Characterisation of the Ca^{2+} signaling pathway involved in the control of Temperature Dependent Locomotion by Neuronal Calcium Sensor-1 in *Caenorhabditis elegans*

Thesis submitted in accordance with the requirements of the University of Liverpool for the degree of Doctor in Philosophy by

Paul Anthony Christopher Todd

September 2016

Abstract

Calcium (Ca^{2+}) signaling is critical in regulating a number of neuronal functions including synaptic transmission, axonal growth, development and neurotransmitter release / recycling. The EF-hand containing Ca^{2+} binding protein Neuronal Ca^{2+} Sensor 1 (NCS-1) has been shown to be important in a number of these processes. NCS-1 is a member of the NCS family of proteins encoded in mammals by 14 genes. Ca^{2+} bound NCS-1 exposes a hydrophobic binding domain through an altered conformation allowing regulation of downstream processes, dependent on a diverse range of target proteins.

Many interacting partners have been identified for NCS-1, some of which are common to Calmodulin (CaM) with others unique to NCS-1. Mammalian NCS-1 has been shown to regulate PQ-type voltage-gated Ca^{2+} channels (VGCCs), although evidence of a direct interaction between the two proteins has been lacking. The initial part of this study investigated interactions between NCS-1 and PQ-type VGCCs (CaV2.1). Within the CaV2.1 C-terminal tail, there are two Ca^{2+}-sensor binding regions; the CBD (CaM binding domain) and the IM/IQ domain. Through cell transfection and fluorescence based experiments, an interaction between these two proteins was established. Co-expression of NCS-1 and a PQ channel C-terminal domain led to the appearance of hallmark aggregated cellular structures. Furthermore, the kinetic behaviour of NCS-1 and PQ in these cells was significantly different to those observed when each protein was expressed in isolation.

The second part of this study used *C. elegans* as a model organism to study *in vivo* interactions of NCS-1. In *C. elegans* NCS-1 is primarily found in the nervous system, with highest expression in sensory neurons. Previous studies have identified a defect in isothermal tracking in an *ncs-1* defective *C. elegans* animal. When tested in a locomotion assay, characterised in this thesis, the locomotion rate of wild-type *C. elegans* decreased at an elevated temperature of 28^{o}C whilst the *ncs-1* null *C. elegans* showed a slight yet significant increase in locomotion at the elevated temperature. During this project a reversible paralysis phenotype was identified in the temperature dependent locomotion assay (TDLA). In the second part of the project this assay was exploited to quantify the paralysis phenotype in various mutant *C. elegans* strains.

Based on the mammalian NCS-1 interactome, a sub-set of protein orthologues were identified within the *C. elegans* nervous system as potential interacting proteins to be studied. It was established that potential targets were TRP1 & 2, ARF-1.1 and PI4K of which various double mutants were generated through *C. elegans* genetic crosses. The double mutants identified a genetic interaction between ARF-1.1 and NCS-1 in the TDLA suggestive of a possible functional interaction. Additional studies using a chemical inhibitor of phosphatidylinositol 4kinaseIIIβ suggests a potential network comprising PI4K-1, NCS-1 and ARF-1.1 regulates this behaviour. These findings allowed a partial elucidation of the interactions and functional relationships between these proteins in a physiological context with an identifiable behavioural output.

Acknowledgements

After an amazing 3 years on this project there are too many people to thank without writing another 20 pages. Firstly and most importantly I would like to thank my three amazing supervisors; Bob for all his insights, for being the mastermind behind the project and for always maintaining a detailed knowledge of the project whilst giving me the freedom to carry on with the project, Lee 'the Protein King /doodlepoll disliker' for all your invaluable assistance in the construction of the various constructs and all your help with the fluorescence experiments and cameleon studies and finally Jeff 'the Canadian *C. elegans* boss' for answering all my questions through the project and with your maintained patience when the RNAi experiments were ongoing and for helping with my question about *C. elegans* imaging. Words cannot express how much I appreciate all the help from my supervisors both in answering my questions and keeping an overview of the project in the weekly & monthly meetings and for making the lab an enjoyable space to work in, putting up with my music and making me laugh at times my face actually hurt. Seriously, you have made completing this research a joy and I think that was the most beneficial and conducive working environment for myself. An extra thanks to you all for reading my thesis drafts and giving me comments and support.

I would also like to thank Professor Alexei Tepikin for allowing me usage of the microscopes in Blue Block, for also being a superb head of the Wellcome Trust at the time of me joining the programme. Thanks must also be given for Professor Judy Coulson for the use of the qPCR machine. Regarding other PIs I would like to thank Professor Alan Morgan for his insights into this project through the weekly worm (nematode) meetings and for helping me obtain some of the *C. elegans* strains, I also appreciate the spontaneous meetings with Dr. Tobias Zech who showed a genuine interest in *C. elegans* when I attempted to use the microscope on 4th floor and Professor Barry Campbell for questioning me on my project and for our random chats about anything… and everything. Furthermore to Professors Silvie Urbe and Ian Prior thank you for my yearly APRs and for being impartial advisors during these meetings.

I also would like to say my thanks to other Principal investigators at the University of Liverpool for attending my end of year talks, although they both had their own unique issues of a random Skype call and an incorrect title on the programme but apart from those, the questions asked during these helped me tremendously during my project. I would also like to thank the Wellcome Trust for funding myself during this research and I am proud to have been accepted onto this course and supported by such a great Trust.

Secondly, I would like to thank the other members of Red block and our adopted members. Past members (James Johnson, Leanne Bloxam, Victoria Martin, Matt Edmonds, Hannah McCue, Pryank Patel, Xi Chen, Dayani Rajamanoharan and Jennifer Mak (sup buddy)), present members (Shiquan Wong, Charlotte Nugues, Nordine Helassa) including our adoptive members (Erica Brockmeier, Helen Tanton, Steven Dodd, Louise Thompson and Francesca De Faveri) for all your smiles, your cheery attitudes and for making the last 3 years a pleasure and making me excited to come to labs each day, even when experiments were not going well. A special thanks to Victoria Martin for the amazing start to the NCS-1 project and for enticing me to come back to the lab during my MRes. To the MRes who have passed through the lab over the years, your daily questions and lunch time chats will also be missed. To you all I cannot express my thanks. You have all been great friends over the past 4 years and have kept me focused and committed over the course of this project and I truly hope that whatever you do with your futures it is enjoyable. A special mention to Dr. Hannah McCue for her assistance in generating the *C. elegans* strains through injections and to Shiquan Wong for her help assessing the PIK-93 bioaccumulation in *C. elegans*.

To the future members of the lab, Red block is the best place to work and the research completed here is awesome, trust me, and it is an enjoyable place to carry out research with a great team of PIs who are more than willing to help. Also any future members of the lab, feel free to read this thesis and for those of you who do get onto a PhD, my advice and comments are to keep reading and keep learning, whilst it will be like a rollercoaster with many rapid ups and downs, overall it will most likely be the best years of your life to date; and if you make friends half as great as those I made, you should count yourselves lucky. NCS-1 is the best protein and don't you forget it!

To my fellow PhD peers I would like to thank you for all the nights out, the laughs and the chats in the corridors; during the University symposiums and such. A special thanks to my fellow Wellcome Trust cohort Matthew Concannon for putting up with living with me for 3 years, Bronwyn Dawson for living with me for 1 year; for your shared *C. elegans* frustrations, your help during demonstrating and for your chats and for hearing me vent, Jennifer McNamee for listening to my random stories and for always being around when I needed someone to talk with or to destress and finally Michela Pulix for being one of the greatest people and friends I have met during my PhD, the random walks we took into Sefton Park, your random office times, your help during demonstrating, the nights out and for always knowing how to make me smile when I was stressed or feeling down. To you all I am happy we were put together for the past 3-4 years and although we rarely went out altogether, I enjoyed those times and you definitely got me through the last 3 years.

A super special thanks to the Haemotech BiotechYES team (I have already thanked you all but you need another thanks), Dayani, Jennifer, Bronwyn and Helen you made BiotechYES so enjoyable, the late nights, getting told off by hotel security, the discussions, the many many meetings, the learning experiences, the help with the different aspects, helping pull the project together to make such a strong product (HT112) and the stressful practises before the Manchester regionals and the London finals. I would not change a thing about the whole experience… except maybe thinking of the idea of uncaffinated coffee, not that I am bitter or anything. To all the teams at BiotechYES that year, thanks for making the experience so amazing especially to the Leeds team Geltide solutions who were there both for the Manchester regionals and the London finals and were such a great team to compete alongside.

To my old Lancaster University friends Emma Stafford, Rachel Kendall, Michael Weatherby, Sally Malcolm and Hannah Southworth; thanks for the random meetups and for your support over the course of this postgraduate study, you always made me laugh. To my friends from Manchester, specifically Mark Kendall and Matthew Thomas, and their families, who helped take my mind off my project when it was overwhelming me and for giving me suitable distractions in the forms of online games or through nights out and visits to Liverpool. I am so grateful for your support.

A big thanks also to my internal and external examiners; Doctor Antonius Plagge and Professor Lindy Holden-Dye; I hope you enjoyed reading this thesis as much as I enjoyed completing the research and formulating the overall thesis. I thank you for your time and for your comments.

Nearing the end now I promise, thanks to Lucy Clark my amazing girlfriend for putting up with me during my thesis write up, for keeping me smiling and on target when I swayed from work, procrastinated or lost motivation, I would not have finished this thesis on time was it not for you. A little thanks for also helping me learn the 'correct' way to say Scones and Oregano; and for showing the many wonders of Yorkshire. To Lucy and your family (Carol, Andy, Sophie, Katie and Ben) for letting me into your home during my thesis write up and for showing an interest in my work as well as being supportive during the time I was probably at my grumpiest and most stressed out. Immense thanks to you all.

Finally, I promised to save the best until last, I would like to thank my family. To my mum, Dawn; thank you for coming up to see me over the last few years (a special niece delivery service), for listening to me rant and stress and remind me there is light at the end of it all. To my Dad, Anthony; thank you for helping me move and for supporting me when I moved back home. I cannot state how much I appreciate all your support and I am proud to be your son. To my sisters Hayley, Jennifer and Aimee, and my nieces Leilani and Seirianne, thanks for being there when I needed you, for coming to visit me, for drawing me pretty pictures and for covering me in food when you did come to visit (those last 2 points are more towards my nieces but not discounting my other family members). To my pet dog Fudge who is sadly no longer with us, your cuddles and affection always helped me calm down. The unconditional love and support from my family, for listening to me stress and for helping me chill out and calm down when I was unduly getting into a tizz, without you I would have struggled greatly over the past few years.

Publications

Work presented in this thesis has been published in part in the following papers:

LIAN, L. Y., PANDALANENI, S. R., TODD, P. A., MARTIN, V. M., BURGOYNE, R. D. & HAYNES, L. P. 2014. Demonstration of Binding of Neuronal Calcium Sensor-1 to the Ca2.1 PQ-Type Calcium Channel. *Biochemistry*.

TODD, P. A., MCCUE, H. V., HAYNES, L. P., BARCLAY, J. W. & BURGOYNE, R. D. 2016. Interaction of ARF-1.1 and neuronal calcium sensor-1 in the control of the temperature-dependency of locomotion in Caenorhabditis elegans. *Sci Rep,* 6**,** 30023.

Table of Contents

Abbreviations

α – alpha
ACAP – ATP GAP with coiled coiled domain
ACh – Acetylcholine
ADP – Adenosine Diphosphate
ADF – Amphid dual F
AFD – Amphid finger-like D
AGAP – GTP-binding domain ARF GAP
AIA – Amphid interneuron A
AIB – Amphid interneuron B
AIY – Amphid interneuron Y
AIZ – Amphid interneuron Z
ANOVA – Analysis of Variance
AP – adaptor proteins
ARAP – Arf Rho GAP
ARF – ADP ribosylation factor
ARF-1.1 – ADP Ribosylation factor 1.1
ARL – ARF like
ARP – ARF related protein
ASAP – ARF GAP with SRC homology 3 domain
ASE – Amphid single E
ASG – Amphid single G
ASI – Amphid single I
ATP – Adenosine Triphosphate
AUA – Lateral ganglia of head interneuron
AVK – Amphid, Nerve ring, ventral cord interneuron K
AWA – Amphid winged A
AWB – Amphid winged B
AWC – Amphid winged C

β – beta
BAG – Head sensory neuron
BIG – Brefeldin-A-resistant GEF

BSA – Bovine serum albumin

C. elegans – *Caenorhabditis elegans*
cAMP – Cyclic adenosine monophosphate
$[Ca^{2+}]$ - Ca^{2+} concentration
$[Ca^{2+}]_i$ – intracellular calcium concentration
Ca^{2+} - Calcium ion
CaBPs - Ca^{2+} Binding Proteins
CaBP1 - Ca^{2+} Binding Protein 1
cADPR – Cyclic Adenosine Diphosphate Receptor
$CaCl_2$ – Calcium chloride
CaM – Calmodulin, Ca^{2+} modulated protein
CaMK II – Calmodulin dependent protein kinase II
$Ca_V1.2$ – Voltage gated Ca^{2+} channel family 1.2
$Ca_V1.3$ – Voltage gated Ca^{2+} channel family 1.3
$Ca_V1.4$ – Voltage gated Ca^{2+} channel family 1.4
$Ca_V2.1$ – Voltage gated Ca^{2+} channel family 2.1
$Ca_V2.2$ – Voltage gated Ca^{2+} channel family 2.2
$Ca_V2.3$ – Voltage gated Ca^{2+} channel family 2.3
Ca_V2x – Voltage Gated Ca^{2+} channel family 2x
CBD – Calmodulin binding domain
CDI – Ca^{2+} dependent inactivation
CDF – Ca^{2+} dependent facilitation
CFP – Cyan fluorescent protein
CGC – *Caenorhabditis elegans* Genetics Centre
cGMP – Cyclic Guanosine monophosphate
CICR - Ca^{2+} Induced Ca^{2+} Release
Cl^- - Chloride ion
CNS – Central Nervous System
CO_2 – Carbon dioxide
CREB – cAMP Response element binding proteins
CRISPR – Clustered Regularly Interspaced Short Palindromic Repeats
cT – cultivation temperature

∆ - delta

D. rerio – Danio rerio

D. melanogaster – Drosophila melanogaster

D2R – Dopamine D2 receptor

DAG- Diacylglycerol

DIC – Differential interference contrast

DMEM – Dulbecco's modified eagle medium

DMSO – Dimethyl sulfoxide

DNA – Dioxyribose nucleic acid

Dop – Dopamine

DREAM - calsenilin/KChIP3

dsRNA – double stranded RNA

DVA – Nerve ring, dorsal cord interneuron

E. coli – Escherichia coli

EDTA – Ethylenediaminetetraacetic acid

EF – E & F helices of parvalbumin, Ca^{2+} binding motif

ER – Endoplasmic Reticulum

Eri-1 – enhanced RNAi

EGA6 – Exchange factor for ARF6

F1 – Filial 1 hybrid

F2 – Filial 2 hybrid

FBS – Fetal bovine serum

FLIP – Fluorescence loss in photobleaching

FLP – Head sensory neuron

FRAP – Fluorescence restoration after photobleaching

FRET – Förster resonance energy transfer

GABA – γ-aminobutyric acid

GAPs – GTPase activating proteins

GCs – Guanylyl cyclases

GCAPs – Guanylate cyclase activating proteins

gDNA – Genomic DNA
GDP – Guanosine Diphosphate
GEFs – Guanine nucleotide exchange factor
GFP – Green fluorescent protein
GIT – G-protein coupled receptor kinase interacting protein
GMP – Guanosine monophosphate
Glu – Glutamate
Gly – Glycine
GPCRs – G-protein coupled receptors
GRK – G-protein coupled receptor kinases
GTP – Guanosine triphosphate

H. sapiens – *Homo sapiens*
HCLP-1 – Hippocalcin like protein 1
HSN – Midbody motor neuron
Hsp-1 – Heat shock protein 1

IP3 / $InsP_3$- Inositol triphosphate
($Ins(1,4,5)P_3$) – Inositol 1,4,5 triphosphate
$InsP_3Rs$ – Inositol triphosphate receptor
IPTG – Isopropyl β-D-1-thiogalactopyranoside
IT – Isothermal tracking

Kan – Kanamycin
KChIPs – Potassium (K^+) Channel interacting proteins
KCl – Potassium chloride
kDa – kilo Dalton

LB – Lysogeny broth
LB agar – Luria-Bertani
LGCC – Ligand Gated Ca^{2+} channel
Lin-15b – Abnormal cell lineage
LKU – lipid kinase unique
LTD – Long Term Depression

LTP – Long Term Potentiation

Mb – Megabases
mCh – mCherry
$MgCl_2$ – Magnesium chloride
ml – millilitre
mm – millimetre
ms - milliseconds
Mut – Mutant
Myr – myristoylation domain

N.A. – numerical aperture
Na^+ - Sodium ion
NaCl – Salt
nCaS – Neuronal Ca^{2+} sensor
NCS – Neuronal Ca^{2+} sensor
NCS-1 – Neuronal Ca^{2+} sensor 1
NCX – Na+/ Ca^{2+} exchange
NEAA – Non-essential amino acids
NGM – Nematode Growth Medium
NH_2 – Amino terminal
NMDA – N-methyl-D-aspartate
NMDARs – NMDA receptors
nM – Nanomolar
nm – Nanometer
NSF – *N*-ethylmaleimide-sensitive factor

O_2 – Oxygen
-OH – Hydroxyl domain
ORF – Open reading frame
OSM-6 – Osmotic avoidance abnormal

PA – Phosphatidic acid
PBS – Phosphate buffered saline

PCR – Polymerase Chain Reaction

PDE – phosphodiesterase

Pen/Strep – Penicillin / Streptomycin

PFA – Paraformaldehyde

pH – Partial pressure of Hydrogen

PH – Plekstrin homology

PHA – Phasmid A

PHB – Phasmid B

PHC – Phasmid C

PI3K – Phosphoinositide-3-OH kinase

PIFK/ PI4K- Phosphatidylinositol-4-kinase

PI4KIIIβ – Phosphoinositide 4-kinase III beta

PI4P – Phosphatidylinositol 4-phosphate

PIK-93 – N-(5-(4-Chloro-3-(((2-hydroxyethyl)amino)sulfonyl)phenyl)-4-methyl-2-thiazolyl)-acetamide

PIP2 – Phosphatidylinositol 4,5-bisphosphate

PI – Phosphatidylinositol

$PI(4,5)P_2$ – Phosphatidylinositol 4,5-bisphosphate

PIP(4,5)K – Phosphatidylinositol 4-phosphate 5-kinase

PKC – Phosphokinase C

PLC – Phospholipase C

PLD – Phospholipase D

PLCβ1- Phospholipase C beta 1

pm1 – Pharyngeal muscle

PM – Plasma membrane

PMCA –PM Ca^{2+} ATPase

PVC – Ventral cord interneuron C

PVD – Ventral cord interneuron D

qPCR – Quantitative PCR

rab-3 – RAB family

Rde-1 – RNAi defective

RH – regulator of G-protein signaling homology domain

RIA – Head, nerve ring interneuron A

RIB – Head, nerve ring interneuron B

RIM – Head, nerve ring interneuron M

RMG – Head interneuron G

RNA – Ribose nucleic acid

RNAi – Ribose Nucleic Acid interference

ROC – Receptor operated channels

ROI – Region of interest

rpm – rotations per minute

RyRs – Ryanodine receptors

S. cerevisiae – *Saccharomyces cerevisiae*

SAR – Secretion-associated and Ras-related

Ser – Seratonin

SEM – Standard Error of the Mean

SERCA – Sarco/endoplasmic reticulum Ca^{2+} ATPase

Sid-1 – Systemic RNAi defective

SNARE – Soluble NSF Attachment Protein Receptor

Snb-1 – Synaptobrevin

Snt-1 – Synaptotagmin

SOC – Super optimal broth with catabolite repression

SOCC – Store-operated Ca^{2+} channel

SOCE – Store-operated Ca^{2+} entry

STIM – Stromal interacting protein-1

SR – Sarcoplasmic reticulum

Src- sarcoma

TDL – Temperature Dependent Locomotion

TDLA - Temperature Dependent Locomotion Assay

TGN – Trans Golgi network

TRP – Transient Receptor Potential

TRPA - Transient Receptor Potential Ankyrin

TM – Transmembrane

TPCs – Two pore channels

TRPC - Transient Receptor Potential Canonical

TRPM - Transient Receptor Potential melastatin

TRPML - Transient Receptor Potential mucolipin

TRPN - Transient Receptor Potential no mechanoreceptor potential

TRPP - Transient Receptor Potential Polycystin

TRPV - Transient Receptor Potential Vanilloid

Ts – thermotactic set point

Ttx-3 – abnormal thermotaxis

UK – United Kingdom

µg – microgram

µM- Micromolar

Unc-18 – Uncoordinated 18

v/v – volume per volume

VGCC – Voltage Gated Ca^{2+} channel

VILIPs – Visinin- like proteins

WT – Wild type

w/v – weight per volume

YFP – Yellow fluorescent protein

Chapter 1: Introduction

Introduction

1.1 Calcium signaling

The calcium ion (Ca^{2+}) is a universal signalling species that emerged in prokaryotic life, with more varied and specialised functions arising with multicellular organisms (Cai et al., 2015, Bootman et al., 2001b). The divalent Ca^{2+} ion has been widely studied for its roles in regulating a vast number of processes within cells. Ca^{2+} is one of the most versatile cellular messengers currently known (Berridge et al., 2000, Bootman et al., 2001a), regulating a plethora of responses over different time frames (microseconds to years) (Petersen et al., 2005). Cells have developed mechanisms to shape Ca^{2+} signals in space, time and amplitude to elicit a range of responses (Bootman et al., 2001a, Berridge et al., 1998).

Intracellular Ca^{2+} is maintained at a resting level of ~100 nM (Berridge et al., 2000). When elevated above this basal concentration, the 'Ca^{2+} signalling network' is engaged (Figure 1.1) resulting in activation of a four stage pathway. Firstly an external or internal cellular signal elicits a rise in cytoplasmic Ca^{2+} ($[Ca^{2+}]_i$) either through Ca^{2+}-release from intracellular Ca^{2+} stores (mitochondria or endoplasmic reticulum (ER)) or entrance of extracellular Ca^{2+} across the plasma membrane (PM). $[Ca^{2+}]_i$ levels can rise to several μM under such circumstances (Ashby and Tepikin, 2001, Bootman et al., 2001a). Elevated Ca^{2+} acts as a secondary messenger, stimulating numerous Ca^{2+}-sensitive processes.

Using self-regulating mechanisms (Figure 1.2), Ca^{2+} is expelled from the cytoplasm, removing Ca^{2+} from the cell or into storage organelles through a range of channels (Cai et al., 2015, Berridge et al., 1998, Bootman et al., 2001a, Bootman et al., 2001b). Either side of the PM there exists a more than 10,000 fold change in $[Ca^{2+}]$, with systems in place to maintain a low intracellular $[Ca^{2+}]$ (Cai et al., 2015, Clapham, 2007). Cells require vast amounts of energy to maintain a low $[Ca^{2+}]_i$ as too high a $[Ca^{2+}]$ is cytotoxic.

Ca^{2+} elevations can occur through different pathways (Bootman et al., 2001a, Berridge et al., 1998). These can be grouped into: Ligand-gated Ca^{2+} channels (LGCC), Voltage-gated Ca^{2+} channels (VGCC) and Store-operated Ca^{2+} channels (SOCC). LGCCs include the Inositol 1,4,5 triphosphate ($Ins(1,4,5)P_3$) binding to its receptor ($InsP_3Rs$) (Berridge, 1993) or modulation of Ryanodine receptors (RyR) by cyclic ADP Ribose (cADPR) and Ca^{2+} (Berridge et al., 2000). VGCCs are activated following PM depolarisation whilst SOCCs are stimulated after intracellular Ca^{2+} stores are depleted (Bootman et al., 2001a, Bootman et al., 2001b).

IP3Rs are ubiquitously expressed with RYRs enhanced in neurons, cardiac and skeletal muscles (Cai et al., 2015). Increased Ca^{2+} in one cellular region sensitises RYRs to Ca^{2+} (Berridge, 1993, Berridge et al., 1998, Bootman et al., 2001a). This is similar to $InsP_3Rs$ which are inhibited above a threshold [Ca^{2+}] (>300 nM), remaining active between 100-300 nM Ca^{2+} (Berridge et al., 2000, Bootman et al., 2001a). Either IP_3Rs or RYRs are able to stimulate Ca^{2+} release from the ER, an important task for diversifying the Ca^{2+} signals. In non-excitable cells, and some excitable cells, SOCC are involved in Store-operated Ca^{2+} entry (SOCE). Here ER Ca^{2+} depletion is sensed by STIM proteins which in turn regulate Orai channels to maintain the Ca^{2+} signal (Cai et al., 2015). SOCE is utilized during exocytosis.

Components of the Ca^{2+} signalling toolkit permit translocation of Ca^{2+} over the PM (Berridge et al., 2000, Bootman et al., 2001a, Cai et al., 2015). The importance of this system is that Ca^{2+} has the ability to regulate the pathway itself, preventing overstimulation or cytotoxic levels of Ca^{2+}. Either IP_3Rs or RYRs are able to stimulate Ca^{2+} release from the ER, an important task for diversifying the Ca^{2+} signals, producing a more versatile signalling network (Berridge et al., 1998, Bootman et al., 2001a, Bootman, 2007, Roderick et al., 2007).

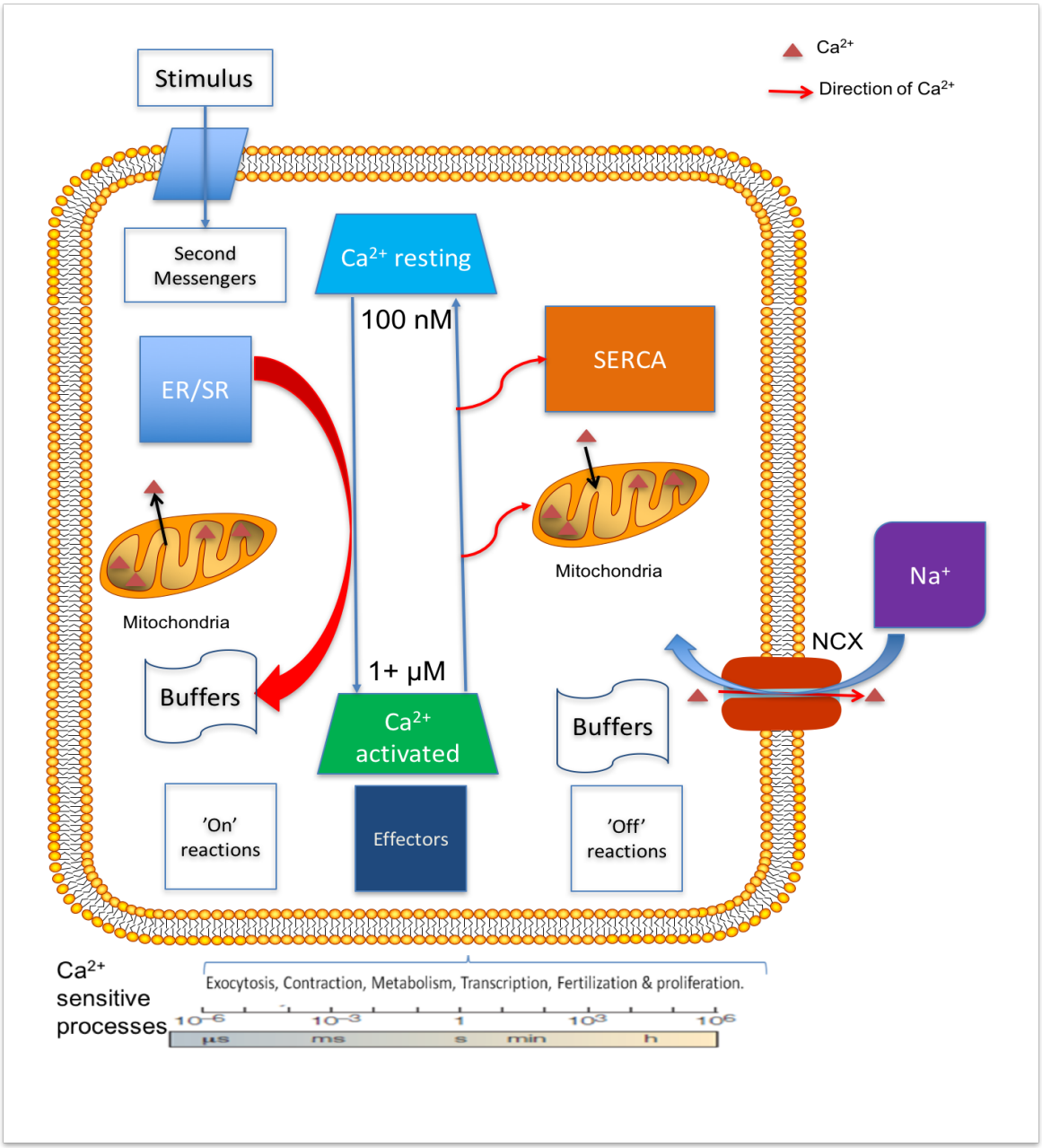

Figure 1.1 Ca^{2+} signalling toolkit/ network: Ca^{2+} enters cells to transduce and transmit external or internal signals to elicit a cellular response. Ca^{2+} can be released from internal organelles such as the mitochondria or be released from the endoplasmic reticulum (ER) or the sarcoplasmic reticulum (SR) to raise cytosolic Ca^{2+}. Signals can be stopped through several mechanisms. Mitochondria can sequester Ca^{2+} to buffer the intracellular compartment. Ca^{2+} is transported into the ER/ SR through the sarco/endoplasmic reticulum Ca^{2+} ATPase (SERCA) or expelled from cells using pumps and channels. Figure adapted from (Clapham, 2007, Berridge et al., 2000, Bootman et al., 2001a, Cai et al., 2015).

Ca^{2+} acts as a secondary messenger during muscle contraction, gene transcription, cell proliferation, exocytosis, fertilisation, cell survival and cell death (Berridge et al., 1998, Bootman et al., 2001a, Bootman et al., 2001b, Bootman, 2007, Petersen et al.,

2005, Pedersen et al., 2005) using a network of signalling partners to elicit downstream pathways (Bootman et al., 2001a). This requires a number of Ca^{2+} binding proteins which will be discussed later in this thesis (Burgoyne and Weiss, 2001, Haynes et al., 2006, Haynes et al., 2007). Multicellular organisms require communication between cells using complex signalling systems (Cai et al., 2015, Roderick et al., 2007, Bootman et al., 2001a, Berridge et al., 2000).

Ca^{2+} signalling has been well investigated showing the effect movement of Ca^{2+} has on cells (Figure 1.1 and 1.2), the channels involved and its diversity using G-protein coupled receptors (GPCRs) (Berridge et al., 2000, Berridge et al., 2003, Bootman et al., 2001a, Bootman et al., 2001b, Bootman, 2007). Research is ongoing regarding the two pore channels (TPCs) in respect to Ca^{2+} signalling, although their importance in release of lysosomal Ca^{2+} has been investigated (Brailoiu et al., 2009, Patel et al., 2010, Ruas et al., 2010).

Ca^{2+} released from IP3Rs are referred to as Ca^{2+} 'blips' or 'puffs' whilst those from RYRs are named Ca^{2+} 'quarks' or 'sparks'. Ca^{2+} 'blips' or 'quarks' stimulate a single Ca^{2+} channel with a localised response ~2 μM for ~ 200 ms (Berridge et al., 2000, Berridge et al., 2003, Bootman et al., 2001a, Bootman et al., 2001b). Ca^{2+} 'puffs' or 'sparks' stimulate a cluster of channels in a co-ordinated manner, persisting longer than Ca^{2+} 'blips or quarks' (~500 ms) and diffuse ~6 μM (Bootman et al., 2001b). Ca^{2+} 'blips' or 'quarks' can stimulate neighbouring receptors forming a Ca^{2+} wave after overcoming the cellular Ca^{2+}-buffering mechanisms which restrict Ca^{2+} signals (Berridge et al., 1998, Berridge et al., 2000, Bootman et al., 2001a, Berridge et al., 2003).

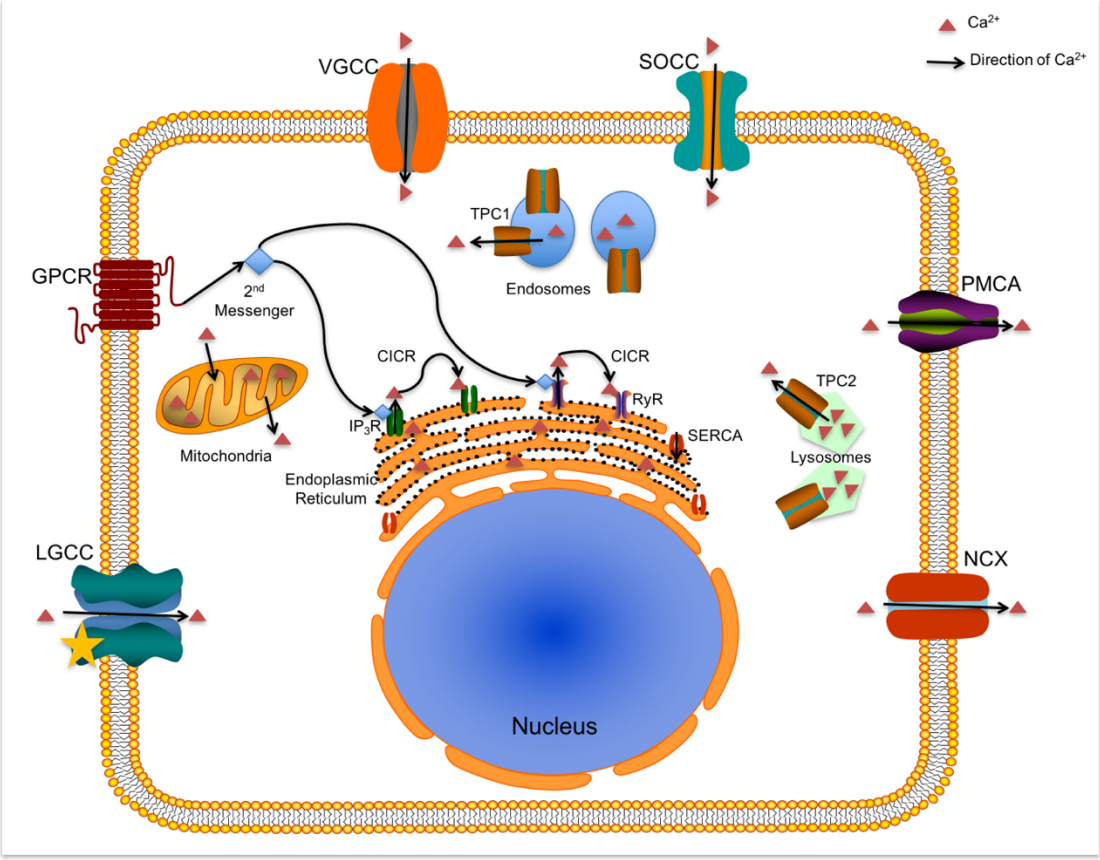

Figure 1.2 Ca^{2+} signalling overview: Influx of Ca^{2+} into the cell is mediated primarily by VGCC with LGCC and SOCC assisting in this process. Ca^{2+} also enters cells through agents binding to GPCRs resulting in the production of second messengers resulting in the activation of IP_3Rs and RYRs. This can lead to signal propagation by CICR. Lysosomes can release stored Ca^{2+} via the TPCs. Ca^{2+} leaves cells through different mechanisms such as NCX (Na^+/ Ca^{2+} exchange) or PM Ca^{2+} ATPase (PMCA). Figure adapted from (Clapham, 2007, Berridge et al., 2000, Bootman et al., 2001a, Bootman et al., 2001b).

Ca^{2+} is able to induce Ca^{2+} release (Ca^{2+} induced Ca^{2+} release (CICR)) (Figure 1.1 and 1.2). Separate mechanisms for Ca^{2+} release exist which are dependent on hormones and growth factors binding to receptors, stimulating hydrolysis of phosphatidylinositol 4,5-bisphosphate (PIP_2) by phospholipase C (PLC) producing $InsP_3$ and diacylglycerol (DAG). The level of hormone applied to cells is proportional to the frequency of Ca^{2+} spikes. Ca^{2+} signals are important throughout the entire body, and are fundamentally important to the normal operation of neuronal and cardiac tissue (Bootman et al., 2001b, Roderick et al., 2007, Catterall and Few, 2008, Catterall et al., 2013). This thesis focuses on the role of Ca^{2+} in specific aspects of nervous system function.

1.2 EF hand: A Ca^{2+} binding motif

This thesis focuses on investigating EF-hand containing Ca^{2+} binding proteins, more than 200 proteins in the human genome contain EF hands, making this one of the largest single motif protein families (Schwaller, 2009, Iacovelli et al., 1999). EF hands were identified in 1973 in Parvalbumin and are named after Parvalbumin's E and F regions (Clapham, 2007, Yanez et al., 2012).

EF-hands commonly occur in pairs. EF-hands consist of a helix loop helix structure (~12 amino acids in total) where Ca^{2+} binds in the loop region (Figure 1.3), linking the two helix regions. Within the EF-hand key residues have been identified; positions 1, 3, 5, 7, 9 and 12 required for correct Ca^{2+} positioning (Yanez et al., 2012). Residues 1, 3 and 5 predominantly being aspartate, position 12 being a glutamate. Specific EF hand containing proteins can undergo a conformational shift when bound to Ca^{2+} (Burgoyne and Weiss, 2001, Burgoyne, 2007, Burgoyne and Haynes, 2014) to expose hydrophobic features, permitting interactions with partner proteins.

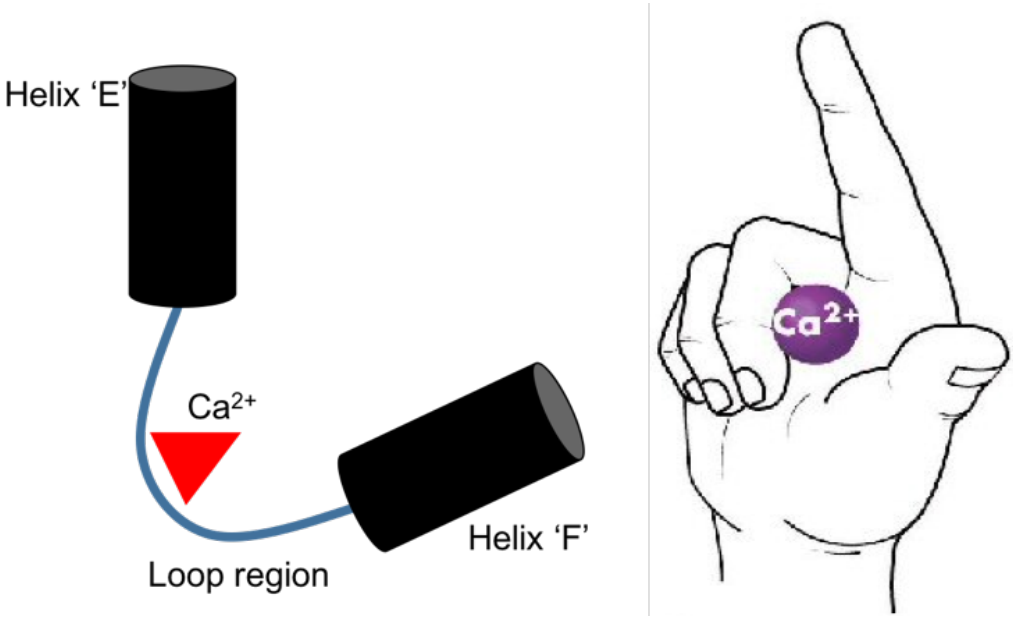

Figure 1.3 EF hands: A structural diagram of the EF hand similar to a thumb and forefinger structure of a hand where Ca^{2+} sits at the base of the two appendages (helices). Ca^{2+} binds to the loop region between the helices. Adapted from (McCue et al., 2009, Burgoyne, 2007).

1.3 Neuronal Calcium

The central nervous system (CNS) is able to process, store and transfer information through a series of regulated and complex patterns of Ca^{2+} signals generated by an interplay between a range of Ca^{2+} channels, pumps and exchangers and decoded into cell biological outputs by a diverse array of Ca^{2+}-sensing proteins (Haynes et al., 2012b). Ca^{2+} plays a vital role in neuronal sensory input, signal transmission and regulation of neuronal signaling (Bootman et al., 2001a, Criddle et al., 2007, Petersen et al., 2005).

Animal behaviour can be regulated through changes in intracellular free Ca^{2+}, transmitted via Ca^{2+} sensor proteins, relaying cellular signals to evoke protein-protein interactions. Neurons express a number of Ca^{2+} sensor proteins (McCue et al., 2010b) such as synaptotagmin I. Ca^{2+} bound synaptotagmin I, is utilized during fast neurotransmission (Nonet et al., 1993, Fernandez-Chacon et al., 2001) alongside other EF-hand containing proteins (Figure 1.3) (McCue et al., 2010b). Numerous neuronal processes are Ca^{2+}-dependent including regulated exocytosis of neurotransmitters, modulation of ion channel activity, development and regulation of neuronal gene expression. Recent studies identified the potential presence of aberrant Ca^{2+} signaling in a number of neurodegenerative disorders (Brini et al., 2014, Mattson and Magnus, 2006, Camandola and Mattson, 2011, Ames et al., 2012).

Neuronal Ca^{2+} signals are highly diverse, potentially due to restricted expression of proteins in different neurons, with various post-transcriptional modifications (myristoylation or palmitoylation) to alter protein locations (O'Callaghan et al., 2002, O'Callaghan et al., 2003).

Through molecular pathways, Ca^{2+} controls patterns of synaptic facilitation and depression to regulate synaptic connectivity and architecture, dictating higher level abstract processes of learning and memory acquisition (Yan, 2014). Synaptic efficiency is altered by Long Term Potentiation (LTP) and Long Term Depression (LTD) (Brini et al., 2014) through synaptic transmission, to modulate learning and memory.

LTP occurs using Ca^{2+} signals in the μM scale for a matter of seconds; LTD occurs following a Ca^{2+} signal on the hundreds of nM scale for longer time frames using Ca^{2+} entry via N-methyl-D-aspartate (NMDA) receptors (Malenka and Bear, 2004, Bear and Malenka, 1994). Ca^{2+} in neurons modulates axonal growth, synaptic strength and neural plasticity (Zhang et al., 1995, Moreno et al., 2016, McGinnis et al., 1998, McCue et al., 2010b, Zucker and Regehr, 2002, Chen et al., 2001, Bennett, 1999, Ghosh and Greenberg, 1995).

1.3.1 Calcium sensor proteins

Ca^{2+} sensor proteins can be broadly grouped into two sub-families; the Ca^{2+} binding proteins (CaBPs) and the Neuronal Ca^{2+} sensor (NCS) family (Haeseleer et al., 2000, Haynes et al., 2012a, Burgoyne, 2007, Burgoyne and Weiss, 2001, Burgoyne and Haynes, 2012). Members of these families are related to Calmodulin (CaM), each containing four EF-hands (Burgoyne and Haynes, 2014, Burgoyne and Haynes, 2010, Burgoyne, 2007).

The Ca^{2+}-binding / sensor proteins display distinct cellular and tissue distribution, present either intracellular or extracellular to stimulate or inhibit signalling (Yanez et al., 2012, Kabbani et al., 2002, Iacovelli et al., 1999).

1.3.2 Calmodulin

In 1970, the primordial EF-hand protein, Calmodulin (Calcium Modulated Protein (CaM)) (148 amino acid), was first identified (Stevens, 1983, Clapham, 2007, Yanez et al., 2012). Present in all plant and animal cells, CaM is the most abundant Ca^{2+} sensor protein, showing high conservation, a useful tool for studying Ca^{2+} sensors (Zhang et al., 1995, Yanez et al., 2012). CaM regulates numerous physiological processes including exocytosis, cell motility, modulating intracellular Ca^{2+} levels and assembly of the cytoskeleton. Partner proteins of CaM are well known including Ca^{2+}/CaM-dependent protein kinase II which mediates many CaM dependent functions (Yamauchi, 2005). CaM has four functional EF hands arranged in pairs, N-terminal and C-terminal lobe (DeMaria et al., 2001, Berridge et al., 2000). The ability of CaM to interact with >300 partner proteins stems from its highly mobile linker region

orientating the structure of CaM (Chattopadhyaya et al., 1992, Babu et al., 1988, Ikura and Ames, 2006).

Under changes in $[Ca^{2+}]_i$, many EF-hand containing proteins undergo a conformation change (Ikura and Ames, 2006), permitting binding to downstream partner proteins. Upon binding Ca^{2+}, CaM undergoes a conformational change, increasing its Ca^{2+} affinity 10 fold (Berridge et al., 1998, Zhang et al., 1995).

1.3.3 Calcium Binding Proteins (CaBPs)

The CaBPs were first identified in vertebrates (McCue et al., 2010a), further allowing diversification in the Ca^{2+} signal in higher organisms. CaBPs show higher resemblance to CaM than the NCS proteins in sequence homology. Each member contains four EF-hands albeit some are inactive (Figure 1.4) (McCue et al., 2009). CaBP 7 & 8 contain a C-terminal transmembrane domain whereas CaBP 1 & 2 have an N-terminal myristoylation sequence, similar to members of the NCS family.

The myristoylation sequence restricts CaBP protein localisation to membranes, further diversifying the Ca^{2+} signal. Caldendrin is the longest splice isoform of CaBP1 that does not contain an *N*-myristoylation motif. Members of the CaBP family share a number of similar interacting proteins with CaM; resulting in different outcomes. In respect to L-type Ca^{2+} channels, CaM bound L-type channels causes Ca^{2+} dependent inactivation (CDI) and reduced Ca^{2+} influx. CaBP1 bound L-type Ca^{2+} channel blocks CDI and increases Ca^{2+} influx (Findeisen and Minor, 2010, Findeisen et al., 2013).

In regards to $Ca_V1.2$ channels, the N-terminal portion of CaBP1 induces inhibition of CDI and induction of Ca^{2+} dependent facilitation (CDF), thereby modulating channel activity, with the C-terminus acting as a protein anchor (Findeisen and Minor, 2010).

CaBP1 is present within neurons, CaBP4 is however present in retinal cells as well as neuronal cells, assisting in regulating photoreceptor Ca^{2+} signals (Lee et al., 2007). CaBP4 was proposed to be involved in neurotransmitter release at synaptic terminals

(Haeseleer et al., 2000, Haeseleer, 2008). The rationale behind using CaBP1 as a control for later studies is due to its presence in neurons and its N-terminal myristoylation sequence.

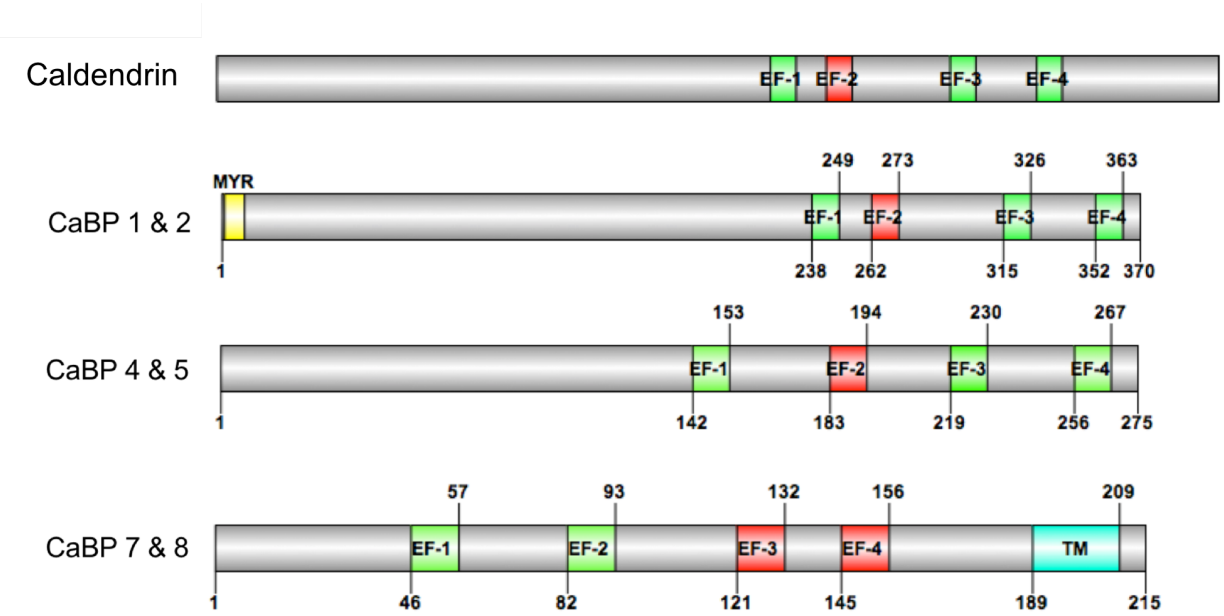

Figure 1.4 CaBP structures: CaBP family members are structurally distinct from CaM, each contain 4 EF-hands albeit with different active (green) and inactive (red) EF-hands. CaBP1 & 2 have an N-terminal myristoylation domain allowing membrane association. Membrane association in CaBP7 & 8 occurs via its C-terminal transmembrane domain.

CaBP7 and 8 are believed to be regulators of PI4KIIIβ (McCue et al., 2010a, McCue et al., 2010b). Under low [Ca^{2+}], CaBP7 and 8 inhibit kinase activity of PI4KIIIβ; in the presence of high [Ca^{2+}], NCS-1 binds to PI4KIIIβ stimulating its kinase activity, enhancing trafficking from the Trans Golgi Network to the PM (Mikhaylova et al., 2009).

1.3.4 NCS family

The Neuronal Calcium Sensor (NCS) family of proteins are a sub-family of the CaM like proteins highly expressed in neurons (Burgoyne and Weiss, 2001), each of which contain up to 4 active EF-hands (Figure 1.5), with less than 20 % homology with CaM (Brini et al., 2014, Burgoyne and Weiss, 2001). NCS family members are present in specific cell types including neurons and retinal cells. Interestingly, NCS family members hold non-redundant functions as over-expression of one family member

does not compensate for the loss of another NCS member (Heidarsson et al., 2012, Heidarsson et al., 2013, Pandalaneni et al., 2015). NCS family members bind Ca^{2+} at sub-micromolar concentrations (Burgoyne and Haynes, 2012, Rousset et al., 2003) confirming their biological activity as high-affinity sensors compared to low affinity Ca^{2+} buffers.

Mammalian NCS proteins are encoded by 14 conserved genes, with critical roles in regulation of neurotransmitter release, gene transcription, ion channel regulation, cell growth/ survival and synaptic functions (Burgoyne and Haynes, 2012, McFerran et al., 1998, Pongs et al., 1993, Burgoyne, 2007). The NCS family contains 5 sub-families; Class A (NCS-1 / Frequenin), Class B (visinin-like proteins (VILIPs)), Class C (Recoverin), Class D (Guanylate cyclase activating proteins (GCAPs) and Class E (voltage gated Potassium (K^+) channel interacting proteins (KChIPs)) (Burgoyne and Haynes, 2012). NCS family members have differing Ca^{2+} affinities. This research focused on NCS-1.

Ca^{2+} bound NCS-1 adopts a compact globular shape, this differs from Ca^{2+} bound CaM which forms an extended dumbbell shape (Burgoyne and Weiss, 2001, Burgoyne, 2007, Burgoyne and Haynes, 2010, Clayton et al., 2013b). Numerous NCS family members contain an N-terminal modification, myristoyl or palmitoyl acylation that in most cases mediates permanent or reversible membrane association. A Ca^{2+} / myristoyl switch mechanism was suggested as a regulatory mechanism, only being exposed in a Ca^{2+} bound protein (O'Callaghan et al., 2002, O'Callaghan et al., 2003). Some maintain an exposed lipid group in the absence of Ca^{2+} permitting spatial alterations under changing [Ca^{2+}]. Myristoylation is also able to furnish a structural role in certain NCS family members and in GCAP-1 is essential for structural stability, extending the physiological functionality of this modification in the NCS family (Haynes and Burgoyne, 2008).

NCS-1, the primordial member of the NCS family, was first identified in *Drosophila melanogaster (D. melanogaster)* (frequenin) (Pongs et al., 1993), and is the most diversely expressed member of the NCS family. NCS-1 orthologues have been identified in many organisms ranging from Yeast to Humans (Burgoyne and Haynes, 2012, Pongs et al., 1993, Hendricks et al., 1999). VILIPs arose in Nematodes,

Recoverin and GCAPs in amphibians and KChIPs first identified in mammals (Burgoyne and Weiss, 2001).

NCS-1 unlike CaM does not contain 4 active EF hands due to a Cysteine-proline substitution in EF hand-1 and contains an N-terminal myristoyl group (using a conserved glycine at position 2) allowing association with membranous structures (Heidarsson et al., 2013, Ames et al., 2012, Jeromin et al., 2004, Hilfiker, 2003, Taverna et al., 2002). The cellular distribution of the NCS family members is unique allowing diverse functions to be carried out in different cell types (Burgoyne and Weiss, 2001).

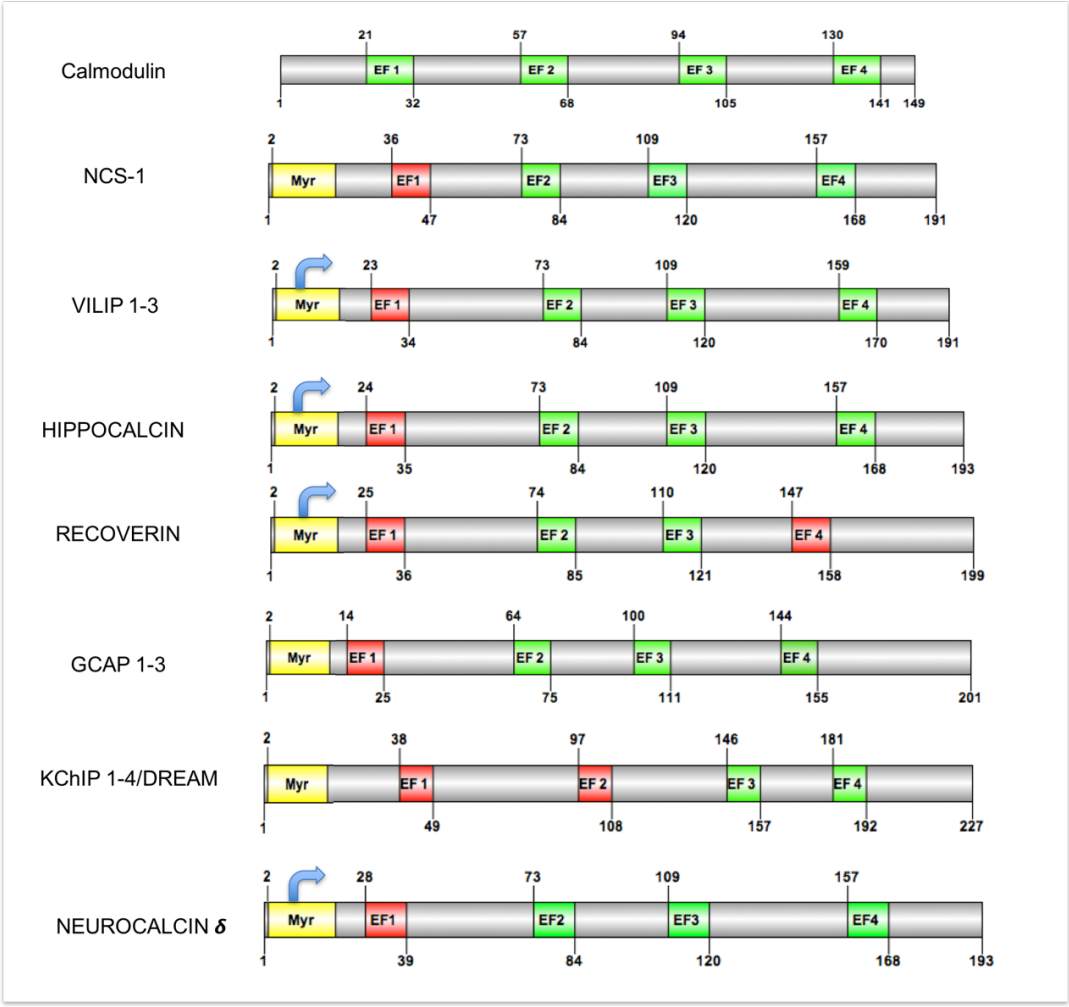

Figure 1.5 NCS family: A detailed structure of the NCS family members with the canonical Ca^{2+} binding protein CaM. Active (green) and inactive (red) EF-hands are represented. Members that are known to undergo a Ca^{2+}-myristoyl shift are highlighted using arrows. Figure adapted from (Raghuram et al., 2012, Viviano et al., 2016, McCue et al., 2010b).

Protein	Active EF hands	Ca^{2+} affinity μM	Concentration of Ca^{2+} bound EF hands μM	References
Hippocalcin	3	0.324	49.72	(O'Callaghan et al., 2003)
NCS-1	3	0.440	29.37	(Aravind et al., 2008)
DREAM	2	~1.000	19.37	(Osawa et al., 2005)
Caldendrin (CaBPs)	2	7.000	16.54	(Wingard et al., 2005)
CaM	4	5.850	49.18	(Faas et al., 2011)

Table 1.1 NCS family Ca^{2+} affinity: Through various studies and equations the affinity of proteins able to bind Ca^{2+} has been calculated. Members of the NCS and CaBP family have been studied alongside CaM, adapted from (Raghuram et al., 2012).

NCS-1 has a higher affinity for Ca^{2+} than CaM. Mammals contain a single NCS-1, one Recoverin, three members of the GCAPs, four members of the KChIPs and five of the VILIP proteins; the recoverin and GCAPs are found solely in the retina (Burgoyne, 2007). Studies have identified the presence of several or all of the NCS family proteins in neurons which are likely to perform distinct functions. Upon examination of the expression profiles, sub-cellular localisations and biophysical properties of the various NCS proteins and CaM highlights that each protein fulfils a unique physiological function(s), multiple sensors present within the same cell type enhances a cells ability to respond to an enhanced range of Ca^{2+} signals.

Other mammalian NCS family functions include signal transduction, gene expression (VILIPs) (De Castro et al., 1995, Few et al., 2005) and light adaptation in the retina (GCAPs and Recoverin) (Ames et al., 2012, De Castro et al., 1995). GCAPs activate guanylyl cyclases (GCs) in the retina as Recoverin inhibits rhodopsin kinase increasing light sensitivity in mammals (Burgoyne and Weiss, 2001, Burgoyne, 2007, Burgoyne and Haynes, 2010). KChIPs are primarily located within the brain and interact with voltage-gated potassium channels, an important role for KChIP2 is found in the heart (Roderick et al., 2007, Kuo et al., 2001).

1.4 NCS-1 and its functions

NCS-1, the primary member of the NCS family, shows a highly conserved sequence (Pongs et al., 1993). Slight changes in [Ca^{2+}] can be detected by NCS-1. NCS-1 predominantly localizes to the Golgi apparatus and PM (Hilfiker, 2003).

NCS-1 the most widely expressed of the NCS family has identified roles in neurotransmitter release (McFerran et al., 1998, Pongs et al., 1993, McFerran et al., 1999), VGCC activities (Weiss et al., 2000, Tsujimoto et al., 2002), short term synaptic plasticity LTD (Jo et al., 2008, Sippy et al., 2003), and synaptic activity (assisting in vesicle fusion at the pre-synaptic terminal (Karp, 2010)). Yeast (*Saccharomyces cerevisiae* (*S. cerevisiae))* NCS-1 is essential for survival, via interactions with Pik1, a phosphatidylinositol-4-kinase (PI4K) orthologue (Hilfiker, 2003, Hendricks et al., 1999). Mammalian NCS-1 and PI4K interact, assisting in neuronal secretion and constitutive exocytosis under NCS-1 overexpression (Hilfiker, 2003).

NCS-1 in neurons regulates Dopamine D2 receptor (D2R) phosphorylation and trafficking. NCS-1 could be a targeted treatment for Schizophrenia and neurodegenerative disorders (Brini et al., 2014, Burgoyne and Haynes, 2012). NCS-1 mutations affect its ability to bind specific partner proteins; key residues between EF3 and EF4 assist in target specificity (Ames et al., 2012, Bourne et al., 2001, Aravind et al., 2008, Rajaram et al., 2000).

A preliminary mammalian NCS-1 interactome has been produced from various protein-protein interaction screens (Figure 1.6 adapted from (McCue et al., 2010b, Burgoyne and Haynes, 2012, Haynes et al., 2006)). Known functional implications of these interactions include neuronal outgrowth, synaptic transmission, learning and memory (Pongs et al., 1993, Saab et al., 2009). Some of these interactions remain to be fully established regarding their Ca^{2+} dependency.

NCS-1 has three EF-hands able to bind Ca^{2+}, under normal physiological conditions, EF2 and EF3 are thought to be Mg^{2+} bound. When bound to Mg^{2+}, NCS-1 has a lower affinity to Ca^{2+} than the apo form (~90 nM as opposed to ~440 nM in the apo form)

(Aravind et al., 2008) preventing non-specific activation (Ames et al., 2012, Burgoyne and Weiss, 2001, Burgoyne and Haynes, 2014, Aravind et al., 2008).

NCS-1 overexpression increases neurotransmitter release in *Drosophila*, Ca^{2+}-dependent exocytosis, learning and memory in *Caenorhabditis elegans* (*C. elegans*) (Heidarsson et al., 2012, McFerran et al., 1998, Pongs et al., 1993, Gomez et al., 2001). During *Danio rerio (D. rerio)* development, NCS-1 is required for semi-lunar canal formation (Burgoyne, 2007, Hendricks et al., 1999).

Highlighted in the protein-protein interaction screens were ARF1 and PI4KIIIβ (PI4K), supporting past research regarding a relationship between these proteins (Haynes et al., 2005, Haynes et al., 2006, Haynes et al., 2007, Burgoyne and Haynes, 2014). Similarly these allow secretion of components for inner ear development of the vestibular apparatus (Petko et al., 2009).

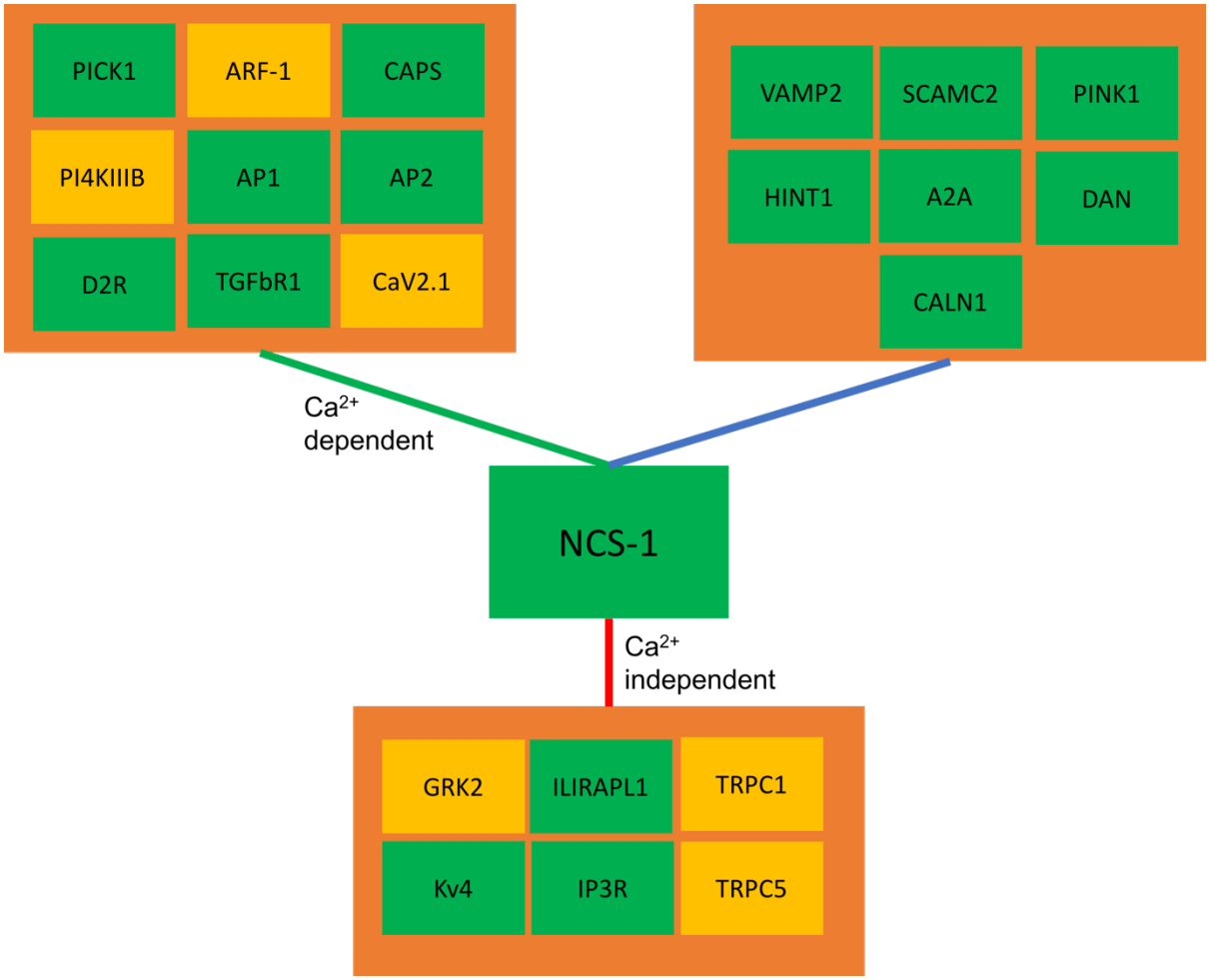

Figure 1.6: Simplified interactome of mammalian NCS-1: Known interactors of mammalian NCS-1 were identified and homologues of these proteins within *C. elegans* determined. Interactions with mammalian NCS-1 can be classified as either Ca^{2+} dependent (top left box) or Ca^{2+} independent (bottombox). Not all interactions with mammalian NCS-1 have been fully elucidated (top right box). Proteins identified within the AIY interneuron pair highlighted (yellow boxes). Figure adapted from (McCue et al., 2010b, Burgoyne and Haynes, 2012). The importance of the AIY neuron and the potential interacting partners will be highlighted later in this thesis (chapter 1.7-1.7.3)

Many partner proteins overlap with CaM however a number of unique partner proteins are known (Haynes et al., 2006, Haynes et al., 2007), being either Ca^{2+} dependent or independent interactions. AIY specific expression of NCS-1 in *C. elegans* allows for temperature dependent locomotion (TDL) behaviours. Of interest were orthologues of the mammalian interactome which were AIY specific or proteins neuronally expressed in *C. elegans*. The majority of interactions with NCS-1 shown above have not been fully validated functionally (Burgoyne and Haynes, 2014, Haynes et al., 2005, Haynes et al., 2006, Haynes and Burgoyne, 2008).

1.4.1 NCS-1 partners

C. elegans lacking NCS-1 present with aberrant thermosensory behaviours (Gomez et al., 2001, Hedgecock and Russell, 1975). The expression of NCS-1 in the AIY neuron of *C. elegans* is sufficient to recapture temperature dependent phenotypes (Martin et al., 2013). This along with other aspects of NCS-1 in *C. elegans* will be further elaborated on later in this thesis (section 1.6 onwards). The identity of its downstream partner protein is unclear; using a mammalian NCS-1 interactome, potential partner proteins were selected in *C. elegans* using the selection criteria of being present in neurons or specifically in the AIY neuron; any of which that elicited a temperature dependent phenotype were discounted due to the nature of our research assay. Of specific interest was the relationship between NCS-1, Arf-1.1 and PI4KIIIβ (Hobert, 2013).

1.4.2 VGCC

CaM and NCS-1 share multiple interacting proteins, including the VGCCs; our focus was upon the PQ-type channels of the $Ca_V2.1$ (Voltage gated Ca^{2+} channels 2.1) family. Regarding CaM and its interaction with PQ-type channels (Figure 1.7), CaM plays a role in short-term synaptic plasticity (Leal et al., 2012, Mochida et al., 2008, Burgoyne and Haynes, 2014). Open $Ca_V2.1$ channels are bound by CaM at their IQ domain; with Ca^{2+} initially binding to its C-terminal EF-hands; persistent channel opening allows Ca^{2+} binding to the N-terminal EF-hands.

The N-terminal lobe of CaM interacts with the Calmodulin binding domain (CBD) (Figure 1.7), inducing CDI; mutations in which prevents inactivation (Findeisen and Minor, 2010, DeMaria et al., 2001, Burgoyne and Haynes, 2014). Mutations in the C-terminal lobe of CaM on the other hand inhibits CDF (DeMaria et al., 2001, Lee et al., 2002, Lee et al., 2000, Tadross et al., 2013). One hypothesis is that residual Ca^{2+} acts as 'facilitation sensors' to CaM, resulting in various downstream effects (Catterall, 2000). With CaM containing 4 active EF hands and no presence of an N-terminal myristoylation site, one theory is that CaM is able to bind to $Ca_V2.1$ channels different to other Ca^{2+} sensor proteins (Catterall, 2000).

The C-terminal domain of the PQ-type channels contain a IQ (also known as an IM domain) and CBD domains (Catterall and Few, 2008, Catterall, 2000, Lee et al., 1999, Lee et al., 2003), involved in CaM dependent modulation of the $Ca_v2.1$ channel activity (Erickson et al., 2001, Erickson et al., 2003). A high density of Ca^{2+} in nerve terminal active zones is required to inactivate $Ca_V2.1$ channels (Catterall, 2000). Channel regulation is more complicated than presented here with evidence suggesting the β2a-subunit is more susceptible to CaM mediated CDF and CDI than other isoforms of this subunit (Lee et al., 2000).

1.4.2.1 Structure of the PQ-type Ca^{2+} channel

Of the various VGCCs within the Ca_v2x family, the PQ-type channels are pre-synaptic Ca^{2+} channels, able to initiate neurotransmitter release through interactions and modulation by specific Ca^{2+}-binding proteins; contributing to synaptic plasticity (Lee et al., 2002, Few et al., 2005). PQ-type channels are also able to b post-synaptic. Changes in Ca^{2+} influx affects synaptic functions through altered short-term plasticity (Zucker and Regehr, 2002).

The α_1-subunit of the PQ-type channels consists of 4 repeating units, each containing 6 transmembrane domains with cytosolic N and C-terminal tails (Figure 1.7) (Catterall, 2000, Catterall et al., 2013). Previous research has identified the IQ domain as the site of interaction between NCS-1 and PQ-type channels (Lian et al., 2014).

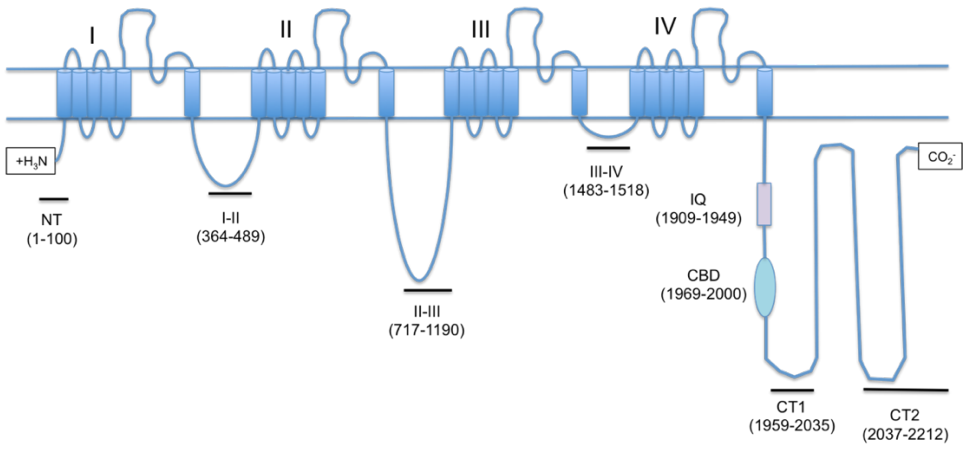

Figure 1.7 PQ structure: The PQ VGCC consists of multiple sub-units; the α_1-subunit has 4 repeating domains, each containing 6 TM domains. NCS-1 binds to the PQ channel at the IQ/IM domain; both the N and C-termini are cytosolic (adapted from (Catterall, 2000, Burgoyne and Haynes, 2014)).

1.4.2.2 Ca^{2+} sensor proteins modulate $Ca_V2.1$ channels

Neuronal Ca^{2+} channels, including the $Ca_V2.1$ PQ-type channels can be modulated by various EF-hand containing Ca^{2+} sensor proteins (Figures 1.3, 1.5, 1.6 & 1.7) in either a Ca^{2+}-dependent or independent manner (DeMaria et al., 2001, Lee et al., 2002, Haynes et al., 2006). Ca^{2+} bound EF-hand containing proteins undergo a conformational shift, exposing binding interfaces permitting interaction with downstream effectors (Burgoyne and Haynes, 2012, Dason et al., 2009, Dason et al., 2012). Regulation of PQ-channels is critical to maintain normal neuronal function (Lee et al., 2000, Lian et al., 2014, Brini et al., 2014, Lee et al., 1999, Lee et al., 2002, Tsujimoto et al., 2002).

Synaptic transmission and neurotransmitter release is primarily initiated by members of the $Ca_V2.1$ channel family (N, PQ and R-type currents) (Tsien et al., 1991, Mochida et al., 2008, Catterall and Few, 2008). The α pore forming subunits of the Ca_V2x family contains multiple transmembrane spanning domains (Figure 1.7). Through association with additional accessory sub-units this allows the assembled channel complex to function in trafficking and regulatory behaviours (Catterall and Few, 2008, Catterall, 2000).

1.4.2.3 PQ-type channels interactions with nCaS proteins

The PQ-type channels are regulated by various Ca^{2+} sensors (Burgoyne and Haynes, 2014). Numerous identified nCaS family members, are able to displace CaM from regulatory binding sites which in turn confers distinct forms of regulation (Catterall, 2000, Catterall and Few, 2008, Christel and Lee, 2012). CaBP1 is able to inactivate PQ-type channels. In this case, CaBP1 binds to the CBD within the α-domain of PQ-type channels in a Ca^{2+}-independent manner resulting in rapid inactivation of channel activity (Lee et al., 2002).

In contrast to this effect, another nCaS known to interact with the PQ-type channel is VILIP-2; upon co-transfection into cells VILIP-2 increases CDF whilst inhibiting CDI

(Few et al., 2005, Lautermilch et al., 2005, Burgoyne and Haynes, 2014) through binding to both the IQ and CBD domains. These opposing effects on channel activity represents the diversity of effects on neuronal Ca^{2+} signals, using different proteins. Members of the CaBP family are also known to interact with and regulate a range of VGCC types altering the channel activity by activating or inactivating CDF and CDI (Table 1.2).

VGCC	Type	CDF	CDI	References
CaV1.2	L-type	CaBP1 (increase)	CaM (increase), CaBP1 (decrease), Caldendrin (decrease), CaBP5 (decrease)	(Peterson et al., 1999, Zuhlke et al., 2000, Tippens and Lee, 2007, Zhou et al., 2004, Rieke et al., 2008)
CaV1.3	L-type		CaM (increase), CaBP 1,2,3, & 4 (decrease)	(Cui et al., 2007, Lee et al., 2007, Yang et al., 2006, Yang et al., 2014, Schrauwen et al., 2012)
CaV1.4	L-type		CaBP4 (decrease)	(Shaltiel et al., 2012)
CaV2.1	PQ-type	CaM (increase), VILIP-2 (increase), NCS-1 (increase), CaBP-1 (decrease)	CaM (increase), CaBP1 (decrease), VILIP-2 (decrease)	(DeMaria et al., 2001, Lee et al., 2003, Lee et al., 2002, Lautermilch et al., 2005, Tsujimoto et al., 2002, Weiss et al., 2000)
CaV2.2	N-type		CaM (increase)	(Liang et al., 2003)
CaV2.3	R-type		CaM (increase)	(Liang et al., 2003)

Table 1.2 CDF and CDI: Overview of different VGCCs and factors which increase or decrease their levels of CDF or CDI, adapted from (Burgoyne and Haynes, 2014). A number of Ca^{2+} binding proteins are included in this table acting upon levels of CDF and CDI. The effects of the proteins on CDF and CDI are outlined in this table (increase or decrease).

1.4.2.4 NCS-1 and its interaction with PQ VGCC.

Studies have shown NCS-1 and its orthologues undertake some of their neuronal functions through interacting with orthologues of the $Ca_V2.1$ protein family. In *Drosophila melanogaster*, frequenin (the NCS-1 orthologue) interacts with cacophony (the $Ca_V2.1$ PQ-type VGCC orthologue) to help regulate neuronal signaling (Dason et al., 2009, Dason et al., 2012). Recent studies using X-ray crystallography have

elucidated the structure of NCS-1 under various conditions to identify protein-protein interactions (Ames et al., 2012, Rousset et al., 2003, Tsujimoto et al., 2002).

To date research suggests NCS-1 interacts with the PQ VGCC at the IQ/IM domain (Catterall and Few, 2008). NCS-1 has been shown to downregulate expression of various VGCC in a β-subunit specific manner (Rousset et al., 2003). Hypothesized binding sites of NCS-1 and various proteins were obtained using data from characterized interactions which occur using the C-terminus of NCS-1 (Heidarsson et al., 2012).

Previous research has shown the importance of PQ-type channels in maintaining neuronal function. This research looked at NCS-1 and its interaction with PQ-type channels at the PM, as NCS-1 is a potential regulator of PQ-type channels (Lian et al., 2014). A lethal phenotype is shown in *C. elegans* lacking PQ-type channels, as such developing a method to test interactions in a living animal is advantageous to elucidate behavioural patterns and protein-protein interactions.

1.4.3 TRP

The mammalian NCS-1 interactome generated from protein-protein interaction screens (Figure 1.6) identified the Transient Receptor Potential (TRP) cation channels, primarily moving Na^+ and Ca^{2+} across the PM, as a potential interacting partner (Song and Yuan, 2010, Pedersen et al., 2005, Clapham, 2007). TRP channels consist of a six transmembrane spanning protein with a pore domain situated between TM domains 5 and 6. TRP channels form homo or heterotetramer structures (Pedersen et al., 2005), regulation of the TRP channels is thought to occur through the N and C termini which are both present intracellular (Ramsey et al., 2006, Song and Yuan, 2010).

Originally, TRPs were first identified in *D. melanogaster* when investigating responses to light (Ramsey et al., 2006, Pedersen et al., 2005). A *Drosophila* mutant with a transient response to light suggested the presence of TRP channels (Pedersen et al., 2005, Ramsey et al., 2006). The first TRP gene was cloned in 1989 (Montell and Rubin, 1989). To date more than 30 members have been identified within this family

(Pedersen et al., 2005). Like other protein channels, TRPs are affected by temperature changes, pH and other environmental signals (Ramsey et al., 2006, Clapham, 2007). Cell types usually contain multiple TRP sub-types (Pedersen et al., 2005).

Seven sub-families are known for the TRP channels based on their amino acid sequence; including TRPC (canonical) (TRPC1 first cloned in 1995 (Wes et al., 1995, Petersen et al., 1995)), TRPV (vanilloid), TRPM (melastatin), TRPN (no mechanoreceptor potential C) TRPA (ankyrin), TRPP (polycystin) and TRPML (mucolipin), as outlined previously (Ramsey et al., 2006, Montell, 2005, Venkatachalam and Montell, 2007, Latorre et al., 2009, Pedersen et al., 2005).

Most of the TRP channels are Ca^{2+} permeable (Cai et al., 2015), assisting in sensing environmental factors through chemical and physical stimuli. Cation current through TRP channels depolarises cells, necessary to transmit action potentials. TRPs and their activity are involved in various cellular functions and diseases (Ramsey et al., 2006, Clapham, 2007, Nilius et al., 2005, Venkatachalam and Montell, 2007). In non-excitable cells, TRPs stimulate voltage-dependent channels to stimulate different processes such as; transcription, translation and contraction (Song and Yuan, 2010). In certain animals, including *C. elegans*, TRP channel activity has been linked to longevity (Talavera et al., 2008, Xiao et al., 2013, Zhang et al., 2015).

1.4.3.1 TRPN

TRPN to date contains a single identified member containing ~29 Ankyrin repeats, found in *C. elegans, Drosophila* and zebra fish (*D. rerio*) (Sidi et al., 2003, Walker et al., 2000). In *Drosophila*, TRPN1 knockout resulted in cessation of mechanosensation and a loss of auditory response in *D. rerio* larvae.

1.4.3.2 TRPA

TRPA1 is the primary member of the Ankyrin TRPs, containing numerous Ankyrin repeats at its N terminus, ~14 repeats (Song and Yuan, 2010, Story et al., 2003). TRPA1 forms non-selective cation channels present in the ear (Pedersen et al., 2005,

Corey et al., 2004). It is under dispute whether TRPA1 is activated by cold (Jordt et al., 2004).

1.4.3.3 TRPC

Commonly in the C-terminal tail of TRPC members, an invariable sequence is found, known as a TRP box (EWKFAR) (Pedersen et al., 2005). Sequence similarity between different members of the TRPC family is high ~75%, with members being activated by phospholipase Cβ1 (PLCβ1) (TRPC1, 4 & 5) or Diacylglycerol (DAG) (TRPC 3, 6 & 7) (Ramsey et al., 2006, Song and Yuan, 2010, Pedersen et al., 2005). Interestingly, TRPC1 is believed to be DAG insensitive, instead acting as a mechanosensitive cation channel, converting membrane stretch into cation signals (Pedersen et al., 2005).

DAG is able to activate TRP channels on the PM, here named receptor-operated channels. Activation of TRP channels in this manner releases Ca^{2+} from the ER and SR, allowing store operated Ca^{2+} entry (Pedersen et al., 2005). Therefore insensitivity to DAG reduces the ability for ions to cross the PM through TRP channels downstream of the RTK or GPCR signaling pathway converting membrane phospholipids into IP3 and DAG with the help of PLC (Minke, 2006). Differential activation and inhibition of TRPC family members can occur, with TRPC4 and 5 able to be activated in the presence of micromolar concentrations of lanthanides, the presence of which inhibits other TRPC members (Pedersen et al., 2005).

TRPs, as with the PQ-VGCCs, also interact with CaM with TRPC3 & 6 showing a higher affinity for CaM than other TRPC members. Translocation of TRP channels is important for their functions, interestingly TRPC5 translocates to the PM in a PI3K, Rac and phosphatidylinositol 4-phosphate 5-kinase (PIP(4,5)K) dependent manner (Bezzerides et al., 2004). In rodents, TRPC2 is required for pheromone detection, however in humans TRPC2 is considered a pseudogene, potentially acting as a Ca^{2+} signal in spermatozoa (Pedersen et al., 2005, Song and Yuan, 2010, Wes et al., 1995, Lucas et al., 2003).

1.4.3.4 TRPV

Members of the TRPV family, in humans and mice have been identified as sensors of noxious temperatures (Song and Yuan, 2010, Caterina et al., 2000). TRPV1-4 each form outwardly rectifying cation channels with different selectivity of Ca^{2+} to Na^{+}. Distinct roles of thermosensation and osmosensation have been identified for TRPV channels (Pedersen et al., 2005). TRPV5 and TRPV6 form constitutively active inwardly rectifying Ca^{2+}-selective cation channels, being tightly regulated by $[Ca^{2+}]_i$. Each TRPV family member contains between 3 and 5 NH_2-terminal Ankyrin repeats. Activation of the TRPV channels differs depending on the temperature threshold, which can be reduced through PKC activation or decreased levels of $PI(4,5)P_2$ (Pedersen et al., 2005).

TRPV channels are present in other organisms including *C. elegans* (Osm-9) and *Drosophila* (Nan) (Pedersen et al., 2005). In the kidney and intestines, reuptake of Ca^{2+} is partially completed through TRPV5 and TRPV6 family members respectively, TRPV6 binds directly to CaM (den Dekker et al., 2003, Lambers et al., 2004).

1.4.3.5 TRPP

TRPP channels have been reported in disease such as autosomal dominant polycystic kidney disease, namely TRPP1. Structurally, TRPP1 contains 11 TM domains with TRPP2 and other TRPP members having 6 TM domains. TRPP1 and 2 are expressed widely with other TRPP members showing restricted localisation (Pedersen et al., 2005). TRPP2 contains a Ca^{2+} binding EF-hand however this lacks a TRP domain, potentially functioning as an intracellular Ca^{2+} channel.

Nonselective cation channels formed by TRPP1 are present in kidney, pancreas, heart, blood and testes (Ramsey et al., 2006, Song and Yuan, 2010). During mouse development, TRPP1 assists in formation of cardiac, skeletal and renal cells. TRPP2 forms cation channels in the kidney, testes and eye, activated following an increase in $[Ca^{2+}]_i$ (Ramsey et al., 2006, Song and Yuan, 2010, Venkatachalam and Montell, 2007).

1.4.3.6 TRPML

Three members have been identified currently for the TRPML subfamily (TRPML1-3), the initial member being TRPML1 (mucolipin), mutations in which lead to lysosomal storage diseases, TRPML assists in controlling lysosomal Ca^{2+} levels (Pedersen et al., 2005). TRPML1 whilst being present on lysosomes is inhibited at low pH. Currently, less is known regarding TRPML2 and 3. Of the TRP subfamilies, the TRPML family is restricted to vesicles, late endosomes and lysosomes present intracellular and form nonselective cation channels (Montell, 2005, Ramsey et al., 2006, Song and Yuan, 2010, Yao et al., 2005). This is also the case for TRPV1 and TRPM8 acting intracellular (Pedersen et al., 2005, Cai et al., 2015, Bootman et al., 2001a).

1.4.3.7 TRPM

TRP channels are conserved through evolution with animals expressing TRPs in different tissues (Chatzigeorgiou et al., 2010, Latorre et al., 2009, Pedersen et al., 2005, Song and Yuan, 2010).

TRPM channels exhibit variable permeability to Ca^{2+} and Mg^{2+}, TRPM4 and TRPM5 being Ca^{2+} impermeable with TRPM6 and TRPM7 being greatly Ca^{2+} permeable (Nilius et al., 2005, Pedersen et al., 2005). Splice variants and mutations in TRPM channels are present in melanoma metastasis (TRPM1), human hypomagnesemia, secondary hypocalcemia (TRPM6) and myogenic cerebral artery vasoconstriction (TRPM4). TRPM5 is involved in taste sensation, TRPM7 in Mg^{2+} homeostasis and TRPM4 in activated T lymphocytes (Montell, 2005, Nilius et al., 2005, Pedersen et al., 2005, Song and Yuan, 2010, Venkatachalam and Montell, 2007).

TRPM1 (melastatin) acts as a tumour suppressor protein, expression of which is decreased in melanoma patients (Pedersen et al., 2005, Grimm et al., 2003). Gating of TRPM4 and 5 occurs through increased $[Ca^{2+}]_i$,TRPM5 activity is also increased through $PI(4,5)P_2$, which previously was shown to inhibit TRPV1 (Pedersen et al., 2005). Interestingly, TRPM7 has been shown to be involved in neuronal cell death and regulating cell cycle progression (Aarts et al., 2003, Wolf and Cittadini, 1999).

Altered expression and regulation of TRP channels is implicated in hypertension (Song and Yuan, 2010). Another of the binding partners for TRPC is enkurin, able to bind to TRPC1, 2 and 5 present in sperm (Sutton et al., 2004). Enkurin interacts with Phosphoinositide-3-OH kinase (PI3K) potentially linking TRPCs with Ca^{2+} sensing mechanisms (Sutton et al., 2004, Pedersen et al., 2005). Key serine/threonine and tyrosine residues present within TRP channels are able to undergo phosphorylation (Pedersen et al., 2005). TRPC3 to become available for activation must undergo src-mediated tyrosine phosphorylation (Vazquez et al., 2004).

1.4.4 ARF

ADP Ribosylation Factors (ARFs) are part of the Ras superfamily of proteins (Chavrier and Goud, 1999) able to bind GTP; containing 6 members (ARF1-6), omitting other ARF related proteins (Lu et al., 2001, Amor et al., 1994, Chavrier and Goud, 1999). These 6 members are sub-divided into 3 ARF classes ARF1-3 (class I), ARF4-5 (class II) and ARF6 (class III) each showing ubiquitous expression (Moss and Vaughan, 1995, Donaldson and Honda, 2005). The ARF family also includes the ARL (ARF like), ARP (ARF-related proteins) and SAR (Secretion-associated and Ras-related) proteins (Nakano and Muramatsu, 1989), which appear to contain similar sequence homology and in some cases, similar functions with the ARF proteins (Pasqualato et al., 2002, Lu et al., 2001, Nie et al., 2003, Boman and Kahn, 1995). Members of the ARF family are approximately 20 kDa (Nie et al., 2003, Boman and Kahn, 1995).

The ARF family, identified in the 1980's, are highly conserved between species; present in all eukaryotic organisms examined, with ARF class I being the most conserved (Moss and Vaughan, 1995, Kahn et al., 1991). ARL1 due to its N-terminal myristoylation sequence is present on the Golgi apparatus in vesicular-tubular structures (Boman and Kahn, 1995). Loss of ARF1 in Yeast results in slow growth, cold sensitivity and a greater sensitivity to fluoride; furthermore, in Yeast, over- or under-expression of ARF proteins affects cell viability (Kahn et al., 1991).

ARF functions depend on its interacting proteins including; structural proteins, lipid metabolising enzymes and proteins which bind ARF-GFP with as of yet undefined functions. ARFs interact with GEFs (Guanine nucleotide exchange factors) and GAPs

(GTPase-activating proteins) regulating their activity and permitting specificity (table 1.3) (Nie et al., 2003, Donaldson and Honda, 2005, Chavrier and Goud, 1999). ARF members bind directly to protein coats including adaptor protein (AP)-1, 3 and 4; resulting in trapping vesicle cargo/ receptors as part of the mannose 6-phosphate pathway (Nie et al., 2003, Donaldson and Honda, 2005, Chavrier and Goud, 1999, Palmer et al., 1993).

Regulator	Arf specificity	Arf Interface	Localisation	References
GEFs				
BIG1/2	Arf1, -3	Sw1/2	Golgi	(Donaldson and Jackson, 2000, Jackson and Casanova, 2000)
GBF	Arf1, -3, -5	Sw1/2	Golgi	(Donaldson and Jackson, 2000, Jackson and Casanova, 2000)
ARNO/GRP/ Cytohesin	Arf1, -6	Sw1/2	PM	(Donaldson and Jackson, 2000, Jackson and Casanova, 2000, Cherfils and Chardin, 1999, Mossessova et al., 1998)
EFA6	Arf6	Sw1/2	PM	(Donaldson and Jackson, 2000, Jackson and Casanova, 2000)
ARF GEP 100	Arf6	Sw1/2	Cell periphery	(Someya et al., 2001)
GAPs				
ARF GAP1/3	Arf1	Sw2, α-3	Golgi	(Donaldson and Jackson, 2000, Randazzo et al., 2000, Goldberg, 1999)
GIT1/2	Arf1, -3, -5, -6	?	Cell periphery	(Donaldson and Jackson, 2000, Randazzo et al., 2000, Turner et al., 2001, de Curtis, 2001)
ACAP1/2/3	Arf6	?	Cell periphery	(Donaldson and Jackson, 2000, Randazzo et al., 2000, Jackson et al., 2000, Turner et al., 2001, de Curtis, 2001)
ASAP1/2/3	Arf1, -5	Sw1, amino terminus	Focal adhesion	(Donaldson and Jackson, 2000, Randazzo et al., 2000, Brown et al., 1998, Andreev et al., 1999, Turner et al., 2001, de Curtis, 2001)
AGAP1/2/3	Arf1, -5	Sw1, amino terminus	Endosomes	(Nie et al., 2002)
ARAP1/2/3	Arf1, -5, -6	?	Golgi, cell periphery	(Miura et al., 2002, Krugmann et al., 2002, Santy and Casanova, 2002)

Table 1.3 Regulation of ARFs by GEFs and GAPs: ARF family members are activated in a GTP bound state and inactivated in a GDP bound state. Regulation of this mechanism occurs through GAPs and GEFs. Each ARF member has a number of regulatory proteins to assist in their activity and the point of interaction if known has been specified. Abbreviations used: ARNO (ARF nucleotide binding site opener); BIG (brefeldin-A-resistant GEF); EGA6 (exchange factor for ARF6); GIT (G-protein-coupled receptor-kinase-interacting protein); PM; SW1/2 (switch 1 or 2 of ARF). ACAP, AGAP, ARAP and ASAP are all ARF GAPs with a coiled-coil domain (ACAP), GTP-binding domain (AGAP), Rho GAP (ARAP) and an Src homology 3 domain (ASAP). Table modified from (Nie et al., 2003).

ARFs contain an N-terminal myristoylation domain, an N-terminal extension (~10-25 residues) to form amphipathic helices (Pasqualato et al., 2002, Donaldson and Honda, 2005, Palmer et al., 1993). An 'interswitch toggle' between two conformations allows recycling of ARF family members between GTP and GDP bound states (Pasqualato et al., 2002, Amor et al., 1994, Lu et al., 2001). An inability to hydrolyse GTP results in a constitutively active ARF (Moss and Vaughan, 1995, Kahn et al., 1991). Research suggests GTP bound ARF has an exposed interswitch domain, covered when GDP bound (Nie et al., 2003). The C-terminus of ARF allows protein-protein interactions. ARL1 when GDP bound causes Golgi apparatus disassembly; however causes Golgi extension when GTP bound (Lu et al., 2001).

Members of the ARF family function to regulate vesicle trafficking, vesicle biogenesis and actin remodelling (Donaldson and Honda, 2005, Nakano and Muramatsu, 1989); with roles in regulating trafficking on the cis-Golgi, trans-Golgi and endosome (Pasqualato et al., 2002, Lu et al., 2001, Zhao et al., 1997, Palmer et al., 1993). Myristoylated ARF is required for recruitment of coatomer proteins to the Golgi (Palmer et al., 1993, Zhao et al., 1997).

Vesicle transport is fundamentally important in endocytic pathways (Lu et al., 2001, Boman and Kahn, 1995, Donaldson and Honda, 2005). ARF, in its GTP bound state, is able to bind to PI4K resulting in the production of phosphatidylinositol 4,5-bisphosphate (PIP2) and phosphatidic acid (PA), utilised in Ca^{2+} release and membrane remodelling systems (Nie et al., 2003, Boman and Kahn, 1995). Members of the ARF family stimulate Phospholipase D (PLD) in a PIP2 dependent manner (Donaldson and Honda, 2005, Moss and Vaughan, 1995, Amor et al., 1994).

1.4.5 PI4K

Phosphatidylinositol (PI) present in cells is used to produce phosphatidylinositidephosphates (PIPs) which contain a number of regulatory roles (Balla and Balla, 2006). Numerous PIPs are present, generated by specific kinases including Phosphatidylinositol 4-kinaes (PI4Ks), first discovered in 1970-80s (Balla, 2013). The PI4Ks act to synthesise phosphatidylinositol 4-phosphate (PI4P); one of the members of the phosphoinositide family. PI4P functions as part of the trans Golgi

network (TGN), defining the membranes of the Golgi apparatus, the TGN and mediating trafficking to and from the Golgi (Boura and Nencka, 2015).

In humans, two sub-groups of PI4Ks are known, namely type II and type III, both containing α and β forms (Clayton et al., 2013a, Balla, 2013), showing high conservation between Yeast and human. PI4KIII α and β show distinct localisations within neurons of the central nervous system (CNS), indicative of a compartmentalized system within cells of the CNS (Clayton et al., 2013a, Clayton et al., 2013b). Due to multiple phosphorylation sites, various PIPs can be produced. A total of 7 PIPs have been identified to date, not including the parental PI molecule; PI4P, $PI(4,5)P_2$, $PI(3,4,5)P_3$, $PI(3,4)P_2$, $PI(3,5)P_2$, PI3P and PI5P, through esterification of the –OH groups on position 3, 4 and 5 of the inositol ring and addition of a phosphate group (Waugh, 2015, McCrea and De Camilli, 2009, Balla and Balla, 2006).

PIPs assist in determining cellular localisation (McCrea and De Camilli, 2009, Clayton et al., 2013a), maintaining PM acidity and supporting signal transduction. PI4Ps have crucial roles in maintaining levels of $PI(4,5)P_2$ and establishing organelle identity; different cellular membrane domains show different PI distribution (Clayton et al., 2013b). When hydrolysed, PIPs form IP_3 and DAG utilized during Ca^{2+} signalling (Boura and Nencka, 2015, Tewson et al., 2012, Berridge et al., 2003, Bootman et al., 2001a). In the nervous system, PIPs regulate receptor signalling, secretion, endocytosis, ion flux, migration and survival through binding specific proteins or by effecting membrane charge (Waugh, 2015, Takahashi et al., 2014).

A wide range of neurological disorders have been identified as having aberrant PIP activity including stroke, Alzheimer's, Charcot-Marie-Tooth, epilepsy and autism as reviewed in (Waugh, 2015, Clayton et al., 2013a, Clayton et al., 2013b, McCrea and De Camilli, 2009, Balla, 2013).

PIP kinases (PI3K and PI4K) phosphorylate PIPs to form the 7 molecules outlined previously. PI4P levels are maintained through the action of PI4K enzyme isozymes; PI4K2A, PI4K2B, PI4KA and PI4KB (Waugh, 2015). Different PIPs are targeted to specific cellular locations (Clayton et al., 2013a, Clayton et al., 2013b).

Features	PI4KIIα	PI4KIIβ	PI4KIIIα	PI4KIIIβ
Alternative names	PI4KII; PI4K55; 56 kDa type II PtdIns 4-kinase	PI4KII; PI4K55; 56 kDa type II PtdIns 4-kinase	Pik4ca; PI4K230; PtdIns 4-kinase α	Pik4cb; PI4K92; Ptdins 4-kinase β
Yeast homolog	Lsb6p (Pik2p)	Lsb6p (Pik2p)	Stt4p	Pik1p
Estimated MW	55-56 kDa	55-56 kDa	210 kDa	110 kDa
Actual MW	54 kDa	55 kDa	230 kDa	92 kDa
Wortmannin	Insensitive	Insensitive	IC_{50} 50-300 nM	IC_{50} 50-300 nM
Ca^{2+}	Inhibits	Inhibits	No direct effect	No direct effect
Ki (adenosine)	10-70 μM	10-70 μM	Millimolar	Millimolar
Triton X-100	Activates	Activates	Activates	Activates
Km (ATP)	10-50 μM	10-50 μM	~700 μM	~400 μM
Km (PtdIns)	~20-60 μM	~20-60 μM	~100 μM	~100 μM

Table 1.4 PIFKs: Features of the different PIP kinases. Conserved proteins also present in Yeast. Actual protein sizes range from 54-230 kDa, effects of Ca^{2+} on activity is primarily inhibitory for the PI4KII class with no direct effect on the PI4KIII class adapted from (Balla and Balla, 2006).

Deletion of type II PI4Ks in Yeast generates a minimal effect on endosomal trafficking and in actin polymerisation. Type II PI4Ks in humans contain a palmitoylation sequence motif (CCPCC), associating with membranes permits activation, regulating type II PI4Ks. PI4K IIα function in vesicle and endosomal trafficking (Boura and Nencka, 2015).

In *S. cerevisiae*; a homolog of PI4K (PIK1), the orthologue of human PI4KIIIβ, is essential for survival (Bourne et al., 2001, Hendricks et al., 1999, Boura and Nencka, 2015, Balla, 2013). Human PI4K functions within the nucleus and upon the Golgi apparatus (Strahl et al., 2005, Wang et al., 2012, Strahl et al., 2007). PIK1 acting in the secretory pathway of the Golgi synthesizes PI4P, regulating trafficking and autophagy within this organelle (Figure 1.8) (Wang et al., 2012, Balla and Balla, 2006).

Research suggests that prior to PI4K activity, this is first recruited to membranes potentially through the action of Arf1 (Godi et al., 1999, Haynes et al., 2005, Haynes et al., 2007, Balla and Balla, 2006). Other known interactors of PI4K include NCS-1 (Frequenin) however the details regarding this interaction functionally remains to be

fully elucidated (Strahl et al., 2007, Hilfiker, 2003, Taverna et al., 2002, Zhao et al., 2001, Mikhaylova et al., 2009, Haynes et al., 2005).

Both the α and β forms of the PI4KIII family contain a proline rich sequence and a lipid kinase unique (LKU) domain near their N-termini with the C-terminus containing their catalytic domain. PI4KIIIβ also has an identified NCS-1 binding site close to its N-terminus, following from the LKU domain (Clayton et al., 2013b, Balla, 2013), this interaction indicates a potential relationship between PI4P synthesis and Ca^{2+}-sensitive exocytosis (Figure 1.8).

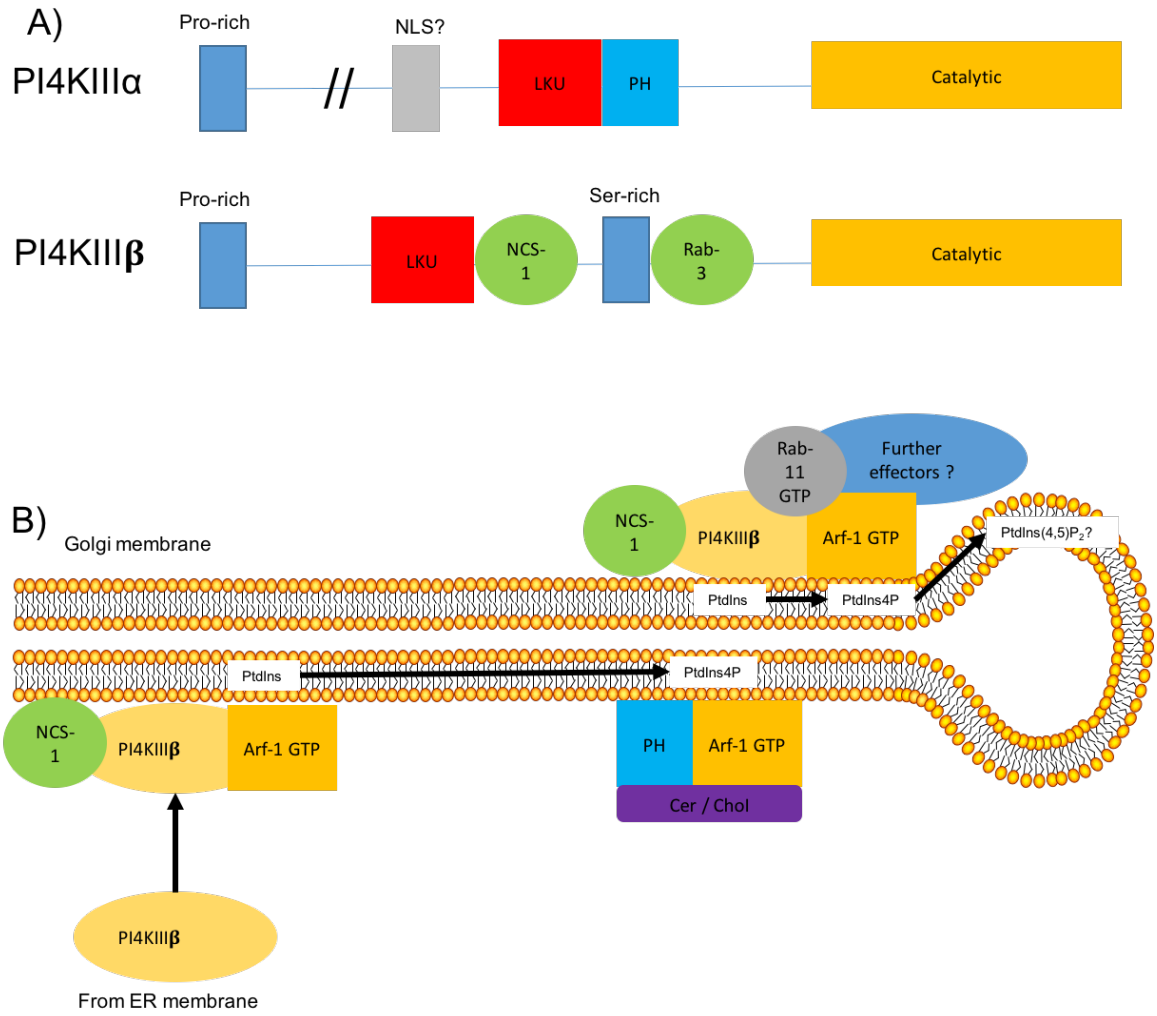

Figure 1.8 PI4KIIIβ localisation on Golgi: A) The PI4KIII class of PIP kinases contain an N-terminal proline rich domain (blue) and a C-terminal catalytic domain (yellow). B) Localisation of PI4KIIIβ with NCS-1 and Arf-1 can be direct, however other proteins are required to produce the different PIP members, some effectors are yet to be elucidated (adapted from (Balla and Balla, 2006)).

The effects of PI4KIIIβ in the Golgi have been described (De Matteis and D'Angelo, 2007, Godi et al., 1999) whereby utilizing Arfs, Rab11 and recruiting other proteins; PI4K assists in budding and cleavage of Golgi transport vesicles. A strong relationship has been identified between ARFs, PI4Ks and NCS-1 at the site of the Golgi (De Matteis and D'Angelo, 2007, Balla and Balla, 2006, Strahl et al., 2007).

1.4.6 GRKs

The mammalian G-protein coupled receptor kinases (GRKs) family contains 6-7 currently identified serine/ threonine protein kinases (Gurevich et al., 2012), acting upon agonist-bound or activated G protein-coupled receptors (GPCRs) as their primary targets (Pitcher et al., 1998, Gurevich et al., 2012). Phosphorylation of these targets causes increased endocytosis, desensitizes receptors; diminishing further signalling events and increases intracellular trafficking (Freedman and Lefkowitz, 1996, Penela et al., 2010, Ribas et al., 2007). Loss of GRK function results in hypersensitivity to GPCR stimulation (Fukuto et al., 2004) Activity of GRKs also depends on interaction with proteins present within cells i.e. CaM alongside non-receptor proteins including PI3K and Akt (Ribas et al., 2007).

Broadly, GRK family members are sub-divided into 3 families; 'visual GRKs' (GRK1 and GRK7 present in rods and cones respectively), β-adrenergic receptor kinases (GRK2 and GRK3) and the GRK4 subfamily (GRK4-6). Between GRK sub-families ~45% sequence homology is present. Each GRK protein is distinct with regards to their regulatory processes (Ribas et al., 2007). Distribution of GRK1, 4 and 7 is restricted to specific organs whilst GRK2, 3, 5 and 6 are expressed ubiquitously. GRK1 was originally named rhodopsin kinase, GRK4 is located in testes, kidney and the cerebellum (Sallese et al., 1997).

GRKs share certain structural features; a catalytic domain (~270 aa) located at the core of GRK proteins (Pronin et al., 1997). This is also present in other serine/ threonine kinases. The catalytic domain of GRKs is located between an N-terminal domain (~185 aa), required for membrane anchoring and recognizing receptors (Garcia-Higuera et al., 1994), and a variable length C-terminal domain (~105-230 aa). Multiple domains have been identified within the N-terminal domain of GRKs including

the RH domain, regulator of G protein signaling homology domain; potentially allowing regulation of GPCRs independently of phosphorylation (Ribeiro et al., 2009). The C-terminus assists in sub-cellular localisation (Penela et al., 2010, Ribas et al., 2007). GRK-2's C-terminal domain contains a plekstrin homology (PH) domain, allowing binding to PIP2; a membrane phospholipid. This interaction poses as a method by which GRK-2, a predominately cytosolic protein, may associate with membranes.

GRKs phosphorylate GPCRs, stimulating recruitment of arrestins which bind to newly phosphorylated receptors, blocking G-protein activation (Penela et al., 2010, Ribas et al., 2007). Arrestin bound receptors are subsequently targeted for clathrin-mediated endocytosis, serving as a resensitization process, translocating receptors back onto PMs. GRKs regulate various cellular processes in a phosphorylation dependent manner, acting upon non-receptor targets including tubulin and β-subunit of the Na^+ channel present in epithelial cells (Penela et al., 2003). Mouse models with defective GRKs have identified unique functional roles for GRK isoforms; knockout GRK2 mice are embryonic lethal, caused by cardiac failure (Kohout and Lefkowitz, 2003, Fukuto et al., 2004). Chemosensation in *C. elegans* utilises GRKs; loss of which results in animals which are not hypersensitive to odorants, identified using behavioural and Ca^{2+} imaging methods (Fukuto et al., 2004, Bargmann, 2006).

Yeast-two hybrid screens have produced a GRK interactome (Ribas et al., 2007). Our focus was upon CaM and Ca^{2+} binding proteins interacting with GRKs (table 1.5) (Iacovelli et al., 1999). CaM operates to inhibit GRK2-6 activity through increased autophosphorylation (Ribas et al., 2007, Pronin et al., 1997). Ca^{2+}-binding proteins modulate GRK activity; Recoverin inactivates GRK1 depending on Ca^{2+} levels (Ribas et al., 2007, Iacovelli et al., 1999, Pronin et al., 1997). GRK2 has been shown to interact with NCS-1, modulating the desensitization of dopamine D2 receptors (Kabbani et al., 2002, Gurevich et al., 2016).

	Recoverin	VILIP	NCS-1	CaM	CaBPs	References
GRK1	++	++	++	-	N/D	(Klenchin et al., 1995, De Castro et al., 1995)
GRK2	-	-	-	+	-	(Chuang et al., 1996, Haga et al., 1997, Pronin et al., 1998)
GRK3	N/D	-	N/D	+	N/D	(Chuang et al., 1996, Boekhoff et al., 1997)
GRK4	N/D	N/D	N/D	+++	N/D	(Sallese et al., 1997)
GRK5	-	-	-	++++	++	(Klenchin et al., 1995, Rhoads and Friedberg, 1997, Pronin et al., 1998)
GRK6	N/D	N/D	N/D	+++	N/D	(Pronin et al., 1997)

Table 1.5: Inhibition of GRKs by CaBP and NCS family members: At the time of publishing, GRK7 remained undiscovered. Some cases, Ca^{2+} sensor proteins were able to inhibit GRKs with different potencies (+) or failed to inhibit GRK activity (-). A sub-set of the interactions, at this time had not been determined (N/D). Table adapted from (Iacovelli et al., 1999).

1.5 C. elegans as a model organism

The nematode *Caenorhabditis elegans* (*C. elegans*), is part of the phylum Nematoda. *C. elegans* in nature is an avascular, non-pathogenic soil dwelling organism (humid and oxygenated environment), fertile and viable between 12-26^{o}C using bacteria as a food source (Gomez et al., 2001). The transparency and small size of *C. elegans* allows light and fluorescence microscopy experiments to be conducted. *C. elegans* are a cheap model organism which were first used in the pioneering work of Sydney Brenner to study genetics (Brenner, 1974). Since the work by Brenner, the field of *C. elegans* research has expanded with later research by the Fire lab first using *C. elegans* to study RNA interference (RNAi) (Fire et al., 1998, Timmons et al., 2003) in their Nobel prize work. Research using *C. elegans* has increased since 1974 (Brenner, 1974) with its genome sequenced (97 megabases (Mb)) in 1998 (C.S.C., 1998), the first multicellular organism to be fully sequenced (with a genome ~1/30th that of the Human genome). *C. elegans* contains ~19,000 genes, with high conservation shown between *C. elegans* and *C. briggsae* however 40% of these genes show conservation between *C. elegans* and mammals assisting in our knowledge of more complex organisms (Kang and Avery, 2009, Tomioka et al., 2006, Alcedo and Kenyon, 2004). Currently *C. elegans* is one of the best understood organisms (Ankeny, 2001).

Strains are defined by their mutations or knockdowns, depending on the alleles affected (Brenner, 1974). *C. elegans* have two sexes, the predominant hermaphrodite (XX) ~99.9% and the male (XO) ~0.1% arising from spontaneous non-dysjunction of the germline. Males are required for genetic crossing (only produce sperm), whilst hermaphrodites are able to self-fertilize (contain both sperm and oocytes) producing genetically identical offspring. Genetic crosses allow protein interactions and signaling pathways to be elucidated (Kashyap et al., 2014).

For the studies outlined in this thesis, *C. elegans* provided a good background for investigations of behaviour and neurotransmission. *C. elegans* provided a good platform for studying protein-protein interactions using an identifiable output. As previous research in the laboratory had identified *C. elegans* as an optimal organism for similar temperature related research, this was taken forward in the current project. As the assay developed in this project required temperature to be raised to a set temperature, this is ideally completed on a small scale to reduce temperature fluctuations during the assay. Development and neuronal processes have been heavily studied within *C. elegans* using behaviours as identifiable outputs. Neuromuscular system activity may be monitored in the intact animal from changes in its response to certain stimuli. These activities may be affected by mutations; phenocopied behaviours between different mutant strains, as tested in this project, suggest genetic interactions.

This was ideal for the current project as a high quantity of animals could be gathered and tested using a high throughput assay and differences clearly noted in behaviours. *C. elegans* is ideal for laboratory settings and it was assumed that processes in *C. elegans* would be resounded amongst other animal species. For the purposes of this project, a plethora of mutant strains had already been generated and were easily obtained from the CGC. With N2 acting as a standard strain that every researcher in the field uses this allows comparison between studies.

Offspring from hermaphrodites produce predominately hermaphrodites, with a small incidence of male production whilst when hermaphrodites are crossed with males, approximately 50% of each form are produced. The overall anatomy of adult *C.*

elegans is essentially the same with the 959 cell lineage being identified (Chalfie et al., 1983, Sulston and Horvitz, 1977, Sulston, 1983, Sulston et al., 1983). The adult male nematode is shorter and thinner than that of the hermaphrodite, with a posterior copulatory organ, whilst this is absent in hermaphrodites, they instead have a vulva around halfway down their body.

C. elegans lifecycle differs with cultivation temperature (cT). Nematodes grown at 15°C live longer than those cultivated at 25°C (Figure 1.9) whist *C. elegans* cultivated at 25°C live for approximately 30 days (Trindade et al., 2013, Zhang et al., 2015, Smeal and Guarente, 1997). A short lifespan is advantageous for high throughput screening and developmental progression investigations (Sulston, 1983, Sulston et al., 1983). Between life cycle stages, *C. elegans* undergo a molt stage (Cassada and Russell, 1975). Adult *C. elegans* are ~1mm long with a diameter of ~80 µm, in the presence of sufficient food. When starved or overcrowded, *C. elegans* enter a dauer stage, a more resilient form allowing survival in less than optimal conditions (Hilliard et al., 2002, Schackwitz et al., 1996, Cassada and Russell, 1975).

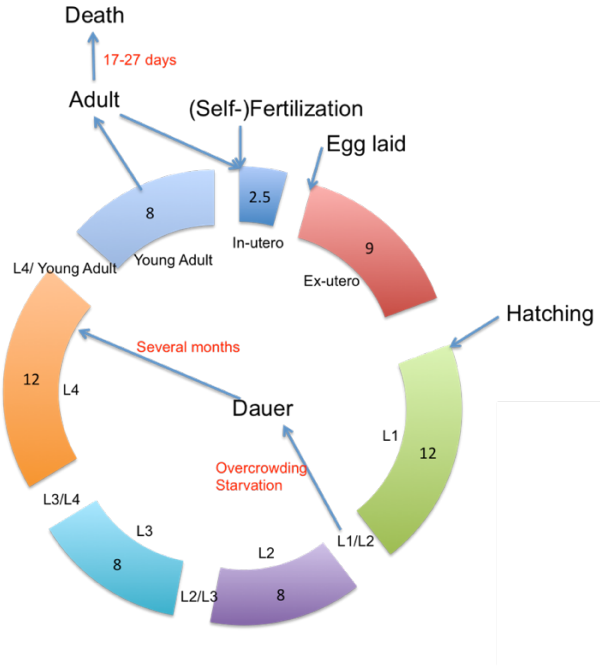

Figure 1.9 life cycle of *C. elegans* at 22°C: The current model of *C. elegans* life cycle including developmental stages. Times on the chart signify hours taken at each stage of the life cycle. Each stage of the life cycle is separated by a molt phase allowing progression to the next stage as the nematode increases in size and maturity. Dauer pathway also indicated as a viable altered lifecycle for *C. elegans* under non-optimal growth conditions. Lifespan adapted from Figure found on www.wormatlas.org.

1.6 C. elegans nervous system

The hermaphrodite *C. elegans* nervous system contains 302 neurons which co-ordinates behaviours in response to environmental stimuli (Alcedo and Kenyon, 2004, Bargmann, 2006, Filingeri, 2015, Kimura et al., 2004, Xiao et al., 2015). The simple yet well mapped nervous system of *C. elegans* makes it ideal in assisting our understanding of more complex behaviours in organisms which contain billions of neurons such as *H. sapiens* (Emmons, 2015, White et al., 1986).

Hermaphrodites contain 302 neurons with 56 glial and supporting cells with males having ~385 neurons with 92 glial and support cells (Sammut et al., 2015, Chalfie et al., 1983, Sulston and Horvitz, 1977, Sulston, 1983, Sulston et al., 1983) allowing different sexual behaviour patterns (Sulston et al., 1980, Kimble and Hirsh, 1979).

Neurons are highly concentrated in the circumpharyngeal nerve ring towards the anterior end, extending to the dorsal and ventral nerve cords (down the dorsal and ventral arms of the nematode), the tail and sensory neurons in the head (Figure 1.10) (White et al., 1986). Serial electron microscopy in 1986 allowed a detailed map of the nervous system connectivity (White et al., 1986, Emmons, 2015).

Approximately 5000 chemical synapses and 600 gap junctions are present in the *C. elegans* nervous system (White et al., 1986). Environmental stimuli such as mechanosensation, chemosensation, food availability, thermosensation, locomotion and generic *C. elegans* reproductive behaviours are detected and behaviour modified to reduce exposure to unfavourable environments (Albertson and Thomson, 1976, Bargmann, 2006, Chalfie et al., 1983, Franks et al., 2006, Gjorgjieva et al., 2014).

The *C. elegans* nervous system is sub-divided into the pharyngeal pumping mechanism for feeding (20 neurons) and the central nervous system (CNS) (282 neurons). These include sensory neurons, interneurons and motor neurons.

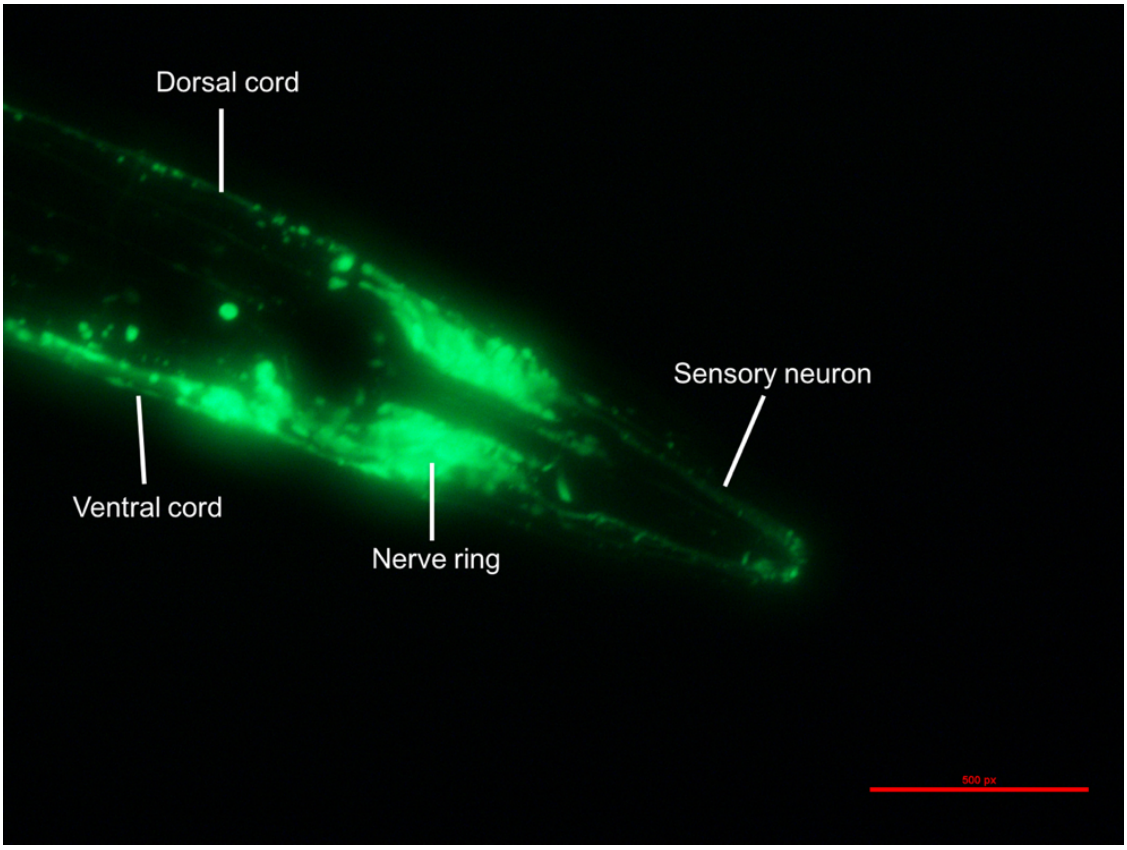

Figure 1.10 Overview of anterior region of adult hermaphrodite *C. elegans* nervous system: The nervous system of *C. elegans* transmits sensed environmental changes from sensory neurons through interneurons at chemical synapses and gap junctions to motor neurons to evoke a response, scale bar represents 10 μm. Here is an example of GFP expression in *C. elegans* neurons under the *rab-3* promoter, expressing GFP in all neurons.

1.6.1 Sensory Neurons

Around 40 classes of sensory neurons are present in *C. elegans*, predominantly in the head of *C. elegans* projecting to the anterior tip, acting during chemosensation, mechanosensation and thermosensation resulting in a range of behaviours (Kuhara et al., 2011, Clark et al., 2006, Kimura et al., 2004, Bargmann et al., 1993, Bargmann, 2006, Mori, 1999, Tsalik and Hobert, 2003).

Sensory neurons in the *C. elegans* head include the amphids, inner and outer labials, anterior deirids and cephalics. Those in the nematode tail are the phasmids and the posterior deirids. A sub-set of sensory neurons are located in the body of nematodes (Altun et al., 2002-2016). Dendritic extensions from the cell body towards the nerve ring allow communication with other neurons (Altun et al., 2002-2016). Synaptic ends

permit communication between neurons through neurotransmitter release forming behavioural outputs (Molnar and Brown, 2010, Barclay et al., 2012, Zhou et al., 2015, Komatsu et al., 1996, Sasakura and Mori, 2013). One example of neurotransmitter functions is to stimulate ionotropic receptors at post-synaptic membranes to allow Ca^{2+} influx; this is a critical feature in the nervous system and heart (Cai et al., 2015, Bennett, 1999, Roderick et al., 2007) however neurotransmitters can also act on pre-synaptic membranes to stimulate a vast range of receptors.

1.6.2 Interneurons

Interneurons receive, process and transmit signals from sensory neurons relaying this to motor neurons to elicit a behavioural response (Altun et al., 2002-2016). The function of interneurons is similar in humans and *C. elegans,* either in the CNS or the nerve ring respectively (Hobert et al., 1997, Tsalik and Hobert, 2003, Altun et al., 2002-2016, Zhou et al., 2015).

1.6.3 Motor Neurons

Motor neurons elicit a behavioural output utilising information from sensory and interneurons by controlling locomotion or the alimentary canal through muscle contraction propelling *C. elegans* forward or backwards (Chalfie et al., 1983, Emmons, 2015, White et al., 1986, Du and Chalfie, 2001, Forrester et al., 1998). Around 30 classes of motor neurons are present in *C. elegans,* innervating different aspects of the nematode for specific behaviours; egg laying, pharyngeal pumping and locomotion (Chalfie et al., 1983, Du and Chalfie, 2001). Motor neurons can receive stimulation from various interneurons, varying the downstream outputs, producing a more complex overlapping signalling pathway. Signaling from upstream neurons to motor neurons shows a complex network with various upstream neurons able to stimulate downstream neurons through various means including gap junctions and chemical synapses. Different types of motorneurons can act in an activation or inhibitory sense, this in *C. elegans* produces the classis thrashing movement owing to opposing contraction and relaxation of the cell wall muscles on the dorsal and ventral sides of the *C. elegans.*

1.6.4 Synapses

Junctions between neurons are known as synapses, described by Sir Charles Sherrington in his Nobel prize work (Molnar and Brown, 2010). Synapses follow a self-regulating system, pre-synaptic neurons switch off signals upon transmission to downstream post-synaptic neurons. Neuronal messages are transmitted down the neuron, the arrival of which opens VGCCs allowing an influx of Ca^{2+} stimulating secretion of neurotransmitter molecules (Figure 1.11 steps 1-3).

Vesicles with packaged neurotransmitters fuse with the PM using the Soluble N-ethylmaleimide sensitive fusion Attachment Protein Receptor (SNARE) complex expelling contained neurotransmitter into the synaptic cleft which diffuses over the synaptic cleft and binds to neurotransmitter specific gated post-synaptic channels (Marx, 2014, Hall, 1972, Altun et al., 2009) (Figure 1.11 steps 4-6). When open, Ca^{2+} enters the post-synaptic neuron. This causes depolarisation of the post-synaptic neuron and transmission of the signal through an excitatory post-synaptic potential. The neurotransmitter molecules are broken down and repackaged to regulate the system, preventing overstimulation (Figure 1.11 steps 7-8). In the case of Acetylcholine, ACh is broken down into Acetyl and Choline to prevent overstimulation. ACh is reformed through various molecular pathways including the Krebs cycle.

Neurons contain N and PQ-type VGCCs to facilitate neurotransmitter release via a Ca^{2+} plume and the SNARE complex; Ca^{2+} binds to synaptotagmin stimulating the final stage of exocytosis and neurotransmitter vesicles (Berridge et al., 2000). Neurotransmitters in *C. elegans* include Acetylcholine (ACh), Glutamate (Glu), Serotonin (Ser), Dopamine (Dop), γ-aminobutyric acid (GABA), potentially Glycine (Gly), Octopamine and neuropeptides used by specific neurons for behavioural responses.

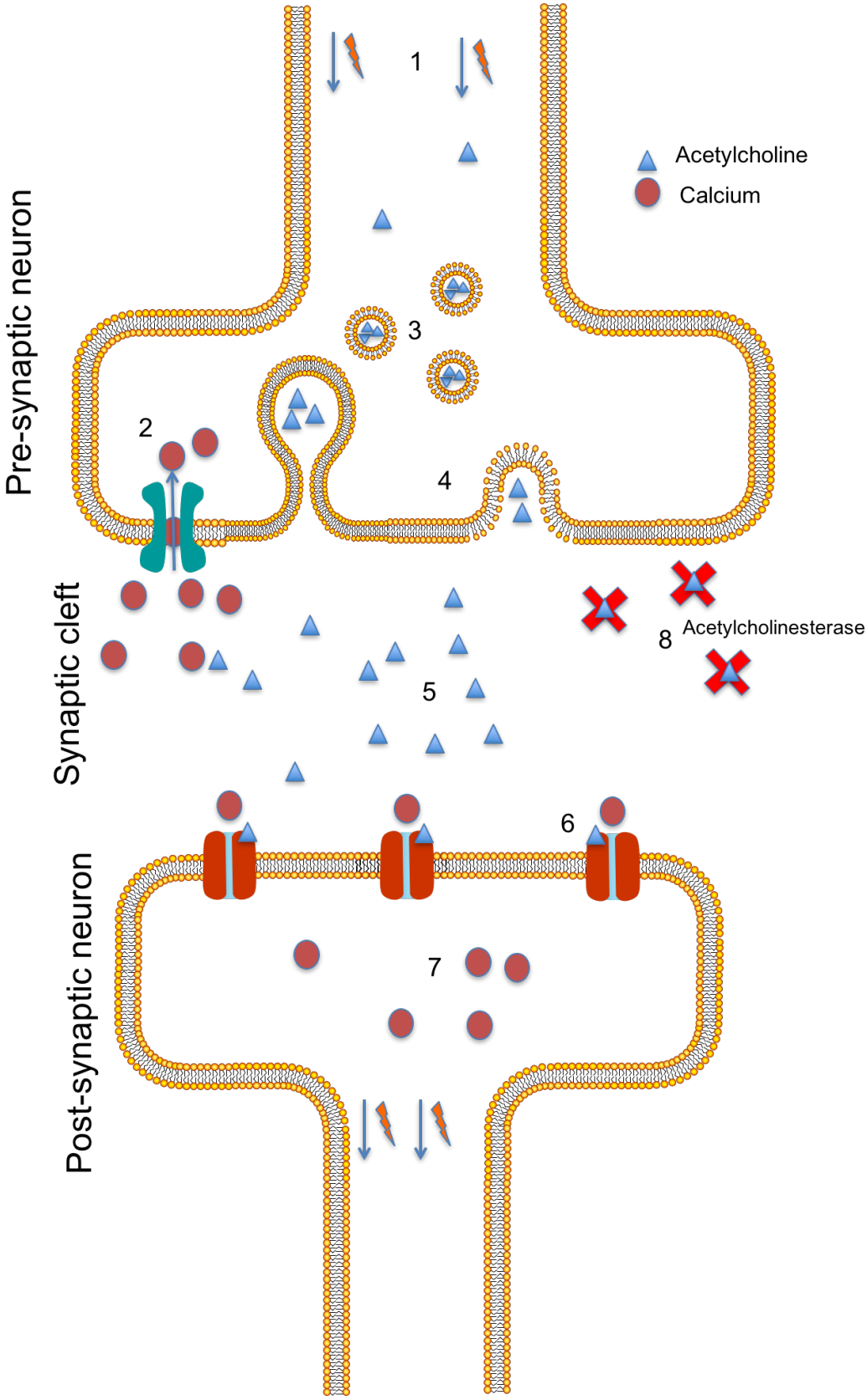

Figure 1.11 Simplified diagram of a synaptic junction. Illustration of a synaptic junction using acetylcholine as a neurotransmitter signalling molecule (Figure adapted from (Marx, 2014)). Neurotransmitter release and progression of the signal is highly organised and undergoes a self-regulating mechanism as outlined on the previous page.

1.6.5 C. elegans as a model organism to study learning and memory

C. elegans is a particularly useful model for studying learning and memory due to its simple neuronal system (302 neurons), researchers are able to map neuronal signaling pathways in this organism more conveniently than in more complex animals. The association of food at a given temperature, associative learning (thermosensation and thermotaxis) has been identified in *C. elegans* with a defined set of behavioural responses (Hedgecock and Russell, 1975, Murakami et al., 2005, Murakami, 2007, Jorgensen and Rankin, 1997, Ryu and Samuel, 2002).

Russell and Hedgecock's work identified the *C. elegans* thermosensory neural network assisting survival in a changing environment (Hedgecock and Russell, 1975) by moving towards their cT. Upon reaching the cT, *C. elegans* remain at this temperature, moving isothermally in a phenomenon referred to as isothermal tracking (IT). This provides a simple learning and memory system. This method of associative behaviour is temporary and can be lost with prolonged starvation, representing a complex interplay between numerous environmental factors; humidity, food availability, oxygen levels and competition define thermotaxis behaviours (Aoki and Mori, 2015).

Migration to a specific temperature (explorative behaviour) and IT (exploitative behaviour) require separate neural processes. To further understand selective behaviours, more research is needed. Analysis of *C. elegans* has enhanced our knowledge of thermosensation and neural processing to regulate behavioural outputs (Kimata et al., 2012).

1.6.6 Thermosensation needed for survival

To survive, animals need to be able to quickly adapt to a changing environment. Currently, neural circuits underlying exploratory behaviours remain poorly understood (Clark et al., 2006). Functionally these behaviours are crucial in understanding how animals learn and adapt. *C. elegans* behaviours are affected by salt concentration (Ardiel and Rankin, 2010, Rose and Rankin, 2001, Tomioka et al., 2006, Hukema et

al., 2006), temperature (Gomez et al., 2001, Mori and Ohshima, 1995, Kimura et al., 2004, Kuhara et al., 2008, Nishida et al., 2011, Ohnishi et al., 2011, Sasakura and Mori, 2013), humidity (Filingeri, 2015, Russell et al., 2014, Zhao et al., 2003), oxygen concentration (Cheung et al., 2005, Possik and Pause, 2015), receptor expression (Malinow and Malenka, 2002, Luscher and Frerking, 2001, Nuttley et al., 2002) along with food availability (Ardiel and Rankin, 2010, Nuttley et al., 2002).

Our focus was on the environmental stressor temperature and its influence on biological processes and thermosensation (Aoki and Mori, 2015, Kimata et al., 2012). *C. elegans* generally reside at temperatures which increase their performance and Darwinian fitness, similar effects noted regarding rearing temperatures in an experience dependent manner. *C. elegans* hold an astute ability to sense temperature changes and move isothermally over a specific temperature (± 0.1 ^{o}C) using specialized mechanisms (Anderson et al., 2011, Gomez et al., 2001, Jurado et al., 2010, Kimata et al., 2012, Kimura et al., 2004, Mori and Ohshima, 1995, Mori, 1999, Nishida et al., 2011, Sasakura and Mori, 2013, Satterlee et al., 2001, Schafer, 2012, Aoki and Mori, 2015, Filingeri, 2015)

1.6.6.1 Thermosensors in mammals

In mammals, as in other organisms; temperature has a profound effect on behaviour (Vriens et al., 2014, Xiao et al., 2015, Brenner et al., 2014). Temperature is one of the two primary environmental factors, alongside food, that affects lifespan in animal models (Xiao et al., 2015, Clarke and Portner, 2010, Cabanac, 1975). Thermoavoidance of extreme harmful temperatures have been well documented in mammals. The most well documented mammalian thermosensors are the TRP channels (Vriens et al., 2014, Xiao et al., 2015, Satterlee et al., 2001), with roles also in mechanosensation, osmosensation and photosensation in many organisms (Talavera et al., 2008, Voets, 2014, Vriens et al., 2014, Palkar et al., 2015).

Different TRP members have been linked with temperature, coining the term thermo-TRPs, regulating a range of temperature related behaviours in organisms. TRPM8 and TRPA1 are cold sensitive, TRPV1-4 and TRPM3 are heat sensitive, able to sense a range of ambient temperatures (Figure 1.12) (Venkatachalam and Montell, 2007,

Ramsey et al., 2006). Some TRP responses are species specific as TRPA1 acts both as a cold sensor (mice and *C. elegans*) and a heat sensor (snakes) (Chatzigeorgiou et al., 2010). Specific isoforms of the mammalian thermosensors and their activities are not fully elucidated although they each operate under specific activation temperatures (Xiao et al., 2015). Mammalian knockouts of specific nocireceptors in early development produces thermo-insensitive mice over different temperature ranges (Pogorzala et al., 2013). Mammalian thermosensation requires a complex feedback loop to sense and respond to a change in temperature, requiring interactions from specific regions of the brain for various desired outputs.

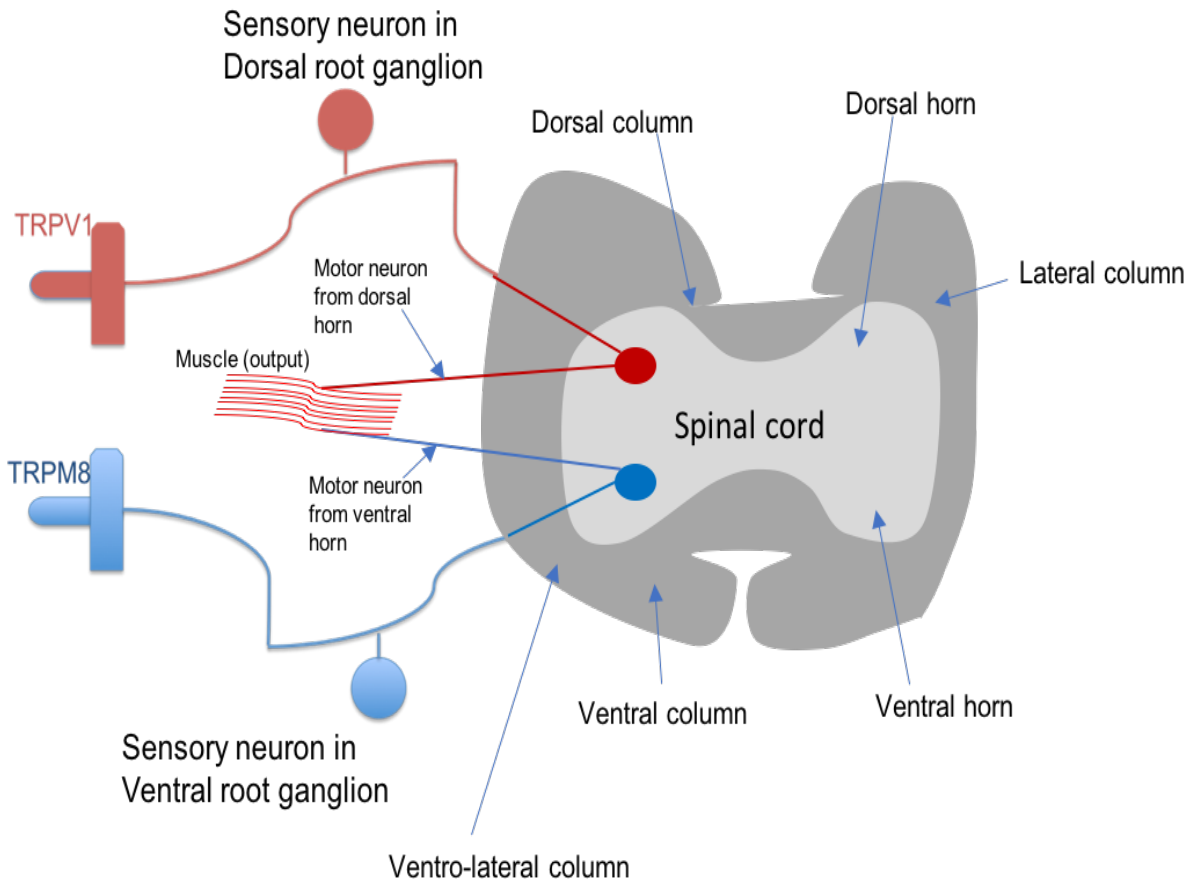

Figure 1.12: Simplified model of mammalian thermosensation: Current model for Mammalian thermosensation using Figures adapted from (Xiao et al., 2015). Transient Receptor Potential (TRP) channels are known to be involved in thermosensation in mammals with connections to spinal cord and specific brain regions. The diagram shows the expected thermosensory pathway for detection of heat and cold variations of temperature. This diagram is over-simplified due to the complexity of mammalian sensory circuits.

1.6.6.2 Thermosensors in C. elegans

The thermosensory neurons in *C. elegans* have been studied in great detail allowing a partial elucidation of the temperature signaling pathway within these specific neurons. The primary thermosensory neurons in *C. elegans* for the thermosensory neural network are the AWC and AFD neurons which are described further in section 1.6.7.

Temperature is known to have significant effects on the physiology, ecology and fitness of ectotherms, which includes *C. elegans* (Anderson et al., 2011). Many ectotherms are known to rely on behavioural adjustments to regulate body temperature to avoid lethal temperatures. In *C. elegans*, dissection of behaviours can be conducted on a single neuron level (Kimata et al., 2012).

Both the AWC and AFD neurons act as critical thermosensors in *C. elegans*, (Figure 1.13) however the precise sensor in these remains unknown (Perkins et al., 1986). *C. elegans* uses cyclic guanosine monophosphate (cGMP) signaling within thermosensory neurons. Laser ablation studies have further aided research into understanding neuronal networks (Mori and Ohshima, 1995).

C. elegans respond rapidly to temperature changes to enhance survival. Ca^{2+} imaging experiments have shown the importance of the past cT regarding Ca^{2+} influx into AWC and AFD neurons, suggesting similar plasticity responses with each responding to even minor elevated temperature changes (from 20-20.4 ^{o}C) yet minimal activity below their cT (Kimata et al., 2012, Kuhara et al., 2008), resulting in incorrect thermotactic behaviours, moving in a cryophilic manner as opposed to thermophilic. Thermosensory neuronal activity depends on cT; the AFD neuron responds at a temperature ~2 ^{o}C under the cT but is unresponsive at colder temperatures (Kimata et al., 2012).

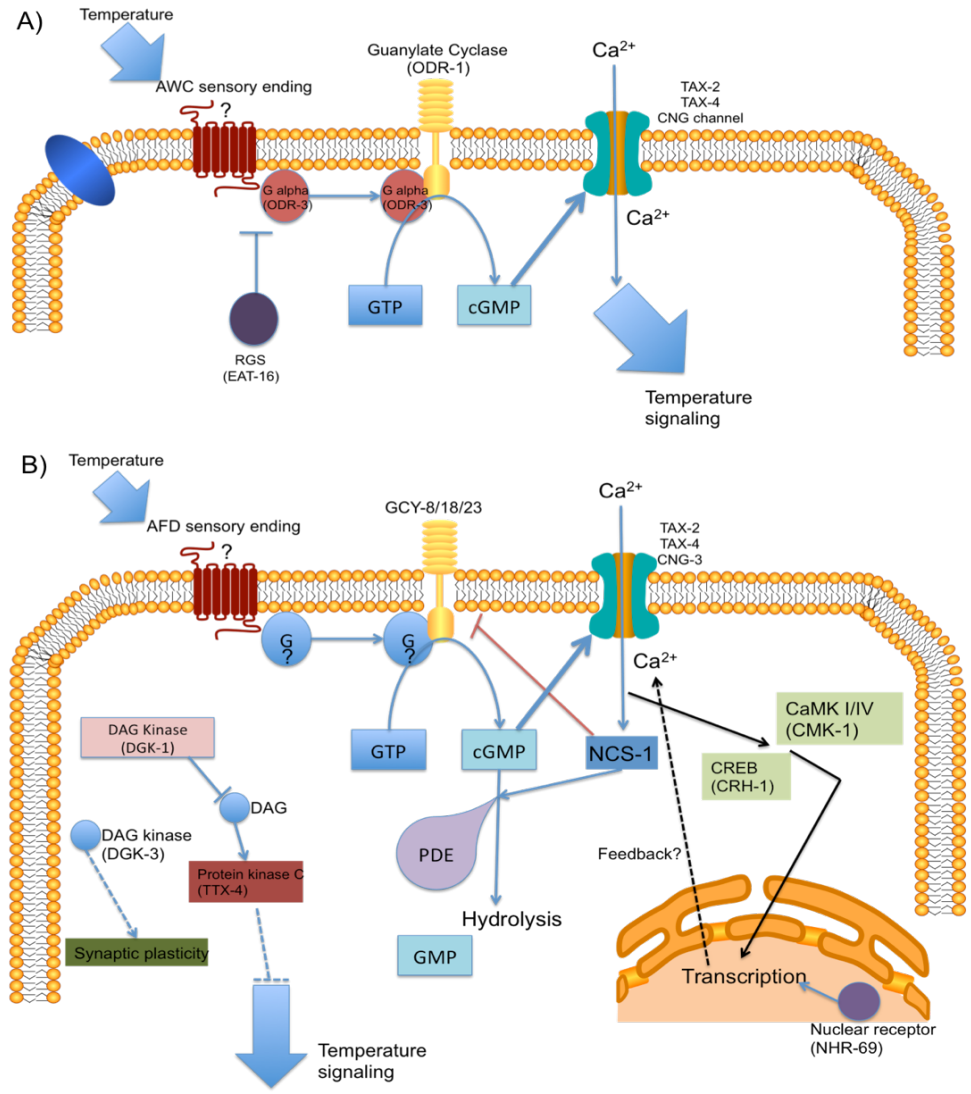

Figure 1.13: Current model of thermosensation in *C. elegans*: The current model for thermosensation in *C. elegans* adapted from (Wang et al., 2013, Aoki and Mori, 2015, Kimata et al., 2012) for the sensory neuron (A) AWC and another sensory neuron involved in thermosensation (B) AFD. Upon detection of a temperature differing from the cT the AWC and AFD neurons are stimulated. (A) Method of temperature sensation from the AWC sensory neuron using cGMP. Currently the temperature sensor is unknown as are some aspects of this mechanistic pathway. (B) Detection of temperature above the cT, or 2 ^{o}C below the cT causes the AFD neuron to be stimulated allowing *C. elegans* to stimulate transcription of specific genes. This pathway is yet to be fully elucidated however NCS-1 is shown as interacting with Phosphodiesterases potentially as a feedback mechanism.

Cameleon Ca^{2+} imaging in the AWC and AFD neurons showed increased fluorescence in response to warming, indicating a role in the thermotaxis neural circuit (Kimata et al., 2012). AWC can alter its response depending on temperature stimuli pattern (Kimata et al., 2012, Kuhara et al., 2008) signifying a complex interaction between specific neurons. Temperature sensation in the AFD sensory end still

occurred following removal from its cell body, which was unable to respond to temperature changes (Clark et al., 2006). Incorrect structure of the AFD sensory end, as in *ttx-1* mutants, result in *C. elegans* showing cryophilic behaviours (movement to a lower temperature) as opposed to thermophilic (movement to a higher temperature) when on a temperature gradient (Satterlee et al., 2001).

TRPA1 is present in *C. elegans* PVD multi-dendritic nocireceptor neurons, able to extend lifespan by a cold induced Ca^{2+} influx (Chatzigeorgiou et al., 2010, Xiao et al., 2013). Other studies to date have not clearly identified TRP channels in thermosensation of ambient temperature in *C. elegans*. AFD ion channel mutations; TAX-4 (Komatsu et al., 1996), TAX-2 (Coburn and Bargmann, 1996) or CNG-3 (Smith et al., 2013), lead to athermotactic phenotypes, random movement on temperature gradients. Dynamic AFD responses are gated by cGMP resulting in thermophilic or cryophilic activities, when unable to hydrolyse cGMP, through a loss of phosphodiesterase 2 (PDE-2) abnormal AFD responses to temperature stimuli occur (Wasserman et al., 2011, Wang et al., 2013, Kimata et al., 2012).

1.6.7 Thermosensory neural network in C. elegans.

The *C. elegans* nervous system allows for a significant range of behaviours (Aoki and Mori, 2015). Since the work in 1975 by Russell and Hedgecock and the identification of IT to a pre-determined cT (Hedgecock and Russell, 1975); the thermosensory neural network has been intensively studied showing how thermotactic behaviours allow *C. elegans* to navigate spatial thermal gradients through an experience dependent manner (Clark et al., 2006). Extended starvation perturbs the thermosensory neural network, suggesting rapid learning mechanisms are in place to locate favourable environments. Animals sought a different temperature as they had learnt, and remembered, that their cT had limited food availability, presenting a behavioural plasticity relationship between food and temperature based on experience. Absence of food, an ‘unfavourable’ environment increases *C. elegans* dispersion on a thermal gradient (Mori and Ohshima, 1995, Ye et al., 2008, Ryu and Samuel, 2002).

A study using an *ncs-1* null *C. elegans* showed a defect in thermosensation (Gomez et al., 2001). Thermosensation in *C. elegans* includes thermotaxis and thermoavoidance which each use different neurons and mutations in different genes (Schafer, 2012, Wittenburg and Baumeister, 1999). IT is an example of thermotaxis, *C. elegans* showing IT are generally within less than 3^{o}C of their cT (Hedgecock and Russell, 1975, Jurado et al., 2010, Mori and Ohshima, 1995). Advancements in research equipment such as automated tracking microscopes, has allowed a greater insight into the different aspects of *C. elegans* behaviours and movement providing databases of identified behaviours (Yemini E., 2013, Tsalik and Hobert, 2003).

C. elegans, when at temperatures which differ from their cT, present different behavioural responses: thermophilic (migrate to a higher temperature), cryophilic (migrate to a colder temperature) and atactic/ athermotaxis (unaffected by temperature) (Ghosh et al., 2012, Ryu and Samuel, 2002, Gomez et al., 2001).

NCS-1 is present within the AFD, AWC and AIY neurons of the thermosensory neural network (Figure 1.14, adapted from (Nishida et al., 2011, Mori, 1999, Gomez et al., 2001, Kuhara et al., 2008)), more information about NCS-1 in *C. elegans* will be presented in section 1.7.3. The AIY and AIZ neurons are critical for signal processing and integration, although they drive opposing thermotaxis responses; whilst the AIY is required for positive thermotaxis (thermophilic behaviours), the AIZ is needed for negative thermotaxis (cryophilic behaviours) (Kimata et al., 2012, Gomez et al., 2001, Garrity et al., 2010, Martin et al., 2013, Hobert et al., 1997). Activity of the AFD neuron is coupled with AIY stimulation via synaptic interactions (Clark et al., 2006).

The thermosensory neural network contains two thermosensory neurons (AWC (Biron et al., 2008) and AFD outlined in section 1.6.6.2 (Chung et al., 2013, Clark et al., 2006, Kimura et al., 2004, Nishida et al., 2011)), analysed by neuronal Ca^{2+} imaging and *C. elegans* assays. The AFD sensory neuron has been proposed to store a memory of the thermotactic set-point (T_S). Knowledge of these neurons, and their links to learning and memory is ongoing (Kimata et al., 2012, Kimura et al., 2004, Kuhara et al., 2008, Mori et al., 2007). Laser ablation studies have excluded some neurons previously believed to be involved in thermosensory memory and provided supporting knowledge for other members of the thermosensory network including the AIY and AIZ neurons

(Ma and Shen, 2012, Chung et al., 2013, Gomez et al., 2001, Martin et al., 2013). Ablation of the AIY neuron, or failure to differentiate the AIY neuron (*ttx-3* mutant) cause cryophilic phenotype (Mori and Ohshima, 1995, Hobert et al., 1997).

Increases in [Ca^{2+}] have been shown following an increase in temperature in AFD neurons, with an identifiable decrease in intracellular Ca^{2+} when temperature is lowered (Clark et al., 2006, Mori and Ohshima, 1995, Kimura et al., 2004). A lowered [Ca^{2+}] then leads to reduced glutamate activity; increasing ACh activity causing a thermophilic response. Evidence points towards the AFD neuron being able to excite the AIY neuron, causing depolarization; yet inhibition of the AFD neuron increases Ca^{2+} levels in AIY indicating a potential inhibitory pathway (Narayan et al., 2011, Kuhara et al., 2011). Previous studies also suggested that the AFD can negatively regulate the AIY neuron via release of glutamate allowing cold sensation (Ohnishi et al., 2011).

Research into the AFD neuron has provided a significant amount of insights into the initial stages of thermosensation. Expression of PKC-1 in the AFD neuron is sufficient to rescue thermophilic behaviours. An interplay between *C. elegans* neurons and their intestines in cold sensation has been proposed, acting as a form of cold sensation and avoidance (McGhee, 2007). No clear sensor is known for the AWC or AFD neurons at this time.

Ca^{2+} in various molecular pathways, can modify behaviours under stressful conditions. Of the EF-hand containing Ca^{2+}-binding proteins, the NCS family have been implicated in the thermosensory neural network, specifically NCS-1. The target(s) of NCS-1 within this network however are not well characterised.

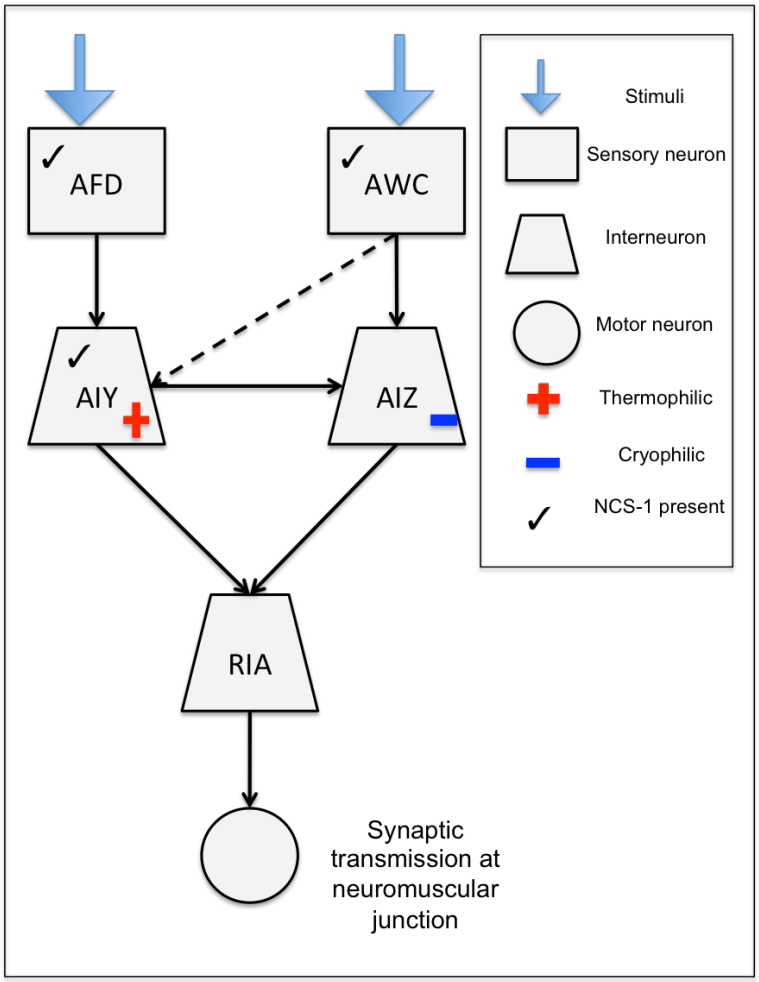

Figure 1.14: Current model of isothermal tracking and memory within the thermosensory neural network for *C. elegans*: The current wiring model for thermosensation in *C. elegans* using neurons showing behavioural plasticity. The sensory neurons AWC and AFD detect and store temperature information which then stimulates the AIY (thermophilic behaviour) or the AIZ (cryophilic behaviour) leading onto the RIA interneuron to evoke a response in locomotion from motor neurons. Figure adapted from (Garrity et al., 2010, Gomez et al., 2001, Martin et al., 2013).

1.7 AIY neuron and its synaptic partners

The *C. elegans* neuronal connectome has identified synaptic connections between specific neurons. As the AIY neuron is important for the temperature dependent locomotion phenotype utilized in this research (Martin et al., 2013), it is interesting to identify other behaviours which the AIY neuron contributes to. These behaviours include negative thermotaxis in conjunction with its synaptic partners which include sensory, inter and motor neurons for behaviour plasticity and relation to specific thermal cues (Figure 1.15, 1.16 and table 1.6).

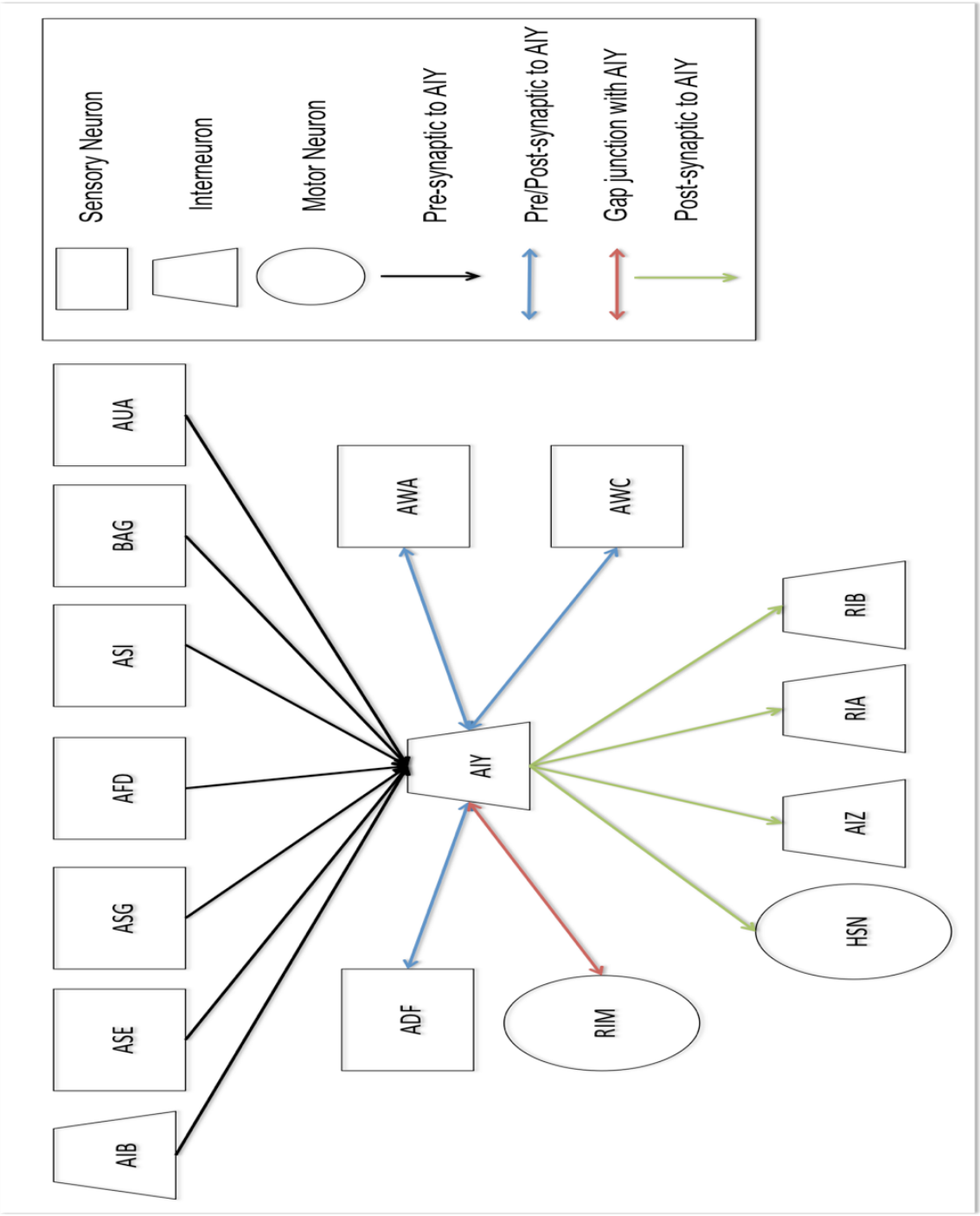

Figure 1.15 Pre and post synaptic connections with AIY interneuron: Current identified pre and post synaptic connections with the AIY interneuron of *C. elegans*. Current connectome of the AIY neuron with identified chemical synapses and gap junctions. Signal flow has been presented as pre and post-synaptic connections with the AIY neuron solely with pre-synaptic neurons appearing left of the AIY neuron and post-synaptic to the right of the diagram. Those acting as pre and post synaptic with AIY are present above and below the AIY neuron as are the known gap junctions of AIY. Figure adapted from (Bhatla, 2016).

Neuron & type	Location	Pre/ post AIY	Function	References
AIY - interneuron	Ventral ganglion, amphid	N/A	IT, Thermosensory neural network, cholinergic signaling, ablation causes cryophilic movement and loss of IT, regulates forward movement	(Altun et al., 2002-2016, Ishihara et al., 2002, de Bono and Maricq, 2005, Mori and Ohshima, 1995, Gomez et al., 2001, Kuhara et al., 2008, Kuhara et al., 2011, Tsalik and Hobert, 2003, Ohnishi et al., 2011)
AFD - sensory	Lateral ganglia, amphid neuron	Pre	Thermosensor, CO_2 detector, cGMP signaling, IT, responds to noxious temperature for thermal avoidance, increasing turn rate	(Wang et al., 2013, Wasserman et al., 2011, Mori et al., 2007, Kuhara et al., 2008, Ma and Shen, 2012, Hedgecock and Russell, 1975, Tsalik and Hobert, 2003, Liu et al., 2012, Biron et al., 2008)
AWC - sensory	Lateral ganglia	Pre/post	Thermosensation, IT, *C. elegans* sexual attraction, Chemosensation, Chemotaxis against volatile odorants (isoamylalcohol), searching and turning behaviours, cGMP signaling	(Biron et al., 2008, Beverly et al., 2011, Kuhara et al., 2008, Altun et al., 2002-2016).
AIZ- interneuron	Ventral ganglion	Post	Ablation stimulates thermophilic behaviour, cryophilic, downreguated under starvation, dispersion from cT	(Sasakura and Mori, 2013, Kuhara and Mori, 2006, Chalasani et al., 2007, Gray et al., 2005)
RIA- interneuron	Head	Post	Thermosensation, mutation causes athermophilic or cryophilic behaviours	(Gomez et al., 2001, Mori and Ohshima, 1995)
ASE- sensory	Lateral ganglia	Pre	Chemosensation of salts, CO2 detection, can be partially covered in the absence of ASE by other neurons	(Bargmann, 2006, Komatsu et al., 1996, Bargmann and Horvitz, 1991, Altun et al., 2002-2016)
ASI- sensory	Lateral Ganglia	Pre	IT, chemosensation of lysine, locomotion by stimulating local search behaviour, negative thermotaxis (Figure 1.16)	(Biron et al., 2008, Beverly et al., 2011, Bargmann and Horvitz, 1991, Gray et al., 2005, Ma and Shen, 2012)

AWA-sensory	Lateral ganglia	Pre/post	Chemosensation to specific molecules, regulates *C. elegans* sexual attraction with AWC and ASK neurons	(Bargmann et al., 1993, White and Jorgensen, 2012).
AIA & AIB-interneurons	Ventral and Lateral ganglion respectively, amphid neurons	Pre	Responds to noxious temperatures, thermosensation, searching and turning behaviour, negative thermotaxis, AIA ablation increases reversal, AIB ablation decreases reversal	(Liu et al., 2012, Altun et al., 2002-2016, Ma and Shen, 2012)
ASG-sensory	Lateral ganglia	Pre	Control entry into dauer state (inhibits entry), lifespan regulation, chemotaxis to water soluble attractants (Na^+ and Cl^-), ASE is the primary chemotaxis neuron	(Schackwitz et al., 1996, Bargmann, 2006)
BAG-sensory	Anterior to nerve ring	Pre	CO_2 avoidance, decrease in O_2 sensation, ablation affects lifespan (increases)	(Hallem and Sternberg, 2008, Altun et al., 2002-2016, Bhatla, 2016)
AUA-sensory	Lateral ganglia	Pre	Social feeding behaviour	(Coates and de Bono, 2002, Bhatla, 2016)
ADF-sensory	Lateral ganglia	Pre/Post	Sole serotonergic sensory neuron, chemotaxis to Na^+ and Cl^-,inhibit dauer stage entry, enhance or inhibit synaptic transmission of other neurotransmitters	(Bargmann and Horvitz, 1991, Altun et al., 2002-2016, Bhatla, 2016)
RIM- motor	Head	Pre/Post, connected via gap junction	Locomotion, reversal movements, photostimulation reverses locomotion, optogenetic ablation increases reversal. RIM inhibits reversal initiation during locomotion	(Altun et al., 2002-2016, Bhatla, 2016).
HSN- motor	Around midbody close to vulva	Post	Hermaphrodite specific, stimulate egg laying	(Chalfie et al., 1983, Bhatla, 2016)
RIB-interneuron	head	Post	Gap junctions with other neurons, process and integrate external information to alter behaviour	(Altun et al., 2002-2016, Bhatla, 2016)

Table 1.6: AIY and its synaptic partners. Roles for the synaptic connections with the AIY neuron are known, leading to functions of thermoavoidance, negative thermotaxis, CO_2 avoidance, O_2 sensation, reversal phenotypes and possibly other unestablished processes. The study of neuronal networks is critical in understanding behaviours.

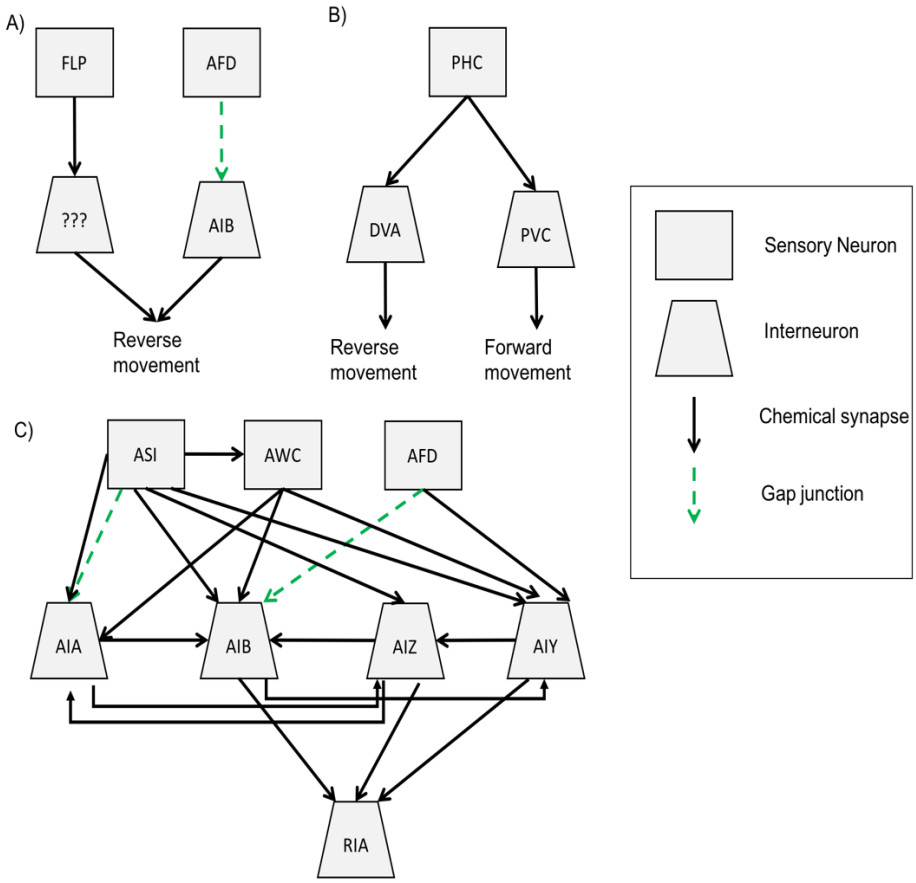

Figure 1.16: Wiring diagram of Thermoavoidance and Negative thermotaxis. Wiring diagram for the identified head and tail neurons of *C. elegans* linked with thermoavoidance, diagrams A & B adapted from (Liu et al., 2012) with diagram C showing the wiring diagram of negative thermotaxis adapted from (Ma and Shen, 2012). A) Sensation of a harmful temperature by neurons in the head of *C. elegans* causes a reversal of locomotion to evade temperature extremes. B) Sensing of detrimental temperatures in the tail of *C. elegans* can induce either forward or reverse motility to evade harmful temperatures. This is regulated by two separate pathways derived from the PHC neuron signaling to either the DVA (reverse locomotion) or the PVC (forward locomotion) interneurons for the behavioural response. C) Currently proposed negative thermotaxis circuit including proposed chemical synapse and gap junction transmission between neurons. Some of the same neurons involved in the thermosensory neural network are active in the proposed negative thermotaxis circuit with the addition of the ASI sensory neuron and the AIA and AIB interneurons.

1.7.1 Thermoavoidance

Organisms detect changes in temperature to avoid stressful environments, in *C. elegans* multiple neurons assist in sensing temperature, detecting changes of ≤0.05 ^{o}C (FLP, PHC, PVC, AFD) to cause a behavioural change (Wittenburg and Baumeister, 1999, Liu et al., 2012) (Figure 1.16). *C. elegans* avoid harmful

environments as this affects fertility and food seeking behaviours, thermoavoidance is unaffected by cT.

1.7.2 Calcium binding proteins in C. elegans.

Over 200 *C. elegans* proteins are predicted to have Ca^{2+} binding properties, a number of these have been classified as 'EF-hand only' proteins totaling approximately 65 members. This includes *C. elegans* equivalents of CaM (cmd-1), cal1-8 and NCS family proteins (7 genes in total ncs1-7). NCS 1-3 have been identified and evaluated in more detail with NCS 4-7 yet to be fully evaluated (Table 1.7 and Figure 1.17) (Rajaram et al., 2000, De Castro et al., 1995, Hobert, 2013).

1.7.3 NCS-1 in C. elegans

NCS-1 in *C. elegans* is present in 1 muscle cell type, 1 motor neuron, 10 pairs of sensory neurons and 2 interneuron pairs. The *C. elegans* NCS family of proteins contains 7 separate genes (NCS-1 to NCS-7), however of these NCS-4 to NCS-7 are homologous to KChIPs (table 1.7). As stated previously, NCS-1 in *C. elegans* shows involvement in Long term potentiation (LTP), Long term depression (LDP), learning and memory as well as a variety of other functions as shown below (table 1.8).

C. elegans protein	*Homo sapiens* homolog	% identical	Number of identified EF hands	EF hand positions
NCS-1	NCS-1	76	3	2,3,4
NCS-2	HCLP-1	51	3	2,3,4
NCS-3	NCS-1	67	4	1,2,3,4
NCS-4 isoform a	KChIP-1	35	3	2,3,4
NCS-4 isoform b	KChIP-4	34	3	1,2,3
NCS-4 isoform c	KChIP-1	32	3	2,3,4
NCS-5 isoform a	Neurocalcin-delta	22	1	4
NCS-5 isoform b	Neurocalcin-delta	22	1	4
NCS-6	KChIP-2	30	2	3,4
NCS-7	KChIP-1 & 2	39	3	2,3,4

Table 1.7: *C. elegans* NCS-1 family homology to *H. sapiens*: NCS family proteins (sequences taken from Wormbase.org) compared with Human genome sequences using protein blast (NCBI blastP). The predicted Ca^{2+} binding EF hands identified using Interpro.EMBL. Identified EF hands classified using Uniprot.org in conjunction with Smart.EMBL and Interpro.EMBL (Chen et al., 2015, Topalidou and Chalfie, 2011, Camon et al., 2003, Mulder et al., 2003, Rajaram et al., 2000, Raghuram et al., 2012).

Protein sequence similarity searching has allowed comparisons to be made between the 7 *C. elegans* NCS proteins and the human protein counterparts. Mammalian NCS proteins share homology with *C. elegans* counterparts. For *C. elegans* NCS-1 and NCS-3, these are most similar to mammalian NCS-1 whilst NCS-2 through blast searching is most like mammalian Hippocalcin like protein-1 (HCLP-1).

Potentially, NCS-1 compensates for NCS-3 as in *ncs-3* null *C. elegans*, no abnormal behaviour was identified (Rajaram et al., 2000). For the newly identified *C. elegans* NCS proteins, NCS-4 to NCS-7, these share homology with a number of different mammalian NCS proteins, specifically KChIP 1, 2 and 4 and Neurocalcin delta, albeit with a low sequence homology (<50%) in all cases. At this time, the later NCS proteins have not been fully analysed hence more work is required in order to make firm conclusions regarding their status as NCS proteins (Figure 1.17).

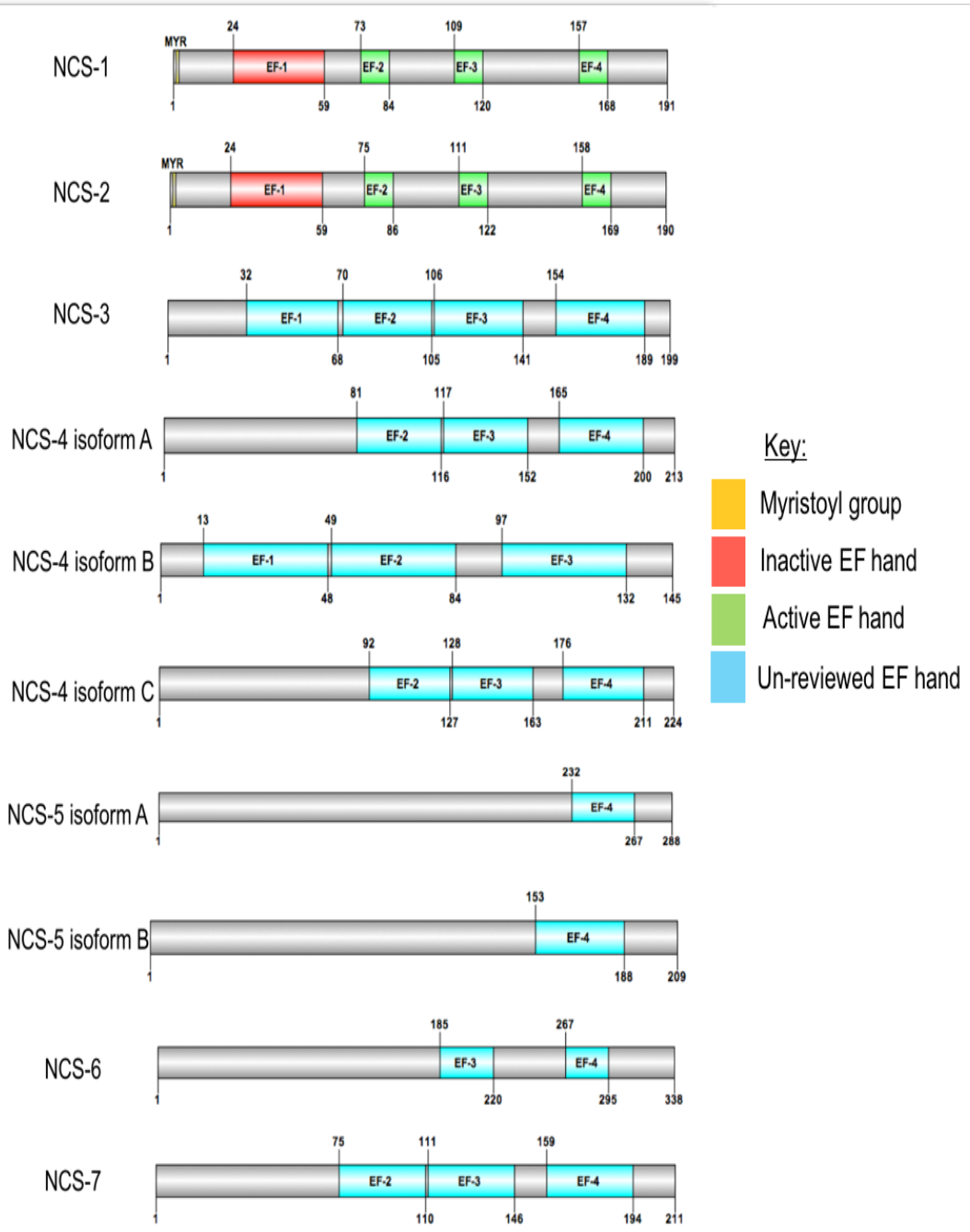

Figure 1.17 *C. elegans* NCS family members: NCS 1-3 have been previously studied however NCS 4-7 were recently identified, as such their structures and the confirmation of their active and inactive EF hands remains to be determined. Multiple splice variants have been identified for NCS-4 and NCS-5, awaiting review.

Neuron	Neuron/ Cell type	Neuron signaling molecule	Function
AWC (L,R))	Sensory neuron (Amphid)	Glutamatergic	Chemotaxis to volatile odorants (benzaldehyde, butanone, isoamylalcohol, 2,3 pentanedione and 2,4,5 trimethylthiazole) and Thermosensor roles
ASE (L,R)	Sensory neuron (Amphid)	Glutamatergic	Chemotaxis to water solble attractants (Na^+, Cl^-, cAMP, biotin and lysine)
AWB (L,R)	Sensory neuron (Amphid)	----	Avoidance from 2-nonanone, 1-octanol (Troemel et al., 1997)
BAG (L,R)	Sensory neuron	Glutamatergic	CO_2 avoidance (Bretscher et al., 2008, Hallem and Sternberg, 2008) and O_2 sensation (Skora and Zimmer, 2013, Zimmer et al., 2009)
PHB (L,R)	Sensory neuron (Phasmid)	Glutamatergic and possibly Serotonergic	Modulate Chemorepulsion
AWA (L,R)	Sensory neuron (Amphid)	----	Chemotaxis to diacetyl, pyrazine, trimethylthiazole and required for sexual-attraction in males (Pereira et al., 2015, Hobert, 2005, Altun-Gultekin et al., 2001, Ishihara et al., 2002, de Bono and Maricq, 2005, Kuhara and Mori, 2006, Chalasani et al., 2007, Gray et al., 2005, Bargmann and Horvitz, 1991)
AFD (L,R)	Sensory neuron (Amphid)	Glutamatergic	Thermosensation (ablation causes athermotactic) and locomotion (Tsalik and Hobert, 2003, Kuhara et al., 2008, Beverly et al., 2011, Mori and Ohshima, 1995)
ADF (L,R)	Sensory neuron (Amphid)	Serotonergic	Couple environmental food signals with serotonin neurotransmission (Jafari et al., 2011), Chemotaxis (to cAMP, biotin, Cl^-, and Na^+) and controls entry into dauer state (Bargmann and Horvitz, 1991, Schackwitz et al., 1996)
ASG (L,R)	Sensory neuron (Amphid)	Glutamatergic and Serotonergic (under hypoxic situations)	Chemotaxis to water soluble attractants (Pocock and Hobert, 2010), entry into dauer state and life span regulation (Alcedo and Kenyon, 2004, Bargmann and Horvitz, 1991, Schackwitz et al., 1996)
PHA (L,R)	Sensory neuron (Phasmid)	Glutamatergic	Modulate chemorepulsion behaviour (Hilliard et al., 2002) and part of the neuronal circuit that functions in mate-searching behaviour of males (Barrios et al., 2012)
AVK (L,R)	Inter neuron	----	----
AIY (L,R)	Inter neuron	Cholinergic	Roles in behavioural patterns involving temperature or chemical cues (Bono and Maricq, 2005, Ishihara et al., 2002), thermotaxis (Beverly et al., 2011, Ardiel and Rankin, 2011, Sasakura and Mori, 2013, Ohnishi et al., 2011), locomotion (Gray et al., 2005, Tsalik and Hobert, 2003) and regulates lifespan and starvation response (Kang and Avery, 2009, Shen et al., 2010)

RMG	Motor neuron	----	Operates in pheromone attraction and social behaviour, integrates signals from various sensory neurons modulating their chemosensory responses (Lockery, 2009, Macosko et al., 2009)
pm1	Muscle cell	N/A	Part of the pharynx muscles, one of eight consecutive rings encircling the pharynx (Albertson and Thomson, 1976, Avery and Thomas, 1997, Franks et al., 2006, Hedgecock and Thomson, 1982)

Table 1.8: NCS-1 neuronal locations with functions: *C. elegans* NCS-1 has been identified to be present in 1 muscle cell type, 1 motor neuron, 10 pairs of sensory neurons and 2 interneuron pairs, identified through GFP expression. The function of NCS-1 in the majority of these neurons has been investigated thoroughly (table 1.8 adapted from (Gomez et al., 2001)). Functional importance of NCS-1 within each specific cell type shows a diverse and complex interplay with NCS-1 and its partner proteins, NCS-1 is present in both left and right neurons (L,R).

Previous studies showed that NCS-1 over-expression has a positive effect on memory function; earlier memory acquisition and extended timeframe of memory retention prior to memory extinction in comparison to N2 or *ncs-1* null *C. elegans* (Figure 1.18) (Hedgecock and Russell, 1975, Gomez et al., 2001). Systematic knockout of the functional EF-hands in NCS-1 (EF 2,3 and 4) when expressed in *ncs-1* null *C. elegans* failed to recapitulate memory functions back to wild-type levels suggesting this is Ca^{2+} dependent (Gomez et al., 2001).

Specific neuronal rescue of NCS-1 identified a critical role for NCS-1 in the AIY neuron for IT and memory (Gomez et al., 2001). No clear evidence to date has suggested a role for NCS-1 in thermoavoidance or negative thermotaxis (Figure 1.15 and 1.16). A novel temperature dependent phenotype has previously been identified in *ncs-1* null *C. elegans* which identified that these retained and showed a slight yet significant increase in locomotion at elevated temperatures which was not found in N2 animals (Martin et al., 2013)

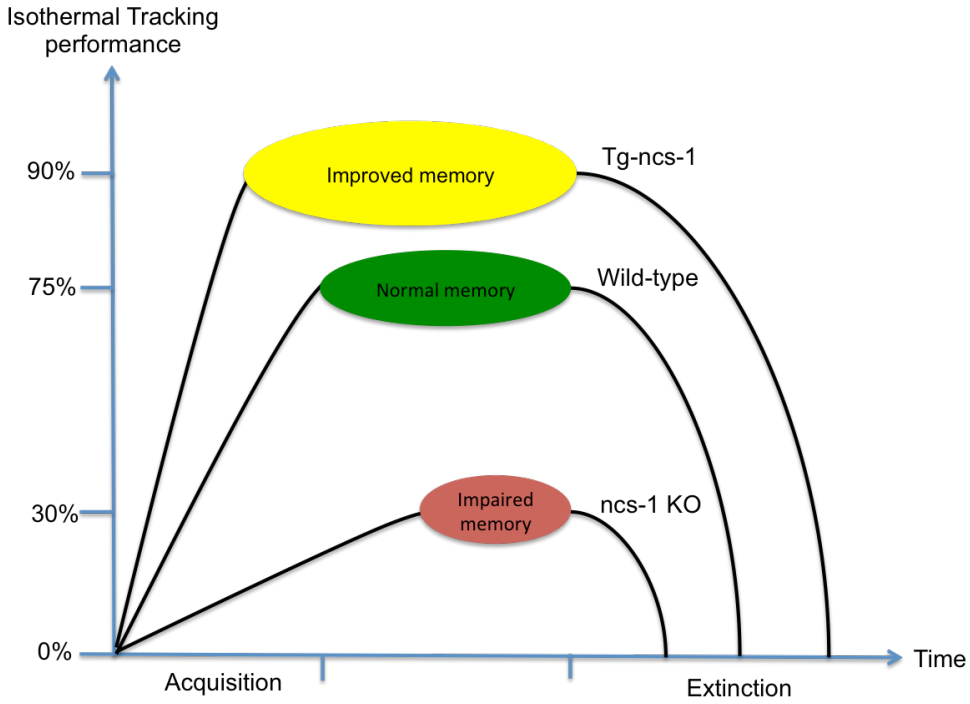

Figure 1.18 Establishment of memory, duration and extinction: Loss of NCS-1 perturbs memory establishment and results in a shorter time to extinction. Over-expression of NCS-1 resulted in a shorter acquisition time and a longer time to memory extinction. Figure adapted from (Gomez et al., 2001).

1.8 Paralysis phenotype

Whilst there are many different forms of thermal behaviours within *C. elegans* this project focused primarily upon the temperature dependent locomotion under elevated temperature using a quantifiable locomotion assay readout. A novel phenotype was previously identified within our laboratory (unpublished Dr. Jeff Barclay) causing paralysis in *C. elegans* under noxious temperature ceasing locomotion. Previously, *C. elegans* locomotion was assessed at elevated temperature with N2 showing the characteristic paralysis phenotype within the initial 10-minute equilibration period. Animals would then resume locomotion in response to a continued exposure to the noxious temperature with a variable recovery time from paralysis. Preliminary research identified this behaviour, yet further characterisation was not completed.

1.9 Factors affecting Thermosensation

Complex crosstalk between neuronal pathways is common to generate specific behaviours. These neuronal networks help understand the diversity of signaling.

Following on from the thermosensory neural network (Figure 1.14) and with the information from table 1.6, the AIY neuron is involved in a range of other processes, for example negative thermotaxis (Figure 1.15 & 1.16) through synaptic connections. Multiple factors affect the mechanisms for thermosensation; as such in thermosensory experiments, these must be adequately controlled and accounted for. Environmental factors such as humidity, odor sensation (chemotaxis), light and non-environmental factors i.e. locomotion are suggested to affect thermosensation (Figure 1.19).

1.9.1 Humidity

Regarding humidity, Russell et al 2014 identified an interplay between mechanosensation and thermosensation in their model of humidity sensation (Russell et al., 2014), using FLP neurons (mechanosensation) which undergo stretching when exposed to abnormal humidity levels; signaling to return to normal humidity environments. *C. elegans* with an inactive AFD neuron (required for thermosensation) are unable to detect humidity levels, as thermosensation is required for humidity sensation, reverse cross-talk might also be present for optimal thermosensation. A change in either of these environmental influences can affect *C. elegans* behaviours; as such correct sensation of these is critical for survival. *C. elegans* behaviour is plastic associating food with a set humidity or a specific temperature (Tsalik and Hobert, 2003, Russell et al., 2014).

1.9.2 Locomotion

Animals are required to move to avoid stressful situations; in *C. elegans* reversal phenotypes and dispersion involve the AIY, and possibly the ASE (odorant sensor), neurons (Tsalik and Hobert, 2003, Pocock and Hobert, 2010, Peymen et al., 2014). Deficiency of the AIY neuron increases hyper-reversal locomotion. Due to association of specific plate conditions with locomotion direction to seek favourable environments, the behaviours are again believed to be plastic. The AIY is not a command interneuron (Figure 1.19), however can alter reversal phenotypes through the AIZ (decreased reversal), RIM and RIB (increase reversal) interneurons (Zheng et al., 1999).

The reversal behaviour of the aforementioned neurons is dependent on the AIY neuron as loss of this causes no change in the level of reversal in *C. elegans*. All processes which utilize the AIY neuron, a key member of the thermosensory neural network, could themselves affect thermosensation.

Thrashing as a form of locomotion in *C. elegans* is dependent on parallel signals causing the muscle cells on the ventral / dorsal side to contract as the opposing side of the *C. elegans* relaxes, resulting in movement. Thrashing here was defined as a complete movement of the head from one side of the animal, across the midpoint and back to the same side of the animal (Ventral to Dorsal and back to Ventral classes as one thrashing motion).

1.9.3 Chemosensation

Chemosensation and chemotaxis of molecules is another factor potentially influencing thermosensation. The detection of NaCl occurs through the ASE (L/R) neurons which signals through the AIY interneuron. In this example, Na^+ is detected by ASEL and Cl^- by ASER (Satoh et al., 2014, Pierce-Shimomura et al., 2001, Filingeri, 2015, Zheng et al., 1999). The pathway for NaCl detection and chemotaxis involves the AIA, AIB or AIY neurons. As the AIY neuron is implicated in this pathway, the NaCl concentration can potentially influence thermosensation (Pierce-Shimomura et al., 2001, Filingeri, 2015, Sasakura and Mori, 2013, Sasakura et al., 2013).

Each of these factors were taken into account during the course of this research to the best of my abilities through completing the temperature dependent locomotion assays in the same room using the same microscope lighting and all experiments were completed using Dent's solution with 0.1% Bovine serum albumin (BSA) to limit any external variables. As thermosensation is a plastic response, all animals tested were grown under the same conditions on Nematode Growth Media (NGM) and were assayed from well fed plates using *C. elegans* of the same age range (young adult to day 2 adults).

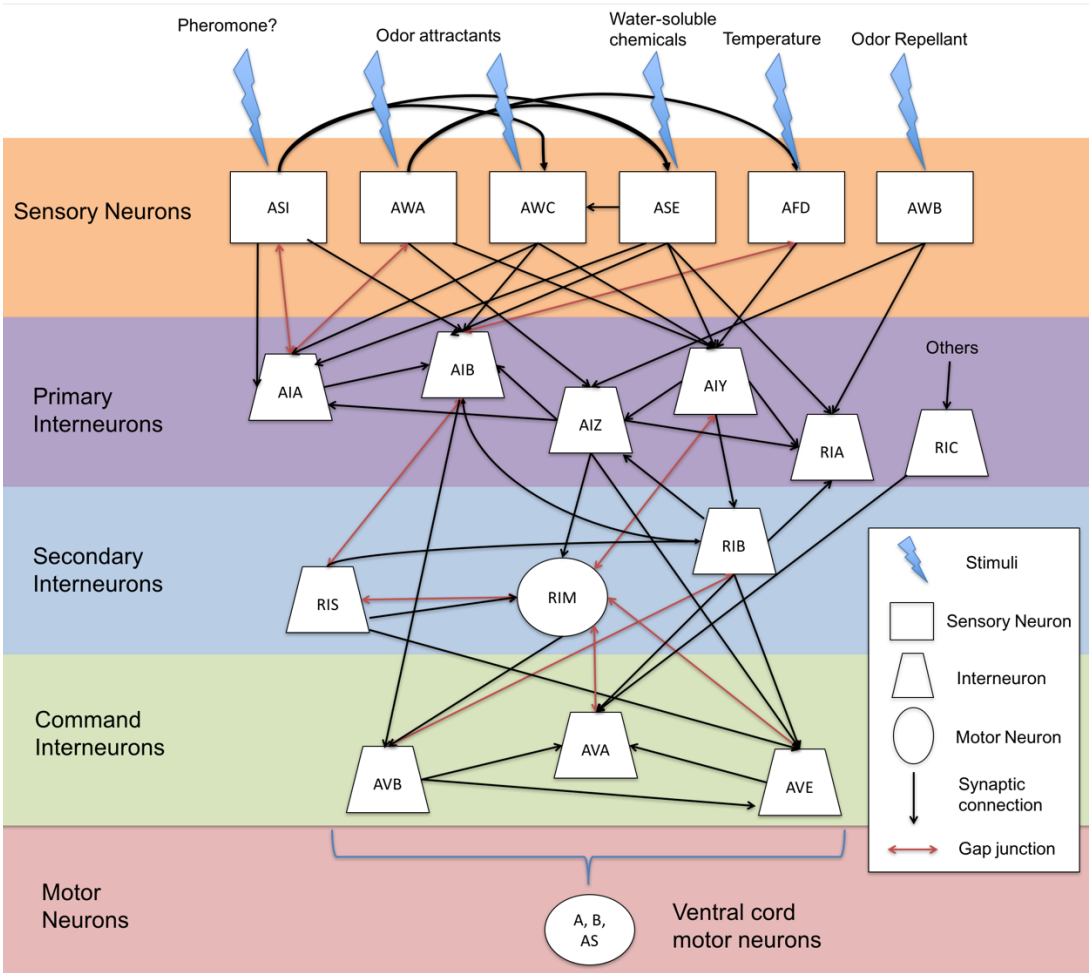

Figure 1.19 Example of the neuronal network inclusive of the AIY neuron: The AIY neuron is critical in thermosensory behaviours. Synaptic connections with other neurons lead to a range of behavioural outputs. The complex interplay between neurons suggests different factors may affect thermosensation The AIY is a primary interneuron, signaling to downstream neurons to elicit a motor output using either dorsal or ventral motorneurons. Studies into neuronal networks have gained much interest recently with more remaining to be established.

1.10 Aims and Objectives:

Using transfected cell lines, as no interaction has been fully established between NCS-1 and PQ, the first part of this research aims to:

1. Identify an interaction between PQ and NCS-1
2. Test intramolecular Cameleon between NCS-1 and PQ

If successful, this could be taken forward into *C. elegans* as the model organism for the second part of this research. For the second part of this research, a number of NCS-1 interacting proteins were analysed using a quantifiable behavioural output.

The second part of the research aims to:

3. Characterise TDL assay
4. Identify NCS-1 interacting partners using the TDLA
5. Re-capture TDL behaviours through RNAi
6. Elucidate relationship between NCS-1, PI4K and ARF-1.1

Chapter 2: Materials and Methods

2.1 Protein Methods

2.1.1 Plasmid construction

Automated dideoxy DNA sequencing was performed in both 5' and 3' directions by The Sequencing Service, University of Dundee, UK.
Complimentary oligonucleotides encoding the myristoylation consensus sequence from Lck kinase (Oz et al., 2013)) containing 5' XhoI and 3' HindIII overhangs were annealed and ligated directly into HindIII/XhoI digested N1-EYFP and N1-mCherry vectors to create new plasma membrane targeting constructs (Myr-EYFP and Myr-mCh). The ligated plasmids were used to transform competent XL-1 *Escherichia coli* (*E. coli)*.

Transformed bacteria were grown on Kanamycin (kan 30 µg/ml) supplemented Luria bertani (LB) agar (1.5% w/v agar, 1% w/v tryptone, 0.5% w/v Yeast extract, 8.56 mM NaCl) plates and for 24 hours at 37^0C. Individual transformant colonies were picked and grown overnight in 5 mls of liquid LB media (1% w/v tryptone, 0.5% w/v Yeast extract, 8.56 mM NaCl) supplemented with 30 µg/ml kan at 37^0C /250 rotations per minute (rpm). Extracted miniprep DNA (Qiagen, UK) was sent for automated dideoxy sequencing to validate correct incorporation and reading frame of the Lck myristoylation sequence.

To create myristoylated PQ-type channel residues 1898-2035, pEYFP-Myr and pmCh-Myr were digested with HindIII and SacII and ligated with a PCR product encoding residues 1898-2035 of the rat PQ channel (Genbank Accession: NM_012918) having complimentary 5' HindIII and 3' SacII overhangs. Ligation reactions were transformed into competent XL-1 *E. coli*, colonies picked and miniprep DNA (Qiagen) extracted for DNA sequencing. These constructs are henceforth referred to as myr-PQ-eYFP and myr-PQ-mCh respectively.

Creation of the new variant Cameleon constructs was completed using standard cloning techniques (used for chapter 3, figures 3.16, 3.18 and 3.19). Here rat NCS-1 and a small or large segment of the rat PQ-type VGCC were included within the

cameleon construct (henceforth referred to as either Partial or Full PQ cameleon respectively). Restriction sites were utilized for assembly of these constructs (see Figure 2.1 below) to create an intramolecular FRET sensor.

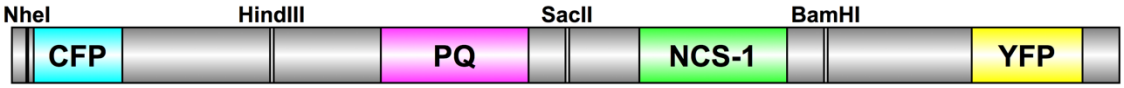

Figure 2.1: Schematic diagram of Cameleon constructs. To allow investigations of PQ and NCS-1 interactions in close proximity, intramolecular FRET sensors were produced with specific restriction sites in place to aid production. Two variations of the cameleon construct were produced with 'Full length PQ' (1898-2035) and 'Partial PQ' (1898-1949) each encompassing the IM domain of the PQ-type channel. Primary experiments used an mCh and EYFP cameleon for analysis with later experiments using CFP/ YFP cameleon. In standard cameleons, binding of Ca^{2+} to the CaM portion of the cameleon allows interaction between CaM and M13 causing a conformational change, resulting in light to radiate from a different wavelength. The novel cameleon produced here uses binding to NCS-1 to then interact with PQ resulting in a conformational change and increased FRET.

2.1.2 Cell culture and transfection

HeLa (Human ovarian cancer cells) and N2A (Mouse Neuroblastoma cells) were maintained in Dulbecco's modified Eagle medium (DMEM) supplemented with 5% (v/v) Fetal Bovine Serum (FBS), 1 % (v/v) NEAA (non-essential amino acids) and 1% (v/v) Penicillin/ Streptomycin (Pen/Strep) at 37 ^{0}C in a humidified atmosphere of 95% (v/v) air and 5% (v/v) CO_2. Cells were passaged at ~80 % confluency. Cells were transfected with 1 µg (24 well plates) or 3 µg (6 well/Matek dishes) of plasmid DNA using 3 µl of Promofectin transfection reagent per µg of plasmid according to the manufacturers protocol. Cells were processed and analysed 24 or 48 hours post transfection.

For Western blot analyses cells were seeded onto 6 well plates using the protocol outlined above. For immunofluorescence, FRET (Förster Resonance Energy Transfer), FLIP (Fluorescence Loss In Photobleaching) and FRAP (Fluorescence Restoration After Photobleaching) protocols cells were plated onto either 13 mm diameter sterile coverslips in 24 well tissue culture trays (fixed cells) or into Matek 30

mm diameter live cell imaging dishes. Cells were allowed to adhere overnight prior to transfection.

Cells were fixed using 4 % (v/v) Paraformaldehyde in Krebs buffer (58.1 mM NaCl, 1.98 mM KCL, 1.3 mM $MgCl_2$, 0.5 mM NaH_2PO_4, 4 mM Glucose, 8 mM HEPES (pH 7.4) and $CaCl_2$ 2 mM). Cells were left in fixative for 6 minutes before drying and mounting onto slides with ProLong Gold antifade glycerol.

2.1.3 Microscopy

Transfected cells were imaged using a Leica TCS-SP-MP fluorescent scanning confocal microscope (Leica Microscopes) and a 63x water immersion lens, numerical aperture (N.A.) =1.2 (live cell experiments) or 63 x oil immersion lens (N.A.=1.3, fixed cells). Fluorophores were excited at 509 nm (YFP), 405 nm (CFP) and 594 nm (mCh) with emissions collected at 582 nm (YFP), 490 nm (CFP) and 620 nm (mCh).

For live cell experiments an acquisition rate of 1 frame/ 5s was employed. Cells were perfused with Krebs buffer and subsequently with Krebs solutions containing 1 µM Ionomycin, 5 µM Thapsigargin, 100 µM Histamine or 5 µM A23187.

To establish interactions between NCS-1 and the PQ Ca^{2+} channel fragment incorporated into the mCh and YFP vectors three different types of experiment were completed. Firstly we attempted to identify this interaction using FRET as described previously (McCue et al., 2013). FRET data was collected by exciting the YFP portion of PQ YFP with a 495 to 510 nm laser line and simultaneous collection of emitted fluorescence between 600 and 650 nm (mCh). These experiments were completed using sensitized emission and acceptor bleaching protocols. To measure FRET through acceptor bleaching, cells were excited using mCh, with corresponding measurements in the YFP emission.

Secondly FRAP experiments were attempted as described previously (Handley et al., 2010). Multiple regions of interest (where co-transfection was present) in transfected cells were selected and photobleached (10 frames). Fluorescence changes were then

measured in these regions to identify shuttling of bleached fluorophores with the unbleached fluorophores from different cellular regions.

Thirdly FLIP experiments were utilized as described previously (Handley et al., 2010). Regions of interest (ROIs) in cells were photobleached and different areas of the cell were then measured to identify the loss of photobleaching in the unbleached regions (suggesting shuttling to the bleached regions).

In addition to these live cell experiments, further analysis of interactions between NCS-1 and PQ-type channels were completed using newly constructed Cameleon constructs (Figure 2.1) which were transfected into HeLa cells and intramolecular FRET activity measured in numerous ROIs, in each experiment numerous ROIs were taken from within the cell with one ROI present in the extracellular region acting as a control background measurement.

2.2 C. elegans Methods

2.2.1 Molecular Biology Methods

2.2.1.1 Plasmid transformation

Prior to completing plasmid miniprep or midiprep protocols, DNA constructs were amplified by using plasmid DNA transformed into chemically competent *E. coli* strain XL1 Blue, prepared in house, via heat shock treatment. An aliquot of XL1 Blue bacteria (50 µl) was thawed on ice before incubation with 0.5 µl of plasmid DNA in pre-chilled round bottomed test tubes for 30 minutes. A heat shock treatment at 42^{o}C for 45 seconds was completed then placed back onto ice for 2 minutes following which 950 µl super optimal broth with catabolite repression (SOC) medium (2% w/v tryptone, 0.5% w/v Yeast extract, 10 mM NaCl, 2.5 mM KCl, 10 mM $MgCl_2$, 20 mM glucose) was added and then incubated at 37^{o}C for 1 hour under continuous orbital rotation (220 rpm). 25 µl of the transformed *E. coli* were subsequently spread onto LB-agar plates (1% w/v tryptone, 0.5% w/v Yeast extract, 1% w/v NaCl, 1% w/v agar) supplemented with the required antibiotic (100 µg/ml ampicillin or 50 µg/ml kanamycin) and cultured overnight at 37^{o}C.

2.2.1.2 Purification of Plasmid DNA

Single *E. coli* colonies grown on the antibiotic containing plates, hence containing the plasmid of interest, were picked for inoculation of 30 ml of LB media (1% w/v tryptone, 0.5% w/v Yeast extract, 9mM NaCl) supplemented with a selection antibiotic and subsequently grown overnight at 37^{o}C under orbital rotation 250 rpm. Cultures were then pelleted by centrifugation (12,000 x g, 10 minutes) and plasmid DNA extracted from the bacterial pellet using QIAprep Spin Miniprep Kit (Qiagen) or a PureYield plasmid Midiprep System (Promega), each completed following the manufacturers guidelines. Plasmid DNA concentration was determined spectrophotometrically with the Nanodrop® Lite (Thermo Fisher Scientific, Waltham, MA, USA) using both 260 and 280 nm.

2.2.1.3 Analysis and isolation of DNA fragments

DNA fragments were separated using Agarose gel electrophoresis, sorting DNA fragments according to size. Agarose gel composed of 1% (w/v) agarose dissolved in Tris-acetate EDTA (TAE) buffer (40 mM Tris, 20 mM acetic acid, 1 mM EDTA). Agarose gels were supplemented with 0.5 µl/ml Sybr Safe (Invitrogen, Paisley, UK) to stain the DNA.

Prior to loading into agarose wells, DNA solutions were mixed with 6x DNA loading buffer (New England Biolabs (NEB)) and separated by gel electrophoresis through a 2% w/v agarose gel, supplemented with SYBR® Safe DNA Gel Stain (Life Technologies) 1:10,000 ratio. Agarose gels were placed into a tank containing TAE buffer at 70 V for ~40 minutes. Size of DNA fragments were analysed using a known marker (Hyperladder 1kb (Bioline)) as a size reference. DNA fragments were imaged using UV light generated by a ChemiDoc XRS (Biorad) utilizing the Quantity One software (BioRad; v4.6.3).

2.2.2 C. elegans strains

C. elegans strains used in this project were wild-type (Bristol N2) or specific mutations obtained from several sources (Table 2.1).

Strain	Gene	Allele	Mutation	Source	Outcrossed
N2	Wild type	*n/a*	n/a	*Caenorhabditis* Genetics Centre (CGC) (University of Minnesota, USA).	N/A
XA406	*ncs-1*	*qa401*	Null, 2149bp deletion including ATG site of NCS-1	CGC	Tc1 (x5)
FX2348	*pifk-1*	*tm2348*	Null, 502bp deletion, 5bp insertion	Mitani laboratory National BioResource Project (NBRP) Nagoya University, Japan.	Information not available
RB1535	*arf-1.1*	*ok1840*	Null 1065bp deletion	CGC	X0
VC160	*trp-1*	*ok323*	Null 1366bp deletion	CGC	UV/TMP (x0)
TQ225	*trp-1*	*sy690*	Null deletion	CGC	UV/TMP (x7)
TQ194	*trp-2*	*sy691*	Null deletion	CGC	UV/TMP (x8)
RB1255	*arf-1.2*	*ok1233*	Null deletion	CGC	UV/TMP (x0)
VC567	*arf-1.2*	*ok796*	Null 1140bp deletion	CGC	UV/TMP (x1)
HA865	*grk-2*	*rt97*	Base pair substitution C/T (wildtype/mutant)	CGC	x4
FG7	*grk-2*	*gk268*	Deletion 1538bp	CGC	x8
NL2099	*rrf-3*	*pk1426*	Null 3015bp deletion, deficient in RNA dependent RNA polymerase (RdRP)	CGC	UV/TMP (x2)
XE1581	wpSi10 II; *eri-1*(*mg366*) IV; *rde-1*(*ne219*) V;*lin-15*B*(n744*) X	*mg366, ne219 and n744*	Selective expression of RNAi constructs within cholinergic neurons with RNAi resistance maintained in other tissues.	CGC (produced by Hammarlund and Firnhaber)	x0

Table 2.1: Strains of *Caenorhabditis elegans (C. elegans)* used in this project. Strains and their known genotype information are included alongside their source. *C. elegans* were sourced from a variety of different laboratories; used for specific experimental measures.

2.2.3 C. elegans husbandry

C. elegans strains were grown and maintained on standard nematode growth media supplemented with the relevant salts (NGM) (50 mM NaCl, 1 mM $CaCl_2$, 1 mM MgSO4, 25 mM KH_2PO_4, 5 µg/ml cholesterol, 0.25% w/v peptone, 2% w/v agar) on either 60mm or 35mm petri plates. Strains were maintained following standard protocol as described previously (Brenner, 1974) and maintained at 20^{o}C. Plates were seeded with 50 µl of *E. coli* OP50 strain as the food source. Between 5-10 young hermaphrodite *C. elegans* were transferred using a sterile tungsten pick (World Precision Instruments), from old, overgrown but not starved plates to fresh seeded NGM plates every generation. Animals were observed using a PZMIV dissecting binocular stereomicroscope (World Precision Instruments) with illumination from either a halogen cold light source or, for GFP expressing strains an epifluorescent UV light when selecting *C. elegans* for assaying or for general maintenance.

Age synchronization of *C. elegans* was completed through either a timed egg lay where 10 young hermaphrodite adult *C. elegans* were transferred as described previously to seeded plates and left for ~16 hours to lay eggs after which the adult *C. elegans* were removed and the eggs left to hatch and larvae to grow for ~36 hours or ~60 hours for progeny to hatch and mature to approximately stage 4 larval/ Day 0 or Day 1 adults respectively. Alternatively a plate of overgrown adult *C. elegans* was washed off using 3.5 ml distilled H_2O and bleached using Sodium hypochlorite (NaClO) (1 ml of 4% v/v NaClO with 0.5 ml of 5 M NaOH).

Animals were briefly vortexed every 2 minutes for 10 minutes before centrifugation (1300 g for 1 minute following which supernatant was removed and 5 ml of dH_2O added and centrifuged 1300 g for 1 minute. Supernatant was removed without disturbing the pellet, leaving 100 µl that is added in a drop wise fashion to a freshly seeded NGM plate.

2.2.4 RNA interference (RNAi) using feeding

RNAi experiments were conducted using standard feeding protocols following standard procedures (Simmer et al., 2002, Simmer et al., 2003, Kamath and Ahringer,

2003, Timmons and Fire, 1998). RNAi in *C. elegans* was completed by feeding (as opposed to via injection or soaking) *C. elegans* HT115 (DE3) bacteria expressing target-gene double-stranded RNA (dsRNA) within the pG-L4440 vector (Timmons et al., 2001, Fraser et al., 2000). HT115 (an *E. coli* strain) lacks dsRNA-specific RNase III however this contains an isopropyl β-D-1-thiogalactopyranoside (IPTG)-inducible T7 RNA polymerase (Timmons et al., 2003) containing the pG-L4440 vector containing gene-specific RNAi trigger sequences. All RNAi feeding clones were obtained from the Vidal *C. elegans* Open Reading Frame (ORF) RNAi feeding library (Source Bioscience, Nottingham, UK) or were specifically obtained directly from Source Bioscience.

Clones of the RNAi constructs were plated out onto 90 mm plates of LB agar (1% tryptone, 0.5% Yeast extract, 1% NaCl, 1.5% agar) supplemented with 100 µg/ml ampicillin and 12.5 µg/ml tetracycline. Bacterial strains for RNAi were streaked onto separate plates from the frozen stocks and incubated overnight at 37^{o}C. A single discreet colony from each plate was subsequently grown in 30 ml LB broth containing 100 µg/ml ampicillin and 12.5 µg/ml tetracycline overnight at 37^{o}C, 250 rpm. Bacterial culture was further incubated with 1 mM IPTG at 37^{o}C for a further 4 hours to increase levels of dsRNA production.

NGM plates supplemented with 100 µg/ml ampicillin and 2 mM IPTG were poured 4-7 days prior to being seeded with 50 µl of the RNAi feeding culture. 5-10 healthy hermaphrodite adults were transferred to RNAi plates ~48 hours after seeding. RNAi plates have reduced RNAi efficiency along with time course, as such fresh RNAi plates were prepared in each experiment. RNAi plates were also maintained in a sealed, covered box in the dark as IPTG is light sensitive. Second generation RNAi fed *C. elegans* were used in the assays described below (results shown in chapter 4). Control feeding RNAi in these experiments consisted of HT115 carrying the empty vector pG-L4440 (no knockdown) as a negative control. For these experiments *hsp-1* was used as the primary positive control as this caused *C. elegans* death.

2.2.5 Genomic DNA extraction and single C. elegans PCR

In order to establish whether a particular *C. elegans* was homozygous or heterozygous for a specific deletion allele, individual animals were picked into 10 µl of *C. elegans* lysis buffer consisting of 5x Phusion® HF buffer (NEB), diluted down to 1x using DEPC treated water and Proteinase K (95µl 1x PCR buffer with 5µl 20 mg/ml Proteinase K) at a concentration of 1 µg/µl, samples were first frozen at -80^{o}C for at least 30 minutes before freeze thawing and undergoing a standard worm lysis protocol through incubation in a thermal cycler at 65^{o}C for 90 minutes, followed by 95^{o}C for 15 minutes. For each subsequent PCR reaction, 2 µl of this lysate was used for genotyping using the primers listed in table 2.2.

Single *C. elegans* PCR was completed in a 25 µl reaction volume consisting of 12.5 µl of OneTaq Quick-Load 2x Master Mix (NEB), 2 µl of template (worm lysis product), forward and reverse primers (0.5 µl of 10 µM) and 9.5 µl of diethylpyrocarbonate-treated (DEPC) water. Specific PCR conditions can be found in table 2.2. Amplified products were analysed using a ChemiDoc XRS after separation on 2% agarose gels (running at 70 volts for ~40 minutes) as described previously.

2.2.6 PCR for double mutants with conditions, primers and product sizes

Investigating	Forward primer	Reverse primer(s)	Annealing temperature (°C)	Extension time (s)
NCS-1 status	CAGTTGAGCATCGTTATTCTG	WT: GATAAGGTATGATTTGGGTTCG	58	90
		MUT: CCGTATTTGAACGTTGCTAC		
Trp-1 status	CAACAGTTGCTCACCTCTATC	WT: CCTCCGCTACCAACATTGGTTC	49	180
		MUT: CGAATTTGTTGTGGAGGCAG		
Trp-2 status	CACTGATGACGTGGATCGCAAGG	CTAAGGGTGAAATATGACGAG	60	90
Arf-1.1 status	CATCGCCAACCAAGGAAAG	WT: CCACATCAGACCTTCGTAGAG	50	120
		MUT: CGACAGAGATCACCAAACATTG		
Arf-1.1 with AttB	GGGGACAAGTTTGTACAAAAAAGCAGGCTCGATGGGCTTATTCTTCTCT	GGGGACCACTTTGTACAAGAAAGCTGGGTCTTATGTCTTCATCTGCTTCTTG	66	60
Pifk-1 status	TATAGGCCGCTGTGCTTTGAATG	WT: GAAGACCGGAGACGATCTTTC	55	90
		MUT: CCCATCAGCACGGTAGGTTTAAA		

Table 2.2: PCR primers and conditions: Primers utilized for the identification of different mutant lines in the generation of double mutants to confirm genetic status of the generated lines. PCR annealing and extension parameters shown for these experiments. PCR conditions also shown for the preliminary construction of injection plasmids. Each PCR consisted of 30 extension cycles.

2.2.7 Male generation and maintenance

In order to generate double mutant strains this was completed by crossing two existing strains. First male N2 *C. elegans* were generated through heat shock of 5-6 L4 hermaphrodites per plate within a 30°C incubator for 6 hours and the progeny screened for male phenotypic characteristics. After males were generated these were propagated by mating L4 hermaphrodites with males of the wild type background using a 4 male : 1 hermaphrodite ratio.

Mating plates were maintained with 16 males and 4-5 L4 hermaphrodites. Male generation is increased after heat shock due to the increased incidence of non-disjunction of the X-chromosome during meiosis leading to a higher incidence of males (Anderson et al., 2010).

2.2.7.1 Double mutant generation (genetic crosses)

Young adult hermaphrodite (pre-gravid) *ncs-1* null (*qa401*) *C. elegans* were crossed with N2 wild-type males to generate *ncs-1* null male *C. elegans* before being crossed with other strains. Between 16-20 young *ncs-1* null males were transferred to a 60 mm seeded (50 µl OP50) NGM plate with the addition of 4-5 young hermaphrodites of various strains (*arf-1.1* null (RB1535), *trp-1* null (VC160), *trp-2* null (TQ194). In the case of the cross between *pifk-1* FX2348 (*tm2348*) and *arf-1.1* null RB1535 (*ok1840*) *C. elegan*s were crossed in a similar manner using *pifk-1* (*tm2348*) null males crossed with *arf-1.1* null (*ok1840*) hermaphrodites.

From this cross approximately 20 F1 cross progeny were singled out onto individual plates and allowed to self-fertilize at 20 ^{o}C. Approximately 48 hours after single animals were placed onto these plates, the original adult *C. elegans* was removed and PCR based genotyping was completed on the original F1 parental organism to identify possible heterozygosity of the two mutant deletion alleles. In these genetic crosses *ncs-1* null males were used as *ncs-1* is present on the X chromosome making crosses more likely to maintain the *ncs-1* null deleterious allele.

Plates which showed heterozygosity for the two mutant alleles of interest (*ncs-1* (XA406 *(qa401*) *+/-)* and a second allele from *arf-1.1* (RB1535 *(ok1840)*), *trp-1* (VC160 *(ok323)*) or *trp-2* (TQ194 *(sy691)*) +/- in each cross had their progeny singled out onto 35 mm seeded NGM plates. The adult *C. elegans* was picked off and PCR genotyped after progeny had been laid, approximately 48 hours after initially being placed onto the fresh plate. This process was continued until a successful, continuous double mutant genotype was identified from the adult lysed *C. elegans*. In all crosses progeny for a series of generations were tested to confirm double mutant genotype.

Strain name	Mutant alleles	Strain 1	Strain 2
AMG 128	*trp-2* and *ncs-1*	XA406 (*qa401*) (*ncs-1* null)	TQ194 (*sy691*) (*trp-2* null)
AMG 145-148	*trp-1* and *ncs-1*	XA406 (*qa401*) (*ncs-1* null)	VC160 (*ok323*) (*trp-1 null*)
AMG 149-152	*arf-1.1* and *ncs-1*	XA406 (*qa401*) (*ncs-1* null)	RB1535 (*ok1840*) (*arf-1.1 null*)
AMG 153-156	*Pifk-1* and *arf-1.1*	FX2348 (*tm2348*) (*pifk-1* null)	RB1535 (*ok1840)* (*arf-1.1 null*)

Table 2.3: List of successful DM: Double mutant strains produced over the course of this research through genetic crosses of different single mutant *C. elegans* strains to form double mutant strains of interest using NCS-1 interacting proteins of interest.

2.2.8 Plasmids used for C. elegans injections

The pDONR201 plasmid (Invitrogen) was used in the various Gateway cloning reactions described below. A GFP marker plasmid for pan-neuronal expression of GFP (pRAB100 [$p_{rab\text{-}3}$*::GFP*]) was obtained from the Nonet Laboratory (Washington, University of St. Louis, USA) with promoter plasmids for sensory neuronal expression (pG[$P_{osm\text{-}6}$]), pan neuronal expression (pG[$p_{rab\text{-}3\text{-}A}$]) being obtained from James Johnson, University of Liverpool.

An AIY neuron specific plasmid was initially obtained from Hobert Lab (Columbia University Medical Center, N.Y.), allowing expression of transgenic proteins within the AIY neuron only, however cloning reactions within this project began using a modified version of this plasmid produced by Dr. Victoria Martin, University of Liverpool (pG[P_{AIY6}*::NCS-1 unspliced*]). The promoter for NCS-1 is present within the introns and exons of the ttx-3 gene present on the X chromosome within *C. elegans*.

2.2.8.1 Gateway cloning

Plasmids created using the Gateway cloning system are illustrated in Figure 2.2, in the case of (P_{ttx-3}*::arf-1.1*) issues during Gateway cloning were experienced hence production of this plasmid used an intermediary newly created plasmid (P_{osm-6}::*arf-1.1*). To create these plasmids expressing *arf-1.1* under different promoters; pan-neuronal *rab-3* [p_{rab-3}::*arf-1.1*], ciliated neurons osm-6 [P_{osm-6}::*arf-1.1*] and AIY neuron specific [P_{ttx3}::*arf-1.1*], *C. elegans arf-1.1* was first amplified from gDNA produced within the laboratory, with the addition of attB sites within the PCR primers resulting in a product of the gene with additional attB recombinase sequences. Products from the PCR reaction were separated on an agarose gel and the PCR product band excised using PureLink® Quick Gel Extraction Kit (Invitrogen). The extracted gene was inserted into the Gateway donor plasmid pDONR201, containing the attP recombinase flanking sequences and cassette, using BP Clonase II recombinase following the manufacturer's instructions (Invitrogen).

BP reaction plasmids from combining pDONR201 with attB-Arf-1.1 was amplified using Bioblue *E. coli* and purified through the standard miniprep protocol as previously mentioned. The presence of attL flanking sequences within the donor vector allowed the gene of interest to be inserted into the destination plasmids pG[P_{osm-6}*::attR*], pG[p_{rab-3}*::attR*] and pG[P_{ttx-3}*::ncs-1*], using LR clonase II according to the manufacturer's instructions.

Initial destination plasmids were formed from the original pPD117.01 plasmid by Dr. James Johnson using standard recombinant cloning procedures. For production of the AIY specific expression of *arf-1.1*, the PAIY-*ncs-1* plasmid provided by Dr. Victoria Martin (University of Liverpool) and the pG[P_{osm-6}*::arf-1.1*] were cut using AscI and BamHI restriction enzymes to remove the promoter region from the specific plasmids. The resulting products were separated on a 1% agarose gel containing 0.1% SYBR Safe and the promoter region of the AIY specific expression plasmid was excised, alongside the backbone of the *arf-1.1* plasmid. The DNA fragments were gel purified according to manufacturer's instructions (Promega) and ligated at room temperature for 30 minutes.

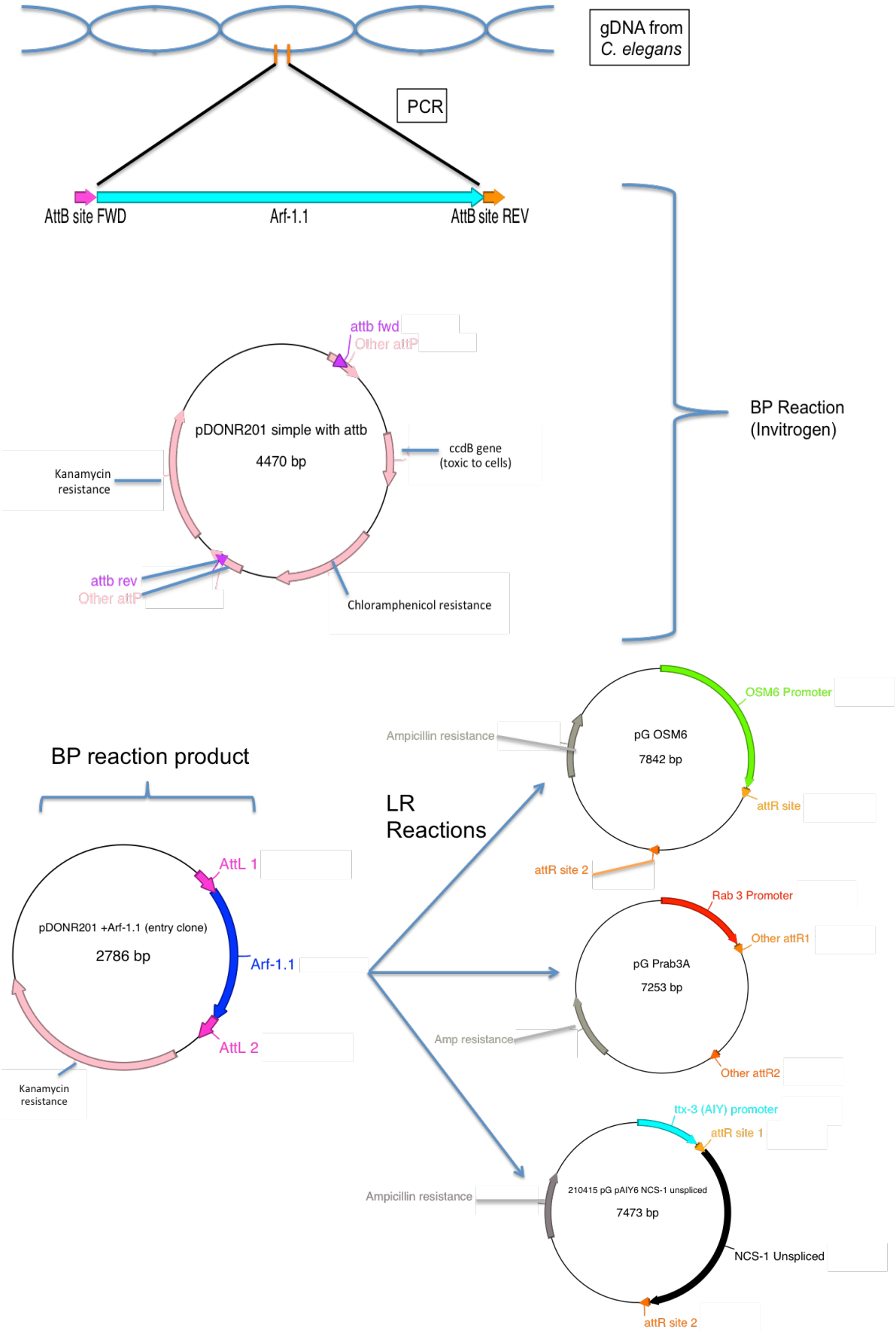
gDNA from
C. elegans
PCR
AttB site FWD
Arf-1.1
AttB site REV
attb fwd
Other attP
pDONR201 simple with attb
4470 bp
ccdB gene
(toxic to cells)
Kanamycin
resistance
attb rev
Other attP
Chloramphenicol resistance
BP Reaction
(Invitrogen)
BP reaction product
AttL 1
pDONR201 +Arf-1.1 (entry clone)
2786 bp
Arf-1.1
AttL 2
Kanamycin
resistance
LR
Reactions
Ampicillin resistance
pG OSM6
7842 bp
OSM6 Promoter
attR site
attR site 2
Rab 3 Promoter
Other attR1
pG Prab3A
7253 bp
Amp resistance
Other attR2
ttx-3 (AIY) promoter
attR site 1
Ampicillin resistance
210415 pG pAIY6 NCS-1 unspliced
7473 bp
NCS-1 Unspliced
attR site 2

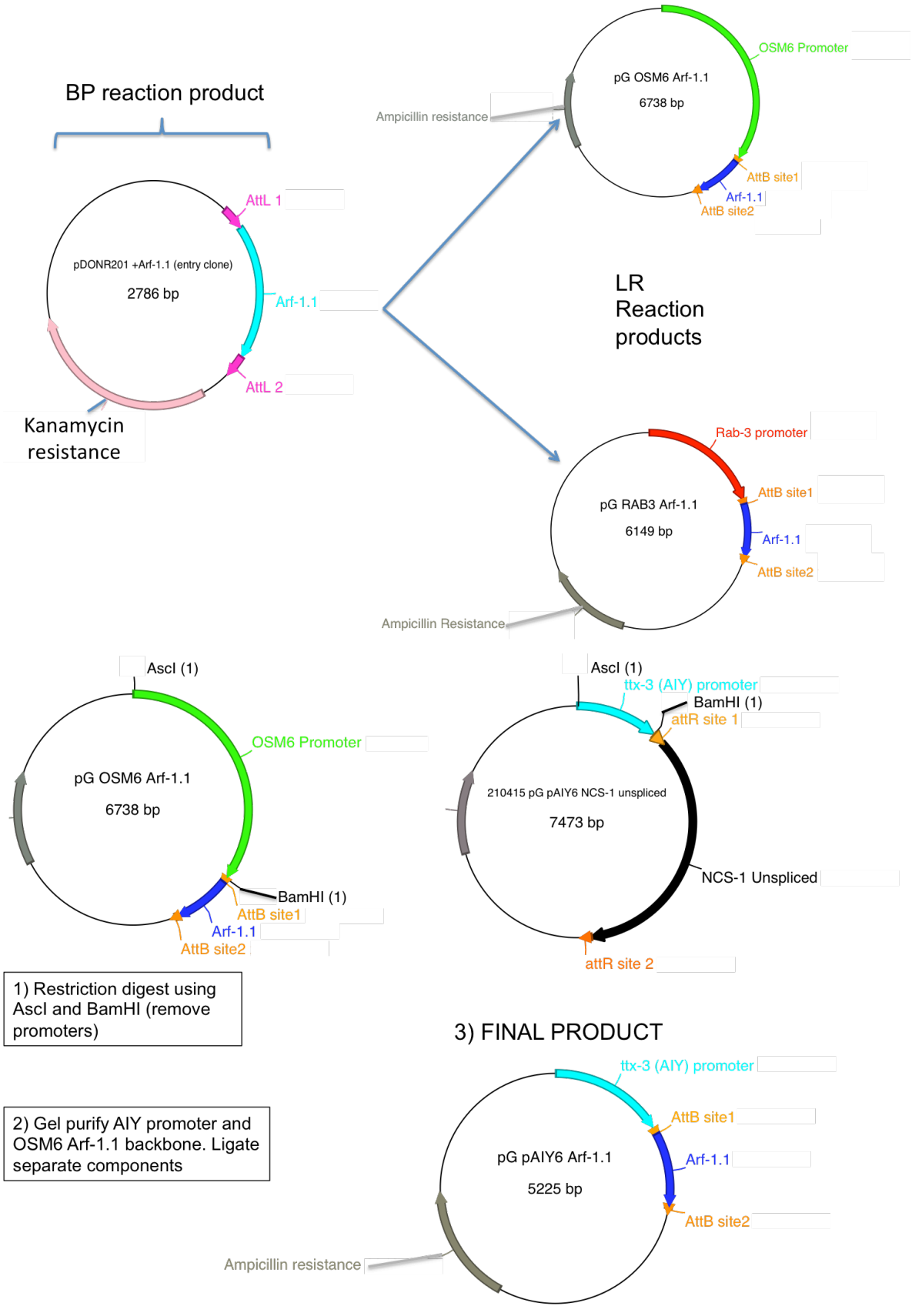
BP reaction product
pDONR201 +Arf-1.1 (entry clone)
2786 bp
AttL 1
Arf-1.1
AttL 2
Kanamycin resistance
pG OSM6 Arf-1.1
6738 bp
OSM6 Promoter
Ampicillin resistance
AttB site1
Arf-1.1
AttB site2
LR Reaction products
pG RAB3 Arf-1.1
6149 bp
Rab-3 promoter
AttB site1
Arf-1.1
AttB site2
Ampicillin Resistance
AscI (1)
pG OSM6 Arf-1.1
6738 bp
OSM6 Promoter
BamHI (1)
AttB site1
Arf-1.1
AttB site2
AscI (1)
ttx-3 (AIY) promoter
BamHI (1)
attR site 1
210415 pG pAIY6 NCS-1 unspliced
7473 bp
NCS-1 Unspliced
attR site 2
1) Restriction digest using AscI and BamHI (remove promoters)
2) Gel purify AIY promoter and OSM6 Arf-1.1 backbone. Ligate separate components
3) FINAL PRODUCT
pG pAIY6 Arf-1.1
5225 bp
ttx-3 (AIY) promoter
AttB site1
Arf-1.1
AttB site2
Ampicillin resistance

Figure 2.2 Formation of p[*rab-3*::*arf-1.*1], p[osm-6::*arf-1.*1] and p[ttx-3::*arf-1.1*]: Standard PCR and restriction digest techniques were utilized to form specific rescue constructs for *arf-1.1* under different promoters. *Arf-1.1* with attB sites was first incorporated into pDONR201 using a BP reaction followed by LR reactions to transfer this into constructs with specific neuronal promoters. Figures produced made using A Plasmid Editor (APE). Plasmids utilized as part of over-expression experiments.

2.2.9 Microinjection

All injections were carried out by Dr. Hannah McCue. Larval stage 4 to Day 1 adult *C. elegans*, including N2, XA406 (*qa401*) (*ncs-1* null), RB1535 (*arf-1.1* null) and AMG149 (*ncs-1 / arf-1.1* null double mutant) were injected using a micropipette needle into their germline cells present within the dorsal gonad. Injection mixtures contained a final concentration of 100 ng/µl DNA. Of this 100 ng, 10 ng/µl was the plasmid of interest (*ncs-1* or *arf-1.1* expression plasmid), 40 ng/µl of GFP marker plasmid and 50 ng/µl of empty pBluscript plasmid (Stratagene), the final volume was made up to 100 µl using dH_2O.

For the purposes of injecting, animals were initially immobilized onto a coverslip coated in a 2% agarose pad and coated with halocarbon oil. Visualisation of the *C. elegan*s for injection used a Nikon Eclipse Ti-S inverted microscope at 20x objective magnification and an Eppendorf micromanipulator was used for positioning of the needle. Animals were re-hydrated after injection by soaking in M9 buffer and transferred to a seeded NGM plate.

Plates were checked for GFP expression observed in progeny. Multiple lines were isolated by transferring single F1 GFP expressing progeny to individual plates, GFP expression in the F2 generation confirmed incorporation of the extra chromosomal plasmid within the animals. Where possible, three separate lines for each plasmid injection were generated and their phenotypes assessed.

Strain injected	Plasmid of interest injected	Neuronal expression	Plasmid with GFP marker	Neuronal expression of GFP	Number of Lines created	Produced by:
N2	$p_{rab\text{-}3}$::*arf-1.1* (40 ng)	All neurons	$p_{rab\text{-}3\text{-}a}$::GFP	All neurons	4	Dr. Hannah McCue
N2	P_{ttx3}::*arf-1.1* (40 ng)	AIY neurons	$p_{rab\text{-}3\text{-}a}$::GFP	All neurons	3	Dr. Hannah McCue
RB1535	$p_{rab\text{-}3}$::*arf-1.1* (40 ng)	All neurons	$p_{rab\text{-}3\text{-}a}$::GFP	All neurons	6	Dr. Hannah McCue
RB1535	P_{osm6}::*arf-1.1* (40 ng)	Sensory neurons	$p_{rab\text{-}3\text{-}a}$::GFP	All neurons	4	Dr. Hannah McCue
N2	$p_{rab\text{-}3}$::*arf-1.1* (10 ng)	All neurons	$p_{rab\text{-}3\text{-}a}$::GFP	All neurons	3	Dr. Hannah McCue
N2	P_{ttx3}::*arf-1.1* (10 ng)	AIY neurons	$p_{rab\text{-}3\text{-}a}$::GFP	All neurons	3	Dr. Hannah McCue
XA406	P_{ttx3}::*arf-1.1* (10 ng)	AIY neurons	$p_{rab\text{-}3\text{-}a}$::GFP	All neurons	4	Dr. Hannah McCue
RB1535	$p_{rab\text{-}3}$::*arf-1.1* (10 ng)	All neurons	$p_{rab\text{-}3\text{-}a}$::GFP	All neurons	3	Dr. Hannah McCue
RB1535	P_{ttx3}::*arf-1.1* (10 ng)	AIY neurons	$p_{rab\text{-}3\text{-}a}$::GFP	All neurons	5	Dr. Hannah McCue
AMG149	$p_{rab\text{-}3}$::*arf-1.1* (10 ng)	All neurons	$p_{rab\text{-}3\text{-}a}$::GFP	All neurons	5	Dr. Hannah McCue
AMG149	P_{ttx3}::*arf-1.1* (10 ng)	AIY neurons	$p_{rab\text{-}3\text{-}a}$::GFP	All neurons	4	Dr. Hannah McCue
AMG149	P_{ttx3}::*ncs-1* (10 ng)	AIY neurons	$p_{rab\text{-}3\text{-}a}$::GFP	All neurons	5	Dr. Hannah McCue

Table 2.4: Transgenic strains produced through microinjection: Injected *C. elegans* strains with over-expression neuronal targeted constructs encoding *arf-1.1* and *ncs-1*. Neuronal targeting sequences using pan-neuronal (rab-3), sensory neurons (osm-6) and AIY specific (ttx-3) promoters. All injections were carried out by Dr. Hannah McCue with GFP expressing progeny identified in later generations by myself.

2.2.10 Imaging

Transgenic *C. elegan*s with confirmed visual GFP expression or wild-type and null strains were immobilized onto a microscope slide in a droplet of M9 buffer containing 10 mM Sodium Azide (NaN3) and a coverslip placed on top. Single animals were imaged using Nikon Eclipse Ti-S inverted microscope with x200 magnification lens. All imaging was completed on Day 1 animals. Fluorescence illumination of transgenic *C. elegans* was used for verification of extra-chromosomal GFP marker expression within injected *C. elegans* lines. Anatomical images of *C. elegans* were obtained using differential interference contrast (DIC).

2.3 C. elegans behavioural assays

2.3.1 Thrashing

Locomotion of the different *C. elegans* strains was completed as a measure of neuronal function. For this assay, day 1 adult hermaphrodite animals were transferred into a 50 µl droplet of Dent's solution (140 mM NaCl, 6 mM KCl, 1 mM $CaCl_2$, 1 mM $MgCl_2$, 5 mM HEPES, pH 7.4 supplemented with 0.1 mg/ml BSA). Individual *C. elegans* were allowed to acclimitise to the Dent's solution for 10 minutes before thrashing rate was quantified. Thrashing was defined as one sinusoidal movement of the animal. Thrashing was measured over a 1 minute period for each individual animal. All experiments were completed at room temperature (~22^{o}C), using *C. elegans* cultivated at 20^{o}C. Animals were first placed onto an unseeded NGM plate to remove any excess OP50 *E. coli* prior to locomotion being tested.

Thrashing here was defined as a complete movement of the head and tail from one side of the animal, across the midpoint and back to the same side of the animal (Ventral to Dorsal and back to Ventral classes as one thrashing motion). Animals which attempted to thrash but failed to pass over the midline and back to the original position were classed as not thrashing. N2 animals were tested on each experimental day, alongside strains of interest. .

2.3.2 Temperature Dependent Locomotion Assay

Initial research in the laboratory looked at temperature dependent locomotion of *C. elegans* by investigating the number of thrashes per minute of *C. elegans* before and after exposure to heightened temperatures (Edwards et al., 2012, Martin et al., 2013). During the course of this investigation a novel paralysis phenotype was identified which a new temperature dependent locomotion assay (TDLA) was utilized for analyzing this phenotype (Todd et al., 2016).

A 35 mm petri dish lid was placed onto a Peltier effect thermoelectric plate (TEtech) to which a 150 µl droplet of Dent's solution was added. Temperature throughout the assay was monitored manually and altered using a thermocoupler and recorded in real-time. Approximately 5, day 1 to day 2 *C. elegans* were placed into the Dent's solution at room temperature (~20^{o}C ±0.5) and left to acclimitise for 5 minutes.

The Dent's solution was then heated to 27^{o}C at which point the timer was started manually. The temperature was allowed to rise to a final temperature of 28.5^{o}C (±0.3). Two different parameters were measured for this assay, firstly the time to paralysis; defined as a complete cessation of motility using thrashing as a measure of locomotion. Preliminary research identified that the paralysis phenotype was temporary and *C. elegans* recovered thus leading to the second parameter; the duration of paralysis. Times for onset and end of paralysis were noted for each individual *C. elegans* within each assay in minutes and seconds before being converted into seconds for each parameter. Duration of paralysis was calculated by subtracting the onset of paralysis time from the end of paralysis time (both in seconds). On each experimental day, N2 animals were tested as well as test strains, this served to remove extraneous variables and also to reduce bias. Animals strains were blinded prior to experiments being conducted.

2.4 Effect of a PI4K inhibitor (PIK-93) on C. elegans TDLA

C. elegans were treated acutely in the presence of a PI4K inhibitor (PIK-93). Initial experiments were completed using DMSO as a control at different concentrations and different time points to elucidate an optimal treatment period and drug concentration.

Later experiments exposed *C. elegans* to PIK-93 over a 1 hour time period in the presence of either 19 nM or 19 µM PIK-93 before undergoing the TDLA as outlined previously. PIK-93 was dissolved into Dent's solution using 1 % DMSO which was also present in the control untreated *C. elegans* assays. *C. elegans* were investigated for their time to paralysis and duration of initial paralysis.

2.5 Extraction of RNA and cDNA synthesis

For each sample, 100 individual adult *C. elegans* were picked into 100 µl RNase-free water into a 1.5 ml Eppendorf tube, *C. elegans* suspension was then centrifuged to the bottom of the tube and 400 µl of Trizol was added. *C. elegans* and Trizol suspension was vortexed for 2 minutes before being frozen overnight at -80 ^{o}C. When all the samples were collected, these were thawed at 37 ^{o}C before being shaken for 40 minutes on an orbital shaker at 4 ^{o}C. A further 200 µl of Trizol® was added, tube quickly vortexed prior to being left at room temperature for 5 minutes, 140 µl of Chloroform was subsequently added before vortexing and left at room temperature for 3 minutes.

The *C. elegans*, Trizol® and Chloroform suspension was subsequently centrifuged at 12,000 x G for 15 minutes at 4 ^{o}C and the top layer (~200 µl) was carefully transferred to a fresh 1.5 ml Eppendorf. To which an equal volume of Chloroform was added prior to centrifugation (12,000 x G for 5 minutes at 4 ^{o}C). Aqueous layer was removed (~200 µl) and placed in a fresh 1.5 ml Eppendorf. RNA precipitated using an equal volume of 70 % Ethanol in RNase-free water. Final suspension transferred to a Qiagen RNeasy spin column with a 2 ml collection tube before centrifugation at 8000 x G for 15 seconds. Flow through was discarded and DNase treatment occurred using Qiagen RNase free DNase kit according to manufacturer's instructions. RNA was eluted into RNase-free water using manufacturer's instructions and quantified using a Nanodrop 1000 spectrophotometer (Thermo Fisher Scientific). Quantified RNA was synthesized into cDNA using GoScript^{TM} Reverse Transcription System (Promega) according to manufacturer's instructions, 5 µg of RNA was used and a final volume of 20 µl was produced.

2.6 Quantitative PCR (qPCR) analysis of C. elegans NCS-1 levels

The produced cDNA was required for qPCR analysis. From the cDNA, 1 µl per well was used with 9 µl of iTAQ Universal SYBR Green mastermix, containing forward and reverse primers, iTAQ and nuclease free water according to manufacturer's instructions (BioRad). A final volume of 10 µl per well was generated in a 96 well white wall qPCR plate (BioRad) and plate contents spun to the bottom of the wells through centrifugation. Plates were assayed using a CFXconnect (BioRad) machine; and fluorescence measured and quantified each cycle. Results were gathered and analysed omitting any results which failed to generate a signal. Results were compared against 3 internal controls and a final ΔΔct value and fold change compared to N2.

Chapter 3 Results: Investigating the interaction between NCS-1 and PQ-type (CaV2.1) Ca^{2+} channel

3.1 Introduction

The $Ca_V2.1$ class of Ca^{2+} channels is pivotal in exocytosis of neurotransmitters; modulation of these channels is therefore essential to ensure regulated release of neurotransmitters (Lian et al., 2014). Modulation of $Ca_V2.1$ channels is required to regulate Ca^{2+}-dependent responses to changes in levels of $[Ca^{2+}]_i$; including processes such as CDF and CDI. These processes allow the opening of $Ca_V2.1$ channels in response to increased $[Ca^{2+}]_i$ or inversely speeds up channel inactivation in the presence of high $[Ca^{2+}]_i$ (CDF and CDI respectively). To date, the interactions between $Ca_V2.1$ channels, specifically within their C-terminal domains and Ca^{2+} sensor proteins have been studied extensively with some mechanisms underlying CDF and CDI identified, the structural basis of the interaction remains to be fully elucidated.

Structurally, the $Ca_V2.1$ channel contains two specific conserved domains within its C-terminal cytoplasmic tail responsible for CaM binding. The first of these is an IQ related motif; which in regards to $Ca_V2.1$ is an IM domain (DeMaria et al., 2001). The second is a CaV specific CBD distal to the IQ motif (Lee et al., 1999). CaM modulates activity of $Ca_V2.1$ for short term synaptic plasticity (Leal et al., 2012, Mochida et al., 2008). Under low $[Ca^{2+}]_i$, CaM interacts with the IQ domain of open $Ca_V2.1$ channels using EF hands present within its C-terminal lobe as these have a higher affinity for Ca^{2+} than the N-terminal lobe EF hands. The N-terminal EF hands interact with the CBD after the $[Ca^{2+}]_I$ increases. Evidence suggests that a functioning C-terminal lobe is essential for CDF with a functional N-terminal lobe required for CDI and partially active in CDF (Lee et al., 2000, Lee et al., 2002, Lee et al., 2003, DeMaria et al., 2001).

PQ channel modulation by CaM appears to be more complicated than initially believed. Whilst a Ca^{2+}-dependent interaction is required in the C-terminus of CaM with the PQ-channel at the site of the IM domain, a Ca^{2+}-independent interaction between the N-terminus of CaM is required to stabilize the interaction (Lee et al., 2003). Precise residues of the IM domain which are required in order to bind to the N- and C- lobes of CaM have only partially been elucidated through crystal structures however these present contradicting evidence (Kim et al., 2008).

CaM shares a number of its binding partners with other Ca^{2+} sensor proteins, this is the case for PQ-type Ca^{2+} channels. This adds another layer of complexity onto this system. The CBD of the $Ca_V2.1$ Ca^{2+} channel interacts with CaBP1, in a Ca^{2+}-independent manner resulting in quicker CDI when compared to CaM (Lee et al., 2002).

Of the neuronal Ca^{2+} sensor proteins, VILIP-2 is a known interactor of the PQ type $Ca_V2.1$ Ca^{2+} channels. Through a Ca^{2+}-dependent interaction, VILIP-2 binds the CBD, competing with CaM for binding and results in a slower CDI, or through binding the IM domain, this enhances levels of CDF (Few et al., 2005, Lautermilch et al., 2005). Whilst NCS-1 has been shown to modulate PQ-type VGCCs, through a voltage-independent manner (Burgoyne and Weiss, 2001), the exact nature of this interaction has not been fully elucidated. A wealth of evidence suggests NCS-1 and PQ channels interact as NCS-1 assists in PQ channel facilitation in nerve terminals and decreases $Ca_V2.1$ Ca^{2+} currents (Tsujimoto et al., 2002, Few et al., 2005, Lautermilch et al., 2005).

In neurons, NCS-1 and PQ are present in presynaptic microdomains. Neurotransmitter release in *Drosophila* involves Frequenin 1 and 2 (Frq-1 & 2) and knockout of these proteins affected neurotransmitter release (Koizumi et al., 2002, Taverna et al., 2002, Dason et al., 2009, Dason et al., 2012). The current study aimed to identify the interaction between NCS-1 and PQ Ca^{2+} channels through Ca^{2+} signaling experiments. As NCS-1 is believed to interact with PQ at its IM motif, plasmid constructs with added myristoylation domains (taken from (Oz et al., 2013)) were utilized to study this interaction (Lian et al., 2014).

To identify an interaction between full length $Ca_V2.1$ and NCS-1 is experimentally problematic. To overcome the issue, a small section of the $Ca_V2.1$ channel was used. As the C-terminal domain of the intact PQ α-domain is normally anchored to the plasma membrane, a myristoyl domain was attached to the fragments; acting as a surrogate membrane anchor (Gomez et al., 2001, Jeromin et al., 2004).

The primary aim of the present study was to identify using different experimental measures whether NCS-1 and PQ-type channels directly interact as suggested

indirectly in previous studies (Tsujimoto et al., 2002, Weiss et al., 2000, Weiss and Burgoyne, 2001, Dason et al., 2009).

3.2 Results

3.2.1 Production of a plasmid encoding a C-terminal regulatory domain of the PQ Voltage Gated Ca^{2+} Channel.

The overall aim of this section of research was to investigate potential interactions between NCS-1 and the PQ VGCC. To do so, novel plasmids encoding fluorescent membrane targeted versions of rat PQ α subunit residues 1898-2035 (encompassing both the IM and CBD motifs (Mochida et al., 2008, DeMaria et al., 2001)) were created, in line with preliminary research suggesting the interaction occurs within this domain (Lian et al., 2014).

Myristorylation domains and PQ fragments were incorporated into empty parental colour tag vectors; forming myr-PQ tagged plasmids (Figure 3.1a). Plasmids were produced using specific restriction sites; positive plasmids were analysed through restriction digestion, identifying the presence of the myristoylation and PQ cassettes (Figure 3.1b). Restriction digests of the produced plasmids (mCh or YFP X-S (XhoI - SacII) and H-S (HindIII - SacII) respectively) were produced to establish the incorporation of the myristoylation domain (H-S) or the myr-PQ domain (X-S).

Plasmid expression in cells was analysed by transfecting HeLa cells with the produced constructs using two different transfection reagents, to determine whether this is reliably transfected to a sufficient degree, and samples lysed 24 hours post transfection. Transfected protein expression analysis was completed through Western blotting of cell lysates with anti-GFP (to detect myr-PQ-eYFP) and anti-RFP (to detect myr-PQ-mCh) antibodies (Figure 3.1c).

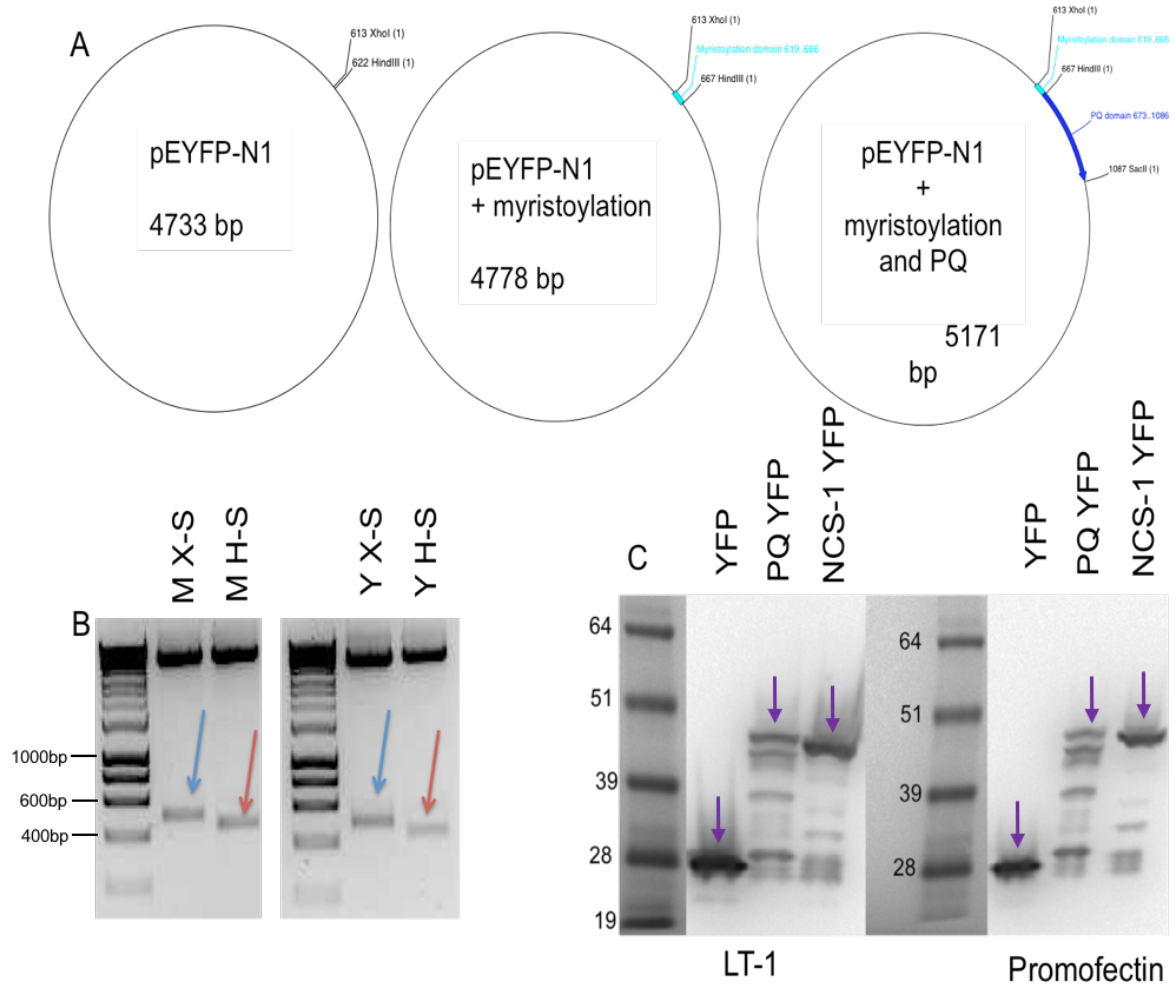

Figure 3.1: Production of plasmids containing Myristoylation domain and PQ fragment. **(A)** Diagrammatic form of process taken to form myr-PQ plasmids, a more physiologically relevant construct, from an empty N1 vector. **(B)** Presence of the myr-PQ domain was analysed through restriction digestion. Lanes 2 and 5 show the myristoylated PQ domain (~450 bp shift) with lanes 3 and 6 showing the myristoylated plasmid (~400 bp shift) further details in Figure 3.1A. Vectors were digested using HindIII with SacII (Myristoylation tagged insert (red arrows)) and XhoI with SacII (myr-PQ (blue arrows)), Market represented by Hyperladder 1kb. **(C)** Western blot showing lysates from transfected HeLa cells, using two different transfection reagents to test efficiency. Blotting for YFP to identify size of transfected proteins, Marker represented by See-blue 2-Plus Prestained (Invitrogen). Correct protein sizes highlighted with purple arrows.

The estimated protein size of YFP/ mCh is 26 kDa, with the myristoylation domain and PQ fragment each increasing the construct size by approximately 2 kDa and 11 kDa respectively. The estimated size of the myristoylated PQ construct is therefore 39 kDa. Colour tagged NCS-1 is ~48kDa (22 kDa for NCS-1 and 26 kDa for the colour tag). Figure 3.1c highlights that all expressed proteins migrated in the expected region of

the gel (between 39 and 51 kDa) by comparison with molecular weight standards. Altered protein migrations here are due to the addition of NCS-1 or myr-PQ (~22 kDa, lanes 3, 4, 7 and 8).

3.2.2 Localisation of myr-PQ-eYFP and myr-PQ-mCh in HeLa cells.

Localisation of myr-PQ plasmids (myr-PQ-mCh and myr-PQ-eYFP) was assessed through confocal microscopy following transfection into HeLa cells. HeLa cells are a commonly used mammalian cell line for protein localization studies due to their ease of transfection and clear morphology. Transfected proteins encoded by plasmids were present on internal-cellular membranes in addition to the plasma membrane, in line with the known localisation for NCS-1 due to its N-terminal myristoylation modification (Figure 3.2) (Jeromin et al., 2004, Ames et al., 2012, Heidarsson et al., 2013, Chen et al., 2001, Dason et al., 2009, de Barry et al., 2006, Gomez et al., 2001).

An unexpected but interesting phenotype was apparent when cells were co-transfected in that NCS-1, in the presence of myr-PQ, was observed in enlarged myr-PQ positive cellular inclusions absent from cells expressing NCS-1 in isolation. It should be noted that this aggregation phenotype was seen in a number of cells transfected with the myristoylated PQ fragment alone however this co-expression data suggests that NCS-1 traffics to the same aggregates in a myr-PQ dependent manner.

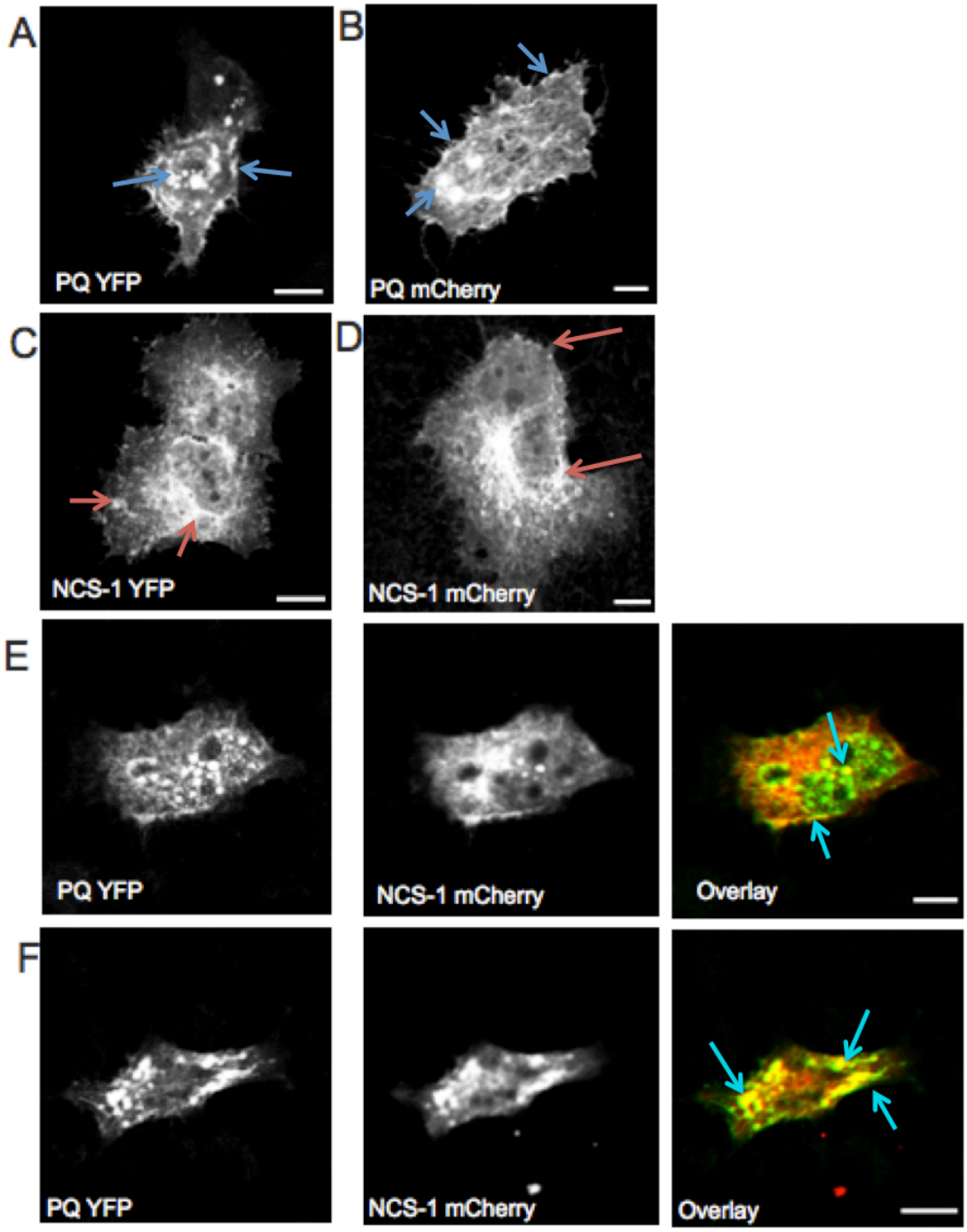

Figure 3.2: Cell localization of transfected protein constructs. Localisation of NCS-1, myr-PQ-eYFP and myr-PQ-mCh in HeLa cells. (A and B) HeLa cells transfected with myr-PQ-eYFP **(A)** and myr-PQ-mCh **(B)** to study cellular localization. Cells were transfected 24 hours post seeding and fixed 24 hours post transfection and imaged. Localisation of transfected constructs to plasma membrane and Golgi apparatus (blue arrows). **(C and D)** show representative images for NCS-1 localisation within cells for the YFP **(C)** and mCh **(D)** tagged constructs, present on cellular membranes; likely the plasma membrane and trans-Golgi network (red arrows). **(E and F)** Evidence of apparent protein aggregation when co-expression of the PQ construct with NCS-1 within HeLa cells (light blue arrows). Scale bars within each panel represents 10 μm.

3.2.3 Effect of myristoylated PQ on the localization of well-established CaBPs.

Many studies have shown that other Ca^{2+} sensing proteins are able to modulate PQ signaling (DeMaria et al., 2001). In order to test the specificity of myr-PQ driven NCS-1 aggregation, the ability of myr-PQ to induce aggregation of other small EF hand containing Ca^{2+} sensing proteins was next examined. For these analyses, an mCh tagged CaM (CaM-mCh) the most widely studied small EF-hand containing Ca^{2+} sensor protein (DeMaria et al., 2001, Lee et al., 1999, Lee et al., 2002, Oz et al., 2013, Raghuram et al., 2012, Zhang et al., 1995), was transfected into HeLa cells alone or alongside myr-PQ-eYFP. When analysed, it was shown that CaM expressed alone exhibited its well characterized diffuse cytoplasmic distribution (Mangels and Gnegy, 1992, McGinnis et al., 1998, Mori et al., 2011). This was unaltered in CaM and myr-PQ-eYFP co-transfected cells (Figure 3.3).

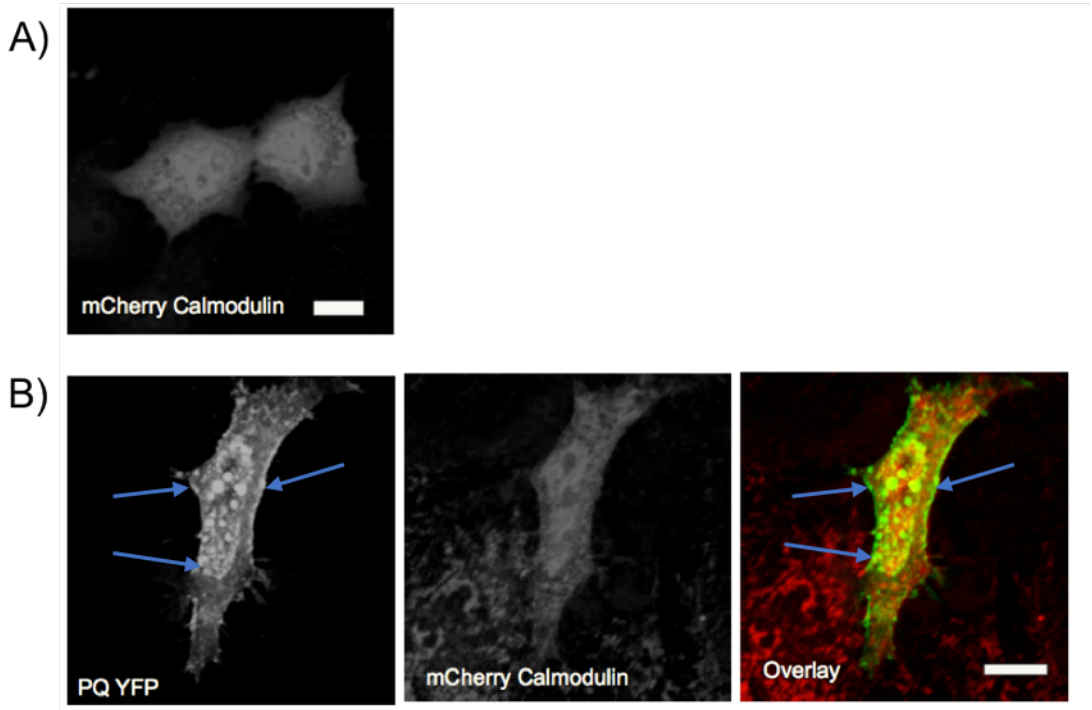

Figure 3.3: Effect of myristoylated PQ on localization of CaM. Fluorescence based microscopy was completed on HeLa cells transfected with mCh-CaM both solo transfected and in conjunction with myr-PQ-eYFP (see Figure 3.1). **(A)** HeLa cells were transfected with mCh CaM and fixed after 24 hours to show the localization of mCh CaM upon transfection into cells. **(B)** Effect of myr-PQ-eYFP on mCh CaM localisation, cells were transfected with 1 µg of each protein for a 24 hour transfection period before fixation in 4% Paraformaldehyde (PFA). Myr-PQ-eYFP localisation highlighted by arrows (blue arrows). Figures include representative images of cells. Scale bar here represents 10 µm.

3.2.4 Effect of myristoylated PQ on the localization of CaBP family members.

Due to the observed effects on the intracellular localization of NCS-1 and CaM the extent of myr-PQ promiscuity for other EF-hand containing small Ca^{2+} binding proteins were tested. Specific focus on CaBP1 and CaBP7; both of which are present on cell membranes, including the Golgi and PM, due to an N-terminal myristoylation sequence or a C-terminal tail anchor respectively (Few et al., 2005, McCue et al., 2009, McCue et al., 2011, McCue et al., 2012). CaBP1 has in previous research been suggested to interact and regulate Ca^{2+} channels including the PQ VGCC (Lee et al., 2002, Wingard et al., 2005, Haynes et al., 2006).

CaBPs localised as expected to cellular membranes (plasma and Golgi membranes) when expressed in HeLa cells (Figure 3.4A) (McCue et al., 2009, McCue et al., 2011, Haynes et al., 2006, Haynes et al., 2012a). Transfection of myr-PQ-eYFP with CaBP1 showed no evidence of co-localisation in enlarged aggregates, similar to previous observed for NCS-1 and CaM (Figure 3.4B). CaBP7 localised to the PM and Golgi (McCue et al., 2009).

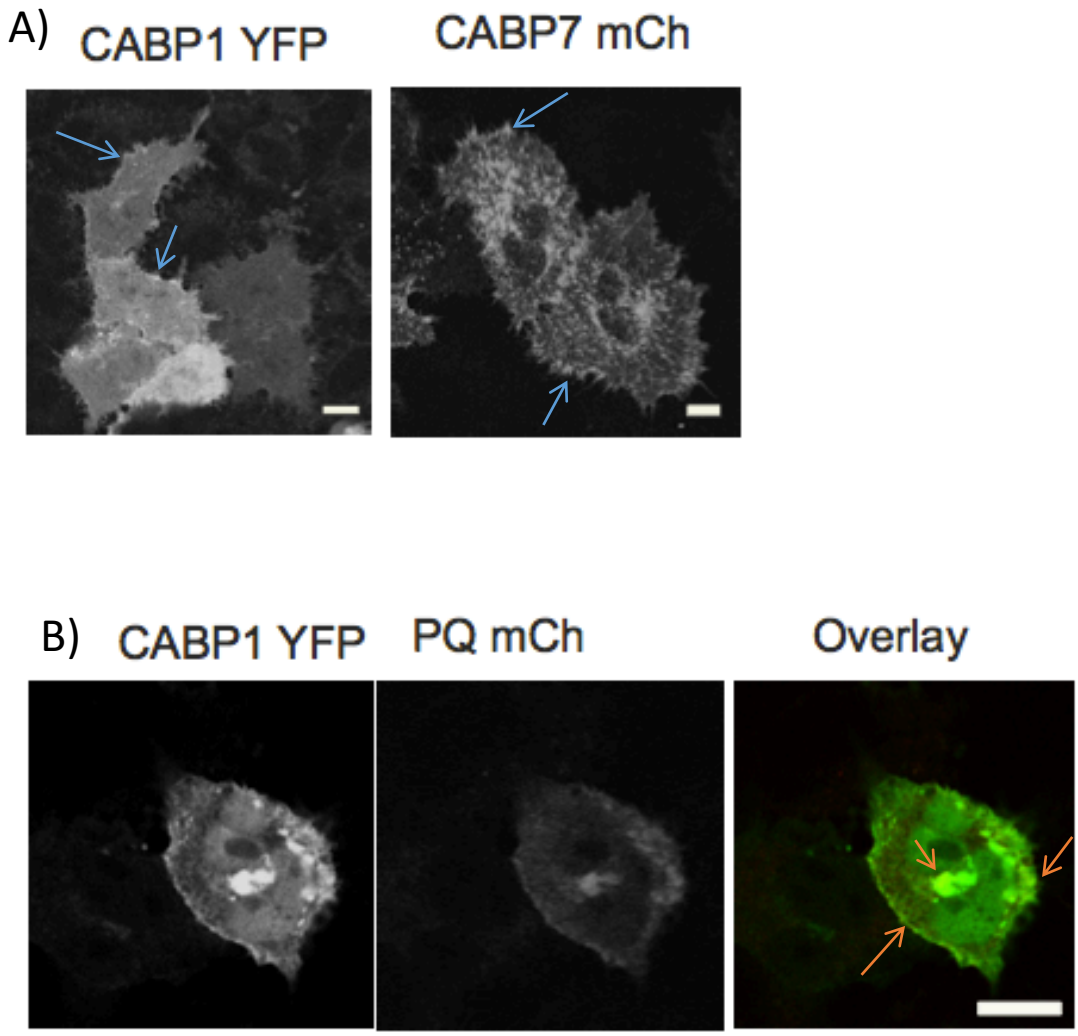

Figure 3.4: Myristoylated PQ and its effect on CaBP protein family members. Fluorescence based microscopy was used on transfected HeLa cells to identify the localization of protein constructs and the effect co-transfection had upon their localization. **(A)** HeLa cells transfected with CaBP1 YFP (left) and CaBP7 mCh (right). CaBP1 has an N-terminal myristoylation site, targeting this to cellular membranes. CaBP7 has a C-terminal Transmembrane domain targeting this also to cell membranes (localisation indicated by blue arrows). **(B)** HeLa cells co-transfected with CaBP1 YFP and myr-PQ-mCh, transfected proteins are localized around the periphery of the cell with some areas of overlap (red arrows). Images of co-transfected CaBP7 mCh with PQ YFP were difficult to identify within cells. Scale bar represents 10 μm.

3.2.5 Testing of constructs in Neuronal cell line (N2A Mouse Neuroblastoma cell line)

Since NCS-1 is enriched in neuronal tissues and the PQ type VGCC is a neuronal specific protein, additional studies were undertaken to examine their interactions in a neuronal cell culture model (Burgoyne and Weiss, 2001, Chen et al., 2001, Dason et al., 2012, Lian et al., 2014, Dragicevic et al., 2014, Burgoyne, 2007, Burgoyne and Haynes, 2012). N2A cells were cultured in a similar manner to HeLa cells and followed the same transfection protocol. Differentiation of N2A cells was completed as described in previous studies using either retinoic acid (Mao et al., 2000) or by serum starvation of cells to stimulate neurite outgrowth (Biernat et al., 2002).

N2A cells were co-transfected with myr-PQ-eYFP, myr-PQ-mCh and NCS-1 expressing constructs to monitor protein localisation. As observed in HeLa cells, aggregate structures were formed in the presence of myr-PQ; the NCS/ CaBP proteins under co-expression with myr-PQ preferentially targeted to these structures as opposed to their normal locations. This suggests the phenomena is cell type independent.

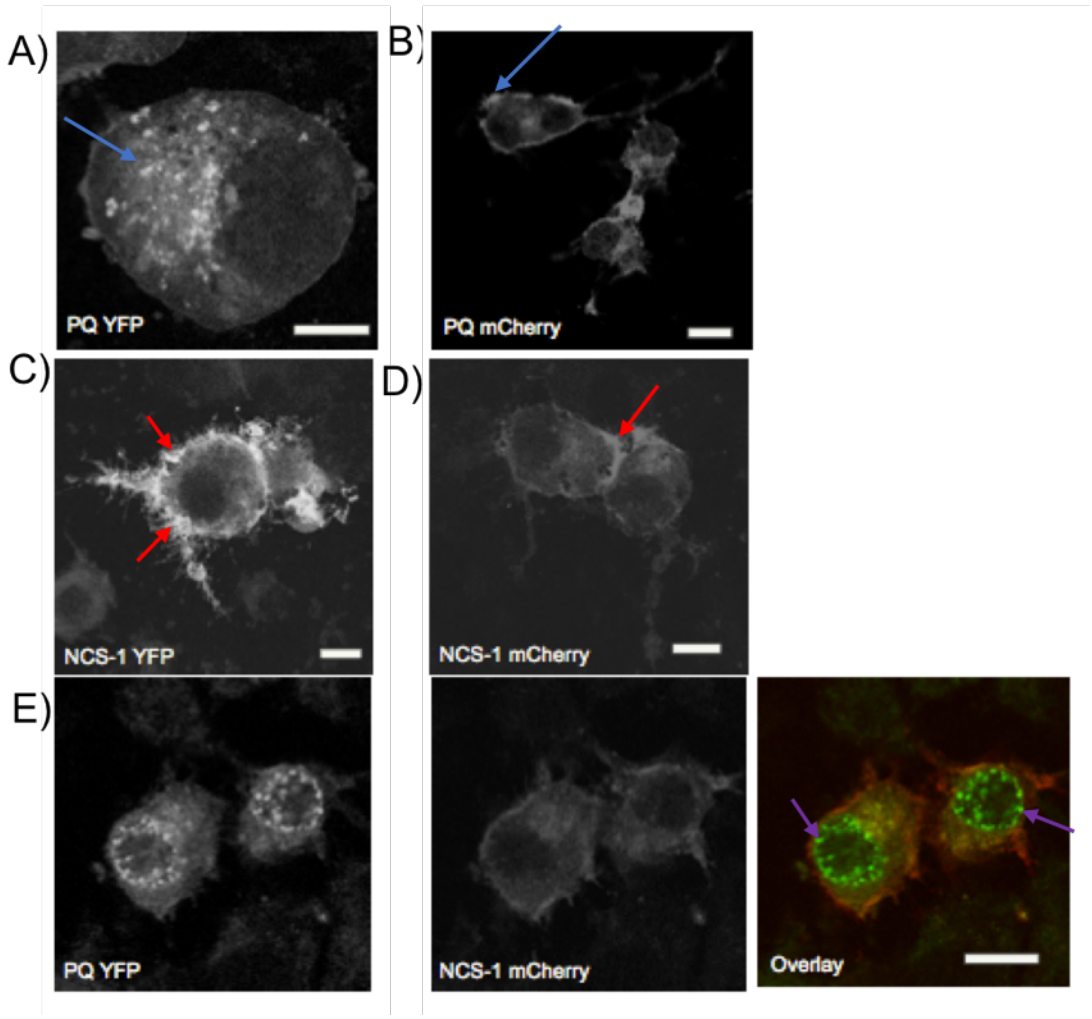

Figure 3.5: Protein localization within a Neuronal cell line (N2A). Plated N2A cells were transfected with protein expression constructs. **(A-D)** N2A cells transfected with (A) myr-PQ-eYFP localized to cell membranes, (B) myr-PQ-mCh also localized to cell membranes (blue arrows), (C) NCS-1 YFP, (D) NCS-1 mCh. In panel C) NCS-1 YFP, localized to cell membranes due to its N-terminal myristoylation site and D) NCS-1 mCh, localized to cell membranes, each when transfected into N2A cells (red arrows). E) Co-transfection of PQ YFP with NCS-1 mCh, presented evidence of co-aggregation within internal structures (purple arrows). Scale bars equivalent to 10 μm.

In transfected N2A cells, transfected proteins localised in all cases (Figure 3.5 A-D) to cell membranes, similar to results gathered from transfected HeLa cells.

Each cell line was treated in the same manner to minimize extraneous variables. Co-transfection of NCS-1 mCh with myr-PQ-eYFP suggested the presence of aggregate, also present in co-transfected HeLa cells. Based on the experiments previously

described, evidence for a potential interaction between NCS-1 and PQ constructs can be suggested.

3.2.6 Effect of myristoylated PQ on related CaM localization in N2A cells.

As CaM is a ubiquitously distributed, well known Ca^{2+} binding protein, the effect Myr-PQ had on its localization within cells was of interest, to ensure no spurious protein translocations were in effect in these cells and to dismiss claims of cell specific responses. N2A cells were transfected with mCh-CaM alone and in conjunction with myr-PQ-eYFP. CaM expressed in N2A cells exhibited a diffuse cytoplasmic localization due to the absence of any membrane targeting motifs, which was unaffected by myr-PQ-eYFP cotransfection (Figure 3.6).

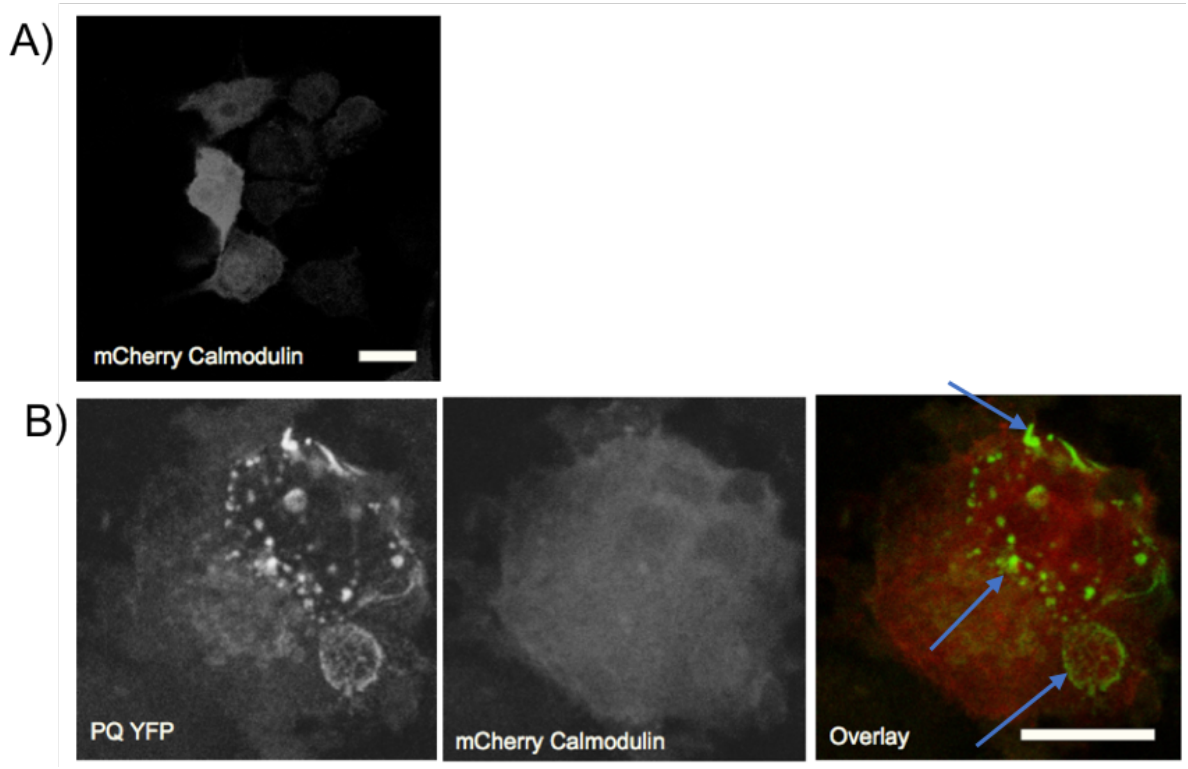

Figure 3.6: Effect of myristoylated PQ on CaM localization in N2A cells. N2A cells were transfected with mCh CaM both on its own and co-transfected with myr-PQ-eYFP. **A)** N2A cells transfected with mCh CaM showing ubiquitous cytoplasmic localisation of the transfected protein. **B)** N2A cells co-transfected with PQ YFP and mCh CaM show similar protein localisations to that shown in HeLa cells, here we see an odd protein localization for PQ YFP around the nuclear envelope (highlighted with arrows) with some evidence of this on the cell periphery. Little effect in regards to altering CaM localization can be identified. Scale bar represents 10 μm; images shown are representative of a wider collection of images.

3.2.7 Effect of co-expression of myr-PQ-eYFP and myr-PQ-mCh on CaBP family members in N2A cells.

Based on previous experiments (Figure 3.4), it is possible that myr-PQ has a slight effect on localisation of CaBP family members. To investigate this possibility further, CaBP1 and CaBP7 localisation were monitored in the presence of myr-PQ following transfection into N2A cells, similar to previous experiments in HeLa cells.

As in HeLa cells; following co-transfection into N2A cells, evidence of co-localisation can be noted (Figure 3.7, yellow regions of interest) between the two inversely colour tagged protein constructs. Cells were imaged using fluorescence microscopy after fixation in 4% PFA. CaBP7 represents a good comparator for NCS-1 under expression in N2A cells as both are neuronally expressed, are known modulators of PI4K and are each localised to cellular membranes.

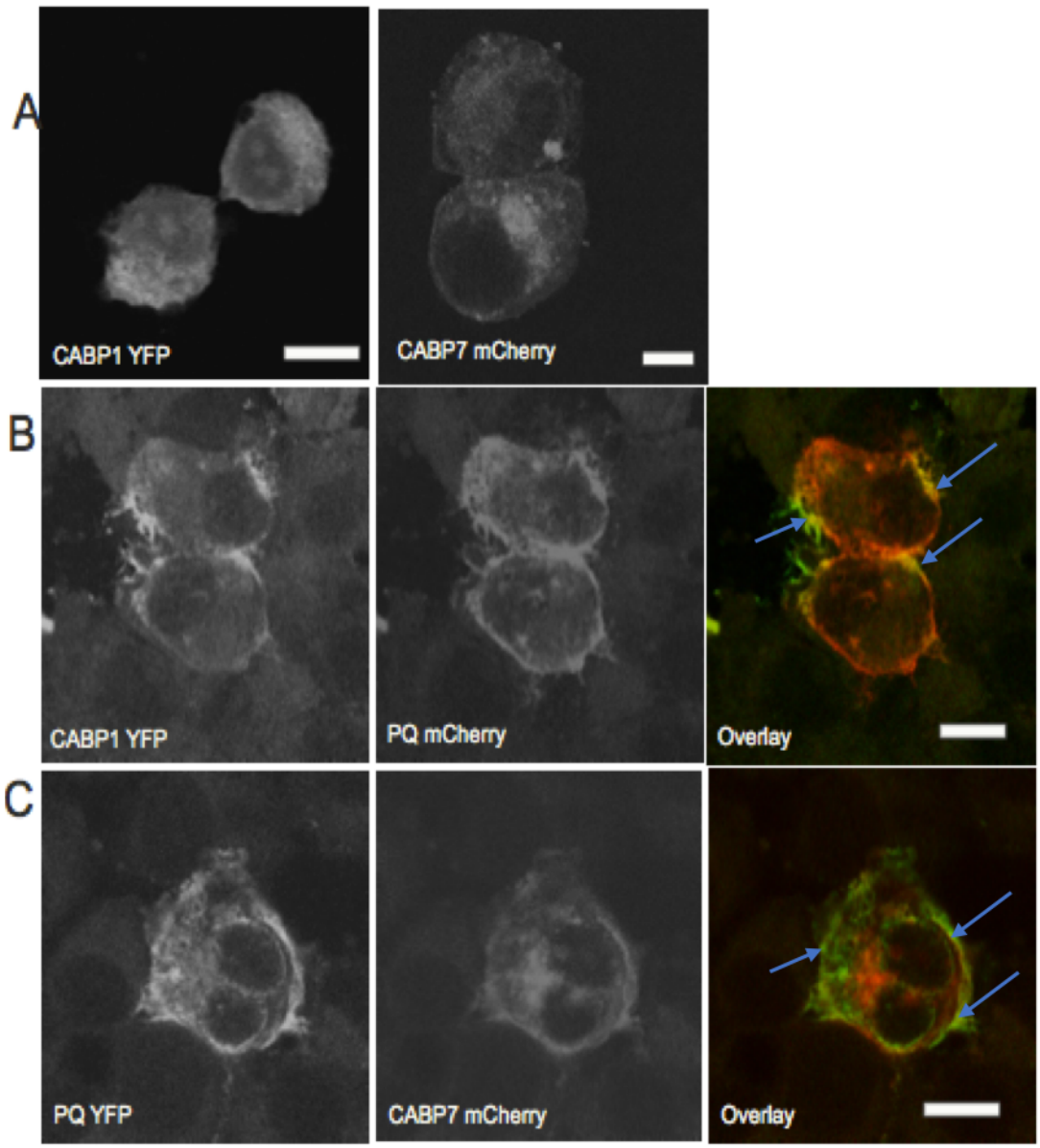

Figure 3.7: Myristoylated PQ and its effect on CaBP protein family members. N2A cells were transfected with CaBP and Myr-PQ constructs (A and B) and fixed after 24 hours. Fluorescence based microscopy was used on transfected N2A cells to identify the localization of protein constructs and the effects of co-transfection on their localization. **A)** N2A cells transfected with CaBP1 YFP (left) and CaBP7 mCh (right). **B)** N2A cells co-transfected with CaBP1 YFP and myr-PQ-mCh. The myr-PQ-mCh shows localisation around the periphery of the cell, as is found for CaBP1 YFP with distinct areas of overlap (blue arrows). **C)** N2A cells co-transfected with myr-PQ-eYFP and CaBP7 mCh evidence of co-localisation on cell membrane (blue arrows). Scale bar represents 10μm.

N2A cell protein localisation analyses were not as conclusive as those from HeLa cells, however evidence for limited domains of co-localisation between the NCS proteins and myr-PQ were evident in transfected cells. Transfected proteins showed

localisations consistent with those observed in previous studies (McCue et al., 2009, McCue et al., 2011, McCue et al., 2012) with proteins localizing to cellular membranes. Partial aggregation for the Myr-PQ construct was seen with some evidence of potential co-localisation with CaBP family members, albeit absent from aggregation structures.

The CaBP family has been studied intensely and their localisation mapped (McCue et al., 2009, McCue et al., 2010b, Haynes et al., 2006, Haynes et al., 2012a). Co-expression of Myr-PQ and the CaBP constructs suggested some evidence of co-localisation however as these were not present in aggregate structures, this indicates that these constructs may interact however not sufficiently enough in N2A cells to remove CaBP family members from the PM (Figure 3.7B and C).

Aggregation structures identified through the course of this research were investigated further within transfected HeLa cells, this will be addressed later in this chapter. Whilst preliminary studies indicted a potential cellular interaction between different CaBPs and the PQ channel subunit, only the novel interaction with NCS-1 was pursued in further detail.

3.2.8 Testing for protein interactions within transfected HeLa cells

Preliminary research suggests that PQ and NCS-1 co-localize and interact within cells (Lian et al., 2014), evidence gathered from this research supports previous research of co-localisation in different cell lines. Kinetic profiles for NCS-1 within live cell experiments have been completed previously (Handley et al., 2010). To investigate whether myr-PQ and NCS-1 interactions were able to alter the kinetic profiles of proteins during translocation, fluorescence profiles were monitored during various live cell experiments treated with 2 μM Ionomycin, 5 μM Thapsigargin or 100 μM Histamine as described in previous research (Handley et al., 2010).

To investigate the potential interactions, and whether this is indicative of *in-vivo* interactions, between NCS-1 and the Myr-PQ constructs, HeLa cells were transfected and imaged using confocal microscopy, as described previously. Collectively three independent methods of investigation were utilized in this research in order to establish whether these proteins were interacting (Lian et al., 2014).

These methods were: 1) Förster Resonance Energy Transfer (FRET); 2) Fluorescence Restoration After Photobleaching (FRAP) and 3) Fluorescence Loss In Photobleaching (FLIP) (Figure 3.8). Firstly, FRET was utilised to measure interactions between a donor and an acceptor fluorophore. Each of these live cell experimental procedures aimed to establish a cellular interaction between myr-PQ and NCS-1.

Secondly FRAP was measured to identify the restored fluorescence in a bleached region of a cell due to protein shuttling between 'pools of protein'. Thirdly experiments using FLIP (a similar method to FRAP) were carried out to measure fluorescence loss from an unbleached region of a cell (inverse study to FRAP). Bleaching of fluorescent proteins allows studies on the energetics of restoration.

Since little is known in regarding the cellular dynamics of the Myr-PQ construct, the present study aimed to determine the kinetic behaviour of these constructs and to identify any changes in these parameters on co-expression with NCS-1.

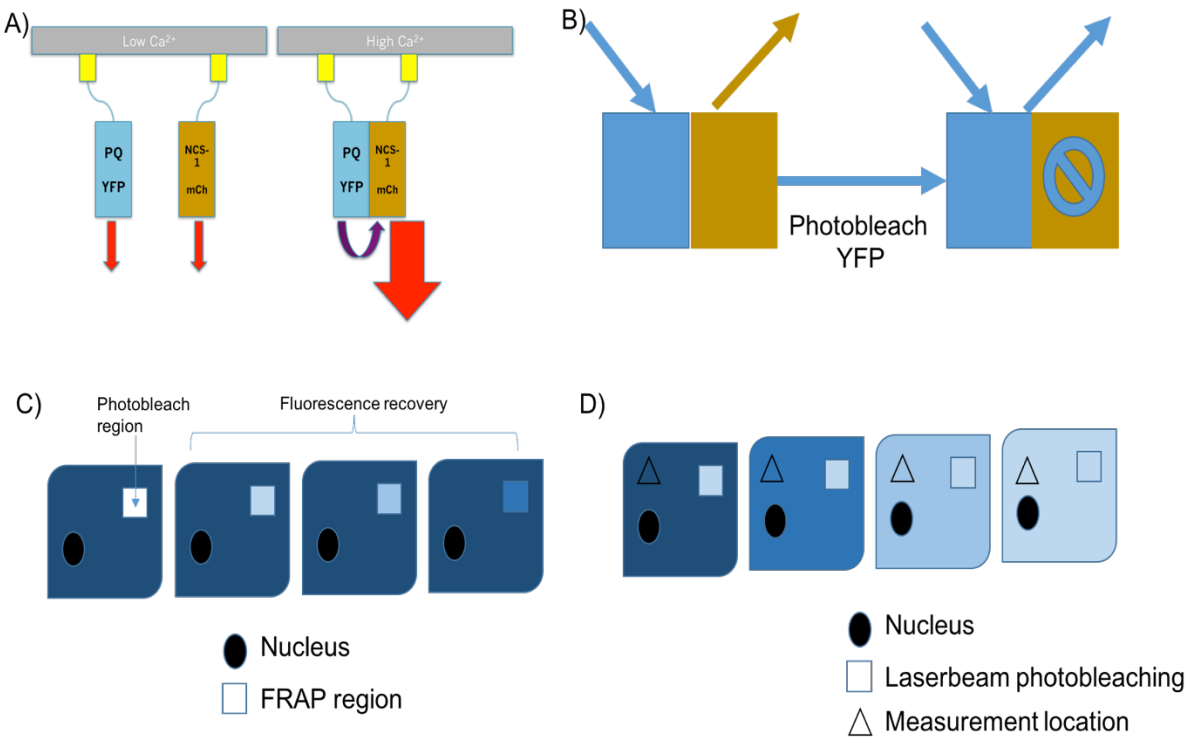

Figure 3.8: Mechanism of interaction studies within live cell experiments. Interaction studies look at a change in fluorescence when two or more proteins interact. A) An example of Ca^{2+}dependent interaction based FRET. When under low Ca^{2+} concentrations (left) the two proteins are unable to interact, both fluoresce when excited by their specific light wavelengths. When under high Ca^{2+} concentrations (right), the transfected proteins undergo conformational shifts, allowing interactions at specific points. Interactions allow colour tags to move closer and allows energy transfer. B) An example of acceptor bleaching FRET, upon exciting CFP as the donor an emission of YFP (left) occurs; under acceptor bleaching emission is through CFP. C) Stages of FRAP over time. A laser excited region of the cell measures recovery of fluorescence over time following photobleaching. D) Stages of FLIP over time. Continuous laser excitation measures decreases in cellular fluorescence following extended photobleaching.

3.2.9 Testing intermolecular FRET between PQ and NCS-1 within transfected HeLa cells.

To identify protein-protein interactions between NCS-1 and Myr-PQ (as shown in recent research (Lian et al., 2014), HeLa cells were co-transfected with NCS-1 and Myr-PQ bound to opposite colour tags, investigating FRET kinetic profiles (Grant et al., 2008, Krebs et al., 2012).

Live cell HeLa experiments were conducted. Cells were transfected for 24 hours before imaging; on the day of imaging, cells were incubated in Krebs buffer (described in methods section) prior to imaging. Live cell experiment dishes were left to equilibrate to room conditions prior to testing. Various buffer/ drug combinations were perfused onto cells using a gravity flow system during imaging.

Perfusion experiments were carried out as described in the methods section using 1 µM Ionomycin, 5 µM Thapsigargin, 100 µM Histamine or 5 µM A23187. Representative images of the live cell experiments are shown (Figure 3.9) to identify protein interactions between myr-PQ-eYFP and NCS-1 mCh.

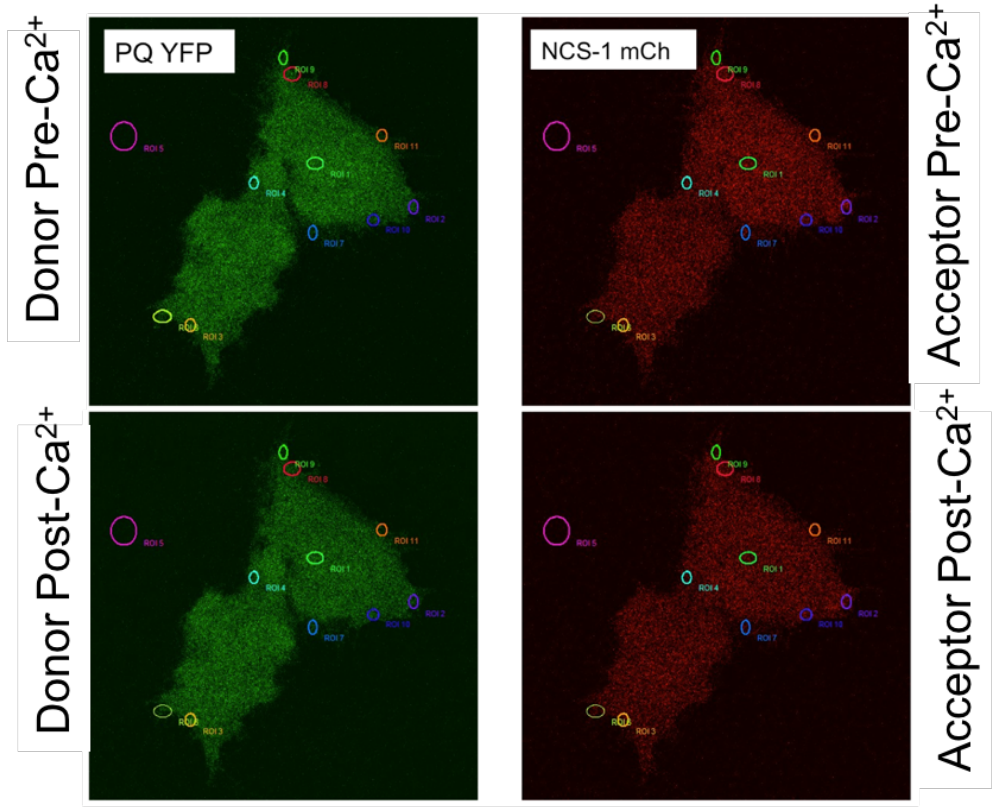

ROI	ROI_1	ROI_2	ROI_3	ROI_4	ROI_5	ROI_6	ROI_7	ROI_8	ROI_9	ROI_10	ROI_11
FRETeff (%)	0	0	2.52	0	12.56	0	12.41	0	0	12.97	0

Mean FRET: Background= 12.56%, Cellular= 2.54%. No reproducible FRET.

Figure 3.9: FRET in transfected HeLa cells: HeLa cells transfected with myr-PQ-eYFP (PQ YFP) along with NCS-1 mCh. FRET was completed by exciting the YFP channel (509nm) and measuring the emission from the mCh channel (620nm), using a set series of parameters as outlined in previous research (Handley et al., 2010). FRET measurements were compared to background FRET to establish whether these results were showing reproducible and reliable FRET signals.

Whilst evidence of co-localisation was noted in these live cell experiments, when comparing FRET levels (areas of co-localisation) to background regions of interest (ROIs), no reproducible FRET could be identified. Multiple ROIs were taken in each experiment compared to one 'background' ROI acting as a control. Identified cellular FRET was much lower than background FRET levels, suggesting this was not the optimum technique for identifying interactions between the co-transfected protein constructs. Current research was unable to identify a reproducible FRET signal. Monitoring protein-protein interactions using FRET is a sensitive process depending on several factors including orientation and spatial separation of the donor / acceptor fluorophores (1-10 nm). Further optimization of the FRET setup is needed for optimal FRET identification.

Multiple ROIs were derived from co-transfected HeLa cells, to measure FRET in numerous regions displaying co-localisation (Figure 3.9). These were compared with an ROI outside of the cell, acting as a background control. Analysis of the various FRET efficiencies shows that the control ROI 'Region 5', lying externally to the cell of interest, has a similar FRET efficiency to 'Regions 7 and 10' present on the plasma membrane of the co-transfected cells.

From this, present research sought to utilize alternative approaches to measure changes in protein interactions, kinetics and localisation through different methods of photobleaching fluorescence based techniques (FRAP and FLIP).

3.2.10 Testing intermolecular FRAP between PQ and NCS-1 within transfected HeLa cells.

With plasma membrane bound protein movement believed to be fluid (Karp, 2010, Cooper, 2000), live cell fluorescence techniques were utilized, to establish whether myr-PQ and NCS-1 interactions altered their membrane mobility. FRAP was first used here to study interactions and kinetic profiles of Myr-PQ and NCS-1 (Handley et al., 2010). As with the FRET experiments, transfected HeLa cells were incubated in Krebs buffer on the day of study and allowed to acclimitise prior to perfusion treatment.

To establish and record baseline fluorescence, the initial 10 frames (approximately 20 seconds) of the experimental series were recorded with perfusion of Krebs buffer, after

which ROIs containing the protein(s) of interest were then bleached for 10 frames, following which post-bleach ROIs were measured for the restored fluorescence (approximately 80 frames, equaling approximately 160 seconds). Multiple ROIs were collected for each cell and multiple cells were collected for analysis.

In order to establish whether restored fluorescence was affected by co-transfection, fluorescence restoration and kinetic profiles were first characterised within live transfected HeLa cells treated as described previously. The various traces for NCS-1 YFP FRAP studies were recorded and analysed with pre-bleach values set as '100%' and post-bleach values analysed in comparison to this for each of the cells measured in these experiments (Figure 3.10), mCh was co-transfected into cells to identify whether this affected kinetic profiles.

Building on previous research from within our laboratory which looked into the kinetic profile of NCS-1 during FRAP experiments (Handley et al., 2010), present research identified similar data, with a change in kinetic profiles being identified when constructs were co-transfected; indicating a potential interaction. The hypothesis for the present research was that interactions between myr-PQ and NCS-1 could alter the fluorescence restoration by altering protein mobility. For each analysed cell, the baseline FRAP profile for NCS-1 YFP was produced through averaging the collected traces from different ROIs present within the same cell.

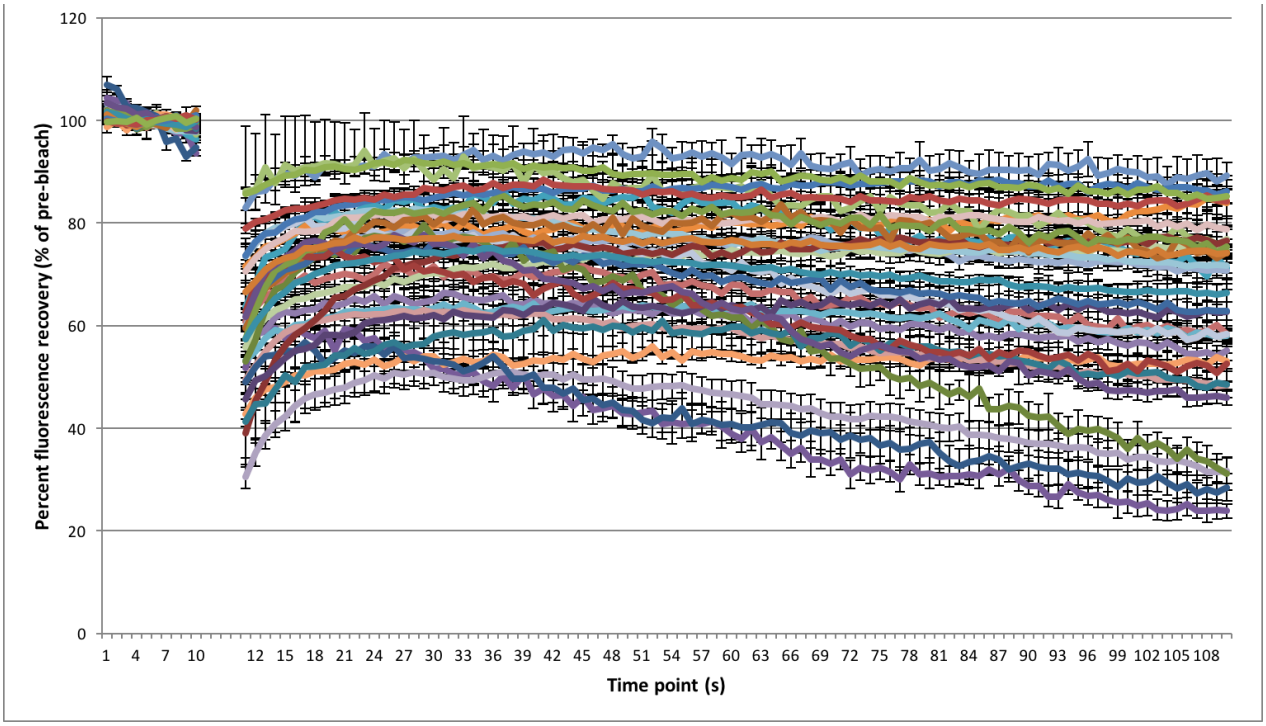

Figure 3.10: Baseline FRAP for NCS-1 YFP: To establish the FRAP signal for NCS-1 YFP, HeLa cells were transfected with NCS-1 YFP with the empty mCh vector. Multiple regions of interest were taken per cell and averaged for each cell to generate a trendline for each individual cell. A total of 17 cells were measured with varying degrees of FRAP shown within the scope of these experiments. Fluorescence of NCS-1 YFP was investigated in these experiments. Cell fluorescence was measured before bleaching occurred (frames 1-10) following which cells were bleached in specific ROIs and fluorescence mapped in the various ROIs. Cell fluorescence recovery was measured over time.

To establish the effect myr-PQ had upon NCS-1 YFP FRAP kinetics (Figure 3.10), co-transfected HeLa cells were utilized as in previous experiments. As before, cells were placed in Krebs buffer on the day of analysis with no added supplements. As described previously, pre-bleach values were set as '100%' and values gathered after bleaching were compared to the pre-bleach value. Under these conditions the FRAP profiles of NCS-1 YFP were analysed (Figure 3.11). Whilst the level of FRAP between experiments varied, evidence of rapid fluorescence restoration within the bleached ROIs is evident for specific cells.

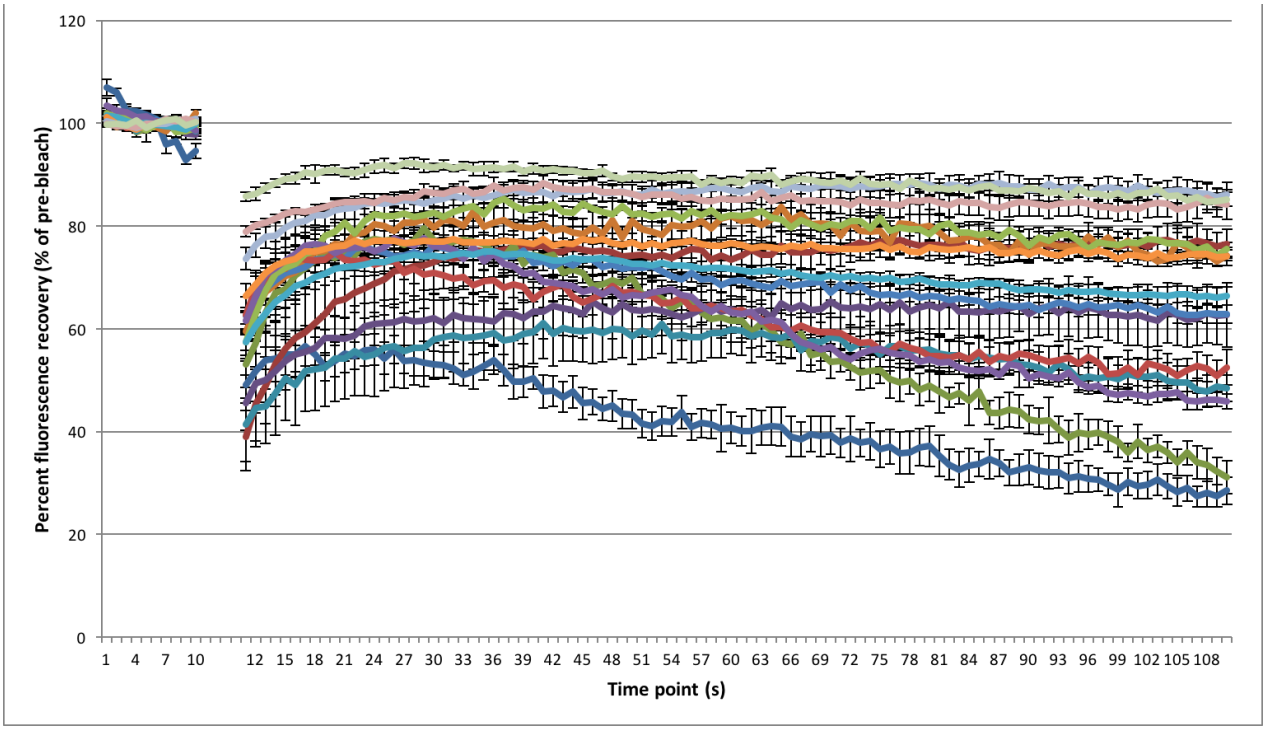

Figure 3.11: The effect of PQ on NCS-1 kinetics: A comparison of FRAP kinetics in co-transfected HeLa cells to identify a potential interaction, following a pre-established FRAP protocol (Handley et al., 2010). A total of 15 cells were used for the analysis with each containing numerous ROIs to form an average per cell, with a focus on kinetics of NCS-1 YFP.

To fully establish the kinetic profiles of NCS-1 YFP when co-transfected with myr-PQ-mCh, an average was generated from the previously generated series of kinetic profiles (Figures 10 and 11). The averages produced for each cell were taken and a single conglomerate average produced for both the NCS-1 YFP (+mCh) and (+myr-PQ-mCh) studies (Figure 3.12). Together these identified whether NCS-1 kinetics were altered or perturbed in the presence of myr-PQ. A baseline allows comparisons with future co-transfection studies. The rationale behind any altered kinetic profiles from co-transfected studies in fluorescence restoration this would be indicative of protein interactions between NCS-1 and myr-PQ in these experiments.

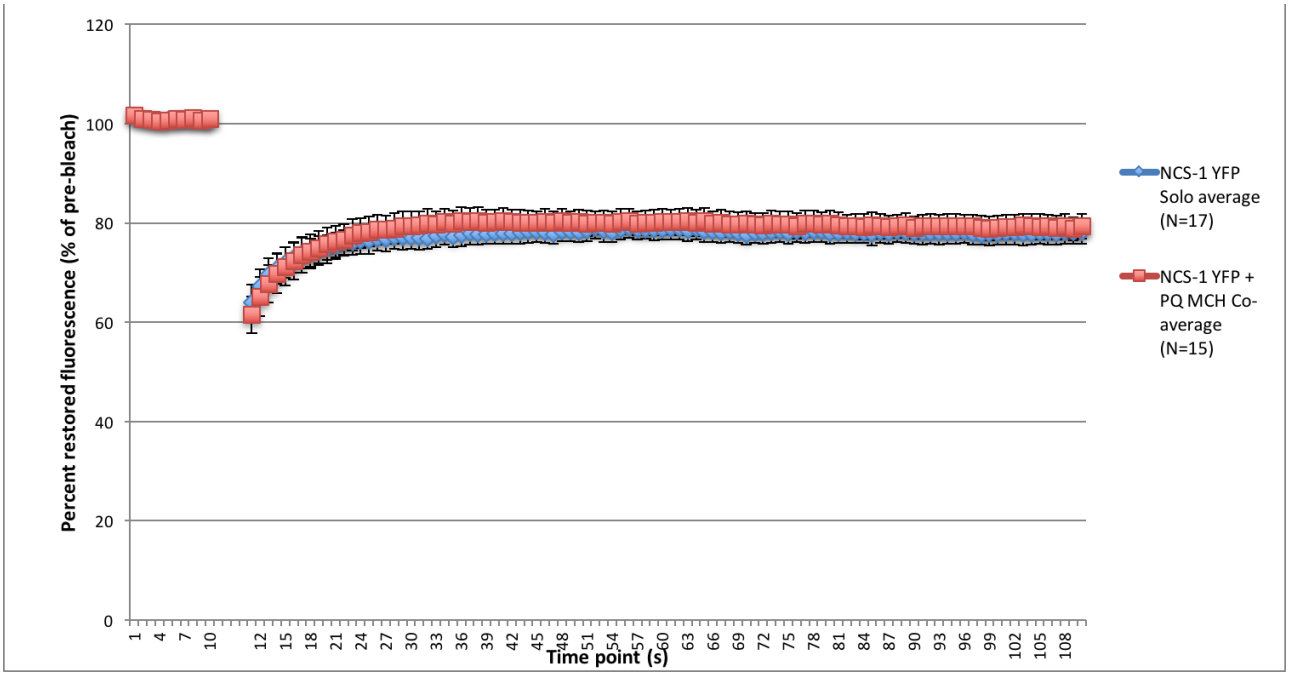

Figure 3.12: Kinetic profiles for NCS-1 and the effect PQ has upon its kinetics: Transfected HeLa cells used in live cell FRAP experiments (transfected with NCS-1 YFP +mCh or NCS-1 YFP + myr-PQ-mCh) were averaged to generate an overall kinetic plot using the conglomerate data set. Plotted data sets identified overlaps between the two conditions. Cells were bleached in multiple ROIs over a period of 10 frames (experimental procedure previously described) and restored fluorescence in these regions was then analysed. In each averaged data set, the 'pre-bleach' values were set as 100% with the 'post-bleach' values as a measure compared to these values. The restored fluorescence reaches a plateau at around 80% restored fluorescence in both experiments.

When taken together, the averages of the individual transfected cells for NCS-1 YFP with mCh vector (Figure 3.10) or myr-PQ-mCh (Figure 3.11) show varied results in regards to the individual cells however when an overall average is generated (Figure 3.12), an overlap between the kinetic profiles is present.

With the data of co-localisation from previous studies in this research, it remains possible the two protein complexes are still interacting albeit unable to be identified with FRAP based protocols, or potentially the interaction did not alter protein mobility. It is clear from these experiments that the fluorescence recovery initially is rapid reaching a plateau of around 80% in each experimental condition within the first minute post bleaching. ROIs were taken from different areas of the cell including the aggresome, PM and cytosol.

3.2.11 Analysis of protein interactions using Fluorescence Loss in Photobleaching

To test further potential methods of identifying interactions between myr-PQ and NCS-1 using altered kinetic profiles, Fluorescence Loss In Photobleaching (FLIP) experiments were carried out. Co-transfected HeLa cells were continuously bleached in regions of co-localisation and fluorescence changes measured in non-bleached regions of the cell to establish and quantify fluorescence loss due to photobleaching. Experiments were carried out with cells maintained in Krebs buffer (pH 7.4). Continuous bleaching of cells identified a steady decrease in fluorescence.

The purpose of this experiment was to identify potential kinetic changes between single transfected cells (NCS-1 YFP + mCh or myr-PQ-mCh + EYFP) when compared with co-transfected cells (NCS-1 YFP + myr-PQ-mCh) to determine whether protein interactions altered kinetic profiles. From the data gathered for the single transfected conditions (Figure 3.13 blue and red lines), different FLIP profiles are present with NCS-1 YFP (+ mCh) showing a more rapid FLIP profile. Interestingly when compared to the co-transfected samples (NCS-1 YFP (+myr-PQ-mCh) (Figure 3.13 green bar)) a similar FLIP profile was found with myr-PQ-eYFP.

This suggests that myr-PQ restricts the movement of NCS-1 as signified by the slower FLIP response thereby altering the kinetic profile. The single transfection control experiments suggest this was not due to the opposite colour tag hence the effect shown in the co-transfection studies signifies an example of interaction between myr-PQ and NCS-1.

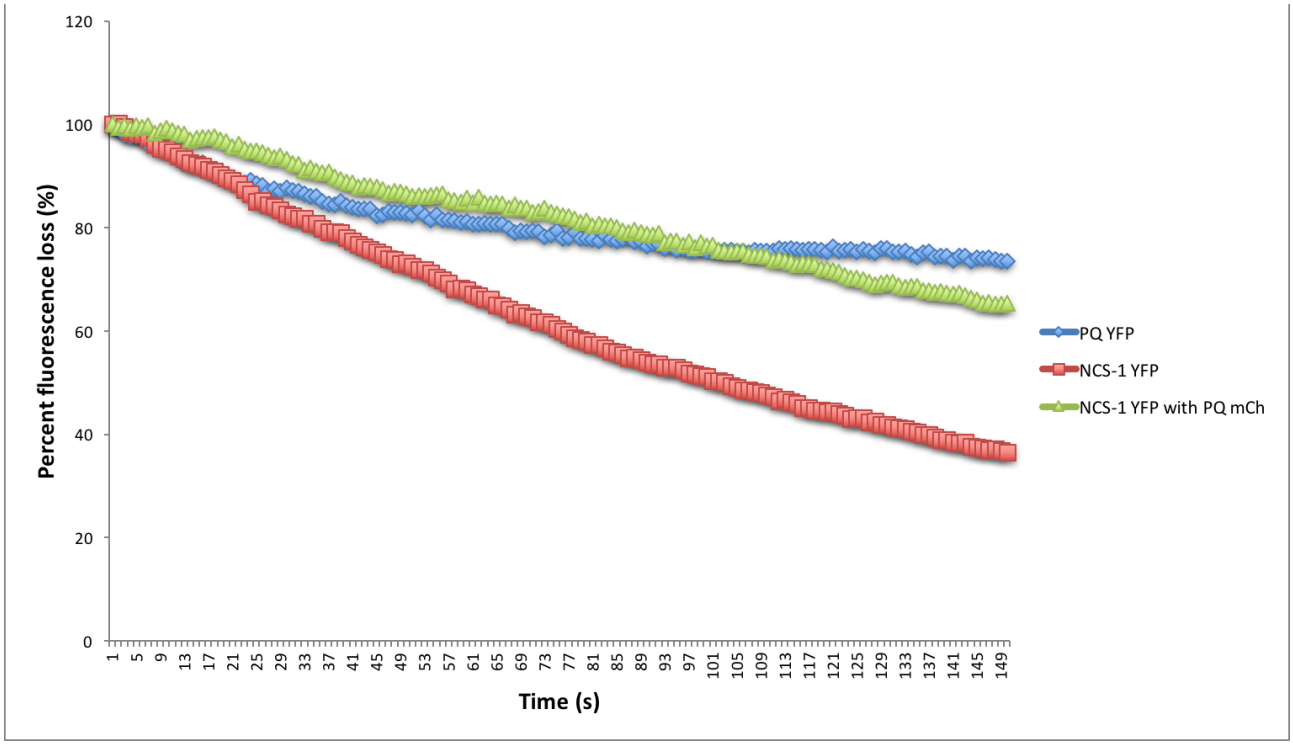

Figure 3.13: Averaged FLIP from transfected HeLa cells. Transfected HeLa cells were used in order to establish whether NCS-1 and PQ interacted, a measure of kinetics changes was established using fluorescence loss. Solo and co-transfected HeLa cells were investigated (N= 4 or 5 cells). Solo transfections generated opposite trends (red and blue bars) with a potential interaction seen in the co-transfection study (denoted by the green bar). Multiple regions of interest were investigated per cell with one region being bleached. Raw data for each individual cell not shown, cells averaged for their FLIP profiles presented here.

Through continuous bleaching, steady shuttling of the 'bleached proteins' into the non-bleached ROIs and shuttling into the bleached regions was occurring due to the fluidity of protein translocation. As in other experiments, fluorescence changes were normalized to initial fluorescence to allow for comparative analysis of FLIP profiles. Dynamic properties of myr-PQ and NCS-1 constructs were elucidated through restoration or loss of fluorescence within transfected cells. In essence these experiments were measuring the abilities of the protein constructs to shuttle between internal compartments thereby altering fluorescence measurements within set ROIs.

3.2.12 Quantifying the level of aggregation structures present in transfected HeLa cells

Through this research, a novel aggregation phenotype has been identified when myr-PQ constructs are co-expressed with various small Ca^{2+} sensor proteins, shown to be

cell line independent as similar structures were identified in HeLa and N2A cell lines. HeLa cells transfected with NCS-1 or myr-PQ constructs (attached to EYFP or mCh prior to transfection (individually and co-transfected)) were imaged as described previously.

Solo transfected samples were co-transfected with the inverse empty colour tag (EYFP or mCh) to exclude the belief that aggregation was caused by the presence of the colour tags. Transfected cells were fixed 24 hours post transfection using 4% PFA. Co-transfected slides were again used as an indicator of interaction between myr-PQ and NCS-1.

Current research serves to corroborate past studies into the kinetic profiles of NCS-1 (Lian et al., 2014, Handley et al., 2010). Research in this section is designed to examine interactions between the PQ-type Ca^{2+} channel and various potential modulators of channel activity, namely various small Ca^{2+} sensing proteins. Through the course of this research, the presence of aggregation structures within cells transfected with myr-PQ alongside NCS-1/CaM/CaBPs was an unexpected yet potentially informative observation. Transfected cells were imaged and aggregation was independently quantified to generate an overall average for the aggregation for the different transfection conditions.

Cells transfected with NCS-1 alone identified no aggregation structures (Figure 3.14), whilst cells transfected with myr-PQ showed aggregate structures in approximately 45% of analysed cells. The absence of aggregate structures when NCS-1 constructs were transfected into cells supports previous research (Haynes et al., 2006, Burgoyne and Weiss, 2001).

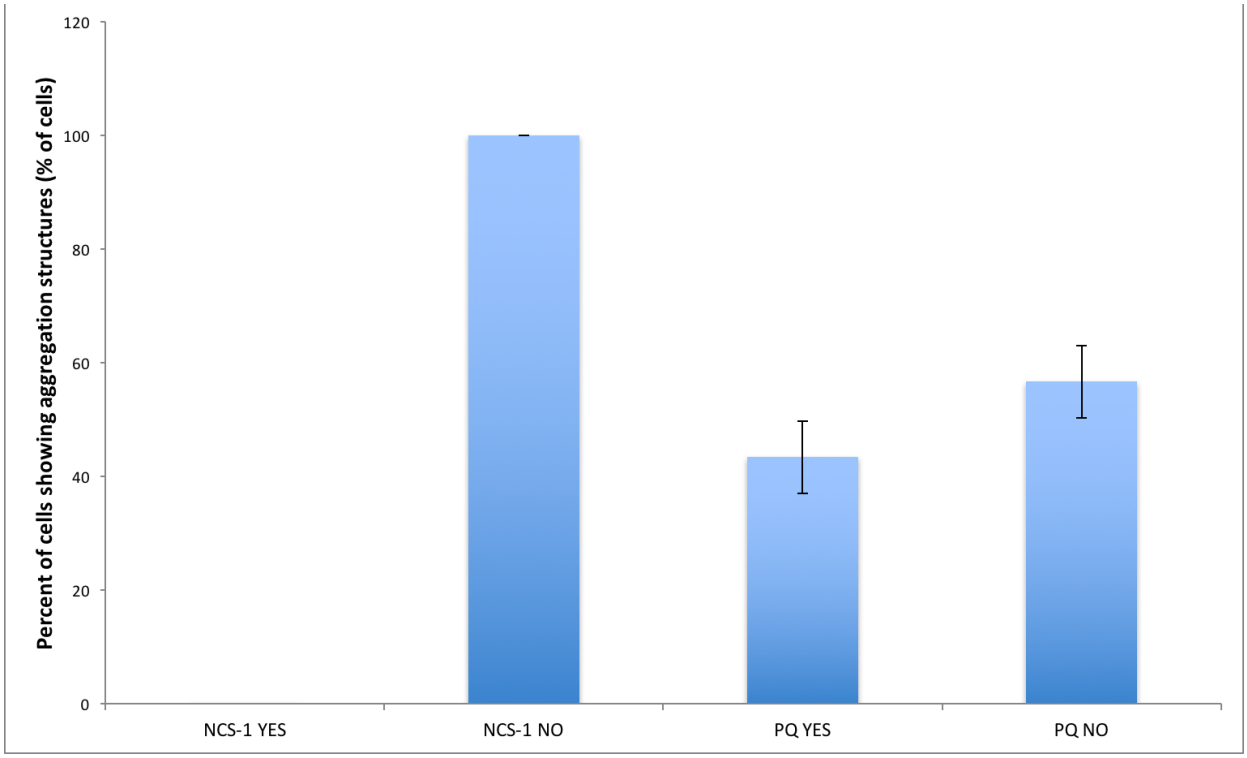

Figure 3.14: Quantified aggregation in HeLa cells co-transfected with inverse colour tag: HeLa cells were transfected using NCS-1 mCh or myr-PQ-eYFP with the inverse empty colour tag and imaged using fluorescence microscopy in order to identify the basal level of aggregation. Co-transfected HeLa cells were taken from three separate experiment slides and multiple cells imaged per experiment (N=67 for NCS-1 mCh transfected cells and N=97 for myr-PQ-eYFP transfected cells). Cells were independently quantified by two individuals and the averages of the scores utilized for this research.

HeLa cells co-transfected with NCS-1 and myr-PQ identified whether these aggregate structures were an example of interactions within cells. Experiments were completed in line with other experiments in this research. Through analyzing the co-transfection cell slides to test the hypothesis that myr-PQ and NCS-1 were interacting, the presence of aggregation structures within HeLa cells transfected with NCS-1 (with the inverse colour tag) rose from 0% to approximately 40% under co-transfection with myr-PQ as shown in Figure 3.15, denoted by yellow structures within cells.

From this observation, it suggested that NCS-1 was undergoing aggregation only in the presence of the PQ construct, suggesting a potential interaction between myr-PQ and NCS-1. The significant change can be seen when looking at the columns of NCS-1 alone and when transfected alongside PQ, showing an increase in the presence of aggregate structures. Both columns (NCS-1 / PQ Yes & No) collectively add to 100%.

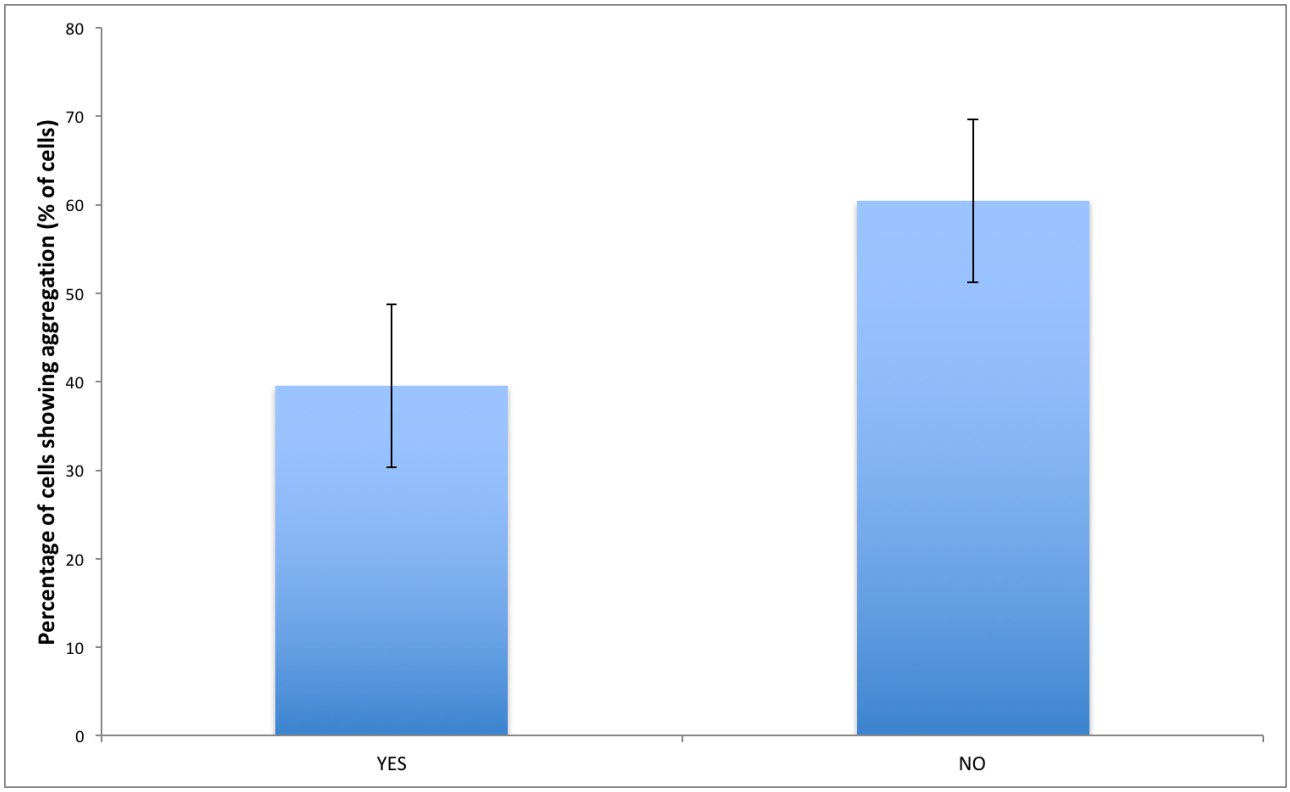

Figure 3.15: The effect of PQ on the aggregation of NCS-1 constructs within cells. HeLa cells were co-transfected with myr-PQ-eYFP and NCS-1 mCh and subsequently imaged using fluorescence microscopy. Images taken were independently quantified for the presence of co-aggregation structures within cells. Three independent slides were produced for each condition (co-transfection of myr-PQ-eYFP with NCS-1 mCh) with a total number of quantified cells of N= 160 cells. Using the quantified data, an overall average was generated for aggregation.

3.2.13 Analysis of newly produced intramolecular FRET sensors

A novel FRET sensor was created using standard PCR based subcloning (see Figure 3.16) similar to the plasmid construction mentioned previously to produce an intramolecular FRET sensor containing both NCS-1 and PQ-type channel fragments. The research here aimed to identify whether intramolecular FRET could enhance identifiable interactions between NCS-1 and PQ-type channels.

As shown previously in this research, intermolecular FRET was unable to establish an interaction between NCS-1 and PQ-type channels (Figure 3.9). The purpose of this research was to increase the opportunity for NCS-1 and PQ to interact spatially by restricting their localization as part of a contiguous intramolecular FRET sensor similar to the CaM based cameleons (Grant et al., 2008, McCue et al., 2013, Miyawaki et al.,

1999) (Figure 3.16). This is different to individual expression of myr-PQ and NCS-1 and detection of intermolecular FRET.

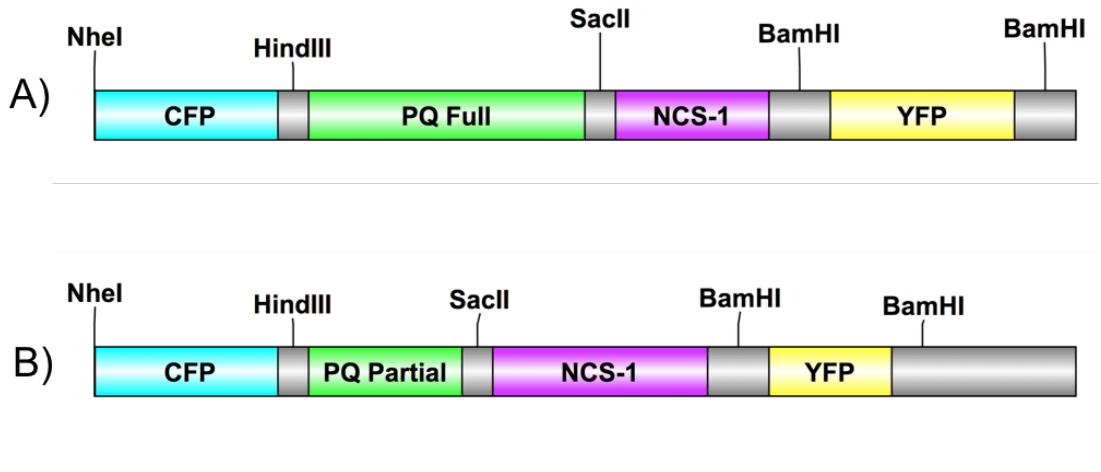

Figure 3.16: Structure of intramolecular FRET sensors. FRET sensors were produced using sequential standard restriction digest techniques. Produced sensors included both NCS-1 and PQ-type channel encompassing the IQ domain. A) Full length NCS-1+PQ cameleon included an extended portion of the PQ domain from 1898-2035 whilst B) Partial length NCS-1+PQ cameleon contained PQ domain 1898-1949.

This study used HeLa cells plated onto 3 cm matek live cell imaging dishes which were subsequently transfected with either GCaMP6 (control transfection), 'PQ-type Full cameleon (PQ 1898-2035)' or 'PQ-type Partial cameleon (PQ 1898-1949)' for a 24 hour time point prior to live cell imaging. Transfected cells were treated as described previously using Thapsigargin and Ionomycin to raise intracellular [Ca^{2+}] to allow the opportunity for FRET to occur. GCaMP6 was used as a control to identify whether Ca^{2+} was increasing in cells under this perfusion system.

The purpose of this series of experiments was to assess the newly produced cameleon constructs to elucidate their ability to measure interactions between NCS-1 and the PQ-type fragment by means of intramolecular FRET signaling. In cells transfected with GCaMP6 (acting as a control), after drug treatment an increase in GFP fluorescence was identified (Figure 3.17). In multiple ROIs present within the cell, a marked increase of GFP fluorescence was identified after drug treatment which was not identified in the extracellular control ROI (ROI 5).

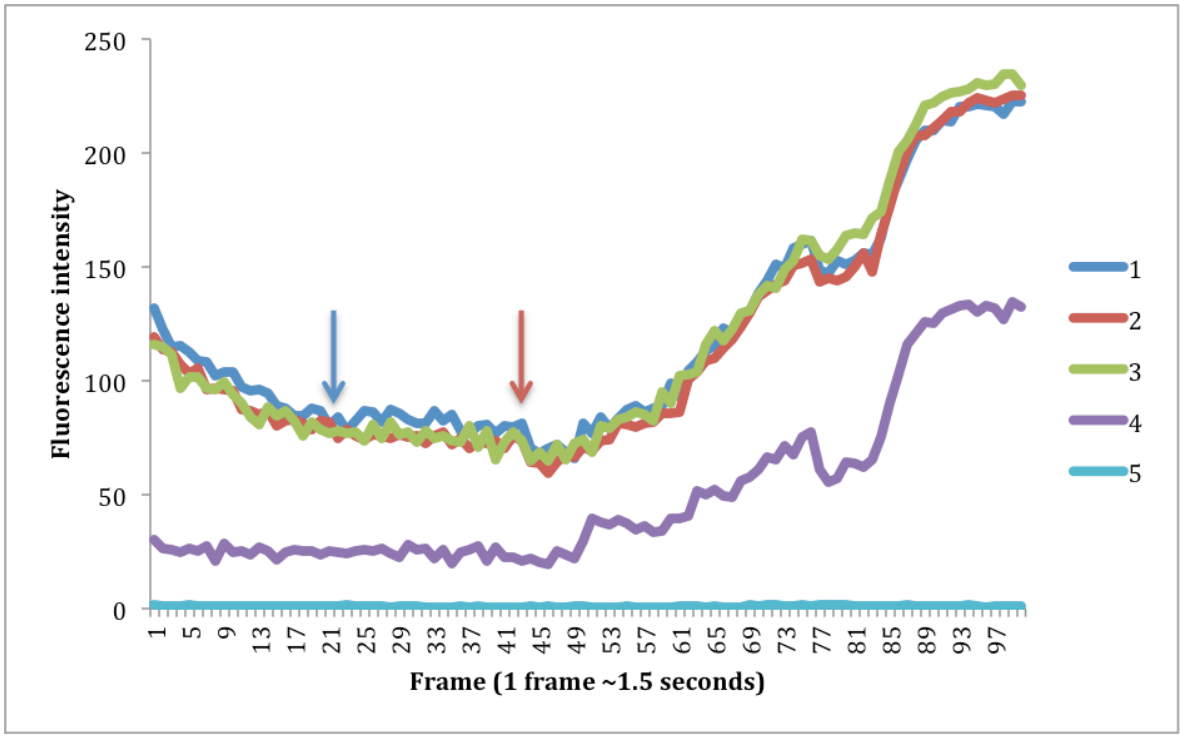

Figure 3.17: The effect of increased [Ca^{2+}] on GCaMP6 GFP fluorescence. HeLa cells were transfected with GCaMP6 and subsequently imaged using fluorescence microscopy under perfusion of Ca^{2+} increasing drugs. Fluorescence intensity taken from multiple ROIs were then analysed for increases in GFP fluorescence. In this research live cells were treated with 5μM Thapsigargin in Krebs buffer at frame 20 (blue arrow) for 30 seconds then with 1μM Ionomycin for 30 seconds before perfusion with Krebs (pH7.4). Representative plot from analysed dish shown above. N= 4 experimental dishes.

Here the fluorescence increase varied in the experimental ROIs however each showed a similar trend in fluorescence increase. The same experimental procedure was applied to HeLa cells transfected with the produced PQ-type variant cameleon constructs to identify their activity when exposed to increases in Ca^{2+} concentration.

In HeLa cells transfected with the 'PQ-type Partial cameleon (1898-1949) when treated with [Ca^{2+}] increasing agents as described previously, varied results were obtained for the FRET signals between dishes. Whilst a positive result was obtained from one of the treated dishes (Figure 3.18a) other dishes transfected with this construct were unable to identify FRET signals (Figure 3.18b).

This variability in the results suggested that the construct does appear to be able to reliably measure intramolecular FRET. Results using this cameleon construct possibly support evidence for a direct interaction between NCS-1 and PQ-type channels within

the region of the IQ domain however this requires further verification (Tsujimoto et al., 2002, Weiss et al., 2000, Weiss and Burgoyne, 2001, Dason et al., 2009, Lian et al., 2014).

Methods were employed to increase the intracellular [Ca^{2+}] to measure FRET activity in a short time course. Whilst the Partial PQ cameleon does suggest an ability to measure intramolecular FRET (and therefore interactions between NCS-1 and PQ), experiments using the same experimental procedure with HeLa cells transfected with the 'Full PQ cameleon (1898-2035)' were unsuccessful in their ability to measure intramolecular FRET (Figure 3.19).

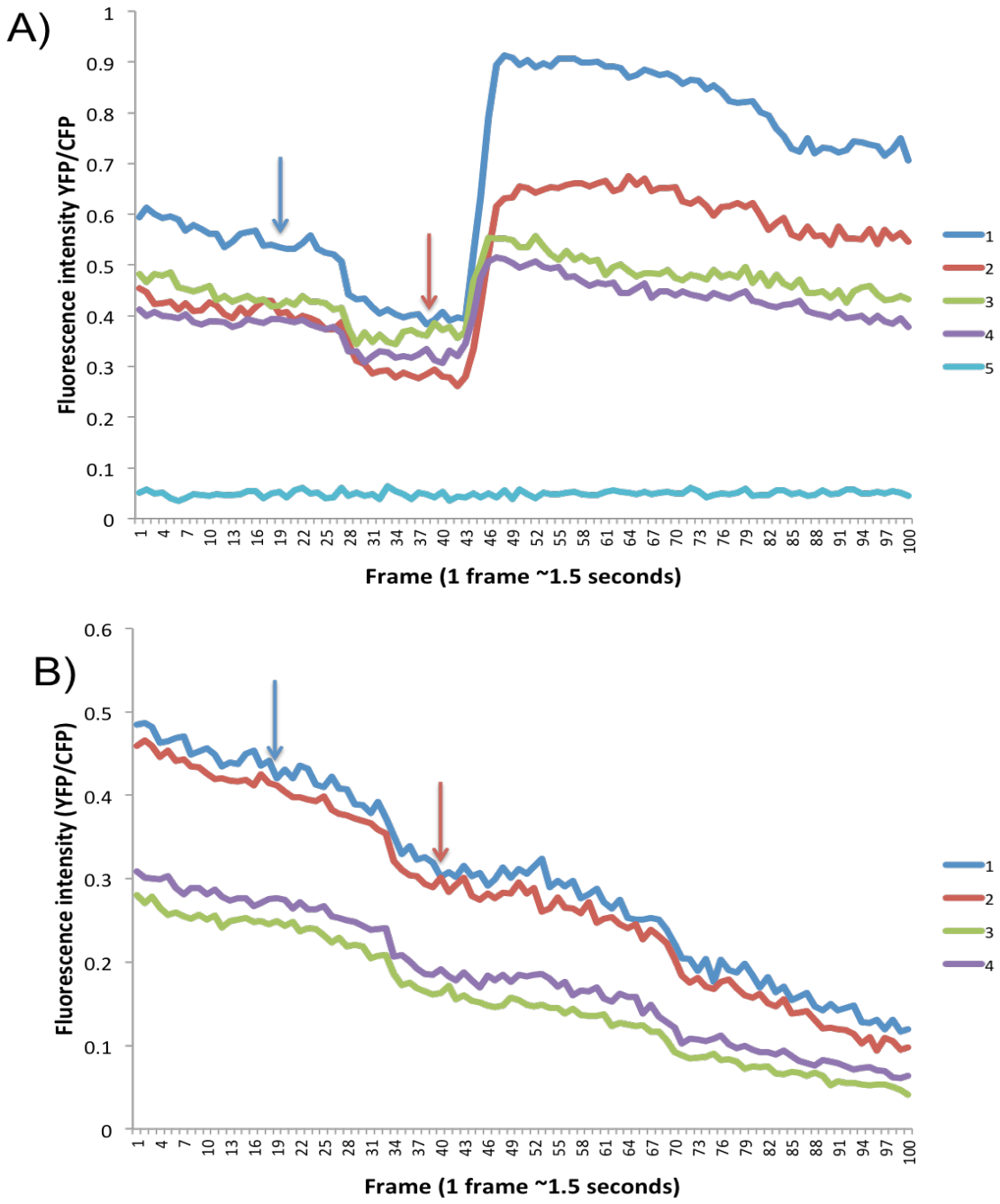

Figure 3.18: Analysis of intramolecular FRET in response to increased [Ca^{2+}]. HeLa cells were transfected with PQ-type Partial cameleon and subsequently imaged using fluorescence microscopy under perfusion of Ca^{2+} increasing agents. Fluorescence intensity taken from multiple ROIs were then analysed for increases in YFP fluorescence indicative of FRET signaling. In this research live cells were treated with 5μM Thapsigargin in Krebs buffer at frame 20 (blue arrow) for 30 seconds then with 1μM Ionomycin (red arrow) for 30 seconds before perfusion with Krebs (pH7.4). Representative plot from analysed dish shown above. N= 4 experimental dishes. Panel A represents a working example of FRET in the PQ-type Partial cameleon with ROI5 acting as an extracellular control. Panel B showed no FRET when using the PQ-type Partial cameleon, suggesting inconsistency in the FRET response.

Whilst the 'Full PQ cameleon (1898-2035)' was unable to generate a measurable FRET signal the reasons behind this are at this time uncertain. As shown previously in this research, FRET signals between two molecules (intermolecular FRET) was difficult to obtain between myr-PQ and NCS-1 using the experimental measures shown previously hence the trial of intramolecular FRET using a longer portion of the PQ-type channel fragment.

With no evidence of FRET in the PQ-full cameleon (Figure 3.19), but some evidence of FRET in the partial PQ cameleon (Figure 3.18), research at this time suggested that these constructs required more in-depth analysis. At this stage of research, some preliminary evidence was generated representing the potential functional usage of the 'PQ-type Partial cameleon' in assessing protein-protein interactions using a smaller portion of the PQ channel.

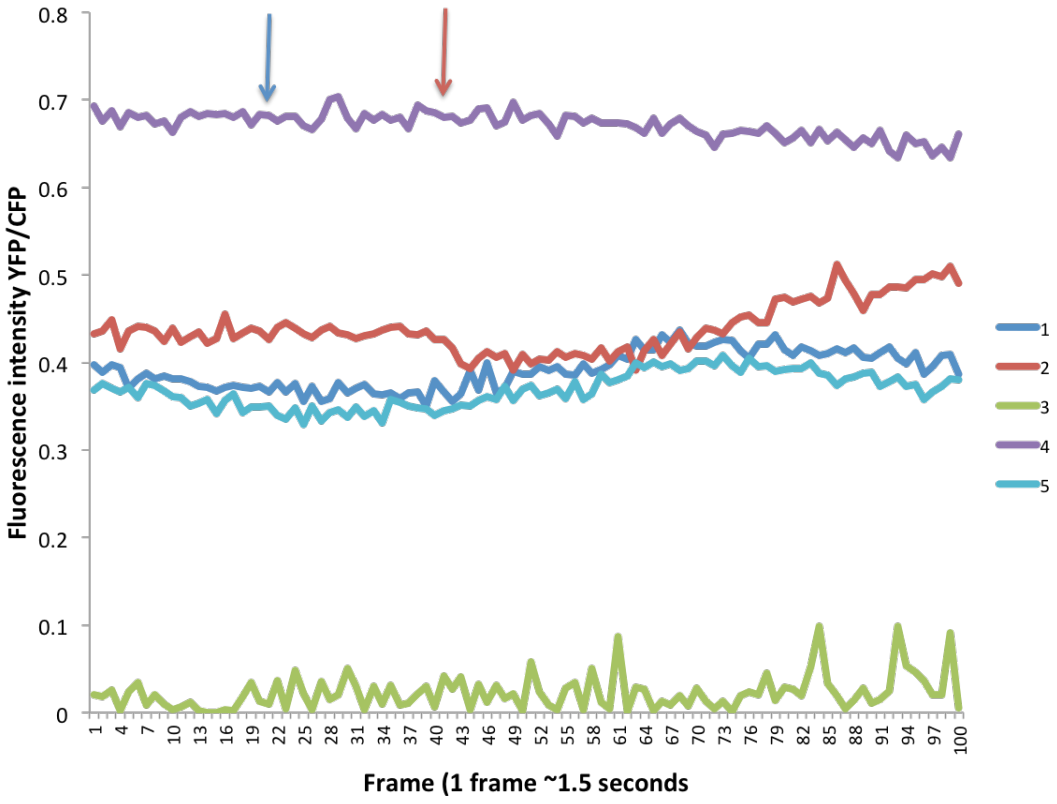

Figure 3.19: Analysis of intramolecular FRET in response to increased [Ca^{2+}]. HeLa cells were transfected with PQ-type Full cameleon (1898-2035) and subsequently imaged using fluorescence microscopy under perfusion of Ca^{2+} increasing agents. Fluorescence intensity taken from multiple ROIs were then analysed for increases in YFP fluorescence indicative of FRET signaling. Cells were treated as described previously. Representative plot from analysed dish shown above. N= 4 experimental

dishes. FRET signals were not identified in the background (ROI 3) or in the experimental ROIs (1,2,4 and 5).

Whilst the transfected dishes were treated using comparable solutions under similar environmental conditions the lack of a FRET signal in the longer cameleon construct ('PQ-type Full cameleon') suggests this was incapable of producing a replicable consistent FRET signal, whilst the shorter cameleon construct presented an example of intramolecular FRET interaction between NCS-1 and PQ.

Background FRET in the experimental dish shown in Figure 3.19 (ROI 3) suggests some spurious changes were altering the signals however with each dish not exceeding >0.15 change in fluorescence intensity in the YFP:CFP ratio this does not support the idea of FRET signals which can be seen in Figure 3.18a where the YFP:CFP ratio changes by >0.3 in the experimental ROIs in comparison to the control ROI present in these experiments.

3.3 Discussion

The aim of this study was to identify and document interactions between a C-terminal regulatory domain of the $Ca_V2.1$ PQ-type VGCC and NCS-1. This work primarily focused on using fluorescence based imaging techniques to monitor protein-protein interactions. Fluorescence based experiments utilized constructs containing the PQ C-terminal residues 1898-2035 as recent research (Lian et al., 2014) had identified this region as containing a site involved in interactions with NCS-1. These two proteins have been identified to interact *in vitro* (Lian et al., 2014) hence further research was undertaken to investigate a potential *ex vivo* association that could be examined in future functional studies using the model organism *C. elegans*.

Within the data presented here, some evidence of degradation of the expressed PQ constructs (myr-PQ-eYFP or myr-PQ-mCh) was observed as shown in Figure 3.1C, however expected membrane localization was apparent when expressed in cells, with protein constructs behaving as expected.

Another reason why the partial PQ fragment was used was that whilst the full length α subunit of the PQ-type channel could be transfected into cells, the expression of this might require additional expression of the β and γ subunits to ensure full function and appropriate trafficking of the channel to the PM. To simplify this analysis, a partial fragment of the α subunit cytoplasmic C-terminal domain was identified and used in these studies. To mimic membrane localization of this domain (as would be found in the intact α subunit), a Lck consensus myristoylation motif was incorporated at the N-terminus of the domain to ensure targeting to the PM (taken from previous research (Oz et al., 2013)).

A pool of NCS-1 is also known to be PM localised through myristoylation (Gomez et al., 2001, Hilfiker, 2003). Targeting both proteins to the PM places them in a physiologically relevant locale and increases the opportunity for relevant interactions to be detected.

When transfected into cells these proteins localized to cell membranes consistent with the PM and Golgi apparatus, as detailed in previous studies (Ames et al., 2012,

McFerran et al., 1999, O'Callaghan et al., 2002). With NCS-1 previously being identified as able to modulate Ca^{2+} signals within neurons (Dason et al., 2009, Dragicevic et al., 2014, Rousset et al., 2003), a detectable interaction with the PQ-type Ca^{2+} channel might represent a useful functional reporter of such signaling activity in intact neurons. Whilst the transfected proteins were able to localize correctly to cellular membranes, it was noted in this research that a portion of the proteins localized aberrantly within cells, shown in multiple cell types including HeLa (Figure 3.2E and Figure 3.3) and N2A cells (Figure 3.5-3.7). With the aggregate structures appearing in numerous cell lines, one hypothesis generated was that the presence of these structures were examples of identifiable domains of NCS-1 interacting with the PQ-type channel fragment.

One interesting observation was noticed within transfected HeLa cells co-transfected with myr-PQ-eYFP and mCh CaM. Under these conditions, CaM localisation was apparently altered in the presence of the myr-PQ-eYFP. Interactions between the PQ domain used during the course of this research and CaM have been shown previously in vitro (Lian et al., 2014). To further elucidate if this is a genuine interaction, further work imaging transfected HeLa cells should be conducted to establish in more detail (through Z-stack analysis) in order to distinguish between localisation in a single plane and within multiple planes. This would provide supporting evidence for true co-localisation.

Alternatively, further evidence of this interaction could be established through immunoprecipitation assays using cells expressing the PQ-type channel fragment. Evidence of this from multiple cell lines would suggest interactions occurring *in vitro*. In addition to this, previous literature has identified that CaM can act to modulate the Ca^{2+} signal from PQ-type channels through modulation and facilitation (DeMaria et al., 2001). CaM was selected for this research as the localisation of this Ca^{2+} sensor within cells has been extensively studied.

Evidence of localisation onto cellular membranes was noted in different cell lines for myr-NCS-1 and other transfected proteins. Through this research, HeLa cells were utilized due their ease of transfection, well defined cellular morphology and well characterized responses to agonists. HeLa cells do not endogenously express PQ

type VGCCs and therefore alternative neuronal like cell culture models which do were additionally explored in these studies (Dason et al., 2012, Gomez et al., 2001, Handley et al., 2010). For this work, N2A cells (Mouse Neuroblastoma) were transfected and protein localization examined. All proteins localized to cellular membranes in a similar manner as observed for HeLa cells. Localisation of the constructs employed in this study is therefore largely independent of cell type and in other analyses the cell type employed was based on ease of transfection and amenability to imaging analysis.

The aim of the present study was to generate *in vivo* sensors to identify NCS-1 driven Ca^{2+} signals which could then be transferred into the nematode *C. elegans* acting as a biosensor of activity during behavioural assays. Initially the generation of the constructs was required, which was achieved using the myristoylation domain alongside the PQ-type channel fragment as described previously (Oz et al., 2013).

The progression from this was the testing of these constructs within various cell lines. This work established that all the constructs localised correctly *ex vivo* and targeted to cellular membranes. From the acquired data, there are few differences between the protein localisations suggesting these proteins can be targeted within different cell lines. The formation of aggregate structures suggested an interaction between NCS-1 and PQ. The imaging technique in live cells aimed to establish a method of visualizing this interaction in real time to be further incorporated into *C. elegans*.

Possible co-localisations were also noted between members of the CaBP family of proteins and the transfected myr-PQ constructs. This is in line with previous research which identified modulation of $Ca_V2.1$ channels (including PQ-type channels) by CaBP1 (Few et al., 2005, Lautermilch et al., 2005, Lee et al., 2002). At this stage, the co-localisation between CaBP family members and myr-PQ has not been fully investigated however I was able to identify evidence of co-localisation in both the cell lines used within this research. The aggregation was stronger in cells transfected with myr-PQ-eYFP suggesting this construct interacts better with co-expressed targets. With evidence of aggregation in cell lines transfected with both myr-PQ and in some cases evidence of co-localised CaBP1 within these structures, this supports previous research for interactions between PQ-type channels and CaBP family members.

Several fluorescence-based techniques were used to investigate changes in protein fluorescence or the kinetic profiles of these constructs, based on energy transfer, fluorescence restoration or depletion (FRET, FRAP and FLIP respectively). Previous research has utilized similar techniques to uncover protein-protein interactions (Handley et al., 2010) and to study the effects of protein kinetics as a measure of interactions. Numerous studies have implicated NCS-1 and Ca^{2+} channels to interact (Dason et al., 2009, Dragicevic et al., 2014, Gomez et al., 2001, Hui et al., 2007), which the present research aimed to expand upon further.

Initially, cells were stimulated using a series of perfusion conditions in order to raise Ca^{2+} levels within cells. Upon stimulation of cells, a consistent replicable FRET signal could not be identified. Whilst this argues that NCS-1 and PQ are not interacting, however it is possible that FRET is not the ideal test for this interaction. The proteins used within this research used the FRET sensor pair of YFP and mCh, whilst this is not the most ideal FRET pair (Grant et al., 2008, Miyawaki et al., 1997, Palmer and Tsien, 2006, Shaner et al., 2005) this was used during the course of this research due to the availability within the laboratory. For this work, a more optimum and promising FRET sensor pair would be the use of CFP-YFP FRET pair of fluorophores as opposed to using mCh and YFP as these are further apart on the light spectrum and provide less optimal donor excitation (Tsien et al., 1991, Tsien, 2009, Wallace et al., 2008).

In accordance with previous research (Handley et al., 2010), stimulation experiments were conducted following similar procedures. Here an example of intermolecular FRET was being studied (FRET between two separate constructs). In light of this and to optimize this further a construct containing both the PQ-type domain and NCS-1 were generated containing both the colour tags (Figure 3.1). This cameleon construct represents an example of intramolecular FRET.

An intramolecular FRET sensor may alleviate some proximity issues thereby assisting in identifying transfected cells. When stimulated, under these conditions, if PQ and NCS-1 were to interact this would cause a change in conformation (a shape change), resulting in an identifiable FRET response. Further issues which are inherently present in FRET based experiments are that this is heavily dependent upon the orientation of

the colour tags. The hypothesized outcome from this type of research would be that as the proteins interacted, by exciting one protein at a specific wavelength, the emission of fluorescence would be from the opposing protein wavelength (Figure 3.8).

When considering the intramolecular FRET signals with the cameleon constructs (Figures 16, 18 and 19), the evidence here suggests a potential mechanism for identifying interactions between NCS-1 and PQ-type channels (Figure 3.18a) however the variability within this suggests that aspects of the experimental design require further optimization. Unfortunately some of the dishes containing the cameleon constructs were subject to focus drift which caused problems when measuring the FRET activity, one example of this is shown previously (Figure 3.18b). Whilst focus drift was an issue, evidence of FRET would be clear in transfected dishes and would represent a rapid shift in fluorescence ratio (Figure 3.18a).

With these cameleon constructs being novel, as ordinary cameleons include M13 as a region as opposed to NCS-1 and PQ, some potential issues could have caused the inability to measure FRET in these systems. Firstly in standard cameleon constructs M13 is approximately 25aa in length allowing folding and flexibility when exposed to higher [Ca^{2+}], however with the PQ region being between 1898-2035 (137aa) in the 'Full PQ cameleon' and between 1898-1949 (51aa) in the 'Partial PQ cameleon' issues of flexibility in the longer constructs could be apparent. By increasing the linker region, this increases the distances between the different colour tags thereby requiring more movement to allow FRET signals. An increase in protein separation however would decrease chances of observing FRET, identification of a minimal interaction motif in the PQ channel would greatly increase the chance of identifying a FRET signal.

Another potential physiological relevance issue is that the NCS-1 in this construct is no longer myristoylated (not bound to cell membranes), which could alter the folding of the protein and the binding to its interacting partners. With FRET signals being complex to obtain due to the specificity of the interaction and the orientation of the colour tags this presents further challenges in this research. One issue which is alleviated by the use of intramoleular FRET is that of analyte concentration as with the two potential interacting partners being in the same construct this reduces the need

for co-transfection and therefore the issue of differential transfection of the two separate constructs (Held, 2005).

With the 'Partial PQ' responding to Ionomycin, this demonstrates this construct can identify and respond to increases in [Ca^{2+}] however with numerous experimental attempts being made and the variable success of these constructs it was therefore determined that ventures down this line of research would be halted.

Whilst this research was unable to establish a consistent, reproducible FRET response, other fluorescence based methods identifying the kinetic profiles of transfected proteins were tested within this research. When co-transfected cells were bleached with a defined region of interest and the restored fluorescence measured post-bleach in the defined ROI (using FRAP), it was noted through this research that the restored fluorescence between the co-transfected (myr-PQ with NCS-1) and solo NCS-1 transfected samples showed no difference in their FRAP kinetic profiles. Some issues we noted during these experiments were due to the range of bleaching which occurred in each dish as well as inherent issues with focus drift when imaging for long periods of time.

Taking into account these experiments were conducted on different days, using different passages of cells; a range of bleaching can be partially explained by these extraneous factors alongside environmental changes or variation in expression levels. When looking at the restoration of fluorescence, in the majority of cases in this research, the fluorescence was restored to a plateau after around 10 frames, supporting findings from previous literature (Handley et al., 2010).

Cells were treated in the same manner for each experiment, however as no discernable difference could be found for the kinetic profiles, this again suggests that myr-PQ and NCS-1 were not interacting. One idea is that, as the two proteins were bound before bleaching, the ROIs tested, after bleaching were saturated with NCS-1 bound to myr-PQ which were unable to detach leading to the similar kinetic profiles generated. Whilst FRAP is a sensitive measure of protein kinetics, issues of photobleaching before or during the experiment can perturb results (Zheng et al., 2011). When looking at FRAP in more detail, the bleaching destroys the fluorophore

however the proteins are still present within this region. If the regions selected for analysis are saturated with proteins, this could prevent proteins translocating into and out of this region. When investigating Ca^{2+} dependent interactions, incubator with a cell permeable Ca^{2+} chelator could be used to alter FRAP/ FLIP profiles.

Whilst in this research the FRET and FRAP series of experiments were unsuitable methods to identify interactions between myr-PQ and NCS-1 a number of recent studies have identified or have postulated of interactions between these proteins (Lian et al., 2014, Catterall and Few, 2008, Mochida et al., 2008, Yan, 2014). The aim of this research was to identify a technique which would allow the visualization of interactions between NCS-1 and myr-PQ containing the IQ/IM domain (1898-2035), which preliminary research identified this as the interaction domain (Catterall and Few, 2008, Mochida et al., 2008, Lian et al., 2014). In the attempt to avoid completing quadruple transfections, this research took only a partial region of this transmembrane protein channel, which previous research identified as being able to identify interactions between PQ and NCS-1 (Lian et al., 2014).

The research outlined to this point suggests that NCS-1 and myr-PQ interactions were unable to be identified through FRET or FRAP based techniques, when looking at the FLIP profiles of NCS-1 transfected into cells with and without myr-PQ, differing FLIP kinetic profiles were identified with NCS-1 co-transfected with myr-PQ showing a FLIP profile corresponding with myr-PQ profiles. Through this an interaction between PQ and NCS-1 could be identified. It should be noted however that for this aspect of the research, the number of experiments completed is relatively low.

One possibility is that the proteins are interacting thereby allowing rapid protein translocation, yet it could be that the proteins post-bleach are moving out of the ROI and subsequently lowering the fluorescence in the surrounding ROIs. Currently the relationship between myr-PQ and NCS-1 in regards to their FLIP profiles have not been fully elucidated. One hypothesis as to why co-transfected cells FLIP profiles act like myr-PQ transfected cells is that the PQ is ‘more dominant’ therefore the interaction is more reducing the level of fluorescence loss.

Aspects of this research also identified aberrant aggregation structures within transfected cells. From previous research, the NCS-1 constructs used within this research are not known to aggregate (Handley et al., 2010), this is supported by research within this project (Figure 3.14), whereas cells transfected with myr-PQ showed evidence of aggregation in approximately 42% of analysed cells. Interestingly, when these protein constructs were co-transfected into cells, the previously un-aggregated NCS-1 constructs now appear to be present within the aggregation structures in approximately 40% of cells imaged, using two independent scorers (Figure 3.15). The presence of the NCS-1 within aggregation structures when co-transfected with myr-PQ provides supporting evidence of interactions between these proteins, as myr-PQ has the ability to 'pull' NCS-1 into these aberrant structures.

In summary, through this research we were able to produce myr-PQ constructs and transfect these into cells to identify their localisation, with further clarification of the localisation of the NCS-1 constructs (shown in previous research (Handley et al., 2010, Haynes et al., 2005)). This research also studied various mechanisms of interaction between NCS-1 and myr-PQ through fluorescence protein-protein interaction methods, the results of which suggested that the optimum method of measuring interactions was to use FLIP as opposed to FRET or FRAP.

Data generated from this research complements previous research for the kinetic profile of NCS-1 in specific fluorescence based procedures (Handley et al., 2010) however the kinetic profile has not been studied in conjunction with myr-PQ. To this end, it was suggested that myr-PQ and NCS-1 interactions are difficult to identify. Through these studies, it is suggested that FRET and FRAP are not able to elucidate these interactions whilst FLIP is sufficient enough for these purposes. These results suggest that under consistent bleaching, proteins are able to move between regions and be visualized whilst with a short bleaching, protein kinetics are more difficult to measure, potentially due to incomplete or insufficient bleaching in these experiments.

Although the present study provides evidence for an interaction between NCS-1 and myr-PQ, further investigation is required to fully elucidate the nature of these interactions. To this end, research utilizing other fluorescence based procedures such

as BiFC assays, electron microscopy to study interactions or NMR to identify structural changes when the two proteins undergo an interaction could be utilized.

3.4 Conclusion

In conclusion, work in this project has identified multiple methods for identifying interactions between NCS-1 and the PQ-type channel encompassing the IQ domain. This supports evidence from previous research regarding interactions between NCS-1 and PQ-type channels (Tsujimoto et al., 2002, Weiss et al., 2000, Weiss and Burgoyne, 2001, Dason et al., 2009, Lian et al., 2014) whilst also building upon the techniques and composition of cameleon constructs. This work supports the role of the IQ domain on the α1 sub-unit of the PQ-type VGCC in interacting with NCS-1. Regarding the aggregate structures present in co-transfected cells, it is probable that these represent interaction structures within cells. To fully elucidate these results further experimental work is required to de-construct the aggregate structures to identify the reasons behind these whilst also optimizing the cameleon transfection and analysis to increase the success rate of successful FRET signals from these constructs.

Chapter 4 Results: Investigation and characterisation of Temperature Dependent Locomotion by NCS-1 and partner proteins in the model organism *C. elegans*

4.1 Introduction

Changes in $[Ca^{2+}]_i$ results in a number of processes depending on the time frame of the Ca^{2+} change. This can result in exocytosis, muscle contraction, fertilization to cell death, gene transcription and changes in ion channel functions (Berridge et al., 1998, Berridge et al., 2000, Berridge et al., 2003, Bootman et al., 2001a). As well as these cellular processes, neural cells use changes in $[Ca^{2+}]_i$ to elicit specific behaviours. These are a result of neural circuits responding to a stimuli in the environment (Katz, 2011).

A key aspect to understanding fully how Ca^{2+} signaling is related to changes in neuronal function that lead to alterations in behaviour is the need to identify the components of the Ca^{2+} signaling pathways; including the essential proteins involved. Understanding the binding mechanisms and the interacting partners required for different behaviours are paramount in decoding neuronal circuits.

Members of the different EF hand containing Ca^{2+}-binding proteins show a broad diversity in regards to their cation binding properties as well as their subcellular targeting. The NCS family members hold a high affinity for Ca^{2+} in comparison to CaM, and a number of these are associated with membranes through post-translational modifications including myristoylation and lipidation (Haynes et al., 2006, Haynes et al., 2007). Correct targeting of Ca^{2+}-binding proteins to the subcellular locations is crucial for their biological processes such as Neuronal Ca^{2+} sensor-1 (NCS-1) interactions with Golgi apparatus allowing trans Golgi movement (Haynes et al., 2005). The NCS family of Ca^{2+} binding proteins respond to changes in $[Ca^{2+}]_i$ to elicit cellular changes which can affect overall behaviour of an organism through interacting with specific binding partners.

This research used the model organism *C. elegans*. *C. elegans* has long been used as a model organism for cellular/genetic mechanisms underlying neurosensory perception and neuroethology in general. The novel temperature-dependent locomotion (TDL) behaviour examined in this chapter potentially reflects a cellular/genetic mechanism underlying a neuroecological phenotype that evaluates

changing animal behaviour and their consequences within the context of the organism's environment.

Currently, the interactome of *C. elegans* NCS-1 has not been fully elucidated, with a number of potential binding partners being hypothesized; based on a mammalian NCS-1 interactome. Previous work has shown a requirement for the Ca^{2+} sensor protein NCS-1 in thermotaxis responses (Gomez et al., 2001) and in changes in locomotion rate following temperature elevation (Martin et al., 2013).

The influence of Ca^{2+} on the structure of NCS-1 in its N and C-termini and the exposure of specific residues of its hydrophobic pocket allow for regulation of interactions. Structural studies have been conducted to specify the binding regions between NCS-1 and a set of its binding partners. In the presence of a binding partner, the C-terminus is hypothesized to translocate out of the hydrophobic binding cleft to permit protein binding.

The functional importance of NCS-1 and a selection of its binding partners have been elucidated including NCS-1 interacting with Dopamine D2 receptors permitting sensitization of these receptors (Kabbani et al., 2002, Lian et al., 2011) and with neuronal Ca^{2+} channels permitting synaptic transmission and exocytosis (Dason et al., 2012, Chen et al., 2001, Dragicevic et al., 2014, Lian et al., 2014). Studies into NCS-1 have characterised many of the functionally important interactions. It is from one such study (Gomez et al., 2001), that emphasized the use of behavioural analysis to study the functional relationship of EF hands and Ca^{2+} binding in neurons to elicit a specific behaviour. This study conditioned *C. elegans* to associate food with a specific temperature, when placed on a temperature gradient; *C. elegans* migrated to this temperature and moved isothermally (Isothermal tracking (IT)).

Previous studies have implicated the AIY neuron as the site of action for NCS-1 in TDL behaviours (Figure 1.14) (Martin et al., 2013). The focus of this chapter centered around the relationship between NCS-1, ARF-1.1 and PIFK-1 in *C. elegans*, with investigations into other hypothesized NCS-1 binding partners including TRP-1, TRP-2, ARF-1.2 and GRK-2. NCS-1 and Arf-1.1 both interact with and stimulate PI4KIIIβ. In non-neuronal cells, over-expression of ARF-1.1 reversed NCS-1 stimulated

inhibition of traffic from the Golgi complex, indicating a potential functional interaction between these two proteins. To explore further the physiological relevance of an ARF-1.1/NCS-1 interaction in a TDL behaviour manner, a specific assay was produced to investigate temperature dependent changes in locomotion in *C. elegans* (Todd et al., 2016).

4.2 Results

4.2.1 Characterisation of the TDL Assay

As preliminary research within the laboratory had identified a novel temporary paralysis phenotype (unpublished data), within *C. elegans* when exposed to a heightened temperature, a revised TDLA was formulated to investigate this phenotype (as outlined in the methods section). This assay measured two distinct parameters; the time to onset of paralysis and the duration of the identified paralysis in different *C. elegans* strains.

Assay characterisation was completed using a range of temperatures to determine the optimal conditions for studying the paralysis phenotype. Preliminary characterisation of the assay was completed on N2 and *ncs-1* (XA406, *qa401*) null *C. elegans* to identify temperatures which allowed high throughput analysis and denoted differences between strains for the assay parameters. Previous studies identified an elevation of temperature to ~28.5^{o}C elicited temperature dependent behaviours (Martin et al., 2013), temperatures between 26^{o}C and 30^{o}C (± 0.5^{o}C) were investigated to fully characterise the assay.

Of the temperatures studied, at 30^{o}C (± 0.5^{o}C) both of the strains tested, N2 wild-type and *ncs-1* null (XA406 (*qa401*)) animals showed a rapid onset of paralysis which at 30^{o}C was not significantly different between the wild-type and mutant strain (Figure 4.1a) albeit a difference was denoted for the duration of paralysis (Figure 4.1b). At the lowest temperature measured, 26.0^{o}C (± 0.5^{o}C), approximately 66% of the *ncs-1* null animals analysed did not paralyse over the time frame of the assay (1 hour), these animals were not included in the final analysis (Figure 4.1c), whilst all the N2 *C. elegans* were able to paralyse. Furthermore at this temperature, no difference was denoted for the duration of paralysis. These temperatures were each deemed unsuitable for high-throughput analysis of animals.

When animals were tested at 28.5^{o}C (± 0.5^{o}C), each animal showed examples of paralysis within a suitable timeframe for high-throughput analysis, with significant differences noted for each of the two parameters of this phenomenon. Ideally for this

research, an optimal temperature was to be found which distinguished wild-type worms from their mutant counterparts. Statistical differences in either parameter suggested the temperature sensing pathway was no longer working as it should; as each parameter was measured against a wild-type background acting as a control. Behaviours which diverged from the control were said to be abnormal.

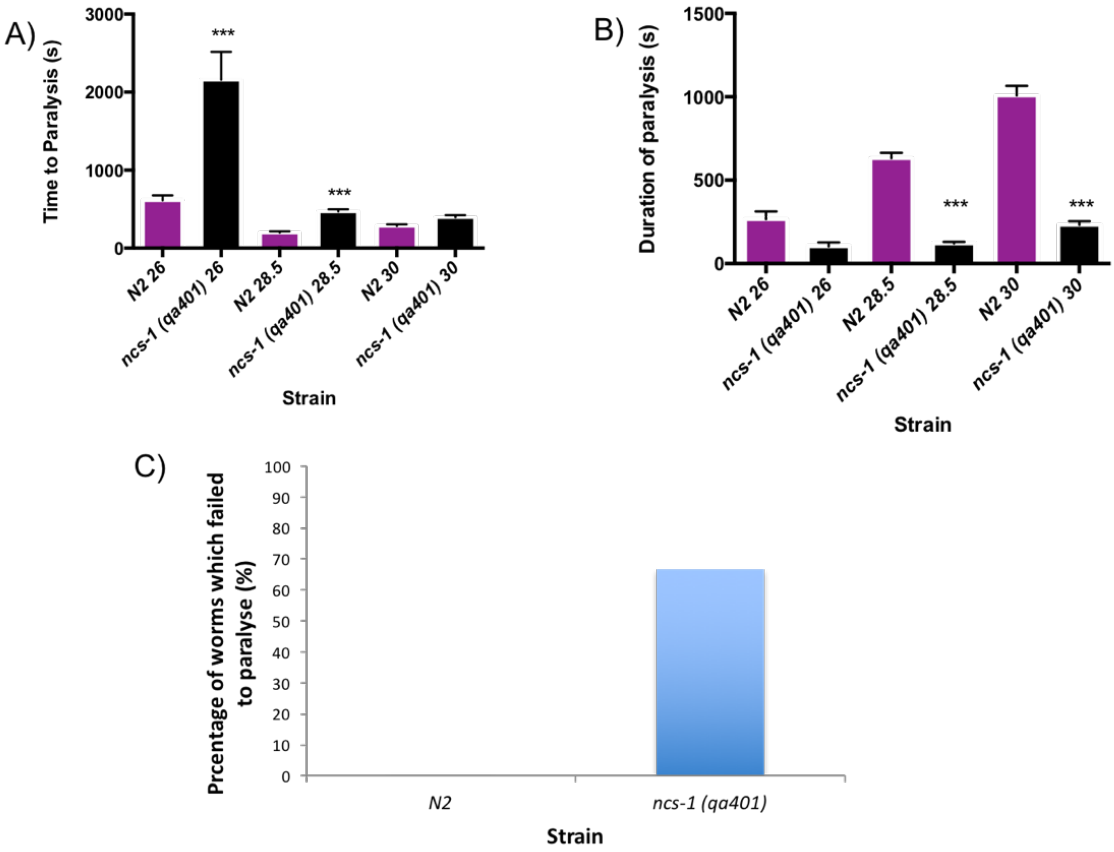

Figure 4.1: Characterisation of optimal temperatures for TDLA. Temperature dependent locomotion assays were completed on 2 separate *C. elegans* strains at various temperatures to elucidate the ideal temperature for subsequent assays investigating worm paralysis behaviours at elevated temperatures. In each case, TDLA was completed as described in the methods section 2.3.2. A) Start of paralysis after heated to defined temperatures. B) Duration of paralysis identified using start of paralysis subtracted from end of paralysis (seconds). C) Percentage of *ncs-1* null worms which failed to undergo paralysis at 26°C. Multiple animals were tested for each strain (N ≥ 15 animals), at 26°C however of the 15 worms tested for *ncs-1* null (*qa401*) only 5 underwent paralysis; for this condition, N = 5 animals. Averages for the different parameters were utilized to assess behavioural responses of the various strains. All data sets were compared with N2 control animals at each temperature (*=p≤0.05, **= p≤0.01, ***= p≤0.001) for start and duration of paralysis determined using one way ANOVA with the use of Sidak correction for multiple comparisons.

4.2.2 Temperature dependent locomotion effects over an extended time frame.

To analyse further the effect temperature had on the behaviour of different *C. elegans* strains, single animals were measured for their thrashing rates at 20°C over a 10 minute time frame (following 10 minute acclimatisation in Dents solution). Locomotion was measured at 1 minute, 5 minutes and 10 minutes and averages generated for each, acting as a measure of neuronal transmission (Figure 4.2).

Previous research within the laboratory has shown that the thrashing rate increased in a specific strain *ncs-1* null (*qa401*) when exposed to an elevated temperature than their cT (Martin et al., 2013). This noted behaviour was not present in other *C. elegans* strains tested. From the data collected, no significant difference could be identified between N2 and *ncs-1* null (*qa401*) *C. elegans* at room temperature, suggesting the neuronal network was unaltered at this temperature.

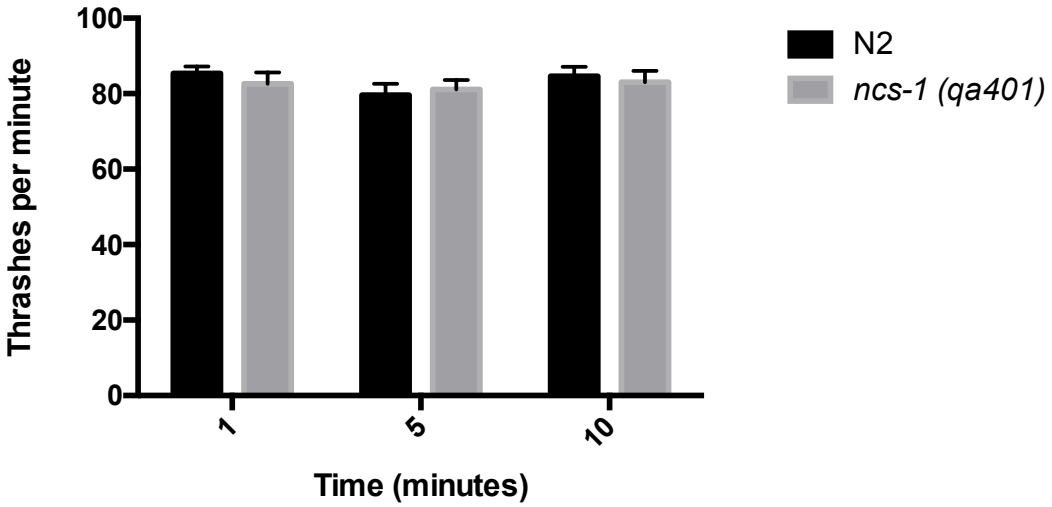

Figure 4.2: Average basal thrashing rate of *C. elegans* at 20°C. *C. elegans* strains were measured for baseline thrashing rates under normal conditions. Single animals were placed into a drop of Dent's solution and the thrashing rate measured at 1 minute, 5 minutes and 10 minutes after addition to the Dent's solution. Thrashing rates were measured over a 1 minute period for each animal and an average generated.

Short and long term responses to temperature were also measured in respect to locomotion. To this end single animals were placed into Dents solution at 20°C and the temperature raised slowly to 28°C (± 0.5°C). The thrashing rate of the animals was

then measured every 5 minutes over a 90-minute time frame. Averages generated for each of the 5 minute intervals (Figure 4.3a). A snapshot of the effect temperature has on locomotion was generated, with N2 dying at elevated temperatures earlier than *ncs-1* null (*qa401*) *C. elegans*. Death of the animals was determined at the 90-minute time point, nematodes which were not moving were mechanically stimulated with a tungsten filament and those which remained immobile were classed as dead. *C. elegans* which were not moving at the 5-minute time points generated a locomotion score of 0, which was included in the analysis, due to the nature of reversible paralysis.

Unlike what was shown during the basal thrashing experiment, the *ncs-1 (qa401) C. elegans* showed an increased locomotion compared with N2 in the same conditions. N2 also showed a higher percentage of paralysis than the *ncs-1* null *(qa401) C. elegans* (Figure 4.3b), duration of paralysis at this stage was not under investigation as this was solely looking at the thrashing rates every 5 minutes.

Of the animals tested in this data set; for N2 the levels of paralysis at the different time points, paralysis was more erratic than the *ncs-1 (qa401) C. elegans*, with the final 3 time points showing 100% paralysis of the N2 animals tested (Figure 4.3b). This is in contrast to the *ncs-1* null *C. elegans* which showed some level of motility at the elevated temperature at the 90-minute time point. The paralysis timeline provided a baseline for this behaviour and also showed differences in the long-term temperature sensation for *C. elegans* when presented with continuous noxious temperatures.

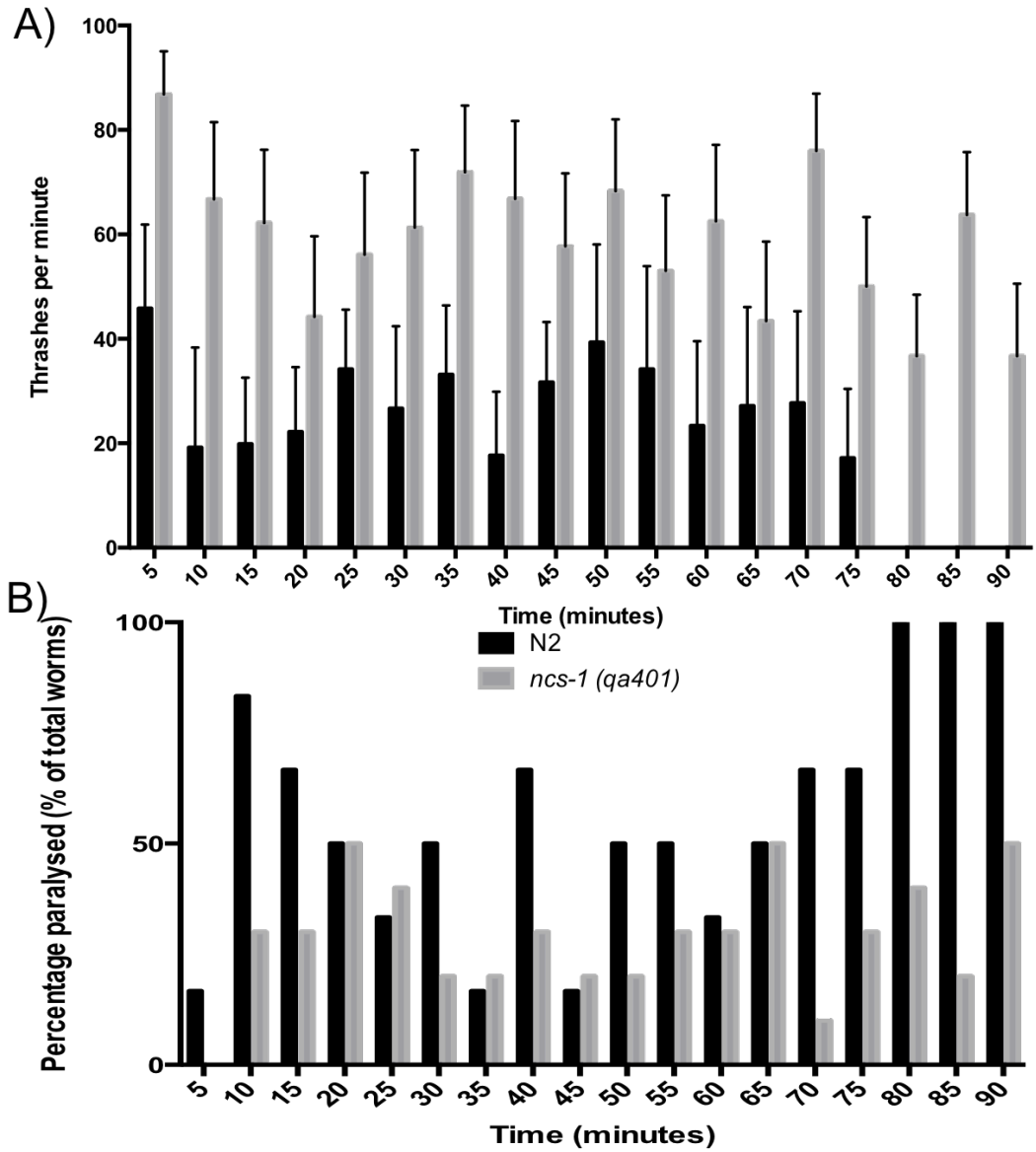

Figure 4.3: Effect prolonged exposure to high temperature has on thrashing rates. Single *C. elegans* were measured for their thrashing behaviours over a 90-minute time frame when exposed to an increased temperature (approximately 28^{o}C). Thrashing rates were measured every 5 minutes up to 90 minutes and the data averaged for each strain. Figure 4.3a shows N2 animals were less motile at the increased temperature with complete cessation of motility after 75 minutes for all of the tested animals whilst *ncs-1* null animals expressed a higher level of motility at the increased temperature and also remained motile up to the end of the time points within this experiment. Cessation of motility was determined through mechanical stimulation of the individual nematodes using a tungsten filament. Paralysis was quantified as any individual worm which failed to thrash more than 5 times within the minute of analysis was classified as paralysed at that time point. Error bars indicate ± SEM.

Average locomotion rates were higher in the *ncs-1* (*qa401*) null *C. elegans* compared to N2 *C. elegans* owing to increased numbers of paralyzed *C. elegans* for the N2s.

The percentage of nematodes which underwent paralysis over the 90-minute time frame shows a repeating pattern with N2 *C. elegans* and ncs-1 null *C. elegans* showing asynchronous pattern of paralysis which differed between the two strains. Whilst N2 animals paralysed earlier and for longer, *ncs-1* null animals paralysed later and recovered quicker.

4.2.3 Analysis of Rescue Strains in the TDL assay.

C. elegans strains with a loss of NCS-1 activity have altered learning patterns including isothermal tracking and also altered temperature dependent behaviours (Gomez et al., 2001, Martin et al., 2013). Previous research in our laboratory by Dr. Jeff Barclay and Dr. Victoria Martin (University of Liverpool) first looked at the locomotive behaviours of different *C. elegans* mutant strains at elevated temperatures compared to locomotion at cultivation temperatures.

Re-expression of NCS-1 in the whole organism using a WT *ncs-1* promoter (WT rescue) or solely in the cholinergic AIY neuron using an AIY specific promoter (AIY rescue) was sufficient to rescue thrashing defects, returning this to wild-type N2 levels (Martin et al., 2013). The new TDLA was utilized as a quantifiable method to identify downstream partner proteins of NCS-1. Assays were completed on multiple animals from different strains to form an average for each strain including mutant and control strains. From these assay parameters, it was discovered that for the wildtype (N2) control strain the onset of paralysis was 457 seconds with a long average duration of paralysis of 711 seconds.

In contrast to this, the *ncs-1* null XA406 (*qa401*) mutant strain had a longer onset of paralysis (average onset of 790 seconds) and a shorter duration of paralysis (average duration of 196 seconds). Significant differences between the strains (N2 and *qa401*) were identified for both parameters. Reintroduction of NCS-1 into *qa401* rescued both parameters of this assay. For the WT rescue the average onset of paralysis was 332 seconds with an average duration of 853 seconds with the AIY specific rescue showing an average onset of 401 seconds and an average duration of 592 seconds (Figure 4.4).

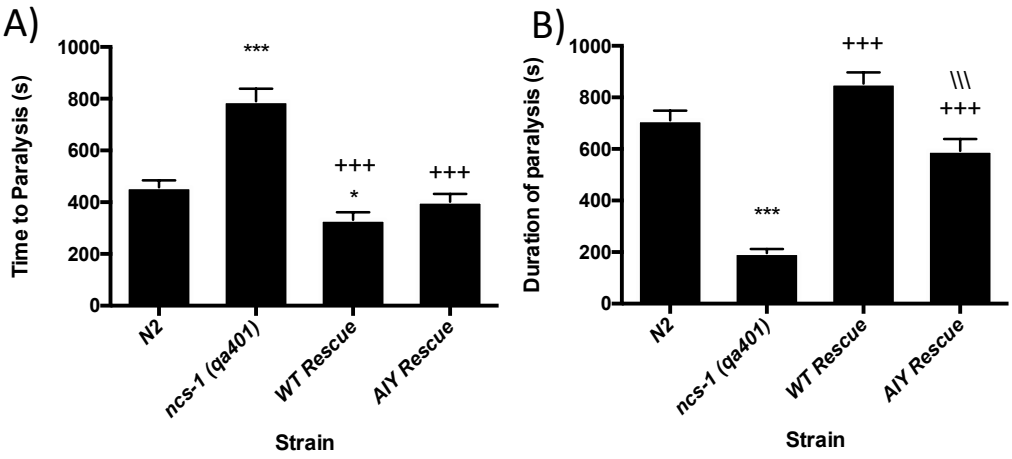

Figure 4.4: Analysis of NCS-1 rescue strains for paralysis behaviours. Temperature dependent locomotion assays were used on various *C. elegans* strains to elucidate the paralysis behaviours for different strains including rescue NCS-1 strains, rescue strains conducted in *ncs-1* null (*qa401)* with *ncs-1* re-expression using a WT *ncs-1* promoter or AIY specific promoter. Paralysis activity measured at 28.5^{o}C (± 0.5^{o}C). Multiple animals were tested for each strain (n≥30 animals) and averages for the different parameters were utilized to understand the behavioural patterns of the various strains. Statistical differences identified using one-way ANOVA (*=p≤0.05, **=p≤0.01 and ***=p≤0.001, *= difference compared to N2, += difference compared to XA406 and \= difference compared to WT rescue). Multiple comparisons were completed on this data set. Statistical differences for the onset and duration of paralysis for each strain was determined using the one-way ANOVA with the use of Dunnetts correction for multiple comparisons.

4.2.4 Testing of RNAi as a means to recapitulate paralysis behaviours

The next approach was to identify functional NCS-1 binding partners in the TDLA using previously characterized/identified binding partners from other types of assays, specifically those present in the nervous system. With the establishment of the baseline behaviours for the paralysis phenotype, the next approach was to assess knock-out or knock-down of selected binding partners, any which were of functional importance in the TDLA were expected to have the same behavioural phenotype as the *ncs-1* null *C. elegans*. An initial approach utilized RNAi (RNA interference) of potential binding partners with a panel of control genes.

The control genes tested for the RNAi panel; Heat shock protein 1 (*hsp-1* (as a lethal positive control)), *L4440* (empty vector negative control) and constituent components of the SNARE complex Synaptotagmin (*snt-1*), Synaptobrevin (*snb-1*) and

Uncoordinated-18 (*unc-18*) to verify sufficient neuronal knockdown in the specific conditions and to show the effect of blocking SNARE complex formation (RNAi conditions outlined in table 4.1). Primary testing looked at the thrashing rates of the RNAi treated animals.

Sample	Gene	Code	Plate	Cell	Chromosome	Obtained from
1	*ncs-1*	C44C1.3	N/A	N/A	X	Source Bioscience
2	*hsp-1*	f26d10.3	10015	H1	IV	C. elegans Vidal RNAi library
3	*L4440*	N/A	N/A	N/A	N/A	C. elegans Vidal RNAi library
4	*snt-1*	F31E8.2	10154	F9	II	C. elegans Vidal RNAi library
5	*snb-1*	T10H9.4	11053	C4	V	C. elegans Vidal RNAi library
6	*unc-18*	F27D9.1	11053	E7	X	C. elegans Vidal RNAi library
7	*pifk-1*	F35H12.4	11081	A12	X	C. elegans Vidal RNAi library
8	*trp-2*	R06B10.4A	11004	C7	III	C. elegans Vidal RNAi library
9	*arf-1.1*	F45E4.1	11041	C6	IV	C. elegans Vidal RNAi library
10	*arf-1.2*	B0336.11	11004	C9	III	C. elegans Vidal RNAi library
11	*arf-1.2 (2)*	B0336.2	10051	D11	III	C. elegans Vidal RNAi library

Table 4.1: RNAi conditions utilized during the subsequent RNAi experiments. RNAi conditions included a set of controls to test efficiency of RNAi within the different *C. elegans* strains along with an RNAi panel using proteins of interest.

4.2.4.1 Quantifying thrashing rates in RNAi treated C. elegans strains

Initial research used the control N2 strain. Upon identifying this was not a suitable model, investigations then progressed onto XE1581 (a cholinergic neuron RNAi specific strain (Firnhaber and Hammarlund, 2013)) and NL2099 (an RNAi hypersensitive strain, *pk1426 (rrf-3*)). These each had specific properties which were useful to elucidate the effect RNAi had upon these different strains. Neuronal activity was quantified through thrashing rates of *C. elegans,* following 2 generations grown on RNAi treatment plates to maximize RNAi treatment. Thrashing assays were completed as this allows quantification of neurotransmission through *C. elegans* motility.

N2 *C. elegans* are not predisposed to have a higher RNAi effect, this work tested the viability of RNAi in *C. elegans* (Figure 4.5). Through treatment of N2 worms using the RNAi panel (taken from Vidal *C. elegans* RNAi clones library), it was found that

thrashing rates were significantly decreased under certain treatment conditions (Figure 4.5).

A partial RNAi effect was shown in the *hsp-1* and in the SNARE complex conditions which showed a decrease in thrashing rates, interestingly in these conditions, RNAi was expected to generate a paralysis or lethal phenotype if sufficient KD was achieved (Morley and Morimoto, 2004, Nonet et al., 1993, Nonet et al., 1998, Simmer et al., 2002, Yu et al., 2013). Similar results were identified in RNAi of a number of the interacting partners of NCS-1 (*trp-2, arf-1.1* and *arf-1.2*).

Similar locomotion rates to untreated worms were shown in *ncs-1* RNAi, L4440 RNAi, *pifk-1* RNAi and *arf-1.2* RNAi (Figure 4.5). At this stage we attempted RNAi on a novel RNAi sensitive neuronal (XE1581) strain, permitting RNAi solely in cholinergic neurons, driving RNAi through *rde-1* and *sid-1* expression of a specialized *C. elegans* negative background lacking *rde-1, eri-1* and *lin-15b* under the expression of *Punc-17* (Firnhaber and Hammarlund, 2013). Our study focused on NCS-1 in the cholinergic AIY neuron.

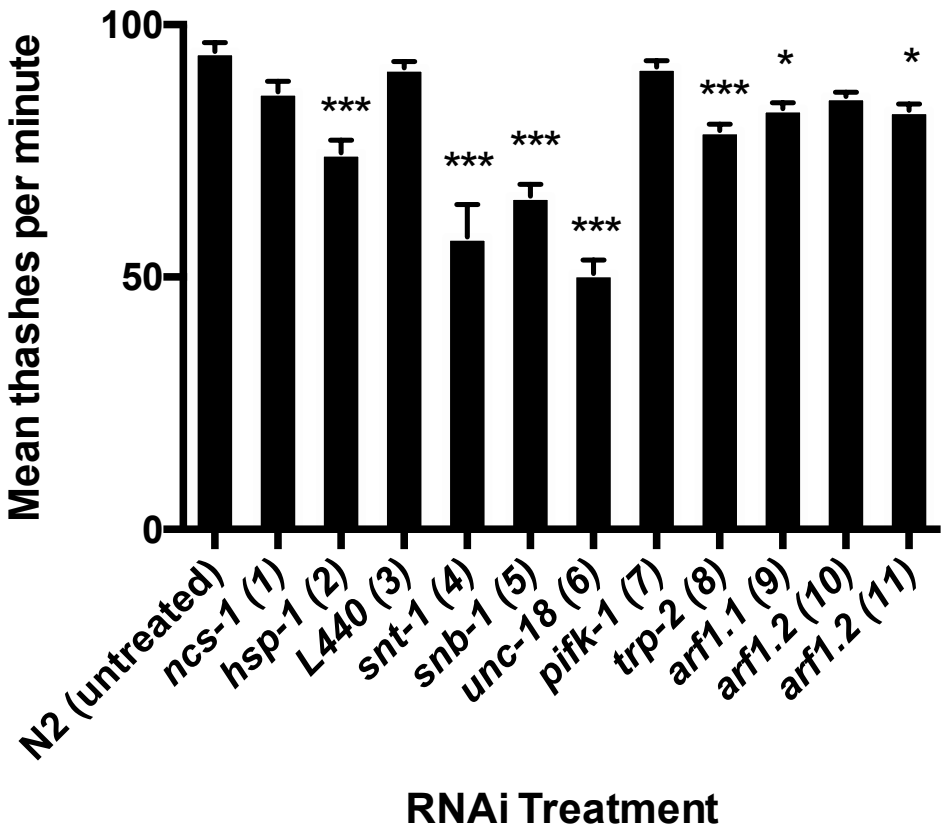

Figure 4.5: Analysis of RNAi induced alterations of thrashing. N2 *C. elegans* underwent feeding RNAi for two generations prior to testing in the thrashing assay. To identify the effect RNAi had upon the thrashing rates of different *C. elegans* strains, animals were treated with bacteria expressing different RNAi constructs. After the F2 generation, single animals were tested for their thrashing rates. Figure 4.5 shows the effect of RNAi on N2 through the thrashing rate quantification. Significant differences were shown in worms which were subjected to RNAi of *hsp-1, snt-1, snb-1, unc-18, trp-2, arf-1.1* and one condition of *arf-1.2*. Locomotion was quantified by counting thrashes per minute of age synchronized day 1 worms at room temperature (20^{o}C) in Dent's solution (n= 15 animals for each condition). All data expressed as average with SEM plotted. Statistical differences were determined using a one-way ANOVA from the package GraphPad Prism 6, significant difference for samples with *=p≤0.05, **=p≤0.01, ***=p≤0.001 comparing with untreated N2 sample, one-way ANOVA with Tukey's correction for multiple comparisons.

4.2.4.2 XE1581

Recently advanced mechanisms have allowed the formation of RNAi specific *C. elegans*, work by (Firnhaber and Hammarlund, 2013) allowed the production of neuron specific RNAi strains, our research used XE1581, as the AIY neuron is the only identified cholinergic neuron expressing NCS-1. This would therefore determine the

effect RNAi had on NCS-1 and the thermosensory pathway in *C. elegans.* Thrashing rates were recorded over a 1 minute period, following a 10 minute acclimatization period.

Comparing thrashing rates against untreated (base-line) thrashing, the different RNAi conditions showed an unexpected yet clear reduction in thrashing rates (Figure 4.6). Of interest, under *ncs-1* RNAi, a significant locomotion reduction was identified along with a number of its binding partners. This reduced thrashing rates has not been shown in previous studies suggesting the altered thrashing rates could be non-specific (Martin et al., 2013). Members of the SNARE complex and *hsp-1* also reduced locomotion, as expected, albeit not paralyzing or being lethal to *C. elegans.* Through presenting RNAi solely in cholinergic neurons, the expected result would be a decrease in the SNARE complex function hence fewer thrashes in the *snt-1, snb-1* and *unc-18* RNAi settings, causing paralysis in these animals. Incomplete RNAi can be seen here as these remained mobile.

Further research was conducted using a more traditional neuronal RNAi sensitive line NL2099 (*pk1926* (*rrf-3*)). Whilst *eri-1* is the traditional strain for RNAi, this strain wasn't suitable for potential research into temperature sensitive behaviours as this is itself temperature sensitive (Kennedy et al., 2004).

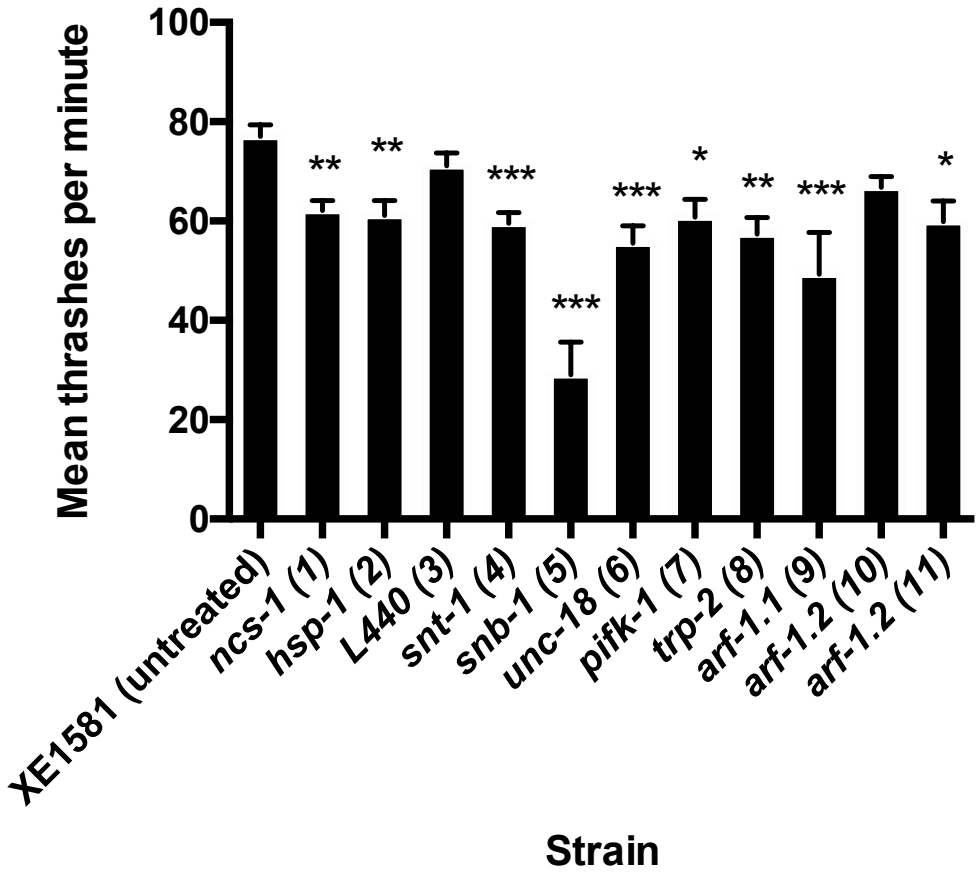

Figure 4.6: Analysis of RNAi induced alterations of thrashing. Effects of RNAi upon the thrashing rates of *C. elegans* designed to allow RNAi in cholinergic neurons alone. Animals were treated with RNAi constructs through feeding RNAi and locomotion rates were assessed for XE1581 untreated compared with XE1581 exposed to an RNAi panel. Significant differences in locomotion rates were discovered for all of the RNAi panel excluding L4440 (negative control) and *arf-1.2* (condition 10, table 4.1) For all conditions at least 10 nematodes were assessed, averaged with SEM plotted for each condition. Statistical differences were determined using a one-way ANOVA from the package GraphPad Prism 6, significant difference for samples with *=p≤0.05, **=p≤0.01 and ***=p≤0.001 compared with XE1581 untreated.

4.2.4.3 NL2099 (rrf-3)

With effects noted in N2 and XE1581 *C. elegans*, analysis was conducted on an RNAi susceptible *C. elegans* strain, NL2099 (*pk1426*), showing a down-regulation of *rrf-3*. NL2099 contains a loss of function within a putative RNA-directed RNA polymerase (RdRP) resulting in a hypersensitivity to RNAi (Simmer et al., 2002, Simmer et al., 2003, Hamilton et al., 2005, Johnson et al., 2005).

A targeted RNAi screen was utilized following on from the previous research. A clear effect can be seen in the *hsp-1* condition causing a complete cessation of movement and reduced growth on plates, as expected. A decrease in locomotion was also noted in the SNARE complex proteins RNAi (*snt-1* and *unc-18*), indicating a possible reduced level of exocytosis hence lowered locomotion (Figure 4.7) when compared to the untreated NL2099 (*rrf-3*) strain.

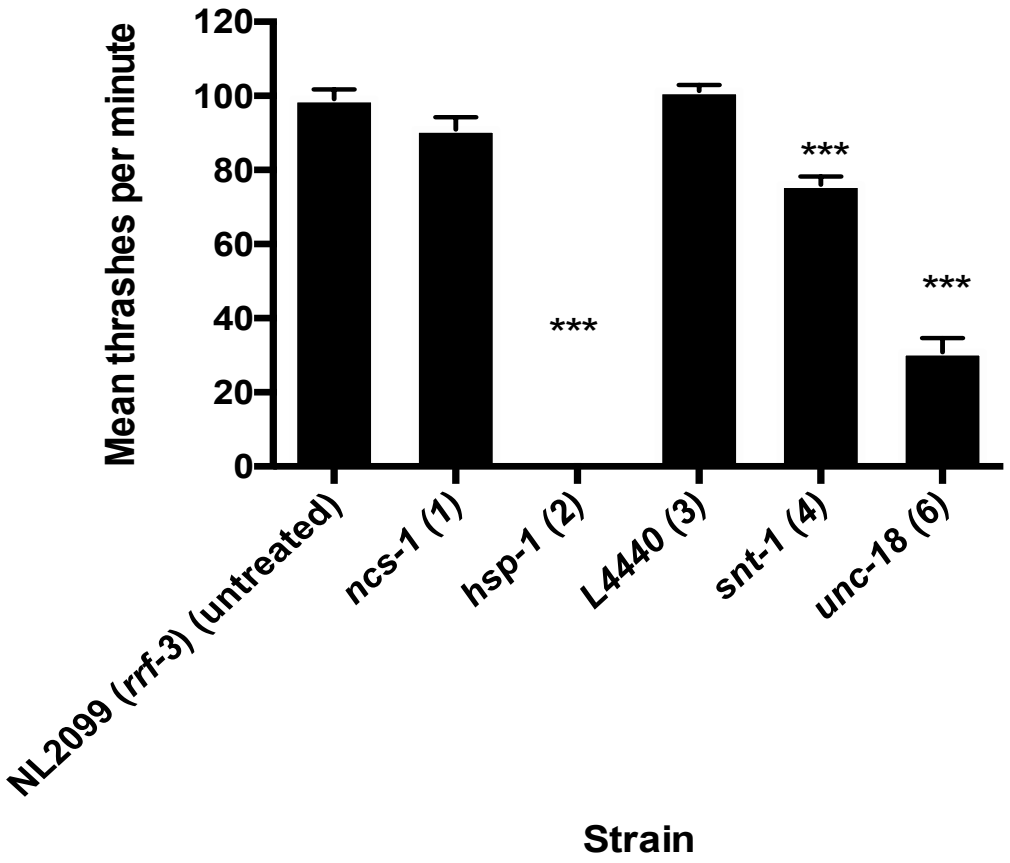

Figure 4.7: Effect of RNAi on locomotive rates in *rrf-3*. Thrashing assays were completed on NL2099 (*rrf-3*) animals (Simmer et al., 2002, Simmer et al., 2003) after pre-treatment with an RNAi panel for two generations. *rrf-3* nematodes treated with RNAi against *hsp-1* caused a complete cessation of movement. RNAi samples taken from Ahringer *C. elegans* RNAi library. N= 20 worms pre treatment. All data expressed as average with SEM plotted. Statistical differences were determined using a one-way ANOVA from the package GraphPad Prism 6, significant difference for samples with *=p≤0.05, **=p≤0.01 and ***=p≤0.001.

NL2099 (*rrf-3*) *hsp-1* RNAi treated *C. elegans* acts as a positive control for the RNAi treatment as this caused complete paralysis/death of the animals. Loss of *hsp-1* (a

member of the *hsp-70* family) (Heschl and Baillie, 1989, Snutch et al., 1988) significantly diminishes protein functions hence leading to death of the organism.

The RNAi panel was not as extensive as when N2 or XE1581 were investigated for NL2099 as the RNAi protocol was being tested on a known RNAi sensitive strain, acting as a positive control. NL2099 showed the extreme effects which were expected to be observed in the other experiments. As RNAi only partially decreases gene function, it is possible a more extreme effect would be present through a more severe gene attenuation. Whilst *hsp-1* RNAi caused cessation of life, suggesting a global effect (as *hsp-1* is present in non-neuronal pharynx cells) (McKay et al., 2003), *C. elegans* under *unc-18* RNAi were motile suggesting incomplete gene function ablation. The expression pattern of *snt-1* and *unc-18* are predominately within the nervous system, RNAi within these conditions is a more precise measure of neuronal knockdown. A sufficient knockdown in thrashing was identified in the RNAi experiments, suggesting it was viable to test in the TDLA.

4.2.5 Analysis of the effect RNAi has upon Temperature Dependent Locomotion

Upon noting an effect on locomotion through feeding RNAi, the next stage was to identify whether RNAi could affect TDL paralysis behaviours as shown in previous knockout strains (Figure 4.4). NL2099 (*rrf-3*) *C. elegans* after the F2 generation grown on RNAi feeding plates (Ohkumo et al., 2008) were subjected to analysis through the TDL assay to assess behavioural changes.

This was working upon the knowledge that NCS-1 has been shown to be present within neurons involved in the thermosensory neural network (AFD, AWC, AFD and AIY) being able to regulate TDL (Gomez et al., 2001, Edwards et al., 2012, Martin et al., 2013). RNAi treated animals were compared with untreated NL2099 *C. elegans.* Interestingly, untreated NL2099 showed a temperature dependent phenotype, different to N2 with a longer onset of paralysis and a shorter duration of paralysis; phenocopying the *ncs-1* null *C. elegans* to an extent. A significant difference was also generated under *ncs-1* and *L4440* RNAi treatment regarding onset of paralysis although not duration of paralysis when compared to untreated NL2099 (Figure 4.8). The parameters of this research suggest an effect on NL2099 in an untreated state,

rrf-3 has been shown to have other temperature sensitive phenotypes in a loss of function variant (Simmer et al., 2002). As such, RNAi was deemed to not be a valid method to assess potential NCS-1 binding partners; as an alternative albeit more widely used approach to the TDLA. For this research, of the methods tested, the TDLA was shown to be the most viable for testing this identified behaviour.

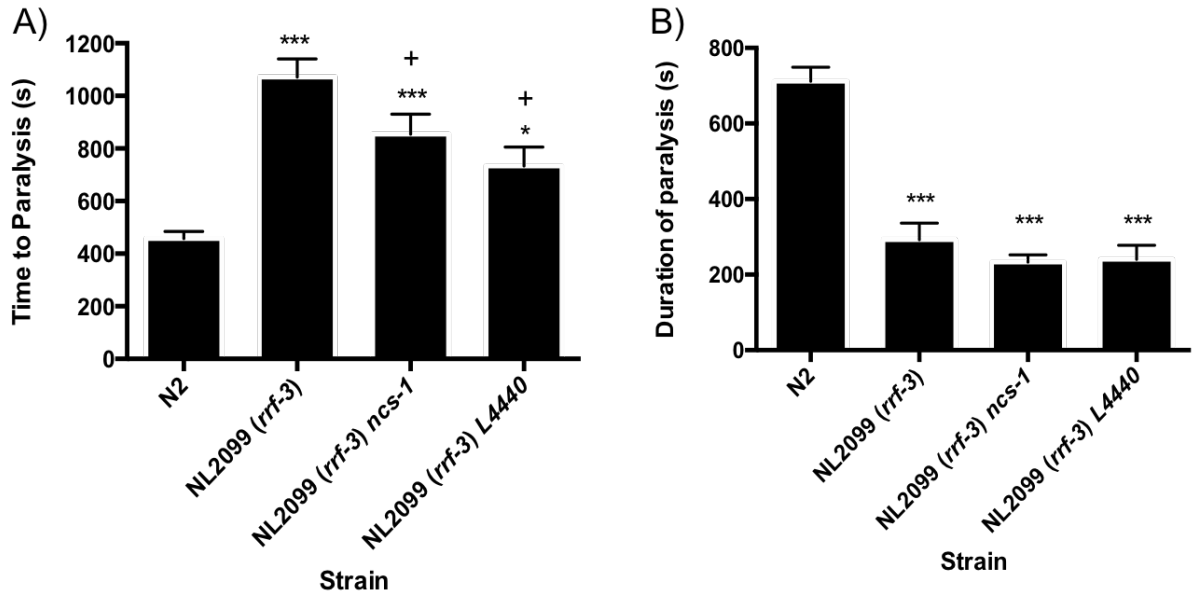

Figure 4.8: The effect of RNAi on TDL behaviour in *C. elegans* using a targeted RNAi panel. RNAi treated F2 generation NL2099 (*rrf-3*) *C. elegans* were subjected to the TDL assay, quantifying their responses to elevated temperature to assess whether RNAi can recapitulate effects seen in other mutant *C. elegans* strains. Parameters measured in this research encompassed the onset of paralysis (time to paralysis (Figure 4.8a)) along with the duration of paralysis (Figure 4.8b). Conditions were compared to N2 or NL2099 (*rrf-3*) untreated *C. elegans* as controls. For each condition n= ≥ 10 animals, all data expressed as average with SEM plotted. Statistical differences were determined using a one-way ANOVA from the package GraphPad Prism 6, one-way ANOVA with Tukey's correction for multiple comparisons (*=p≤0.05, **=p≤0.01 and ***=p≤0.001, * indicates difference from N2 whilst + indicates difference from untreated NL2099 *(rrf-3)*). NL2099 (*rrf-3) L4440* acted as an empty vector control sample.

4.2.6 Identifying potential downstream targets of NCS-1 utilising the TDLA.

NCS-1 holds a number of interacting proteins permitting a range of downstream target processes. To elucidate the downstream functional NCS-1 binding targets in determining the TDLA phenotype (Kuhara et al., 2008, Gomez et al., 2001, Martin et

al., 2013), the behaviour of various *C. elegans* strains was monitored using the TDLA (adapted from (Martin et al., 2013)), looking for phenocopiers of the *ncs-1* null phenotype.

Genes of interest were first identified through a preliminary connectome of mammalian NCS-1 binding partners, taken from various protein-protein interaction screens, which had *C. elegans* orthologues present within the nervous system (Figure 1.6 adapted from (McCue et al., 2010b)). Orthologues which presented a locomotion phenotype when absent in *C. elegans* were omitted as this altered the research parameters. NCS-1 activity in the AIY neuron alone permits rescue of thermosensory behaviours (Martin et al., 2013).

4.2.6.1 Assessing the TDL behaviours of an array of potential NCS-1 interaction partner proteins mutant C. elegans strains.

Mutant *C. elegans* for proteins outlined in the mammalian NCS-1 interactome, if present within neurons or the AIY neurons as the proposed site of action for NCS-1 in TDL behaviours, were obtained from the CGC (Caenorhabditis Genetics Centre), which is funded by NIH Office of Research Infrastructure Programs (P40 OD010440)).

Obtained mutant strains from the preliminary screen were assayed for their TDL behaviours (Figure 4.9). Strains were compared to N2 animals to identify irregular TDL behaviours indicative of their involvement within the TDL pathway as the aberrant TDL behaviour could be due to the gene (Hedgecock and Russell, 1975).

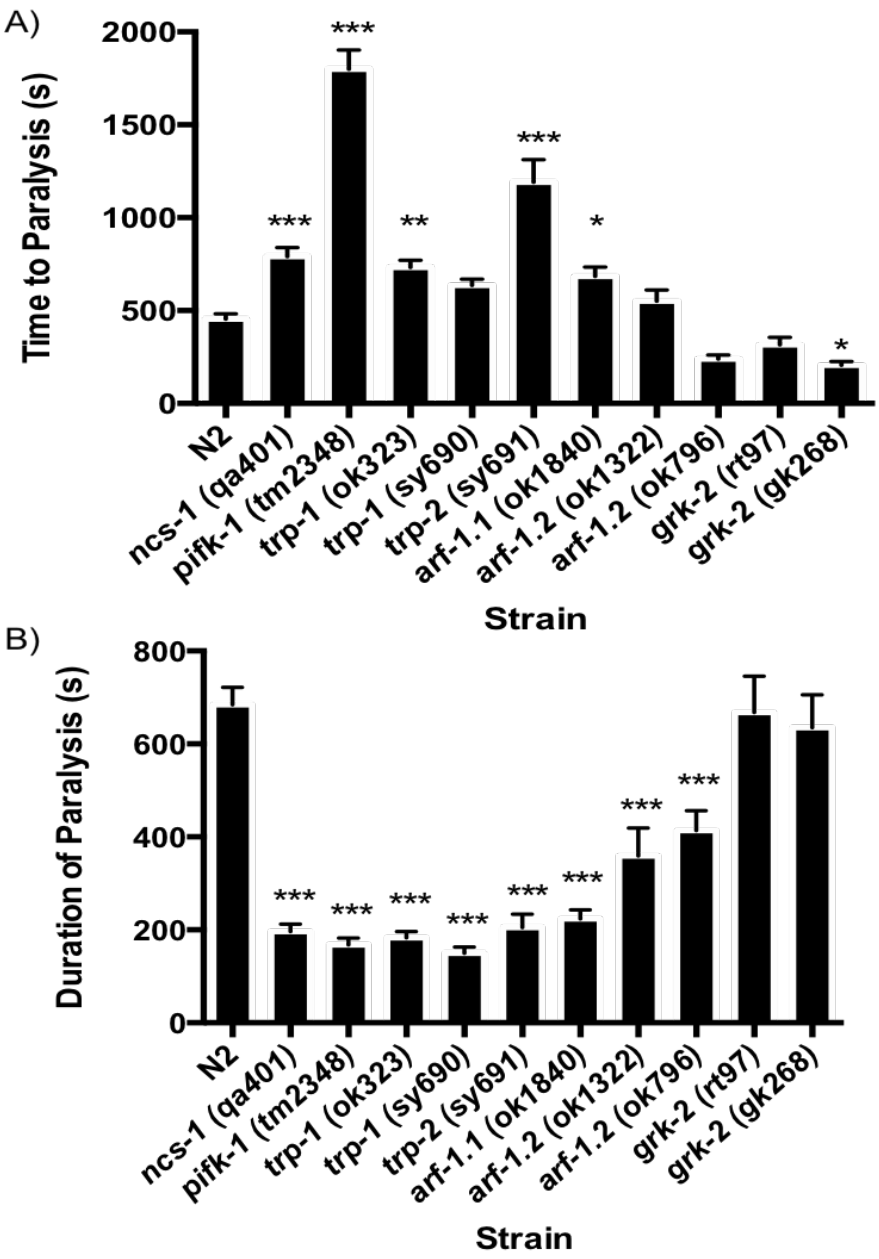

Figure 4.9: Identifying the TDL behaviour of various mutant *C. elegans* strains. Temperature Dependent Locomotion assays were completed using multiple mutant strains of *C. elegans* in an attempt to identify potential targets of NCS-1 within the thermosensory neural network. a) Time to paralysis was measured after worms were placed in Dent's solution on a peltier heating stage and heated to 28.5^{o}C, paralysis was determined as a visible cessation of movement. b) Duration of paralysis was identified from the time the animals recovered from paralysis (regain motor functions), the start of paralysis point (in seconds) was subtracted from the recovery point (in seconds) to generate a duration of paralysis time frame for each animal. Statistical differences were identified by comparing averaged data to that of N2 wildtype animals. Statistical difference demonstrated by one way ANOVA with use of Dunnett correction for multiple comparison (*=p≤0.05, **=p≤0.01 and ***=p≤0.001). N= ≥ 20 animals.

After analysing the mutant strains TDL behaviours, three potential targets were identified as being significantly different (and phenocopied *ncs-1* null) for both research parameters; *pifk-1, arf-1.1, trp-1* and *trp-2*. These strains were taken forward within this research. At this time *grk-2* and *arf-1.2* were discounted as the results were unable to identify reproducible significant difference vs N2 animals.

4.2.7 Generation and identification of double mutant lines.

Using the three identified potential targets of NCS-1, genetic crosses were completed to generate double mutant *C. elegans* strains (of *ncs-1* with the *C. elegans* orthologues of *trp-1, trp-2* and *arf-1.1*) to establish effects on TDL. Genetic crosses between *ncs-1* and *pifk-1* would be problematic as both are present on the X-chromosome. Genetic crosses were confirmed and validated through Polymerase Chain Reaction (PCR) of the parental *C. elegans*. Primers were designed to show wildtype (WT) or mutant (Mut) variants of the DNA fragment (Figure 4.10). Genetic status was checked and verified over multiple generations. Truncated genetic products suggest the gene has been deleted according to PCR status. The absence of a band further identified the genetic status of these genetic lines.

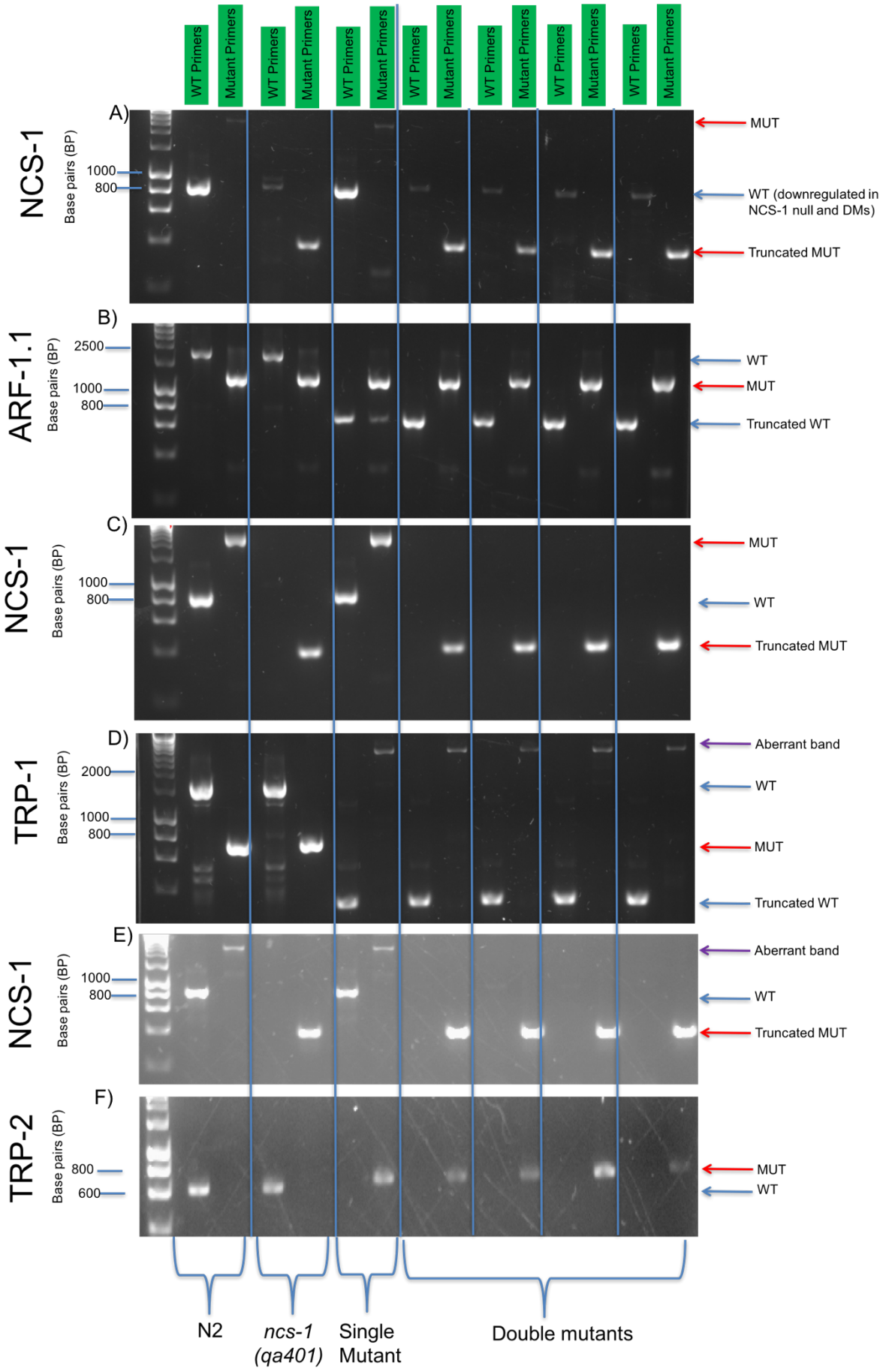
WT Primers
Mutant Primers
A)
NCS-1
Base pairs (BP)
1000
800
MUT
WT (downregulated in NCS-1 null and DMs)
Truncated MUT
B)
ARF-1.1
2500
1000
800
WT
MUT
Truncated WT
C)
NCS-1
MUT
WT
Truncated MUT
D)
TRP-1
2000
Aberrant band
E)
NCS-1
F)
TRP-2
600
N2
ncs-1 (qa401)
Single Mutant
Double mutants

Figure 4.10: PCR validation of Double mutants. A, C, E) Worm lysates from control *C. elegans* strains and newly produced double mutant strains using primers designed against *C. elegans ncs-1*. Single animals were picked to produce worm lysates for PCR. A) A comparison of product size against *C. elegans ncs-1* primers in control strains and *arf-1.1* (*ok1840*) and *ncs-1* (*qa401*) double mutant lines. C) *ncs-1* primers for the *trp-1* (*ok323*) and *ncs-1* (*qa401*) double mutants and E) *ncs-1* primers for the *trp-2* (*sy691*) and *ncs-1* (*qa401*) double mutants. For *ncs-1* a loss of the WT band (blue arrow) should occur with a size difference for the MUT primers (red arrows) B) Gel using worm lysates for control strains alongside double mutant *C. elegans* lines (*ncs-1* and *arf-1.1*), in total 4 lines were produced through genetic crosses, mutant status verified through a size difference when tested using the WT primers (blue arrow). D) Gel using worm lysates for control strains alongside double mutant *C. elegans* lines (*ncs-1* (*qa401*) and *trp-1* (*ok323*)), in total 4 independent lines were successfully produced through this genetic cross and verified using a loss of the MUT band (red arrow) and a size difference for the WT primers (blue arrow). F) Agarose gel using worm lysates for control strains alongside double mutant *C. elegans* lines (*ncs-1* (*qa401*) and *trp-2* (*sy691*)), in total 1 independent genetic line was produced through this cross and verified with a loss of the WT band and a size difference for the MUT primers. All gels loaded with two samples per strain (wild-type primers and mutant primers).

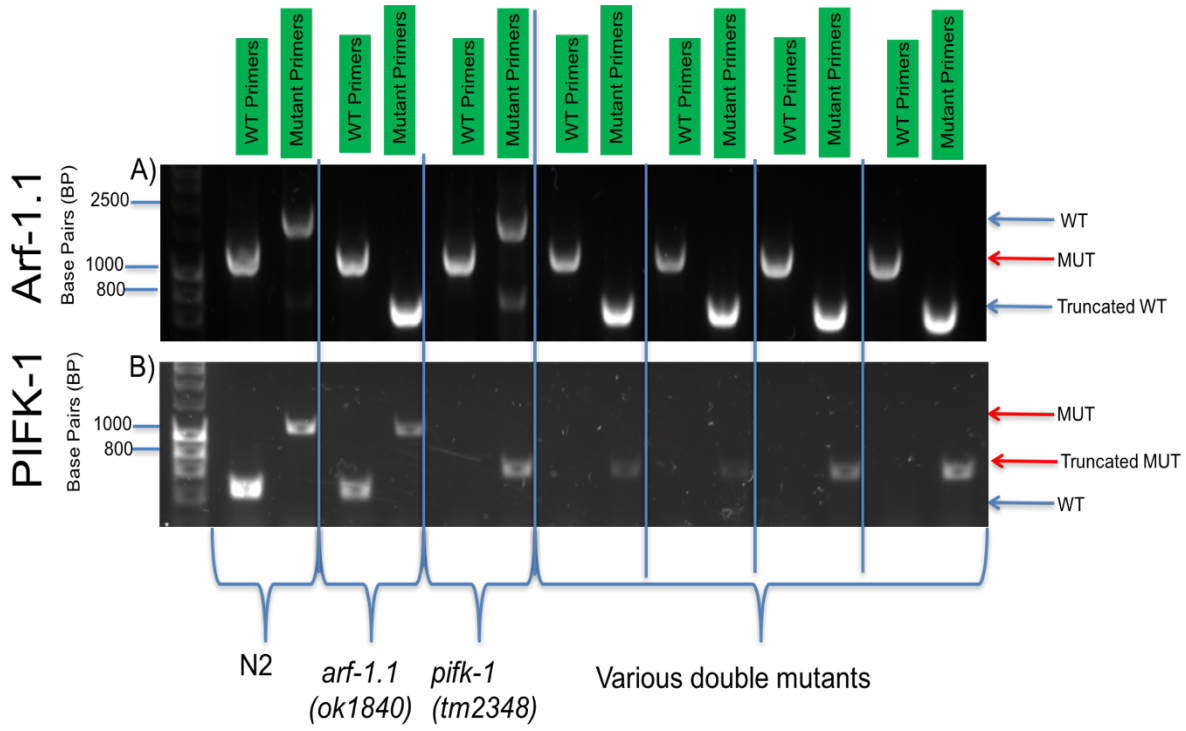

Figure 4.11: PCR validation of double mutant for PIFK-1 (*tm2348*) and Arf-1.1 (*ok1840*). A) Worm lysates from control *C. elegans* strains and newly produced double mutants to verify the status of the *arf-1.1*. For *arf-1.1* a decrease in size for the WT band was identified (blue arrow). B) Worm lysates for control *C. elegans* strains alongside newly produced double mutant lines verifying the status of the *pifk-1* DNA sequence. To verify double mutant status, a loss of the WT band (blue arrow) was identified alongside a smaller DNA fragment for the MUT primers (red arrow). In total 4 independent genetic lines were produced for the *arf-1.1* and *pifk-1 C. elegans* genetic cross.

4.2.8 Effect of induced double mutations on temperature-dependent locomotion

Generated double mutants of *ncs-1* with *trp-1* or *trp-2* showed no difference from the single mutant counterparts for either parameter, showing a longer onset of paralysis and a shorter duration of paralysis (Figure 4.12). Neither a rescue effect or an additive effect was shown. This similar behavioural phenotype is indicative of these proteins acting within the same phenotypic pathway.

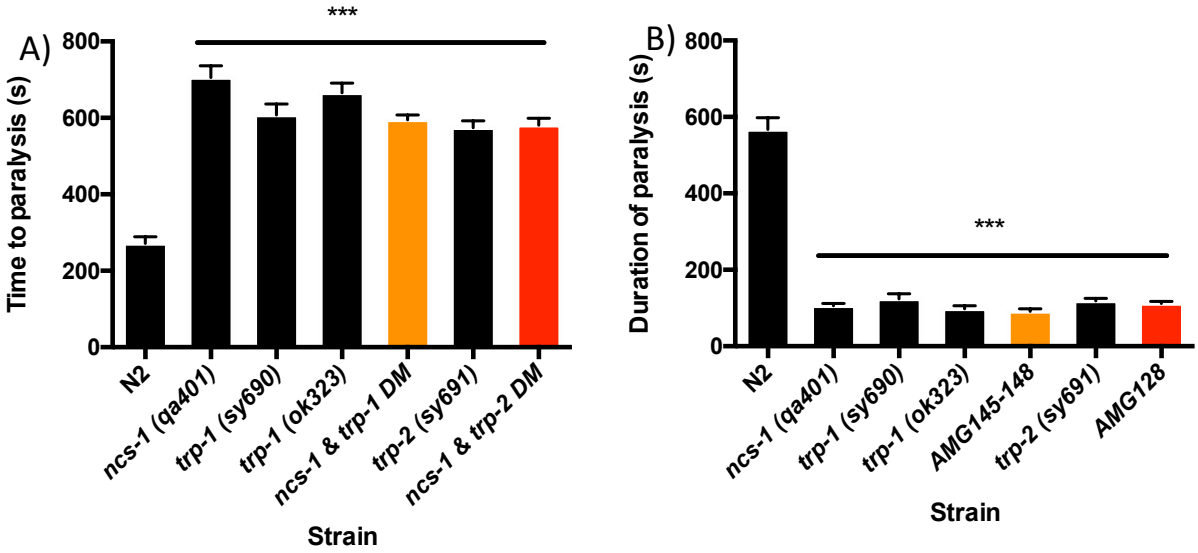

Figure 4.12: Temperature-dependent Locomotion analysis of genetically crossed *ncs-1* and *trp-1 / trp-2 C. elegans* strains A) TDL behaviours of *C. elegans* strains generated through genetic crosses using standard crossing techniques. Single animals were tested for their time to paralysis after exposure to prolonged heat within Dents solution present on a peltier heating stage and exposed to 28.5°C. B) TDL behaviours further derived from the duration of paralysis of the various *C. elegans* strains. Assay started after exposure to 28.5°C heat and recovery identified as continued thrashing of the animals. Where possible double mutant lines were compiled together (*trp-1* double mutants containing 4 separate lines with 1 independent double mutant line generated from *trp-2* genetic crosses with *ncs-1*). All data expressed as means ± SEM. Statistical differences for each strain was determined using one-way ANOVA with use of Dunnett correction for multiple comparison (*=p≤0.05, **=p≤0.01 and ***=p≤0.001). N= ≥ 40 animals.

When assessing the *arf-1.1* and *ncs-1* double mutant, an intermediate phenotype was identified when compared with the single mutant parental strains, significantly different for both parameters from N2 or the single mutant counterparts. The start of paralysis was increased from N2 levels by ~34% (decreased by ~58% of *ncs-1* null paralysis onset) whilst the duration of paralysis decreased from N2 levels by ~38% (increased by ~150% of *ncs-1* null paralysis duration).

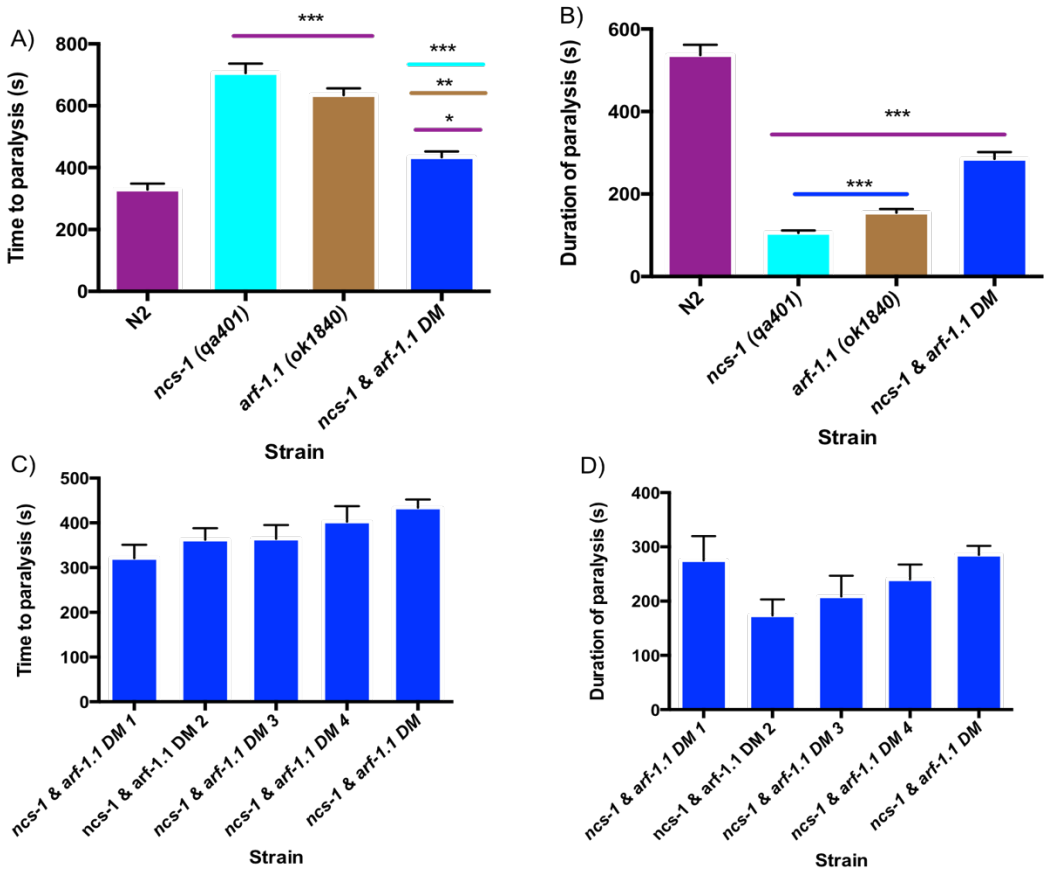

Figure 4.13: Temperature-dependent Locomotion analysis of genetically crossed *ncs-1* and *arf-1.1 C. elegans* strains TDL was assessed through analysing time to paralysis (A, C) and duration of first paralysis (B, D) for a collection of *C. elegans* strains at elevated temperatures when immersed in Dent's solution (pH 7.4). Strains assessed included N2 (wild-type), *ncs-1* null (XA406), *arf-1.1* null (RB1535) and double mutant lines of *ncs-1* and *arf-1.1 C. elegans* generated through genetic crossing the single mutant worms. A, C) TDL behaviours of *C. elegans* strains. Onset of paralysis after exposure to prolonged heat 28.5^{o}C (± 0.5^{o}C) within Dents solution on a Peltier heating stage. B, D) Duration of first paralysis (cessation of movement) of the various *C. elegans* strains was quantified. Paralysis analysed under exposure to heat and recovery identified as continued thrashing of the animals. Double mutant lines were compiled together (*arf-1.1* and *ncs-1* double mutants containing 4 separate lines). All data expressed as means ± SEM. Statistical differences determined using one-way ANOVA with use of Dunnett correction for multiple comparison (*=p≤0.05, **=p≤0.01 and ***=p≤0.001). N= ≥ 15 animals per strain with N= ≥ 40 for all *C. elegans* strains.

4.2.9 Identification of GFP marker expression to indicate injected extrachromosomal array expression.

Mutant *C. elegans* strains were injected with plasmid DNA to form extrachromosomal array constructs to elicit overexpression of genes under specific promoters (as described in section 2.2.8.1). Expression of *ncs-1* or *arf-1.1* under different neuronal promoters; *rab-3* (pan-neuronal), OSM-6 (sensory neurons) and TTX-3 (AIY neurons specifically). Validation of correct promoter localisation was achieved through identification of GFP in the correct locations (p_{rab-3}::GFP expression in all neurons, nerve ring, dorsal and ventral nerve cords) (Figure 4.14 A-C). Rescue experiments completed using 40 ng of EGFP and 10 ng of rescue construct. A total of 3 or more transgenic lines were generated for each rescue condition.

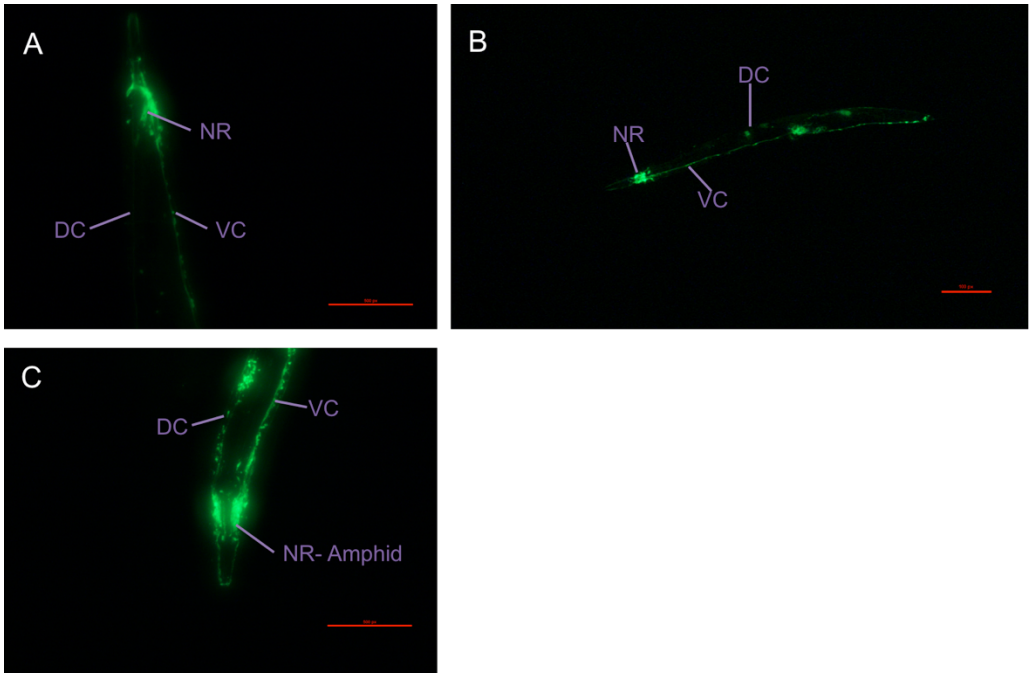

Figure 4.14: GFP expression as a marker for extra-chromosomal injection success for Arf-1.1 at different concentrations. Rescue experiments were conducted using EGFP as a marker for successful injection of extra-chromosomal array. Neuronal localisation was verified through correct EGFP expression through the *rab-3*a promoter (pan-neuronal). Expression can be seen in the Nerve ring (NR), Ventral nerve cord (VC) and Dorsal Nerve cord (DC). Example images show a) N2 [p*rab-3*::GFP p_{rab-3}::*arf-1.1*] b) RB1535 [p_{rab-3}::GFP p_{rab-3}::*arf-1.1*] and c) RB1535 [p_{rab-3}::GFP p_{rab-3}::*arf-1.1*], panels A and B rescued arf-1.1 using 40ng, panel C rescued using only 10ng. Scale bar represents 10 µm.

4.2.10 Effect of overexpressing Arf-1.1 or rescuing Arf-1.1 using different promoters and concentrations.

C. elegans with a transgenic overexpression of *arf-1.1* were assayed using the TDLA. Assayed animals with 40 ng of the overexpression plasmid appeared sick with slower growth although near normal locomotion. Data from multiple lines of transgenic expressing *C. elegans* were compiled and compared with wild-type N2, representing a normal thermosensory pathway and thermosensory locomotion.

Overexpression of *Arf-1.1* in the N2 background decreased the duration of paralysis with no change in the onset of paralysis parameter (Figure 4.15A & B). This effect was phenocopied in RB1535 (*arf-1.1* null) with an overexpression of *arf-1.1*. The nature of ARF-1.1 and its interaction with NCS-1 in the TDL behaviour is yet to be fully elucidated. To reduce toxic effects of the rescue plasmid, new rescue lines were generated utilizing 10 ng transgenic plasmid, as a non-toxic dose (Mello et al., 1991, Evans, 2006, Mariol, 2013).

Rescue experiments were carried out on N2 (wild-type), *qa401 (ncs-1* null), *ok1840 (arf-1.1* null) and *arf-1.1* & *ncs-1* null using GFP expression as a selection marker. Adult GFP expressing *C. elegans* were selected via fluorescence microscopy for TDLA analysis.

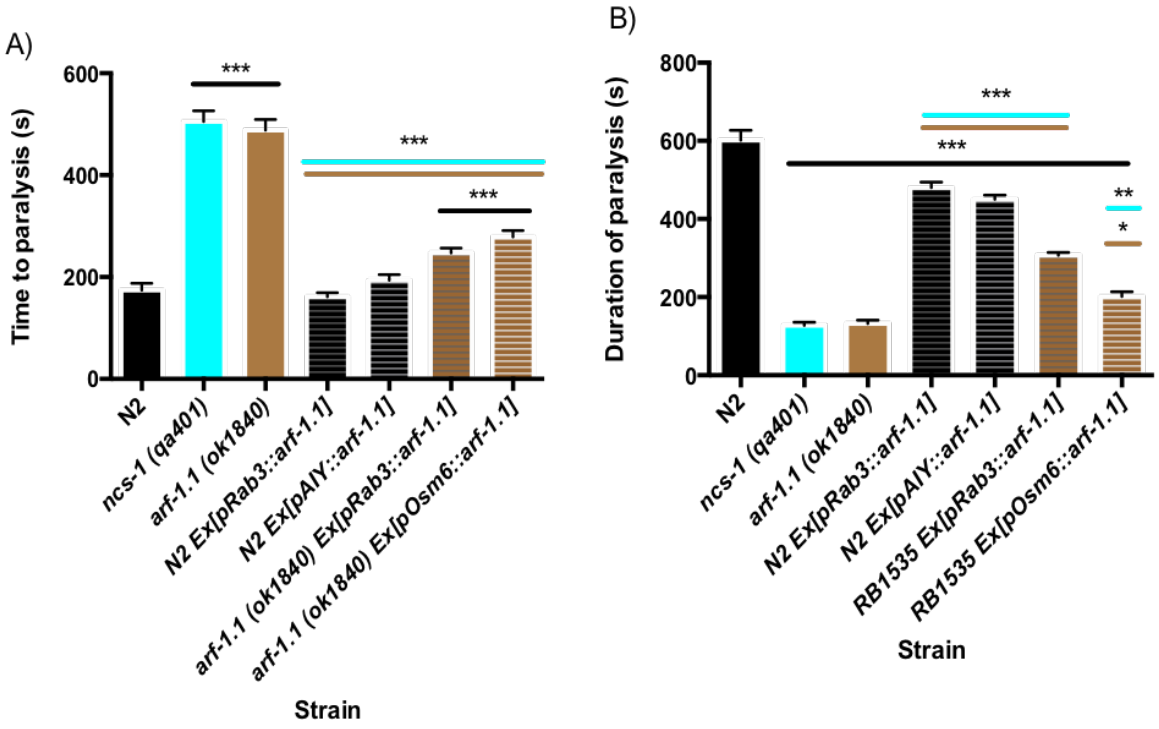

Figure 4.15: Effect of Arf-1.1 rescue and overexpression at 40 ng: A) Temperature-dependent paralysis onset of transgenic worms expressing arf-1.1 under various neuronal promoters, *osm-6* (ciliated neurons), *rab-3* (neurons) and pAIY (using *ttx-3*, as an AIY neuron specific promoter) and all were compared to N2 as an untreated control. Locomotion was assessed using cessation of movement as a marker when placed in Dent's solution and elevated to 28.5°C. B) Duration of paralysis was determined for each line and condition. For all strains and transgenic lines n= ≥40 worms. Each transgenic data set presented used a conglomerate of at least 3 separate transgenic lines that were pooled together. Statistical difference was determined using Dunnett test (*=p≤0.05, **=p≤0.01 and ***=p≤0.001).

C. elegans expressing 10 ng of the overexpression construct appeared healthier with qualitatively normal brood size, growth and motility. Overexpression specifically under the p_{rab-3} and P_{ttx-3} at the 10 ng concentration was assessed. As in the 40 ng expression (Figure 4.15), when injected with 10 ng of the overexpression construct, onset of paralysis was unaffected in the N2 background with a significantly shorter duration of paralysis (Figure 4.16 A,B), this was also shown in the *ncs-1* and *arf-1.1* double mutant with injection of P_{ttx-3}::*ncs-1*, p_{rab-3}::*arf-1.1* and P_{ttx-3}::*arf-1.1* (Figure 4.16 G,H). Neuronal overexpression of *arf-1.1* in RB1535 showed a partial rescue for both onset and duration of paralysis towards N2 levels (Figure 4.16 E,F).

Varying effects from *arf-1.1* overexpression was found for both the onset and duration of paralysis in the different genetic backgrounds. Primarily the duration of paralysis was altered in *C. elegans* lacking ARF-1.1 whilst the onset of paralysis was affected in *C. elegans* lacking NCS-1. In the *ncs-1* null *C. elegans* background, overexpression of *arf-1.1* in the AIY neuron showed a slight decrease in the time to onset of paralysis, with no significant change in the duration of paralysis (Figure 4.16 C,D). Overexpression of *arf-1.1* in the N2 background (Figure 4.16 A,B) had a significantly detrimental effect on the duration of paralysis, increasing its duration further with no change in the onset of paralysis suggesting these are two separate mechanisms working to evoke the reversible paralysis phenotype.

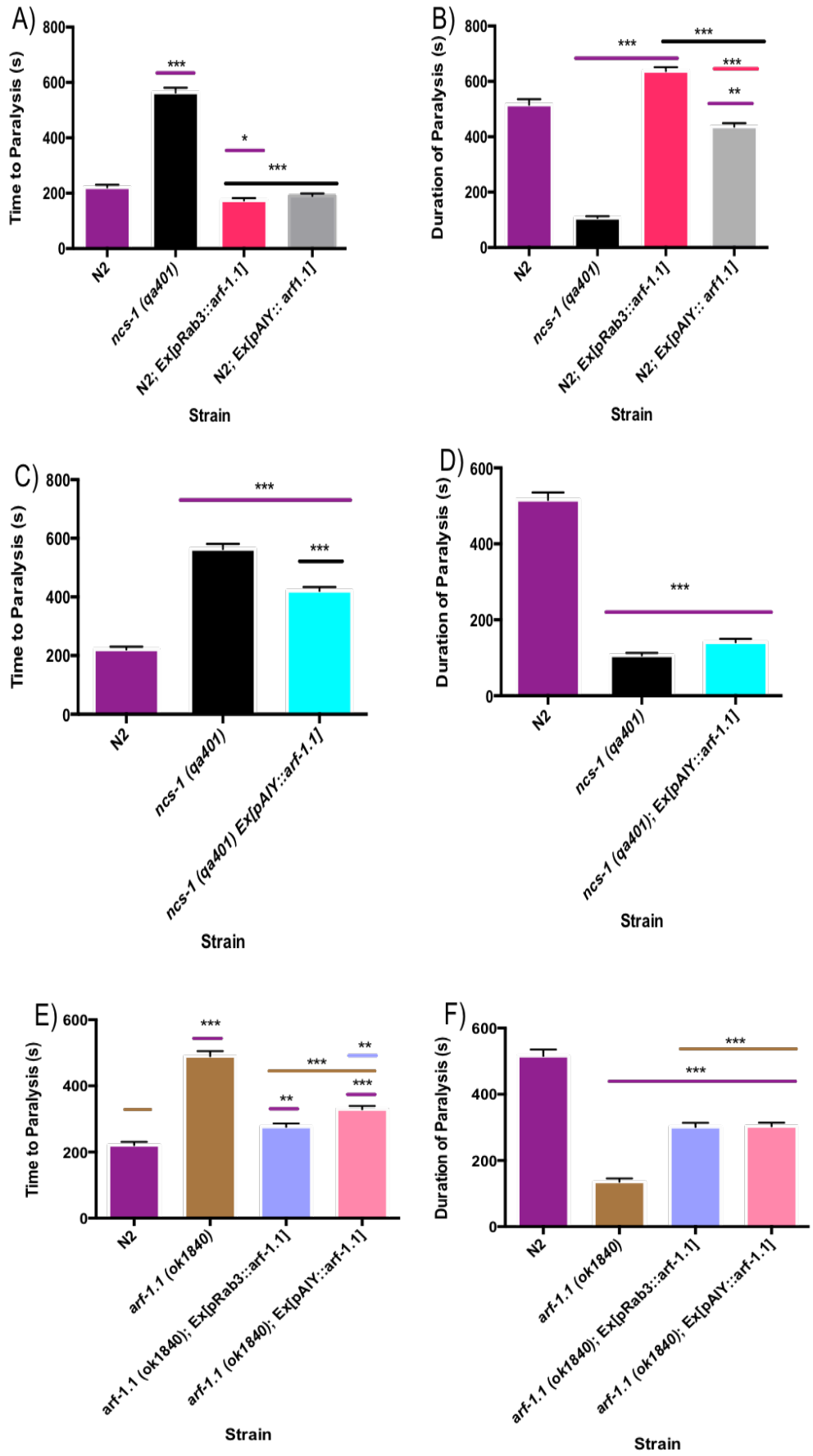
A)
Time to Paralysis (s)
800
600
400
200
0
***
*
***
N2
ncs-1 (qa401)
N2; Ex[pRab3::arf-1.1]
N2; Ex[pAIY:: arf1.1]
Strain
B)
Duration of Paralysis (s)
800
600
400
200
0
***
***
***
**
N2
ncs-1 (qa401)
N2; Ex[pRab3::arf-1.1]
N2; Ex[pAIY:: arf1.1]
Strain
C)
Time to Paralysis (s)
800
600
400
200
0
***
***
N2
ncs-1 (qa401)
ncs-1 (qa401) Ex[pAIY::arf-1.1]
Strain
D)
Duration of Paralysis (s)
600
400
200
0
***
N2
ncs-1 (qa401)
ncs-1 (qa401); Ex[pAIY::arf-1.1]
Strain
E)
Time to Paralysis (s)
600
400
200
0
***
***
**
**
***
N2
arf-1.1 (ok1840)
arf-1.1 (ok1840); Ex[pRab3::arf-1.1]
arf-1.1 (ok1840); Ex[pAIY::arf-1.1]
Strain
F)
Duration of Paralysis (s)
600
400
200
0
***
***
N2
arf-1.1 (ok1840)
arf-1.1 (ok1840); Ex[pRab3::arf-1.1]
arf-1.1 (ok1840); Ex[pAIY::arf-1.1]
Strain

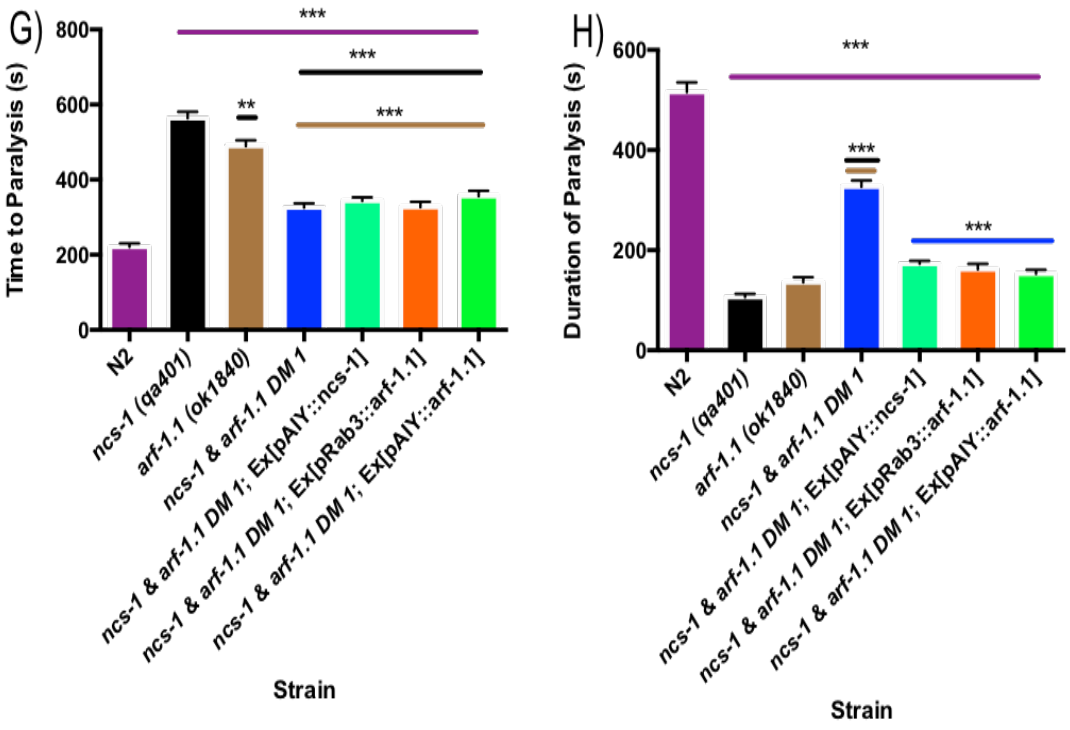

Figure 4.16: Effect of Arf-1.1 overexpression at 10 ng: Overexpression of Arf-1.1 or NCS-1 using different promoters *rab-3* (pan-neuronal), Osm-6 (ciliated neurons) and pAIY (using *ttx-3* as an AIY specific neuron promoter). Overexpression of these constructs was completed using a number of different genetic backgrounds N2 (A, B) XA406 (*qa401*) (C, D), RB1535 (*ok1840*) (E, F) and *ncs-1* (*qa401*) & *arf-1.1* (*ok1840*) double mutant (G, H). A, B) Temperature-dependent paralysis onset (A) and duration (B) of transgenic worms with overexpression of arf-1.1 under the *rab-3* promoter or ttx-3 promoter within the N2 backbone. C, D) Temperature dependent paralysis onset (C) and duration (D) of *ncs-1* null (*qa401*) *C. elegans* with *arf-1.1* rescue within the AIY neurons pAIY (using *ttx-3* as an AIY specific neuron promoter) specifically. E, F) Temperature dependent paralysis onset (E) and duration (F) of *arf-1.1* null (*ok1840*) *C. elegans* overexpressing *arf-1.1* under the *rab-3* and ttx-3 promoters (pan neuronal or AIY specific) G, H) Temperature dependent paralysis onset (G) and duration (H) of a genetically manipulated double mutant *C. elegans* strain (*ncs-1* (*qa401*) & *arf-1.1* (*ok1840*) overexpressing NCS-1 under the pAIY (using *ttx-3* as an AIY specific neuron promoter) and *arf-1.1* under the *rab-3* and ttx-3 promoters. Locomotion was assessed using cessation of movement as a marker when *C. elegans* were placed into Dents solution on a Peltier thermotransduction plate and the temperature raised to 28.5 ^{o}C. All strains and transgenic lines n= ≥40 worms. Transgenic lines were produced in triplicate and data pooled for this experiment. Statistical difference was determined using Dunnett test (*=p≤0.05, **=p≤0.01 and ***=p≤0.001) Samples were compared to each other using a multiple comparisons one way ANOVA.

4.2.11 Thrashing rates of C. elegans used in this thesis

To establish the TDL effects shown were not due to a change in locomotion, *C. elegans* of the strains used during this research were measured for their locomotion rates, as a measure of neuronal transmission. Locomotion was recorded at room temperature with thrashes recorded over a 1 minute period, following 10 minutes in Dents solution allowing the *C. elegans* time to acclimatize. When compared to N2 animals, as a control strain, the other strains were not significantly different to the control strain. The effects identified in the TDLA were therefore unaffected by a change in the locomotive rate of the *C. elegans*.

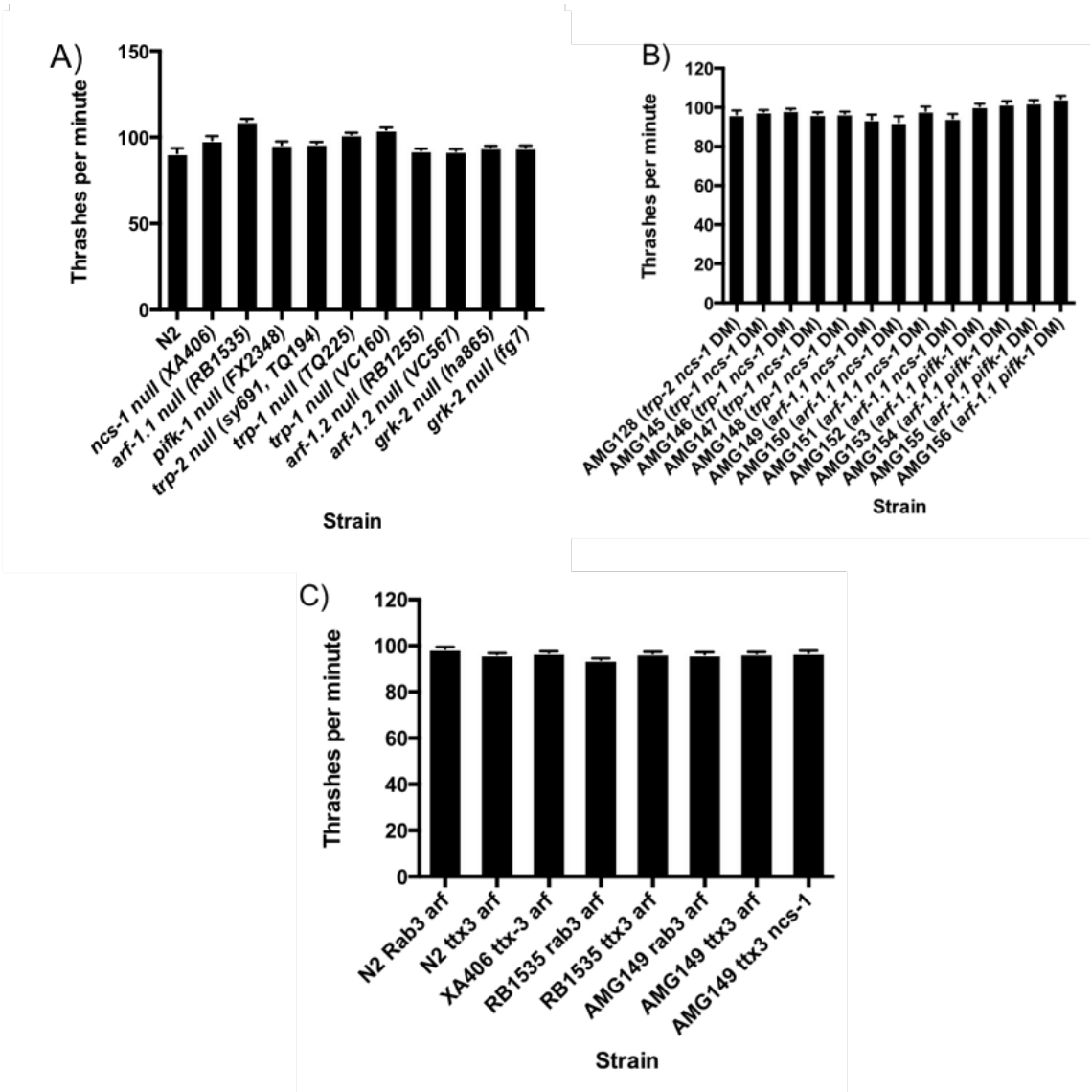

Figure 4.17. *C. elegans* thrashing rates: Thrashing data for all lines used, no statistical difference was identified for any of the lines used throughout this thesis. Locomotion was unaffected in the double mutants or in the over-expression lines, *C. elegans* were tested at room temperature for 1 minute after a 10-minute acclimatization period. For all strains tested, n ≥40 *C. elegans.*

4.2.12 Effect of a mammalian PI4K inhibitor on TDL behaviours in C. elegans

Creation of a double mutant of *pifk-1* and *ncs-1* would have certain technical difficulties, as such experiments sought to use a pharmacological inhibitor. A pharmacological inhibitor of *pifk-1* (PIK-93) was used to assess changes in TDL behaviour. The vehicle for PIK-93 exposure was DMSO. Primary experiments tested whether DMSO at set concentrations altered TDL behaviours. Initial experiments to test optimal DMSO concentration took place using N2 following 1 hour exposure to DMSO using DMSO concentrations between 0.5 % and 2 %. At 1% DMSO no change was identified in the onset or duration of paralysis whilst onset of paralysis was altered at 0.5 % DMSO and duration of paralysis altered at 2 % DMSO (Figure 4.18A & B). Concentration of DMSO remained at 1 % for later assays.

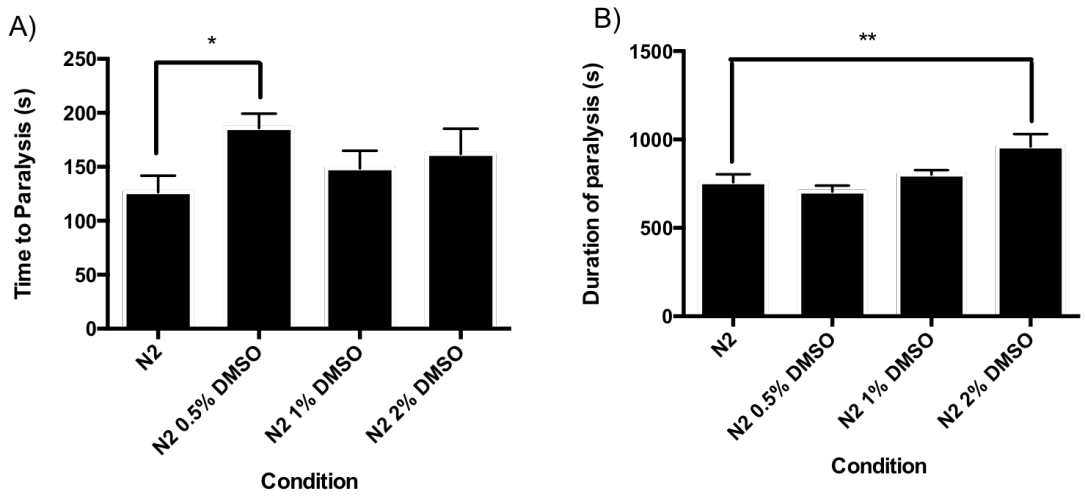

Figure 4.18: Influence of DMSO on TDLA variables. TDL behaviour was assessed in N2 *C. elegans* under different concentrations of a vehicle drug (DMSO) for later PIK-93 experiments. The characterised TDL behaviours of onset of paralysis (A) and duration of paralysis (B) were analysed, compared to untreated N2 as a baseline. At 0.5 % and 2 % DMSO, altered TDL behaviours were identified (onset and duration of paralysis respectively). At 1 % DMSO, no difference was identified when compared with untreated N2 animals. For each group, n ≥12 *C. elegans* assessed. Experiments completed at 28^{o}C ± 0.5^{o}C. Significance indicated as *=p≤0.05, **=p≤0.01 and ***=p≤0.001 compared to untreated N2 controls.

After obtaining the optimal DMSO concentration for TDL assays, exposure time and PIK-93 concentration (19 µM or 19 nM) were assessed for their effects on TDL, using N2 *C. elegans* for assay optimisation. Exposure time ranged from 30 minutes to 2

hours to investigate a 'build-up' effect of PIK-93; longer exposure time induced negative adverse effects on locomotion. After 1 hour PIK-93 exposure at a concentration of 19 µM, onset of paralysis was significantly extended; with a reciprocal decrease in duration of paralysis phenocopying the TDL phenotype identified in *ncs-1* null *C. elegans*. Longer exposure to PIK-93 returned onset of paralysis to basal levels at varying concentrations of PIK-93 (Figure 4.19A & B). These concentrations were selected following a *C. elegans* bioaccumulation model suggesting a poor bioaccumulation of PIK-93 (-7.8224) in *C. elegans* (Burns et al., 2010, Monet et al., 2012).

Over the time course, the TDL behaviour was significantly altered after 1 hour, upon exposure to 19 µM PIK-93. The duration of paralysis in the 2 hour treated *C. elegans* was lower than the 30-minute treatment and the onset of paralysis was slightly lengthened, however due to the extended time point, this may be due to other factors. After testing the pharmacological agent and deducing the optimal conditions to induce a phenocopy of the *pifk-1* null *C. elegans*, assays were completed on a number of *C. elegans* strains.

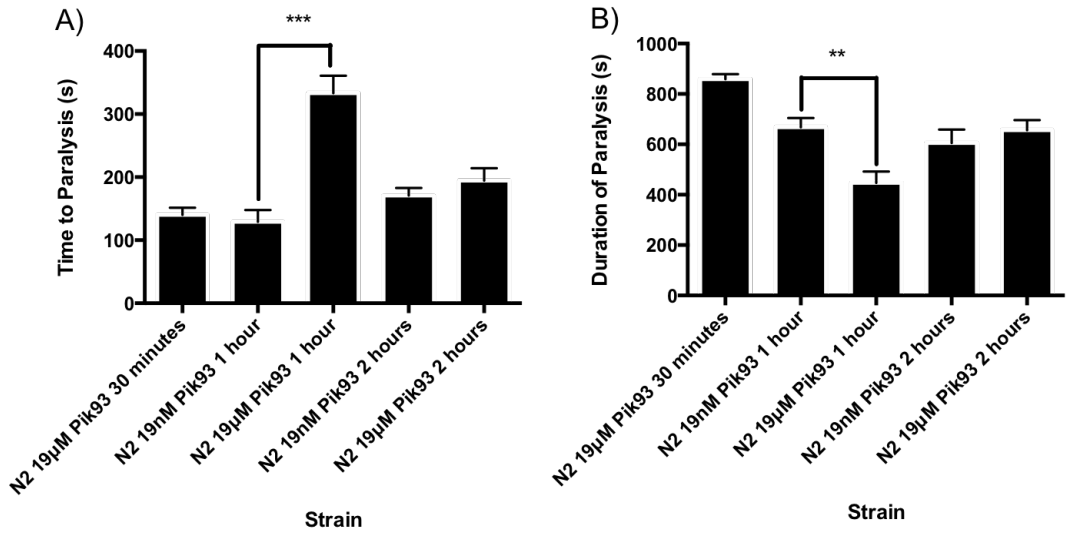

Figure 4.19: Time and drug concentration. N2 *C. elegans* assessed for their TDL behaviours in the presence of PIK-93 over different time frames. A) N2 *C. elegans* onset of paralysis analysed through TDLA, paralysis defined as cessation of movement. B) N2 *C. elegans* duration of paralysis analysed through TDLA, visible thrashing defined the end-point of paralysis. For each group, n ≥ 17 *C. elegans* assessed. Experiments completed at 28°C ± 0.5°C. Significance indicated as *=p≤0.05, **=p≤0.01 and ***=p≤0.001 compared between N2 at same time point

From the previous research (Figures 4.17 and 4.18), we deduced the optimal conditions for PIK-93 effects in *C. elegans;* 1 % DMSO, 1 hour at a concentration of 19 µM PIK-93. Tested strains included N2 (wild-type), *qa401* (*ncs-1* null) and *tm2348* (*pifk-1* null). A TDL phenotype was previously identified in the *pifk-1* null *C. elegans* strain *tm2348* (Figure 4.9). When incubated with PIK-93, neither *ncs-1* null or *pifk-1* null *C. elegans* displayed additive effects to the characterised TDL behaviours (extended onset of paralysis and shorter duration of paralysis). The lack of a response in the presence of a PI4K inhibitor, suggests that NCS-1 and PI4K (*pifk-1*) are present within the same behavioural pathway (Figure 4.20).

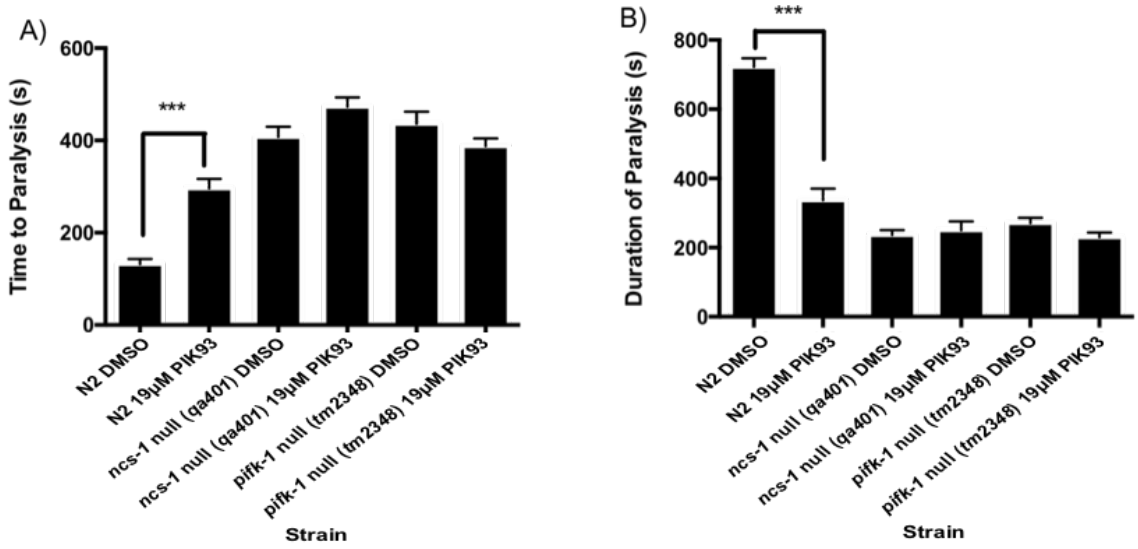

Figure 4.20: Optimal conditions in different *C. elegans* strains. A) Onset of paralysis under PIK-93 exposure in N2, *ncs-1* null and *pifk-1* null *C. elegans.* B) Duration of paralysis under PIK-93 exposure. No additive effect shown for *ncs-1* null or *pifk-1* null *C. elegans*. PIK-93 condition compared to the DMSO condition for the same strain. For each group, n ≥ 30 *C. elegans* assessed. Experiments completed at 28°C ± 0.5°C. Significance indicated as *=p≤0.05, **=p≤0.01 and ***=p≤0.001 compared to DMSO treated N2 controls

4.2.13 Effect on ncs-1 gene expression in mutant and rescue C. elegans strains.

A potential relationship between NCS-1, ARF-1.1 and PIFK-1 in the TDL behaviour pathway has been established. To investigate this relationship at an mRNA expression level further, initial experiments were conducted to identify the expression levels of *ncs-1* in various *C. elegans* strains through quantitative PCR (qPCR). Investigation of *ncs-1* expression was identified in N2, *qa401 (ncs-1* null*), ok1840 (arf-1.1* null*),*

tm2348 (pifk-1 null) and *ncs-1 & arf-1.1* double mutant, along with a number of over-expression controls strains; WT rescue, AIY rescue (Figure 4.4) and N2 over-expression NCS-1.

Preliminary experiments showed an overall increase in the mean gene expression of *ncs-1* in each of the tested strains except *qa401*; however, a significant difference was only present in the WT rescue strain (Figure 4.21 A and B). As these are preliminary experiments, firm conclusions cannot be made at this time regarding the *ncs-1, arf-1.1* and *pifk-1* interaction at a gene expression level. The overall increase in the mean gene expression is indicative of a successful over-expression of *ncs-1* in the rescue lines.

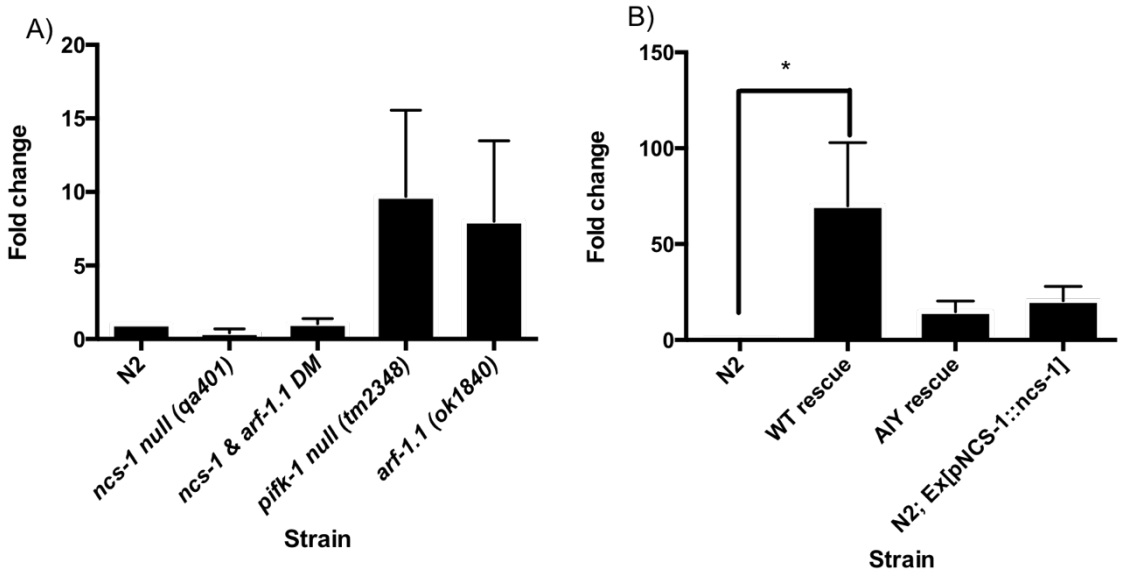

Figure 4.21: Initial qPCR of *ncs-1* in *C. elegans* strains. Levels of gene expression of *ncs-1* was compared to that of the N2 wild-type *C. elegans*. Gene expression levels were calculated using their ΔΔct values to calculate fold change. Fold change was acquired after assessment against three internal controls (PMP1, CDC42 and Y45F10D.4) Each strain contained at least 3 separate samples, and fold changes were generated as a conglomerate of the different *C. elegans* samples. All data expressed as mean ± SEM. Significance denoted by *=p≤0.05, compared with N2 samples. Statistical difference was assessed using one-way ANOVA with Tukey correction.

4.3 Discussion

Owing to its simple neuronal setup of 302 neurons, *C. elegans* has been a critically important model organism for behavioural research. Work into the thermosensory neural network has greatly expanded since the work by Russell and Hedgecock (1975) (Hedgecock and Russell, 1975). Studies have identified the importance of NCS-1 in the AFD and AIY neurons in temperature dependent locomotion (Edwards et al., 2012, Aoki and Mori, 2015, Wang et al., 2013, Martin et al., 2013). Failure to develop the AIY neuron via *ttx-3* ablation resulted in a cryophilic behaviour and an impaired ability to sense and respond to elevated temperatures (Hobert et al., 1997). *C. elegans* which are exposed to prolonged elevated temperatures present with a temporary paralysis phenotype, this is delayed and shortened in *ncs-1* null *C. elegans*. This suggests loss of NCS-1 has a detrimental effect on *C. elegans* in their ability to adapt to noxious temperatures, a defect in their learning and memory processes; intriguing for elucidating the thermosensory neural network.

Whilst structural analysis has been completed on NCS-1 regarding TDL and the thermosensory neural network (Martin et al., 2013, Gomez et al., 2001), the downstream target of NCS-1 in this behaviour is yet to be identified. Preliminary research from our laboratory (unpublished) suggested that PIFK-1 (an orthologue of PI4KIIIβ) was the downstream target of NCS-1 in this behaviour. Through a novel assay, a number of NCS-1 interacting proteins were assessed in regards to the paralysis phenotype. The assay was thoroughly characterised over a range of temperatures using a control and *ncs-1* null mutant strain to identify reproducible effects, significant differences and high throughput analysis.

Computational analysis of previously identified partner proteins of mammalian NCS-1 were checked for the presence of *C. elegans* homologues (Lian et al., 2011, McCue et al., 2010b, Weiss and Burgoyne, 2001, Weiss et al., 2010). Exposure to a prolonged elevated temperature in a liquid solution allowed assessment of locomotion changes and behavioural alterations. Each of the *C. elegans* strains used in this research at room temperature showed normal thrashing rates, suggesting the liquid environment was not detrimental to the nematodes (Figure 4.17).

Previous research showed a slight but significant increase in locomotion when *ncs-1* null (*qa401*) animals were exposed to elevated temperatures (Martin et al., 2013), this was shown to be affected by the rhythmic temporary paralysis phenotype when assessed over a longer time frame, with N2 paralysing earlier than *ncs-1* null (*qa401*) *C. elegans.* Thrashing was monitored every 5 minutes for 90 minutes, presenting a snapshot of the effect the paralysis phenotype has on *C. elegans* locomotion. The TDLA was adapted to specifically investigate the temporary paralysis phenotype through the time to paralysis and duration of first paralysis at elevated temperatures. Previously produced rescue strains, were able to recapture normal TDL behaviours close to N2 levels, suggesting NCS-1 in the AIY neuron is sufficient to rescue TDL behaviours.

Using numerous *C. elegans* backbones, our attempts to recapture the TDL behaviours through RNAi, a process to disrupt mRNA transcription and hence protein synthesis (Fire et al., 1998), were unsuccessful. Using locomotion as the output, the positive controls which we expected to result in lethality or paralysis remained motile, albeit significantly decreased in the N2 and a cholinergic neuron specific RNAi strain (Wang et al., 2005, Firnhaber and Hammarlund, 2013); XE1581 *C. elegans* strains, with only *hsp-1* RNAi having the complete desired effect in NL2099 (*rrf-3*) (Snutch et al., 1988). This is unsurprising as feeding RNAi has a low effect on neurons owing to their resistance (Timmons et al., 2001, Kamath et al., 2001, Kamath and Ahringer, 2003, Asikainen et al., 2005). Whilst XE1581 was thought to be ideal for testing the effect loss of NCS-1 had upon TDL behaviours, as the AIY neuron is the only cholinergic neuron expressing NCS-1, in this work we were unable to elucidate the optimal RNAi conditions. The absence of *rrf-3*, a putative RNA-directed RNA polymerase (RdRP) in the NL2099 *C. elegans* strain is designed for increased sensitivity to RNAi (Simmer et al., 2002, Simmer et al., 2003). This study identified and tested a number of potential targets for NCS-1 in the thermosensory neural network which are suitable for testing in the TDLA.

Preliminary research suggested NL2099 to have a TDL phenotype, similar to that of *ncs-1* null *C. elegans*. To date no temperature sensitive locomotive behaviours have been identified in NL2099 however the result from this study could be due to a small

sample size or through adult starvation affecting responses in their progeny (Rechavi et al., 2014). It is known that NL2099 has temperature sensitive sterility above 25^{o}C (Simmer et al., 2002, Simmer et al., 2003). NL2099 is hypersensitive to somatic RNAi, whilst neuronal cells are more resistant to the RNAi treatment however loss of RdRP affects transcription and translation of many genes (Jia et al., 2009), it is unsurprising a TDL phenotype was identified in this strain, making this unsuitable for our TDL research.

Research has already identified a role for TRP channels in relation to thermosensation in *C. elegans* (Chatzigeorgiou et al., 2010, Montell, 2005, Xiao et al., 2015, Xiao et al., 2013, Zhang et al., 2015), this primarily focuses upon cold sensation and sensation using nocireceptors. Other NCS-1 binding partners in *C. elegans* have not been researched in depth in respect to thermosensation. Through the TDLA, strains from the CGC were assessed for their TDL behavioural patterns, with *grk-2* and *arf-1.2* not being significantly different from N2 wild-type nematodes for the outlined parameters. Loss of these proteins might be rescued by other non-redundant proteins however without more detailed structural data regarding the protein-protein interactions at elevated temperatures, no firm conclusions can be made regarding this.

Binding partners which did replicate the *ncs-1* null phenotype included *pifk-1, arf-1.1, trp-1* and *trp-2* without being lethal, with *pifk-1* null worms showing a remarkable delay in the onset of paralysis. It is known that NCS-1 and PIFK-1 interact (Kapp-Barnea et al., 2003, Zhao et al., 2001, Taverna et al., 2002). It is also intriguing that *arf-1.1* which is known to interact with of both NCS-1 and PIFK-1 (Petko et al., 2009, Haynes et al., 2005, Haynes et al., 2007) also had a mutant thermosensory behaviour phenotype. As ARF-1.1 has roles in vesicle transport, dysfunction in this could lead to abnormal behaviours.

Of interest, the *arf-1.1* mutant worms grew slower than other worms suggesting an important role in development and growth for *arf-1.1*. Double mutants were generated, where possible from the initial TDLA hits to identify if these were operating through a single or separate pathways. Here the research was not looking at thermoavoidance but rather thermosensation, which are controlled by two different neuronal circuits (Ghosh et al., 2012, Glauser, 2013).

A double mutant between *pifk-1* and *ncs-1* was not generated as these are both present on the X-chromosome of *C. elegans* in close proximity. Using XA406 (*ncs-1* null) as the genetic backbone, double mutants with *trp-1, trp-2* and *arf-1.1* were generated and assayed for their TDL behaviours and compared to their single mutant counterparts. Double mutants including *trp-1* or *trp-2* did not alter TDL behaviours yet those with *arf-1.1* showed an intermediary phenotype in this assay. Both NCS-1 and ARF-1.1 interact with PIFK-1. The TDL effect of the *ncs-1* and *arf-1.1* double mutant suggests a relationship between PIFK-1, ARF-1.1 and NCS-1. At this time more research is needed to confirm a genetic interaction between these proteins and their effects on TDL behaviours.

In summary, a number of proteins could be involved in TDL as removal of these alter the paralysis phenotype parameters. This is unsurprising as multiple neurons are required for correct locomotive processes (Gjorgjieva et al., 2014). During this research, in an attempt to remove bias, N2 animals were tested on each experimental day alongside the test animals and were blinded before experiments were conducted. This reduced the likelihood of bias and ensured that any extraneous variables which occurred between experimental days were accounted for.

Injection of overexpression plasmids containing *arf-1.1* or *ncs-1* was thought to be successful through correct expression of EGFP in progeny. To fully confirm presence of the over-expression construct, qPCR should be completed. Initial qPCR experiments were conducted using primers designed against the *ncs-1* deletion site outlined in (Gomez et al., 2001) however, at this time further research is required to elucidate the relationship present between NCS-1, ARF-1.1 and PIFK-1 in the *C. elegans* TDL behaviour phenotype at a genetic level. Rescue using 40 ng was deemed to be detrimental as it resulted in poor growth and fewer progeny, hence a more significant rescue may have been masked by this toxicity. When rescuing with 10 ng of the overexpression construct, *arf-1.1* overexpression in N2 decreased paralysis duration with no effect on the onset of paralysis. This may infer two distinct mechanisms controlling thermosensitive paralysis.

Rescue experiments in *qa401 (ncs-1* null) resulted in a decreased onset of paralysis with no change in the duration of paralysis. With NCS-1 and ARF-1.1 both able to regulate PIFK-1, an interplay between these may control different aspects of the thermosensory paralysis phenotype. Unsuprisingly, expression of *arf-1.1* within the *arf-1.1* mutant backbone showed a partial rescue for both start and duration of paralysis towards N2 levels, albeit incomplete as *arf-1.1* is expressed elsewhere in *C. elegans*.

When analyzing the *ncs-1* and *arf-1.1* double mutant rescue effects, *arf-1.1* re-expression caused no alteration regarding the onset of paralysis however the duration of paralysis was decreased, similar to the *ncs-1* single mutant levels, supporting the hypothesis of two distinct mechanisms for thermosensory paralysis. In these experiments, rescuing effects seemed dependent on the genetic backbone.

From the information gathered for the paralysis phenotype, we are left with two hypotheses. Firstly that the start and duration of paralysis are controlled by two different mechanisms as rescue effects did not affect both parameters. Secondly the temporary paralysis could be a decision making process, when stressed to save energy; nematodes stop moving to save energy whilst the stress is present, since the stress is prolonged *C. elegans* regain movement to avoid the stressor. This second hypothesis is however difficult to assess, with the assay being dependent on thermosensation which is affected by many factors, including humidity and the gradient at which temperature is altered (Kimata et al., 2012, Hedgecock and Russell, 1975, Jurado et al., 2010).

Finally, the relevance of testing a mammalian PI4K inhibitor (PIK-93) on *C. elegans* assists in elucidating whether PI4K acts within the TDL pathway downstream of NCS-1. Optimal conditions were characterised through using 1 % DMSO and treating *C. elegans* in 19 μM PIK-93 for 1 hour. Metabolomic studies could be used to investigate further the accumulation of PIK-93 in the treated *C. elegans.* With no additive effect shown in the *ncs-1* null (*qa401*) or *pifk-1* null (*tm2348*) *C. elegans*, under these conditions for either the onset or duration of paralysis; this is supporting evidence for these both being present in the TDL pathway.

4.4 Conclusion

In conclusion, TDL behaviours in *C. elegans* require NCS-1 expression in the AIY neuron. Loss of NCS-1 perturbs the thermosensory neural network. In this research we were unable to use RNAi to recapitulate the *ncs-1* null TDL phenotype however through the TDLA, a number of potential NCS-1 binding partners were analysed for their TDL behaviour patterns. Of those, a sub-set were taken forward and double mutants generated with *ncs-1*. Through this, *arf-1.1* and *ncs-1* showed an interesting phenotype. It is possible a complex interplay between NCS-1, ARF-1.1 and PIFK-1 is present in respect to TDL behaviours.

Chapter 5: Discussion

5.1 Discussion

To fully understand how Ca^{2+} signaling relates to changes in neuronal function and in turn how this drives behavioural responses, the first task is to fully map Ca^{2+} dependent signaling pathways and to identify the essential proteins involved. Previous work in model organisms has shown the critical importance of the Ca^{2+}-sensor protein NCS-1 in thermotaxis and locomotion changes in response to an elevated temperature regime (Gomez et al., 2001, Martin et al., 2013). *C. elegans* has proven extremely useful in the study of cellular and genetic mechanisms underlying neurosensory perception and neuroethology and work using this system has increased our knowledge of these processes in recent years. The ability to genetically manipulate protein expression specifically in *C. elegans*, and with a completed neuronal network map, cellular mechanisms underlying specific behaviours have begun to be elucidated at the organismal level in *C. elegans*.

Use of the novel TDLA developed over the course of this thesis, allowed a more detailed examination of potential genetic/cellular mechanisms which permit *C. elegans* to adapt to harsh temperatures. Whilst the TDL phenotype is an adaptive response it is also a thermosensory-driven behaviour in an extended exposure to a lethal high-temperature environment. Initially the nematode acts normally at the elevated temperature, thrashing when placed in Dents solution. After some time, however, the worms stop moving. We hypothesise that this is to conserve energy or an attempt to endure the stressful environment. Upon further exposure to the elevated temperature, the animals begin to move normally, potentially to escape the environmental stress.

This new assay provides quantitative assessment of both the time to paralysis and in an extension to this, the duration of the initial paralysis before the animals resume movement. Through this it was feasible to compare temperature dependent phenotypes between different *C. elegans* strains. The assayed behaviour uses the thermotaxis response of *C. elegans* involving the AIY and AFD neurons (Nishida et al., 2011, Kimata et al., 2012, Mori et al., 2007, Sasakura and Mori, 2013, Sasakura et al., 2013). The TDL behavioural assay differs in respect to its genetic requirement when compared to the thermotaxis and temperature avoidance behaviour as

temperature avoidance lacks the requirement for NCS-1 whilst thermotaxis is affected by genes not necessary for the TDL response.

A number of NCS-1 binding partners have been identified including PI4KIIIβ (Hendricks et al., 1999), IP3R (Weiss et al., 2010, Bootman, 2007, Burgoyne, 2007, Burgoyne and Haynes, 2010, Burgoyne and Haynes, 2014), Dopamine D2 receptor (D2R) (Lian et al., 2011) and IL1RAPL1 (Handley et al., 2010). Other interactions have been postulated through various functional and protein-protein binding analyses including ARF-1.1, TRP channels and the PQ VGCCs as part of the $Ca_V2.1$x family. As PQ null *C. elegans* present a paralysed phenotype, two different approaches were incorporated in this work to characterise NCS-1 interactions resulting in the identified TDL behaviour.

The first portion of this work, investigating the PQ type channels interacting with NCS-1 used cell culture based techniques and cameleon FRET sensors to potentially study Ca^{2+} signals in *C. elegans* without presenting a lethal/severe paralysis phenotype whilst the second part of this work used physiological studies of *C. elegans* to analyze behavioural patterns. The PQ interaction was initially identified using the *Drosophila* form of NCS-1 (frequenin) through reverse genetics (Dason et al., 2009, Dason et al., 2012). The development of novel cameleons as tools to investigate the NCS-1 & PQ interaction in the living nematode was one of the primary aims of this section of research, to develop a new FRET sensor which could be used in the nematode, we first wanted to establish an interaction in cells.

Using biochemical methods, the first aims of the project were to create unique myristoylated vectors with colour tags which then had NCS-1 or the IM/ IQ domain of the PQ VGCC added into them; cloning and protein expression were confirmed through sequencing and Western blotting respectively. The addition of the myristoylation domain assisted in producing a physiologically relevant pool of NCS-1 and PQ as both are present on PMs. These tools were then applied to identify potential interactions between NCS-1 and PQ in cells. Proposed interactions between the EF-hand containing Ca^{2+}-sensor proteins, including NCS-1, and the PQ VGCC have previously been identified through functional studies (Lian et al., 2014, Yan, 2014) however prior to this project the interaction was merely proposed. In respect to CaM,

CaBP-1 and VILIP-2; these bind to the IQ/ IM domain and / or the CBD domains present on the C-terminal tail of the channel (Burgoyne and Haynes, 2012, Lee et al., 1999, Lee et al., 2000, Lee et al., 2002, Kim et al., 2008, Liang et al., 2003, DeMaria et al., 2001, Peterson et al., 1999, Yang et al., 2006).

Using myristoylated constructs in co-transfection experiments, co-localisation of the colour-tagged plasmids was observed in a number of cell lines. HeLa cells and a neuronal cell line (N2A) showed examples of co-localisation of PQ with members of the CaBP family, NCS-1 and also a potential interaction between PQ and CaM. This interaction is based on mammalian systems however with the NCS family showing high conservation, it may be possible this interaction is conserved through evolution.

Through a range of live cell imaging techniques, an altered kinetic profile of membrane localisation was identified when co-transfection of myr-PQ and myr-NCS-1 were present within cells. Due to the complexity of FRET and FRAP based techniques these were unable to distinguish a kinetic profile change. FRET is a sensitive method for studying dynamic protein-protein interactions in cells. This technique is based on the close proximity (1-10nm) of donor-acceptor fluorophores, a parameter that can be influenced by a number of factors including fluorophore orientation and relative mobility. It should therefore be noted that absence of a FRET response is not definitive proof of a lack of protein-protein interaction.

FRAP, like FRET relies on protein-protein interactions with the added issue of protein translocation within a specific area as well as protein quantity. With FRAP, the kinetic profiles of the proteins are under scrutiny as is the membrane fluidity. This could therefore not show an interaction between proteins if the proteins are too far from each other or in the incorrect orientation. These are also transient interactions as the proteins are moving into a photobleached region. The kinetic profiles of the bleached proteins may prevent identification of protein-protein interactions in FRAP experiments.

If the cameleon constructs had been reproducible in cells, future work in this section of the project would be to create neuronally targeted plasmids for *C. elegans* to study Ca^{2+} changes and interactions between NCS-1 and the PQ channel in more detail in

specific neurons. This would allow the study of Ca^{2+} signaling in living *C. elegans* under different environmental conditions e.g. extreme heat, changed humidity or when placed in starved / overcrowded environments. Developmental and behavioural insights could be extracted from this work if the constructs worked reproducibly. As mammalian proteins can also be expressed in *C. elegans* this base model could be used to study protein-protein interactions which would be directly applicable to humans and other mammalian species.

Through the course of these experiments, a kinetic change of their membrane mobility was observed for NCS-1 with PQ through FLIP based live cell experiments. This was further supported by the identification of punctate structures present in co-transfected cells which appeared to co-localise NCS-1 into these structures, NCS-1 positive punctate structures were not present when myr-NCS-1 was transfected into cells on its own indicating a positive interaction between NCS-1 and PQ (Lian et al., 2014). This further supports that the interaction domain between NCS-1 and PQ is the IM/ IQ domain on the PQ VGCC (Lian et al., 2014, Burgoyne and Haynes, 2014, McCue et al., 2010b). Protein interactions using live cell techniques were problematic and do not provide any information regarding the structural changes when interactions occur. For the purpose of this thesis, our focus was upon identifying whether the two proteins were able to bind within cells and not specifically investigating the structural changes which occur upon binding.

Based on the results of FLIP analyses it was decided that a novel NCS-1 based cameleon related probe would be developed with the intention of generating a high-resolution cell based sensor for NCS-1/PQ interactions which could be introduced into *C. elegans* in future functional studies. This construct incorporated a short variant of the PQ channel C-terminal domain containing the IQ/ IM domain and the full length NCS-1 in an example of intramolecular FRET (Allen et al., 1999, Atkin et al., 2009, Hendel et al., 2008, McCue et al., 2013, Nagai et al., 2004, Palmer and Tsien, 2006). This NCS-1 based FRET probe contained a PQ domain that was still greater than double the length of the M13 peptide present in the original cameleon probes. This potentially increased the distance between the CFP/YFP donor acceptor fluorophores which could account for difficulty in detecting FRET using this construct. We were able to identify a partial effect when using the cameleon which included the shorter version

of the PQ domain yet not when the longer PQ domain was added to the cameleon construct.

This first part of this thesis provides, with the proven interaction between NCS-1 and PQ at the IQ/ IM domain, a biochemical foundation for further functional research to be conducted. Future work will aim to optimize the NCS-1 cameleon constructs for future cell based studies. This would also allow detailed analysis of *in vivo* NCS-1/PQ specific calcium signaling in various behavioural pathways including the TDL behaviour investigated in the second half of this thesis.

The second part of this thesis carried on from previous work in the laboratory (Martin et al., 2013) to further characterise the TDL behaviour identified in *C. elegans* when placed under extreme prolonged high temperature. *C. elegans* has been extensively used as a simple neuronal model and has also been used to characterise the functions of a number of proteins including NCS-1. Throughout the past 40 years the thermosensory neural network and the requirement of NCS-1 in this has been studied intensely (Gomez et al., 2001, Hedgecock and Russell, 1975). Localisation of NCS-1 is predominately in sensory neurons of *C. elegans* and its expression in the AIY neurons is required for its functions in IT, memory and elevated locomotion at a raised temperature (Gomez et al., 2001, Martin et al., 2013).

Through the modified version of the TDLA, the reversible paralysis phenotype was investigated further following on from the knowledge that the N2 animals showed an earlier onset of paralysis which was longer in duration than the *ncs-1* null *C. elegans.* With this identifiable behavioural phenotype between different *C. elegans* strains and with the knowledge that NCS-1 regulated TDL behaviours in the AIY neuron, a number of proposed NCS-1 binding partners were investigated for their involvement in this pathway based on clues from the mammalian interactome. By testing a number of *C. elegans* strains with mutations in different proteins taken from the mammalian interactome, potential downstream partners of NCS-1 in the TDL behaviour were investigated for their TDL behavioural phenotypes.

Multiple potential targets for NCS-1 regulation in response to Ca^{2+} signaling have been identified, with the most characterised target being the dopamine D2 receptor which

has a clear effect on behaviour in mice (Pandalaneni et al., 2015, Saab et al., 2009, Ng et al., 2016). Prior to this research, no NCS-1 target protein interactions have been directly examined through cellular or biochemical assays specifically for *C. elegans* proteins, with the majority of research being completed on mammalian proteins. With *C. elegans,* the ability to use genetic approaches to study the involvement of potential target proteins in a behavioural phenotype at an organismal level, allows assignment of a functional role for NCS-1 interacting partners in a specific physiological process.

Interestingly, the *C. elegans* NCS-1 shares 76% identity with the human protein. It is therefore worth investigating orthologues of the other partner proteins present in *C. elegans.* Those which were established and tested in this thesis were ARF-1.1 (61% identity), ARF-1.2 (94% identity), GRK-2 (67% identity), PIFK-1 (31% identity), TRP-1 (40% identity) and TRP-2 (47% identity). These proteins show high conservation and therefore we can postulate that the interactions could be conserved between *C. elegans* and humans as has been established for many other protein-protein interactions. It is relevant to establish whether the functional interaction between NCS-1 and PI4KIIIβ orthologues is conserved from Yeast to mammalian proteins.

Through biochemical approaches a three-way interaction has been established between NCS-1, ARF-1.1 and PI4KIIIβ, and shown to affect secretory function in non-neuronal mammalian cells (Petko et al., 2009, Haynes et al., 2005). The interaction between NCS-1 and ARF-1 in a neuronal functional role is yet to be established. Through this current project we identified a role for ARF-1 in the TDL behaviour and to be involved in this behaviour within the AIY neuron, where NCS-1 also functions in TDL behaviours. Mutant strains which were analysed contained mutations for four of the potential NCS-1 targets (*arf-1.1, pifk-1, trp-1 and trp-2)* as these showed similar phenotypes to the *ncs-1* null *C. elegans*. One issue which was present within this project was that for *pifk-1* and *trp-2* only one mutant strain was tested. Further support for *pifk-1* as the potential target was through the use of PIK-93 (an inhibitor of PI4KIIIβ) which extended the time to paralysis and shortened the duration of paralysis when N2 *C. elegans* were treated while this had no effect on the *ncs-1* null or *pifk-1* null *C. elegans*. This suggests an involvement of *pifk-1* in the TDL behaviour in the same pathway as *ncs-1*.

In the TDLA, three of the mutants tested had the most similar phenotype to the *ncs-1* null *C. elegans* (*arf-1.1, trp-1* and *trp-2)*. Double mutants were generated and tested using the TDLA. For the *trp-1* or *trp-2* double mutants with *ncs-1*, no additive effect was shown in regards to the phenotype suggesting these operated in the same pathway. When considering the *arf-1.1 ; ncs-1* double mutant however this showed interactions of an intermediate phenotype when compared to their single mutants. This genetic interaction is a form of reciprocal sign epistasis whereby two deleterious mutations or genes are more beneficial when together than when mutated alone as both mutations impact on the same process. From these results we can hypothesise that both NCS-1 and ARF-1.1 act together to regulate the TDL behaviour.

Through over-expression experiments, testing to see if ARF-1.1 acts in the AIY neurons, we established that over-expression of ARF-1.1 in the AIY neurons alone was sufficient to rescue the TDL phenotype to a similar extent as the pan-neuronal *rab-3* expression of ARF-1.1. Whilst ARF-1.1 is expressed in many cells, our focus was solely on the neuronal expression of ARF-1.1. The *arf-1.1* dependent phenotype is dependent on the ARF-1.1 function in the AIY neurons. The physiological relevance of an interaction at a genetic level could strengthen future proposed methods of action regarding TDL behaviours. Overexpression of ARF-1.1 in AIY neurons when introduced into the *ncs-1* null *C. elegans* was able to rescue the onset of paralysis to a greater extent than the duration of paralysis, paralleled in the *ncs-1* over-expression in the *ncs-1* null *C. elegans.* With this we can suggest that the AIY neurons are more important in respect to regulating the onset of paralysis as opposed to the duration of paralysis in the TDL assay.

It is unsurprising that the pathway for onset and duration of paralysis remains to be fully elucidated as this behaviour most likely involves many stages from temperature sensation through to processing the sensation, motor output and muscle contraction. The two parameters most likely involve multiple genes and cells, some common between the two processes and some being distinct to each parameter. As NCS-1 expression within the AIY neurons alone is sufficient to rescue both parameters, it appears more complex than this as our data suggests different cells and genes are involved as the rescue experiments only appeared to produce a partial rescue; this

was shown with the *arf-1.1* rescue experiments potentially suggesting an involvement of non-neuronal *arf-1.1* in this behaviour.

The work outlined in this thesis provides a good basis for future work to further characterise the downstream target protein of NCS-1 in TDL behaviours. Of interest directly to this project would be the generation of a triple mutant *C. elegans* through Clustered Regularly interspaced short palindromic repeats (CRISPR) and identify the effect this has on the TDL behaviours. One would expect no change to occur in the TDL behaviour in the triple mutant as these all appear to act in the same pathway, however with the effect seen in the *arf-1.1 ncs-1* double mutant, a triple mutant would be of interest within the scope of this research. With this data more targeted experiments could be conducted looking at different cells and the proteins within those cells to form a more complete TDL pathway. As these have all been identified as physiologically important in *C. elegans* TDL behaviour, more specific rescue experiments could be conducted i.e. rescuing *pifk-1* in AIY neurons and identifying whether this rescued the TDL behaviour. Further future work from this project would look at further targeting cameleons constructs into *C. elegans* neurons and investigating the Ca^{2+} signal under elevated temperatures in the AIY neuron and pan-neuronally to identify neuronal responses in this stressor and in response to other stressors such as humidity.

5.2 Proposed mechanism of action

From the information gathered during this project, the relationship between NCS-1, ARF-1.1 and PIFK-1 is yet to be fully elucidated. It is thought that in *C. elegans* NCS-1 acts in the AIY neuron, supported by previous research (Martin et al., 2013). A potential genetic interaction has been identified between NCS-1 and ARF-1.1 suggesting these are acting in the same neuronal pathway resulting in the identified paralysis behaviour. From this research, the proposed model is identified below with NCS-1, ARF-1.1 and PIFK-1 all acting within the AIY neuron.

NCS-1 in the *C. elegans* nervous system acts to generate a plethora of downstream behaviours, many of which are yet to be fully elucidated. With the model organism *C. elegans* being heavily researched, mechanisms of action of specific proteins are beginning to be understood however much remains to be elucidated. In respect to the identified paralysis phenotype, a complex interaction between NCS-1, ARF-1.1 and PIFK-1 has been proposed with NCS-1 signaling upstream of PIFK-1, potentially through ARF-1.1, however more research is required to fully establish this overall pathway.

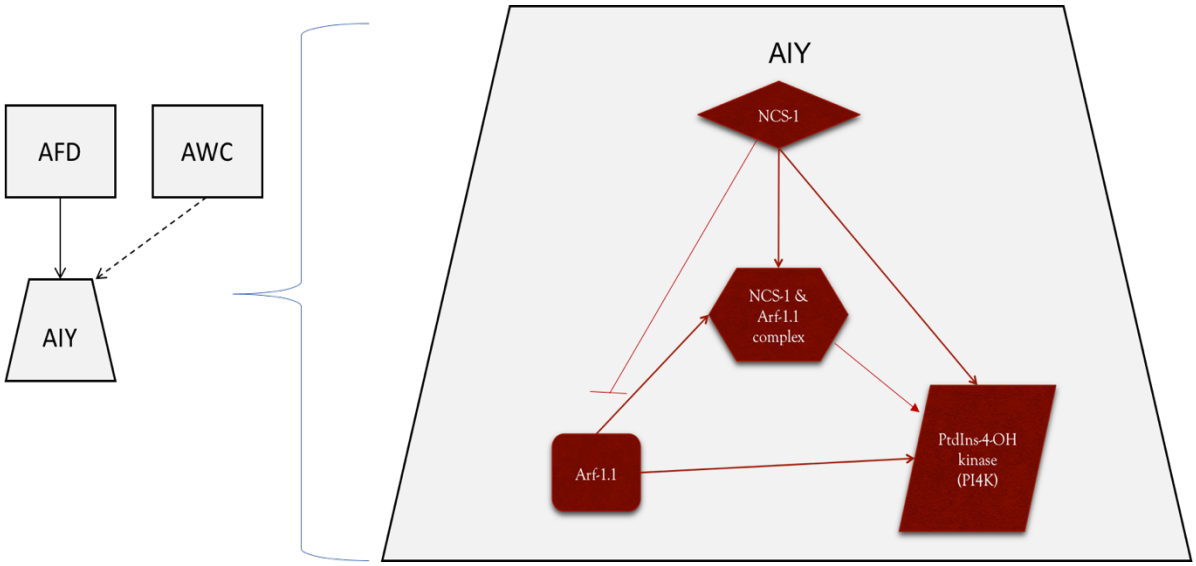

Figure 5.1: Proposed mechanism of action for NCS-1 in TDLA. From the information gathered in this project, NCS-1 is thought to act within the AIY neuron in a signaling pathway involving both ARF-1.1 and PIFK-1 resulting in downstream signaling which results in the paralysis phenotype. Loss of NCS-1 delays the onset of paralysis and extends the duration of paralysis, phenotypes which are both copied in the ARF-1.1 and PIFK-1 null *C. elegans.* This model is still preliminary as more research is required to fully elucidate this pathway. PIFK-1 is believed to be the terminal protein of the three analysed as part of this project.

5.3 Conclusion

In conclusion, this study has also confirmed an interaction between NCS-1 and PQ in a cellular setting through fluorescence based optical techniques. This study has also characterised a quantifiable assay for TDL behaviours utilizing a newly identified novel paralysis phenotype. Significantly, work in this thesis has investigated the significance of a number of potential downstream target proteins of NCS-1 in the TDL behaviour and as such has provided a more detailed functional role for NCS-1 partner proteins in a physiological context.

Chapter 6: References

AARTS, M., IIHARA, K., WEI, W. L., XIONG, Z. G., ARUNDINE, M., CERWINSKI, W., MACDONALD, J. F. & TYMIANSKI, M. 2003. A key role for TRPM7 channels in anoxic neuronal death. *Cell,* 115**,** 863-77.

ALBERTSON, D. G. & THOMSON, J. N. 1976. The pharynx of Caenorhabditis elegans. *Philos Trans R Soc Lond B Biol Sci,* 275**,** 299-325.

ALCEDO, J. & KENYON, C. 2004. Regulation of C. elegans longevity by specific gustatory and olfactory neurons. *Neuron,* 41**,** 45-55.

ALLEN, G. J., KWAK, J. M., CHU, S. P., LLOPIS, J., TSIEN, R. Y., HARPER, J. F. & SCHROEDER, J. I. 1999. Cameleon calcium indicator reports cytoplasmic calcium dynamics in Arabidopsis guard cells. *Plant J,* 19**,** 735-47.

ALTUN, Z. F., CHEN, B., WANG, Z. W. & HALL, D. H. 2009. High Resolution Map of Caenorhabditis elegans Gap Junction Proteins. *Dev Dyn,* 238**,** 1936-50.

ALTUN, Z. F., HERNDON, L. A., CROCKER, C., LINTS, R. & HALL, D. H. 2002-2016. *Wormatlas* [Online]. Available: http://www.wormatlas.org/ [Accessed].

ALTUN-GULTEKIN, Z., ANDACHI, Y., TSALIK, E. L., PILGRIM, D., KOHARA, Y. & HOBERT, O. 2001. A regulatory cascade of three homeobox genes, ceh-10, ttx-3 and ceh-23, controls cell fate specification of a defined interneuron class in C. elegans. *Development,* 128**,** 1951-69.

AMES, J. B., LIM, S. & IKURA, M. 2012. Molecular structure and target recognition of neuronal calcium sensor proteins. *Front Mol Neurosci,* 5.

AMOR, J. C., HARRISON, D. H., KAHN, R. A. & RINGE, D. 1994. Structure of the human ADP-ribosylation factor 1 complexed with GDP. *Nature,* 372**,** 704-8.

ANDERSON, J. L., ALBERGOTTI, L., ELLEBRACHT, B., HUEY, R. B. & PHILLIPS, P. C. 2011. Does thermoregulatory behavior maximize reproductive fitness of natural isolates of Caenorhabditis elegans? *BMC Evol Biol,* 11**,** 157.

ANDERSON, J. L., MORRAN, L. T. & PHILLIPS, P. C. 2010. Outcrossing and the Maintenance of Males within C. elegans Populations. *J Hered,* 101**,** S62-74.

ANDREEV, J., SIMON, J. P., SABATINI, D. D., KAM, J., PLOWMAN, G., RANDAZZO, P. A. & SCHLESSINGER, J. 1999. Identification of a new Pyk2 target protein with Arf-GAP activity. *Mol Cell Biol,* 19**,** 2338-50.

ANKENY, R. A. 2001. The natural history of Caenorhabditis elegans research. *Nature Reviews Genetics,* 2**,** 474-479.

AOKI, I. & MORI, I. 2015. Molecular biology of thermosensory transduction in C. elegans. *Curr Opin Neurobiol,* 34**,** 117-124.

ARAVIND, P., CHANDRA, K., REDDY, P. P., JEROMIN, A., CHARY, K. V. & SHARMA, Y. 2008. Regulatory and structural EF-hand motifs of neuronal calcium sensor-1: Mg 2+ modulates Ca 2+ binding, Ca 2+ -induced conformational changes, and equilibrium unfolding transitions. *J Mol Biol,* 376**,** 1100-15.

ARDIEL, E. L. & RANKIN, C. H. 2010. An elegant mind: learning and memory in Caenorhabditis elegans. *Learn Mem,* 17**,** 191-201.

ARDIEL, E. L. & RANKIN, C. H. 2011. Some like it hot: decoding neurotransmission in the worm's thermotaxis circuit. *EMBO J.*

ASHBY, M. C. & TEPIKIN, A. V. 2001. ER calcium and the functions of intracellular organelles. *Semin Cell Dev Biol,* 12**,** 11-7.

ASIKAINEN, S., VARTIAINEN, S., LAKSO, M., NASS, R. & WONG, G. 2005. Selective sensitivity of Caenorhabditis elegans neurons to RNA interference. *Neuroreport,* 16**,** 1995-9.

ATKIN, S. D., PATEL, S., KOCHARYAN, A., HOLTZCLAW, L. A., WEERTH, S. H., SCHRAM, V., PICKEL, J. & RUSSELL, J. T. 2009. Transgenic mice expressing a

cameleon fluorescent Ca2+ indicator in astrocytes and Schwann cells allow study of glial cell Ca2+ signals in situ and in vivo. *J Neurosci Methods,* 181**,** 212-26.
AVERY, L. & THOMAS, J. H. 1997. Chapter 24 Feeding and Defecation. *C. elegans II. 2nd edition.* Cold Spring Harbor Laboratory Press.
BABU, Y. S., BUGG, C. E. & COOK, W. J. 1988. Structure of calmodulin refined at 2.2 A resolution. *J Mol Biol,* 204**,** 191-204.
BALLA, A. & BALLA, T. 2006. Phosphatidylinositol 4-kinases: old enzymes with emerging functions. *Trends Cell Biol,* 16**,** 351-61.
BALLA, T. 2013. Phosphoinositides: tiny lipids with giant impact on cell regulation. *Physiol Rev,* 93**,** 1019-137.
BARCLAY, J. W., MORGAN, A. & BURGOYNE, R. D. 2012. Neurotransmitter release mechanisms studied in Caenorhabditis elegans. *Cell Calcium,* 52**,** 289-95.
BARGMANN, C. I. 2006. Chemosensation in C. elegans. *WormBook.* Wormbook.
BARGMANN, C. I., HARTWIEG, E. & HORVITZ, H. R. 1993. Odorant-selective genes and neurons mediate olfaction in C. elegans. *Cell,* 74**,** 515-27.
BARGMANN, C. I. & HORVITZ, H. R. 1991. Chemosensory neurons with overlapping functions direct chemotaxis to multiple chemicals in C. elegans. *Neuron,* 7**,** 729-42.
BARRIOS, A., GHOSH, R., FANG, C., EMMONS, S. W. & BARR, M. M. 2012. PDF-1 neuropeptide signaling modulates a neural circuit for mate-searching behavior in C. elegans. *Nat Neurosci,* 15**,** 1675-82.
BEAR, M. F. & MALENKA, R. C. 1994. Synaptic plasticity: LTP and LTD. *Curr Opin Neurobiol,* 4**,** 389-99.
BENNETT, M. R. 1999. The early history of the synapse: from Plato to Sherrington. *Brain Res Bull,* 50**,** 95-118.
BERRIDGE, M. J. 1993. Inositol trisphosphate and calcium signalling. *Nature,* 361**,** 315-25.
BERRIDGE, M. J., BOOTMAN, M. D. & LIPP, P. 1998. Calcium--a life and death signal. *Nature,* 395**,** 645-8.
BERRIDGE, M. J., BOOTMAN, M. D. & RODERICK, H. L. 2003. Calcium signalling: dynamics, homeostasis and remodelling. *Nat Rev Mol Cell Biol,* 4**,** 517-29.
BERRIDGE, M. J., LIPP, P. & BOOTMAN, M. D. 2000. The versatility and universality of calcium signalling. *Nat Rev Mol Cell Biol,* 1**,** 11-21.
BEVERLY, M., ANBIL, S. & SENGUPTA, P. 2011. Degeneracy and neuromodulation among thermosensory neurons contribute to robust thermosensory behaviors in Caenorhabditis elegans. *J Neurosci,* 31**,** 11718-27.
BEZZERIDES, V. J., RAMSEY, I. S., KOTECHA, S., GREKA, A. & CLAPHAM, D. E. 2004. Rapid vesicular translocation and insertion of TRP channels. *Nat Cell Biol,* 6**,** 709-20.
BHATLA, N. 2016. *WormWeb.org - C. elegans Interactive Neural Network* [Online]. Available: http://wormweb.org/neuralnet - c=AIY&m=1 [Accessed 10.05.2016 2016].
BIERNAT, J., WU, Y. Z., TIMM, T., ZHENG-FISCHHOFER, Q., MANDELKOW, E., MEIJER, L. & MANDELKOW, E. M. 2002. Protein kinase MARK/PAR-1 is required for neurite outgrowth and establishment of neuronal polarity. *Mol Biol Cell,* 13**,** 4013-28.
BIRON, D., WASSERMAN, S., THOMAS, J. H., SAMUEL, A. D. & SENGUPTA, P. 2008. An olfactory neuron responds stochastically to temperature and modulates Caenorhabditis elegans thermotactic behavior. *Proc Natl Acad Sci U S A,* 105**,** 11002-7.

BOEKHOFF, I., BRAUNEWELL, K. H., ANDREINI, I., BREER, H. & GUNDELFINGER, E. 1997. The calcium-binding protein VILIP in olfactory neurons: regulation of second messenger signaling. *Eur J Cell Biol,* 72**,** 151-8.
BOMAN, A. L. & KAHN, R. A. 1995. Arf proteins: the membrane traffic police? *Trends Biochem Sci,* 20**,** 147-50.
BONO, M. D. & MARICQ, A. V. 2005. NEURONAL SUBSTRATES OF COMPLEX BEHAVIORS IN C. ELEGANS. http://dx.doi.org/10.1146/annurev.neuro.27.070203.144259.
BOOTMAN, M. 2007. Introduction to Cellular Calcium Signaling. *Calcium Signaling I: Regulation, Mechanisms, Effectors, Role in Disease and Recent Advances.* The Biomedical and Life Sciences collection: Henry Stewart Ltd, London.
BOOTMAN, M. D., COLLINS, T. J., PEPPIATT, C. M., PROTHERO, L. S., MACKENZIE, L., DE SMET, P., TRAVERS, M., TOVEY, S. C., SEO, J. T., BERRIDGE, M. J., CICCOLINI, F. & LIPP, P. 2001a. Calcium signalling--an overview. *Semin Cell Dev Biol,* 12**,** 3-10.
BOOTMAN, M. D., LIPP, P. & BERRIDGE, M. J. 2001b. The organisation and functions of local Ca(2+) signals. *J Cell Sci,* 114**,** 2213-22.
BOURA, E. & NENCKA, R. 2015. Phosphatidylinositol 4-kinases: Function, structure, and inhibition. *Exp Cell Res,* 337**,** 136-45.
BOURNE, Y., DANNENBERG, J., POLLMANN, V., MARCHOT, P. & PONGS, O. 2001. Immunocytochemical localization and crystal structure of human frequenin (neuronal calcium sensor 1). *J Biol Chem,* 276**,** 11949-55.
BRAILOIU, E., CHURAMANI, D., CAI, X., SCHRLAU, M. G., BRAILOIU, G. C., GAO, X., HOOPER, R., BOULWARE, M. J., DUN, N. J., MARCHANT, J. S. & PATEL, S. 2009. Essential requirement for two-pore channel 1 in NAADP-mediated calcium signaling. *J Cell Biol,* 186**,** 201-9.
BRENNER, D. S., VOGT, S. K. & GEREAU, R. W. T. 2014. A technique to measure cold adaptation in freely behaving mice. *J Neurosci Methods,* 236**,** 86-91.
BRENNER, S. 1974. The genetics of Caenorhabditis elegans. *Genetics,* 77**,** 71-94.
BRETSCHER, A. J., BUSCH, K. E. & DE BONO, M. 2008. A carbon dioxide avoidance behavior is integrated with responses to ambient oxygen and food in Caenorhabditis elegans. *Proc Natl Acad Sci U S A,* 105**,** 8044-9.
BRINI, M., CALI, T., OTTOLINI, D. & CARAFOLI, E. 2014. Neuronal calcium signaling: function and dysfunction. *Cell Mol Life Sci,* 71**,** 2787-814.
BROWN, M. T., ANDRADE, J., RADHAKRISHNA, H., DONALDSON, J. G., COOPER, J. A. & RANDAZZO, P. A. 1998. ASAP1, a phospholipid-dependent arf GTPase-activating protein that associates with and is phosphorylated by Src. *Mol Cell Biol,* 18**,** 7038-51.
BURGOYNE, R. D. 2007. Neuronal calcium sensor proteins: generating diversity in neuronal Ca2+ signalling. *Nat Rev Neurosci,* 8**,** 182-93.
BURGOYNE, R. D. & HAYNES, L. P. 2010. Neuronal calcium sensor proteins: emerging roles in membrane traffic and synaptic plasticity. *F1000 Biol Rep,* 2.
BURGOYNE, R. D. & HAYNES, L. P. 2012. Understanding the physiological roles of the neuronal calcium sensor proteins. *Mol Brain,* 5**,** 2.
BURGOYNE, R. D. & HAYNES, L. P. 2014. Sense and specificity in neuronal calcium signalling ☆. *BBA*.
BURGOYNE, R. D. & WEISS, J. L. 2001. The neuronal calcium sensor family of Ca2+-binding proteins. *Biochem J,* 353**,** 1-12.

BURNS, A. R., WALLACE, I. M., WILDENHAIN, J., TYERS, M., GLAEVER, G., G.D., B., NISLOW, C., CUTLER, S. R. & ROY, P. J. 2010. A predictive model for drug bioaccumulation and bioactivity in Caenorhabditis elegans. *Nat Chem Biol,* 6.
C.S.C. 1998. Genome sequence of the nematode C. elegans: a platform for investigating biology. *Science,* 282**,** 2012-8.
CABANAC, M. 1975. Temperature regulation. *Annu Rev Physiol,* 37**,** 415-39.
CAI, X., WANG, X., PATEL, S. & CLAPHAM, D. E. 2015. Insights into the early evolution of animal calcium signaling machinery: a unicellular point of view. *Cell Calcium,* 57**,** 166-73.
CAMANDOLA, S. & MATTSON, M. P. 2011. Aberrant subcellular neuronal calcium regulation in aging and Alzheimer's disease. *Biochim Biophys Acta,* 1813**,** 965-73.
CAMON, E., MAGRANE, M., BARRELL, D., BINNS, D., FLEISCHMANN, W., KERSEY, P., MULDER, N., OINN, T., MASLEN, J., COX, A. & APWEILER, R. 2003. The Gene Ontology Annotation (GOA) project: implementation of GO in SWISS-PROT, TrEMBL, and InterPro. *Genome Res,* 13**,** 662-72.
CASSADA, R. C. & RUSSELL, R. L. 1975. The dauerlarva, a post-embryonic developmental variant of the nematode Caenorhabditis elegans. *Dev Biol,* 46**,** 326-42.
CATERINA, M. J., LEFFLER, A., MALMBERG, A. B., MARTIN, W. J., TRAFTON, J., PETERSEN-ZEITZ, K. R., KOLTZENBURG, M., BASBAUM, A. I. & JULIUS, D. 2000. Impaired nociception and pain sensation in mice lacking the capsaicin receptor. *Science,* 288**,** 306-13.
CATTERALL, W. A. 2000. Structure and regulation of voltage-gated Ca2+ channels. *Annu Rev Cell Dev Biol,* 16**,** 521-55.
CATTERALL, W. A. & FEW, A. P. 2008. Calcium channel regulation and presynaptic plasticity. *Neuron,* 59**,** 882-901.
CATTERALL, W. A., LEAL, K. & NANOU, E. 2013. Calcium channels and short-term synaptic plasticity. *J Biol Chem,* 288**,** 10742-9.
CHALASANI, S. H., CHRONIS, N., TSUNOZAKI, T., GRAY, J. M., RAMOT, D., GOODMAN, M. B. A. & BARGMANN, C. I. 2007. Dissecting a circuit for olfactory behaviour in Caenorhabditis elegans. *Nature,* 450**,** 63-70.
CHALFIE, M., THOMSON, J. N. & SULSTON, J. E. 1983. Induction of neuronal branching in Caenorhabditis elegans. *Science,* 221**,** 61-3.
CHATTOPADHYAYA, R., MEADOR, W. E., MEANS, A. R. & QUIOCHO, F. A. 1992. Calmodulin structure refined at 1.7 A resolution. *J Mol Biol,* 228**,** 1177-92.
CHATZIGEORGIOU, M., YOO, S., WATSON, J. D., LEE, W. H., SPENCER, W. C., KINDT, K. S., HWANG, S. W., MILLER, D. M., 3RD, TREININ, M., DRISCOLL, M. & SCHAFER, W. R. 2010. Specific roles for DEG/ENaC and TRP channels in touch and thermosensation in C. elegans nociceptors. *Nat Neurosci,* 13**,** 861-8.
CHAVRIER, P. & GOUD, B. 1999. The role of ARF and Rab GTPases in membrane transport. *Curr Opin Cell Biol,* 11**,** 466-75.
CHEN, X., RUAN, M. Y. & CAI, S. Q. 2015. KChIP-like auxiliary subunits of Kv4 channels regulate excitability of muscle cells and control male turning behavior during mating in Caenorhabditis elegans. *J Neurosci,* 35**,** 1880-91.
CHEN, X. L., ZHONG, Z. G., YOKOYAMA, S., BARK, C., MEISTER, B., BERGGREN, P. O., RODER, J., HIGASHIDA, H. & JEROMIN, A. 2001. Overexpression of rat neuronal calcium sensor-1 in rodent NG108-15 cells enhances synapse formation and transmission. *J Physiol,* 532**,** 649-59.
CHERFILS, J. & CHARDIN, P. 1999. GEFs: structural basis for their activation of small GTP-binding proteins. *Trends Biochem Sci,* 24**,** 306-11.

CHEUNG, B. H., COHEN, M., ROGERS, C., ALBAYRAM, O. & DE BONO, M. 2005. Experience-dependent modulation of C. elegans behavior by ambient oxygen. *Curr Biol,* 15**,** 905-17.
CHRISTEL, C. & LEE, A. 2012. Ca2+-dependent modulation of voltage-gated Ca2+ channels. *Biochim Biophys Acta,* 1820**,** 1243-52.
CHUANG, T. T., PAOLUCCI, L. & DE BLASI, A. 1996. Inhibition of G protein-coupled receptor kinase subtypes by Ca2+/calmodulin. *J Biol Chem,* 271**,** 28691-6.
CHUNG, S. H., CLARK, D. A., GABEL, C. V., MAZUR, E. & A.D.T., S. 2013. The role of the AFD neuron in C. elegans thermotaxis analyzed using femtosecond laser ablation. *BMC Neuroscience,* 7.
CLAPHAM, D. E. 2007. Calcium signaling. *Cell,* 131**,** 1047-58.
CLARK, D. A., BIRON, D., SENGUPTA, P. & SAMUEL, A. D. 2006. The AFD sensory neurons encode multiple functions underlying thermotactic behavior in Caenorhabditis elegans. *J Neurosci,* 26**,** 7444-51.
CLARKE, A. & PORTNER, H. O. 2010. Temperature, metabolic power and the evolution of endothermy. *Biol Rev Camb Philos Soc,* 85**,** 703-27.
CLAYTON, E. L., MINOGUE, S. & WAUGH, M. G. 2013a. Mammalian phosphatidylinositol 4-kinases as modulators of membrane trafficking and lipid signaling networks. *Prog Lipid Res,* 52**,** 294-304.
CLAYTON, E. L., MINOGUE, S. & WAUGH, M. G. 2013b. Phosphatidylinositol 4-kinases and PI4P metabolism in the nervous system: roles in psychiatric and neurological diseases. *Mol Neurobiol,* 47**,** 361-72.
COATES, J. C. & DE BONO, M. 2002. Antagonistic pathways in neurons exposed to body fluid regulate social feeding in Caenorhabditis elegans. *Nature,* 419**,** 925-9.
COBURN, C. M. & BARGMANN, C. I. 1996. A putative cyclic nucleotide-gated channel is required for sensory development and function in C. elegans. *Neuron,* 17**,** 695-706.
COOPER, G. 2000. *The Cell: A Molecular Approach. 2nd edition.*, Sinauer Associates.
COREY, D. P., GARCIA-ANOVEROS, J., HOLT, J. R., KWAN, K. Y., LIN, S. Y., VOLLRATH, M. A., AMALFITANO, A., CHEUNG, E. L., DERFLER, B. H., DUGGAN, A., GELEOC, G. S., GRAY, P. A., HOFFMAN, M. P., REHM, H. L., TAMASAUSKAS, D. & ZHANG, D. S. 2004. TRPA1 is a candidate for the mechanosensitive transduction channel of vertebrate hair cells. *Nature,* 432**,** 723-30.
CRIDDLE, D. N., GERASIMENKO, J. V., BAUMGARTNER, H. K., JAFFAR, M., VORONINA, S., SUTTON, R., PETERSEN, O. H. & GERASIMENKO, O. V. 2007. Calcium signalling and pancreatic cell death: apoptosis or necrosis? *Cell Death Differ,* 14**,** 1285-94.
CUI, G., MEYER, A. C., CALIN-JAGEMAN, I., NEEF, J., HAESELEER, F., MOSER, T. & LEE, A. 2007. Ca2+-binding proteins tune Ca2+-feedback to Cav1.3 channels in mouse auditory hair cells. *J Physiol,* 585**,** 791-803.
DASON, J. S., ROMERO-POZUELO, J., ATWOOD, H. L. & FERRUS, A. 2012. Multiple roles for frequenin/NCS-1 in synaptic function and development. *Mol Neurobiol,* 45**,** 388-402.
DASON, J. S., ROMERO-POZUELO, J., MARIN, L., IYENGAR, B. G., KLOSE, M. K., FERRUS, A. & ATWOOD, H. L. 2009. Frequenin/NCS-1 and the Ca2+-channel alpha1-subunit co-regulate synaptic transmission and nerve-terminal growth. *J Cell Sci,* 122**,** 4109-21.
DE BARRY, J., JANOSHAZI, A., DUPONT, J. L., PROCKSCH, O., CHASSEROT-GOLAZ, S., JEROMIN, A. & VITALE, N. 2006. Functional implication of neuronal calcium sensor-1 and phosphoinositol 4-kinase-beta interaction in regulated exocytosis of PC12 cells. *J Biol Chem,* 281**,** 18098-111.

DE BONO, M. & MARICQ, A. V. 2005. Neuronal substrates of complex behaviors in C. elegans. *Annu Rev Neurosci,* 28**,** 451-501.
DE CASTRO, E., NEF, S., FIUMELLI, H., LENZ, S. E., KAWAMURA, S. & NEF, P. 1995. Regulation of rhodopsin phosphorylation by a family of neuronal calcium sensors. *Biochem Biophys Res Commun,* 216**,** 133-40.
DE CURTIS, I. 2001. Cell migration: GAPs between membrane traffic and the cytoskeleton. *EMBO Rep,* 2**,** 277-81.
DE MATTEIS, M. A. & D'ANGELO, G. 2007. The role of the phosphoinositides at the Golgi complex. *Biochem Soc Symp***,** 107-16.
DEMARIA, C. D., SOONG, T. W., ALSEIKHAN, B. A., ALVANIA, R. S. & YUE, D. T. 2001. Calmodulin bifurcates the local Ca2+ signal that modulates P/Q-type Ca2+ channels. *Nature,* 411**,** 484-9.
DEN DEKKER, E., HOENDEROP, J. G., NILIUS, B. & BINDELS, R. J. 2003. The epithelial calcium channels, TRPV5 & TRPV6: from identification towards regulation. *Cell Calcium,* 33**,** 497-507.
DONALDSON, J. G. & HONDA, A. 2005. Localization and function of Arf family GTPases. *Biochem Soc Trans,* 33**,** 639-42.
DONALDSON, J. G. & JACKSON, C. L. 2000. Regulators and effectors of the ARF GTPases. *Curr Opin Cell Biol,* 12**,** 475-82.
DRAGICEVIC, E., POETSCHKE, C., DUDA, J., SCHLAUDRAFF, F., LAMMEL, S., SCHIEMANN, J., FAULER, M., HETZEL, A., WATANABE, M., LUJAN, R., MALENKA, R. C., STRIESSNIG, J. & LISS, B. 2014. Cav1.3 channels control D2-autoreceptor responses via NCS-1 in substantia nigra dopamine neurons. *Brain,* 137**,** 2287-302.
DU, H. & CHALFIE, M. 2001. Genes regulating touch cell development in Caenorhabditis elegans. *Genetics,* 158**,** 197-207.
EDWARDS, M. R., JOHNSON, J. R., RANKIN, K., JENKINS, R. E., MAGUIRE, C., MORGAN, A., BURGOYNE, R. D. & BARCLAY, J. W. 2012. PKC-2 phosphorylation of UNC-18 Ser322 in AFD neurons regulates temperature-dependency of locomotion. *J Neurosci,* 32**,** 7042-51.
EMMONS, S. W. 2015. The beginning of connectomics: a commentary on White et al. (1986) 'The structure of the nervous system of the nematode Caenorhabditis elegans'. *Philos Trans R Soc Lond B Biol Sci,* 370.
ERICKSON, M. G., ALSEIKHAN, B. A., PETERSON, B. Z. & YUE, D. T. 2001. Preassociation of calmodulin with voltage-gated Ca(2+) channels revealed by FRET in single living cells. *Neuron,* 31**,** 973-85.
ERICKSON, M. G., LIANG, H., MORI, M. X. & YUE, D. T. 2003. FRET two-hybrid mapping reveals function and location of L-type Ca2+ channel CaM preassociation. *Neuron,* 39**,** 97-107.
EVANS, T. C., ED. 2006. Transformation and microinjection. *In:* WORMBOOK, E. T. C. E. R. C. (ed.) *WormBook.* WormBook,.
FAAS, G. C., RAGHAVACHARI, S., LISMAN, J. E. & MODY, I. 2011. Calmodulin as a direct detector of Ca2+ signals. *Nat Neurosci,* 14**,** 301-4.
FERNANDEZ-CHACON, R., KONIGSTORFER, A., GERBER, S. H., GARCIA, J., MATOS, M. F., STEVENS, C. F., BROSE, N., RIZO, J., ROSENMUND, C. & SUDHOF, T. C. 2001. Synaptotagmin I functions as a calcium regulator of release probability. *Nature,* 410**,** 41-9.
FEW, A. P., LAUTERMILCH, N. J., WESTENBROEK, R. E., SCHEUER, T. & CATTERALL, W. A. 2005. Differential regulation of CaV2.1 channels by calcium-

binding protein 1 and visinin-like protein-2 requires N-terminal myristoylation. *J Neurosci,* 25**,** 7071-80.
FILINGERI, D. 2015. Humidity sensation, cockroaches, worms, and humans: are common sensory mechanisms for hygrosensation shared across species? *J Neurophysiol,* 114**,** 763-7.
FINDEISEN, F. & MINOR, D. L., JR. 2010. Structural basis for the differential effects of CaBP1 and calmodulin on Ca(V)1.2 calcium-dependent inactivation. *Structure,* 18**,** 1617-31.
FINDEISEN, F., RUMPF, C. H. & MINOR, D. L., JR. 2013. Apo states of calmodulin and CaBP1 control CaV1 voltage-gated calcium channel function through direct competition for the IQ domain. *J Mol Biol,* 425**,** 3217-34.
FIRE, A., XU, S., MONTGOMERY, M. K., KOSTAS, S. A., DRIVER, S. E. & MELLO, C. C. 1998. Potent and specific genetic interference by double-stranded RNA in Caenorhabditis elegans. *Nature,* 391**,** 806-811.
FIRNHABER, C. & HAMMARLUND, M. 2013. Neuron-Specific Feeding RNAi in C. elegans and Its Use in a Screen for Essential Genes Required for GABA Neuron Function. *PLoS Genet,* 9.
FORRESTER, W. C., PERENS, E., ZALLEN, J. A. & GARRIGA, G. 1998. Identification of Caenorhabditis elegans genes required for neuronal differentiation and migration. *Genetics,* 148**,** 151-65.
FRANKS, C. J., HOLDEN-DYE, L., BULL, K., LUEDTKE, S. & WALKER, R. J. 2006. Anatomy, physiology and pharmacology of Caenorhabditis elegans pharynx: a model to define gene function in a simple neural system. *Invert Neurosci,* 6**,** 105-22.
FRASER, A. G., KAMATH, R. S., ZIPPERLEN, P., MARTINEZ-CAMPOS, M., SOHRMANN, M. & AHRINGER, J. 2000. Functional genomic analysis of C. elegans chromosome I by systematic RNA interference. *Nature,* 408**,** 325-30.
FREEDMAN, N. J. & LEFKOWITZ, R. J. 1996. Desensitization of G protein-coupled receptors. *Recent Prog Horm Res,* 51**,** 319-51; discussion 352-3.
FUKUTO, H. S., FERKEY, D. M., APICELLA, A. J., LANS, H., SHARMEEN, T., CHEN, W., LEFKOWITZ, R. J., JANSEN, G., SCHAFER, W. R. & HART, A. C. 2004. G protein-coupled receptor kinase function is essential for chemosensation in C. elegans. *Neuron,* 42**,** 581-93.
GARCIA-HIGUERA, I., PENELA, P., MURGA, C., EGEA, G., BONAY, P., BENOVIC, J. L. & MAYOR, F., JR. 1994. Association of the regulatory beta-adrenergic receptor kinase with rat liver microsomal membranes. *J Biol Chem,* 269**,** 1348-55.
GARRITY, P. A., GOODMAN, M. B., SAMUEL, A. D. & SENGUPTA, P. 2010. Running hot and cold: behavioral strategies, neural circuits, and the molecular machinery for thermotaxis in C. elegans and Drosophila. *Genes Dev,* 24**,** 2365-82.
GHOSH, A. & GREENBERG, M. E. 1995. Calcium signaling in neurons: molecular mechanisms and cellular consequences. *Science,* 268**,** 239-47.
GHOSH, R., MOHAMMADI, A., KRUGLYAK, L. & RYU, W. S. 2012. Multiparameter behavioral profiling reveals distinct thermal response regimes in Caenorhabditis elegans. *BMC Biol,* 10**,** 85.
GJORGJIEVA, J., BIRON, D. & HASPEL, G. 2014. Neurobiology of Caenorhabditis elegans Locomotion: Where Do We Stand? *BioScience,* 64**,** 476-486.
GLAUSER, D. A. 2013. How and why Caenorhabditis elegans uses distinct escape and avoidance regimes to minimize exposure to noxious heat. *Worm.*
GODI, A., PERTILE, P., MEYERS, R., MARRA, P., DI TULLIO, G., IURISCI, C., LUINI, A., CORDA, D. & DE MATTEIS, M. A. 1999. ARF mediates recruitment of PtdIns-

4-OH kinase-beta and stimulates synthesis of PtdIns(4,5)P2 on the Golgi complex. *Nat Cell Biol,* 1**,** 280-7.
GOLDBERG, J. 1999. Structural and functional analysis of the ARF1-ARFGAP complex reveals a role for coatomer in GTP hydrolysis. *Cell,* 96**,** 893-902.
GOMEZ, M., DE CASTRO, E., GUARIN, E., SASAKURA, H., KUHARA, A., MORI, I., BARTFAI, T., BARGMANN, C. I. & NEF, P. 2001. Ca2+ signaling via the neuronal calcium sensor-1 regulates associative learning and memory in C. elegans. *Neuron,* 30**,** 241-8.
GRANT, D. M., ZHANG, W., MCGHEE, E. J., BUNNEY, T. D., TALBOT, C. B., KUMAR, S., MUNRO, I., DUNSBY, C., NEIL, M. A., KATAN, M. & FRENCH, P. M. 2008. Multiplexed FRET to image multiple signaling events in live cells. *Biophys J,* 95**,** L69-71.
GRAY, J. M., HILL, J. J. A. & BARGMANN, C. I. 2005. A circuit for navigation in Caenorhabditis elegans.
GRIMM, C., KRAFT, R., SAUERBRUCH, S., SCHULTZ, G. & HARTENECK, C. 2003. Molecular and functional characterization of the melastatin-related cation channel TRPM3. *J Biol Chem,* 278**,** 21493-501.
GUREVICH, E. V., GAINETDINOV, R. R. & GUREVICH, V. V. 2016. G protein-coupled receptor kinases as regulators of dopamine receptor functions. *Pharmacol Res,* 111**,** 1-16.
GUREVICH, E. V., TESMER, J. J., MUSHEGIAN, A. & GUREVICH, V. V. 2012. G protein-coupled receptor kinases: more than just kinases and not only for GPCRs. *Pharmacol Ther,* 133**,** 40-69.
HAESELEER, F. 2008. Interaction and colocalization of CaBP4 and Unc119 (MRG4) in photoreceptors. *Invest Ophthalmol Vis Sci,* 49**,** 2366-75.
HAESELEER, F., SOKAL, I., VERLINDE, C. L., ERDJUMENT-BROMAGE, H., TEMPST, P., PRONIN, A. N., BENOVIC, J. L., FARISS, R. N. & PALCZEWSKI, K. 2000. Five members of a novel Ca(2+)-binding protein (CABP) subfamily with similarity to calmodulin. *J Biol Chem,* 275**,** 1247-60.
HAGA, K., TSUGA, H. & HAGA, T. 1997. Ca2+-dependent inhibition of G protein-coupled receptor kinase 2 by calmodulin. *Biochemistry,* 36**,** 1315-21.
HALL, Z. W. 1972. Release of neurotransmitters and their interaction with receptors. *Annu Rev Biochem,* 41**,** 925-52.
HALLEM, E. A. & STERNBERG, P. W. 2008. Acute carbon dioxide avoidance in Caenorhabditis elegans. *Proc Natl Acad Sci U S A,* 105**,** 8038-43.
HAMILTON, B., DONG, Y., SHINDO, M., LIU, W., ODELL, I., RUVKUN, G. & LEE, S. S. 2005. A systematic RNAi screen for longevity genes in C. elegans. *Genes Dev,* 19**,** 1544-55.
HANDLEY, M. T., LIAN, L. Y., HAYNES, L. P. & BURGOYNE, R. D. 2010. Structural and functional deficits in a neuronal calcium sensor-1 mutant identified in a case of autistic spectrum disorder. *PLoS One,* 5**,** e10534.
HAYNES, L. P. & BURGOYNE, R. D. 2008. Unexpected tails of a Ca2+ sensor. *Nat Chem Biol,* 4**,** 90-1.
HAYNES, L. P., FITZGERALD, D. J., WAREING, B., O'CALLAGHAN, D. W., MORGAN, A. & BURGOYNE, R. D. 2006. Analysis of the interacting partners of the neuronal calcium-binding proteins L-CaBP1, hippocalcin, NCS-1 and neurocalcin delta. *Proteomics,* 6**,** 1822-32.
HAYNES, L. P., MCCUE, H. V. & BURGOYNE, R. D. 2012a. Evolution and functional diversity of the Calcium Binding Proteins (CaBPs). *Front Mol Neurosci,* 5**,** 9.

HAYNES, L. P., MCCUE, H. V. & BURGOYNE, R. D. 2012b. Evolution and functional diversity of the Calcium Binding Proteins (CaBPs). *Front Mol Neurosci,* 5.
HAYNES, L. P., SHERWOOD, M. W., DOLMAN, N. J. & BURGOYNE, R. D. 2007. Specificity, promiscuity and localization of ARF protein interactions with NCS-1 and phosphatidylinositol-4 kinase-III beta. *Traffic,* 8**,** 1080-92.
HAYNES, L. P., THOMAS, G. M. & BURGOYNE, R. D. 2005. Interaction of neuronal calcium sensor-1 and ADP-ribosylation factor 1 allows bidirectional control of phosphatidylinositol 4-kinase beta and trans-Golgi network-plasma membrane traffic. *J Biol Chem,* 280**,** 6047-54.
HEDGECOCK, E. M. & RUSSELL, R. L. 1975. Normal and mutant thermotaxis in the nematode Caenorhabditis elegans.
HEDGECOCK, E. M. & THOMSON, J. N. 1982. A gene required for nuclear and mitochondrial attachment in the nematode Caenorhabditis elegans. *Cell,* 30**,** 321-30.
HEIDARSSON, P. O., BJERRUM-BOHR, I. J., JENSEN, G. A., PONGS, O., FINN, B. E., POULSEN, F. M. & KRAGELUND, B. B. 2012. The C-terminal tail of human neuronal calcium sensor 1 regulates the conformational stability of the Ca(2)(+)(-) activated state. *J Mol Biol,* 417**,** 51-64.
HEIDARSSON, P. O., OTAZO, M. R., BELLUCCI, L., MOSSA, A., IMPARATO, A., PACI, E., CORNI, S., DI FELICE, R., KRAGELUND, B. B. & CECCONI, C. 2013. Single-molecule folding mechanism of an EF-hand neuronal calcium sensor. *Structure,* 21**,** 1812-21.
HELD, P. 2005. *An Introduction to Fluorescence Resonance Energy Transfer (FRET) Technology and its Application in Bioscience* [Online]. http://www.biotek.com/resources/articles/fluorescence-resonance-energy-transfer.html: BioTek. Available: http://www.biotek.com/resources/articles/fluorescence-resonance-energy-transfer.html [Accessed].
HENDEL, T., MANK, M., SCHNELL, B., GRIESBECK, O., BORST, A. & REIFF, D. F. 2008. Fluorescence changes of genetic calcium indicators and OGB-1 correlated with neural activity and calcium in vivo and in vitro. *J Neurosci,* 28**,** 7399-411.
HENDRICKS, K. B., WANG, B. Q., SCHNIEDERS, E. A. & THORNER, J. 1999. Yeast homologue of neuronal frequenin is a regulator of phosphatidylinositol-4-OH kinase. *Nat Cell Biol,* 1**,** 234-41.
HESCHL, M. F. & BAILLIE, D. L. 1989. Characterization of the hsp70 multigene family of Caenorhabditis elegans. *Dna,* 8**,** 233-43.
HILFIKER, S. 2003. Neuronal calcium sensor-1: a multifunctional regulator of secretion. *Biochem Soc Trans,* 31**,** 828-32.
HILLIARD, M. A., BARGMANN, C. I. & BAZZICALUPO, P. 2002. C. elegans responds to chemical repellents by integrating sensory inputs from the head and the tail. *Curr Biol,* 12**,** 730-4.
HOBERT, O. 2005. Neurogenesis in the nematode Caenorhabditis elegans. WormBook.
HOBERT, O. 2013 *The neuronal genome of Caenorhabditis elegans* [Online]. WormBook, doi/10.1895/wormbook.1.161.1,: http://www.wormbook.org/. Available: http://www.wormbook.org/. [Accessed 13.08.2013 2013].
HOBERT, O., MORI, I., YAMASHITA, Y., HONDA, H., OHSHIMA, Y., LIU, Y. & RUVKUN, G. 1997. Regulation of interneuron function in the C. elegans thermoregulatory pathway by the ttx-3 LIM homeobox gene. *Neuron,* 19**,** 345-57.
HUI, K., FEI, G. H., SAAB, B. J., SU, J., RODER, J. C. & FENG, Z. P. 2007. Neuronal calcium sensor-1 modulation of optimal calcium level for neurite outgrowth. *Development,* 134**,** 4479-89.

HUKEMA, R. K., RADEMAKERS, S., DEKKERS, M. P., BURGHOORN, J. & JANSEN, G. 2006. Antagonistic sensory cues generate gustatory plasticity in Caenorhabditis elegans. *Embo j,* 25**,** 312-22.

IACOVELLI, L., SALLESE, M., MARIGGIO, S. & DE BLASI, A. 1999. Regulation of G-protein-coupled receptor kinase subtypes by calcium sensor proteins. *Faseb j,* 13**,** 1-8.

IKURA, M. & AMES, J. B. 2006. Genetic polymorphism and protein conformational plasticity in the calmodulin superfamily: two ways to promote multifunctionality. *Proc Natl Acad Sci U S A,* 103**,** 1159-64.

ISHIHARA, T., IINO, Y., MOHRI, A., MORI, I., GENGYO-ANDO, K., MITANI, S. & KATSURA, I. 2002. HEN-1, a secretory protein with an LDL receptor motif, regulates sensory integration and learning in Caenorhabditis elegans. *Cell,* 109**,** 639-49.

JACKSON, C. L. & CASANOVA, J. E. 2000. Turning on ARF: the Sec7 family of guanine-nucleotide-exchange factors. *Trends Cell Biol,* 10**,** 60-7.

JACKSON, T. R., BROWN, F. D., NIE, Z., MIURA, K., FORONI, L., SUN, J., HSU, V. W., DONALDSON, J. G. & RANDAZZO, P. A. 2000. ACAPs are arf6 GTPase-activating proteins that function in the cell periphery. *J Cell Biol,* 151**,** 627-38.

JAFARI, G., XIE, Y., KULLYEV, A., LIANG, B. & SZE, J. Y. 2011. Regulation of Extrasynaptic 5-HT by Serotonin Reuptake Transporter Function in 5-HT-Absorbing Neurons Underscores Adaptation Behavior in Caenorhabditis elegans.

JEROMIN, A., MURALIDHAR, D., PARAMESWARAN, M. N., RODER, J., FAIRWELL, T., SCARLATA, S., DOWAL, L., MUSTAFI, S. M., CHARY, K. V. & SHARMA, Y. 2004. N-terminal myristoylation regulates calcium-induced conformational changes in neuronal calcium sensor-1. *J Biol Chem,* 279**,** 27158-67.

JIA, Y., LISCH, D. R., OHTSU, K., SCANLON, M. J., NETTLETON, D. & SCHNABLE, P. S. 2009. Loss of RNA–Dependent RNA Polymerase 2 (RDR2) Function Causes Widespread and Unexpected Changes in the Expression of Transposons, Genes, and 24-nt Small RNAs. *PLoS Genet,* 5.

JO, J., HEON, S., KIM, M. J., SON, G. H., PARK, Y., HENLEY, J. M., WEISS, J. L., SHENG, M., COLLINGRIDGE, G. L. & CHO, K. 2008. Metabotropic glutamate receptor-mediated LTD involves two interacting Ca(2+) sensors, NCS-1 and PICK1. *Neuron,* 60**,** 1095-111.

JOHNSON, N. M., BEHM, C. A. & TROWELL, S. C. 2005. Heritable and inducible gene knockdown in C. elegans using Wormgate and the ORFeome. *Gene,* 359**,** 26-34.

JORDT, S. E., BAUTISTA, D. M., CHUANG, H. H., MCKEMY, D. D., ZYGMUNT, P. M., HOGESTATT, E. D., MENG, I. D. & JULIUS, D. 2004. Mustard oils and cannabinoids excite sensory nerve fibres through the TRP channel ANKTM1. *Nature,* 427**,** 260-5.

JORGENSEN, E. & RANKIN, C. 1997. Neural Plasticity. *In:* RIDDLE DL, B. T., MEYER BJ, ET AL., EDITORS (ed.) *C. elegans II. 2nd edition.* Cold Spring Harbor Laboratory Press.

JURADO, P., KODAMA, E., TANIZAWA, Y. & MORI, I. 2010. Distinct thermal migration behaviors in response to different thermal gradients in Caenorhabditis elegans. *Genes Brain Behav,* 9**,** 120-7.

KABBANI, N., NEGYESSY, L., LIN, R., GOLDMAN-RAKIC, P. & LEVENSON, R. 2002. Interaction with neuronal calcium sensor NCS-1 mediates desensitization of the D2 dopamine receptor. *J Neurosci,* 22**,** 8476-86.

KAHN, R. A., KERN, F. G., CLARK, J., GELMANN, E. P. & RULKA, C. 1991. Human ADP-ribosylation factors. A functionally conserved family of GTP-binding proteins. *J Biol Chem,* 266**,** 2606-14.

KAMATH, R. S. & AHRINGER, J. 2003. Genome-wide RNAi screening in Caenorhabditis elegans. *Methods,* 30**,** 313-21.
KAMATH, R. S., MARTINEZ-CAMPOS, M., ZIPPERLEN, P., FRASER, A. G. & AHRINGER, J. 2001. Effectiveness of specific RNA-mediated interference through ingested double-stranded RNA in Caenorhabditis elegans. *Genome Biol,* 2**,** Research0002.
KANG, C. & AVERY, L. 2009. Systemic regulation of starvation response in Caenorhabditis elegans. *Genes Dev,* 23**,** 12-7.
KAPP-BARNEA, Y., MELNIKOV, S., SHEFLER, I., JEROMIN, A. & SAGI-EISENBERG, R. 2003. Neuronal calcium sensor-1 and phosphatidylinositol 4-kinase beta regulate IgE receptor-triggered exocytosis in cultured mast cells. *J Immunol,* 171**,** 5320-7.
KARP, G. 2010. *Cell Biology*, John Wiley & Sons.
KASHYAP, S. S., JOHNSON, J. R., MCCUE, H. V., CHEN, X., EDMONDS, M. J., AYALA, M., GRAHAM, M. E., JENN, R. C., BARCLAY, J. W., BURGOYNE, R. D. & MORGAN, A. 2014. Caenorhabditis elegans dnj-14, the orthologue of the DNAJC5 gene mutated in adult onset neuronal ceroid lipofuscinosis, provides a new platform for neuroprotective drug screening and identifies a SIR-2.1-independent action of resveratrol. *Hum Mol Genet,* 23**,** 5916-27.
KATZ, P. S. 2011. Neural mechanisms underlying the evolvability of behaviour. *Philos Trans R Soc Lond B Biol Sci.*
KENNEDY, S., WANG, D. & RUVKUN, G. 2004. A conserved siRNA-degrading RNase negatively regulates RNA interference in C. elegans. *Nature,* 427**,** 645-9.
KIM, E. Y., RUMPF, C. H., FUJIWARA, Y., COOLEY, E. S., VAN PETEGEM, F. & MINOR, D. L., JR. 2008. Structures of CaV2 Ca2+/CaM-IQ domain complexes reveal binding modes that underlie calcium-dependent inactivation and facilitation. *Structure,* 16**,** 1455-67.
KIMATA, T., SASAKURA, H., OHNISHI, N., NISHIO, N. & MORI, I. 2012. Thermotaxis of C. elegans as a model for temperature perception, neural information processing and neural plasticity. *Worm,* 1**,** 31-41.
KIMBLE, J. & HIRSH, D. 1979. The postembryonic cell lineages of the hermaphrodite and male gonads in Caenorhabditis elegans. *Dev Biol,* 70**,** 396-417.
KIMURA, K. D., MIYAWAKI, A., MATSUMOTO, K. & MORI, I. 2004. The C. elegans thermosensory neuron AFD responds to warming. *Curr Biol,* 14**,** 1291-5.
KLENCHIN, V. A., CALVERT, P. D. & BOWNDS, M. D. 1995. Inhibition of rhodopsin kinase by recoverin. Further evidence for a negative feedback system in phototransduction. *J Biol Chem,* 270**,** 16147-52.
KOHOUT, T. A. & LEFKOWITZ, R. J. 2003. Regulation of G protein-coupled receptor kinases and arrestins during receptor desensitization. *Mol Pharmacol,* 63**,** 9-18.
KOIZUMI, S., ROSA, P., WILLARS, G. B., CHALLISS, R. A., TAVERNA, E., FRANCOLINI, M., BOOTMAN, M. D., LIPP, P., INOUE, K., RODER, J. & JEROMIN, A. 2002. Mechanisms underlying the neuronal calcium sensor-1-evoked enhancement of exocytosis in PC12 cells. *J Biol Chem,* 277**,** 30315-24.
KOMATSU, H., MORI, I., RHEE, J. S., AKAIKE, N. & OHSHIMA, Y. 1996. Mutations in a cyclic nucleotide-gated channel lead to abnormal thermosensation and chemosensation in C. elegans. *Neuron,* 17**,** 707-18.
KREBS, M., HELD, K., BINDER, A., HASHIMOTO, K., DEN HERDER, G., PARNISKE, M., KUDLA, J. & SCHUMACHER, K. 2012. FRET-based genetically encoded sensors allow high-resolution live cell imaging of Ca(2)(+) dynamics. *Plant J,* 69**,** 181-92.

KRUGMANN, S., ANDERSON, K. E., RIDLEY, S. H., RISSO, N., MCGREGOR, A., COADWELL, J., DAVIDSON, K., EGUINOA, A., ELLSON, C. D., LIPP, P., MANIFAVA, M., KTISTAKIS, N., PAINTER, G., THURING, J. W., COOPER, M. A., LIM, Z. Y., HOLMES, A. B., DOVE, S. K., MICHELL, R. H., GREWAL, A., NAZARIAN, A., ERDJUMENT-BROMAGE, H., TEMPST, P., STEPHENS, L. R. & HAWKINS, P. T. 2002. Identification of ARAP3, a novel PI3K effector regulating both Arf and Rho GTPases, by selective capture on phosphoinositide affinity matrices. *Mol Cell,* 9**,** 95-108.

KUHARA, A. & MORI, I. 2006. Molecular physiology of the neural circuit for calcineurin-dependent associative learning in Caenorhabditis elegans. *J Neurosci,* 26**,** 9355-64.

KUHARA, A., OHNISHI, N., SHIMOWADA, T., AND & MORI, I. 2011. Neural coding in a single sensory neuron controlling opposite seeking behaviours in Caenorhabditis elegans. *Nature Communications,* 2**,** 355.

KUHARA, A., OKUMURA, M., KIMATA, T., TANIZAWA, Y., TAKANO, R., KIMURA, K. D., INADA, H., MATSUMOTO, K., AND & MORI, I. 2008. Temperature Sensing by an Olfactory Neuron in a Circuit Controlling Behavior of C. elegans. *Science,* 320.

KUO, H. C., CHENG, C. F., CLARK, R. B., LIN, J. J., LIN, J. L., HOSHIJIMA, M., NGUYEN-TRAN, V. T., GU, Y., IKEDA, Y., CHU, P. H., ROSS, J., GILES, W. R. & CHIEN, K. R. 2001. A defect in the Kv channel-interacting protein 2 (KChIP2) gene leads to a complete loss of I(to) and confers susceptibility to ventricular tachycardia. *Cell,* 107**,** 801-13.

LAMBERS, T. T., WEIDEMA, A. F., NILIUS, B., HOENDEROP, J. G. & BINDELS, R. J. 2004. Regulation of the mouse epithelial Ca2(+) channel TRPV6 by the Ca(2+)-sensor calmodulin. *J Biol Chem,* 279**,** 28855-61.

LATORRE, R., ZAELZER, C. & BRAUCHI, S. 2009. Structure-functional intimacies of transient receptor potential channels. *Q Rev Biophys,* 42**,** 201-46.

LAUTERMILCH, N. J., FEW, A. P., SCHEUER, T. & CATTERALL, W. A. 2005. Modulation of CaV2.1 channels by the neuronal calcium-binding protein visinin-like protein-2. *J Neurosci,* 25**,** 7062-70.

LEAL, K., MOCHIDA, S., SCHEUER, T. & CATTERALL, W. A. 2012. Fine-tuning synaptic plasticity by modulation of CaV2.1 channels with Ca2+ sensor proteins. *Proc Natl Acad Sci U S A,* 109**,** 17069-74.

LEE, A., JIMENEZ, A., CUI, G. & HAESELEER, F. 2007. Phosphorylation of the Ca2+-binding protein CaBP4 by protein kinase C zeta in photoreceptors. *J Neurosci,* 27**,** 12743-54.

LEE, A., SCHEUER, T. & CATTERALL, W. A. 2000. Ca2+/calmodulin-dependent facilitation and inactivation of P/Q-type Ca2+ channels. *J Neurosci,* 20**,** 6830-8.

LEE, A., WESTENBROEK, R. E., HAESELEER, F., PALCZEWSKI, K., SCHEUER, T. & CATTERALL, W. A. 2002. Differential modulation of Ca(v)2.1 channels by calmodulin and Ca2+-binding protein 1. *Nat Neurosci,* 5**,** 210-7.

LEE, A., WONG, S. T., GALLAGHER, D., LI, B., STORM, D. R., SCHEUER, T. & CATTERALL, W. A. 1999. Ca2+/calmodulin binds to and modulates P/Q-type calcium channels. *Nature,* 399**,** 155-9.

LEE, A., ZHOU, H., SCHEUER, T. & CATTERALL, W. A. 2003. Molecular determinants of Ca(2+)/calmodulin-dependent regulation of Ca(v)2.1 channels. *Proc Natl Acad Sci U S A,* 100**,** 16059-64.

LIAN, L. Y., PANDALANENI, S. R., PATEL, P., MCCUE, H. V., HAYNES, L. P. & BURGOYNE, R. D. 2011. Characterisation of the interaction of the C-terminus of the dopamine D2 receptor with neuronal calcium sensor-1. *PLoS One,* 6**,** e27779.

LIAN, L. Y., PANDALANENI, S. R., TODD, P. A., MARTIN, V. M., BURGOYNE, R. D. & HAYNES, L. P. 2014. Demonstration of Binding of Neuronal Calcium Sensor-1 to the Ca2.1 P/Q-Type Calcium Channel. *Biochemistry*.

LIANG, H., DEMARIA, C. D., ERICKSON, M. G., MORI, M. X., ALSEIKHAN, B. A. & YUE, D. T. 2003. Unified mechanisms of Ca2+ regulation across the Ca2+ channel family. *Neuron,* 39**,** 951-60.

LIU, S., SCHULZE, E. & BAUMEISTER, R. 2012. Temperature- and touch-sensitive neurons couple CNG and TRPV channel activities to control heat avoidance in Caenorhabditis elegans. *PLoS One,* 7**,** e32360.

LOCKERY, S. R. 2009. Neuroscience: A social hub for worms. *Nature.* England.

LU, L., HORSTMANN, H., NG, C. & HONG, W. 2001. Regulation of Golgi structure and function by ARF-like protein 1 (Arl1). *J Cell Sci,* 114**,** 4543-55.

LUCAS, P., UKHANOV, K., LEINDERS-ZUFALL, T. & ZUFALL, F. 2003. A diacylglycerol-gated cation channel in vomeronasal neuron dendrites is impaired in TRPC2 mutant mice: mechanism of pheromone transduction. *Neuron,* 40**,** 551-61.

LUSCHER, C. & FRERKING, M. 2001. Restless AMPA receptors: implications for synaptic transmission and plasticity. *Trends Neurosci,* 24**,** 665-70.

MA, X. & SHEN, Y. 2012. Structural basis for degeneracy among thermosensory neurons in Caenorhabditis elegans. *J Neurosci,* 32**,** 1-3.

MACOSKO, E. Z., POKALA, N., FEINBERG, E. H., CHALASANI, S. H., BUTCHER, R. A., CLARDY, J. & BARGMANN, C. I. 2009. A Hub-and-Spoke Circuit Drives Pheromone Attraction and Social Behavior in C. elegans. *Nature,* 458**,** 1171-5.

MALENKA, R. C. & BEAR, M. F. 2004. LTP and LTD: an embarrassment of riches. *Neuron,* 44**,** 5-21.

MALINOW, R. & MALENKA, R. C. 2002. AMPA receptor trafficking and synaptic plasticity. *Annu Rev Neurosci,* 25**,** 103-26.

MANGELS, L. A. & GNEGY, M. E. 1992. Cyclic AMP accumulation alters calmodulin localization in SK-N-SH human neuroblastoma cells. *Brain Res Mol Brain Res,* 12**,** 103-10.

MAO, A. J., BECHBERGER, J., LIDINGTON, D., GALIPEAU, J., LAIRD, D. W. & NAUS, C. C. 2000. Neuronal differentiation and growth control of neuro-2a cells after retroviral gene delivery of connexin43. *J Biol Chem,* 275**,** 34407-14.

MARIOL, M. C., WALTER, L., BELLEMIN, S., GIESELER, K. 2013. A Rapid Protocol for Integrating Extrachromosomal Arrays With High Transmission Rate into the C. elegans Genome. *JoVE (Journal of Visualized Experiments),* e50773.

MARTIN, V. M., JOHNSON, J. R., HAYNES, L. P., BARCLAY, J. W. & BURGOYNE, R. D. 2013. Identification of key structural elements for neuronal calcium sensor-1 function in the regulation of the temperature-dependency of locomotion in C. elegans. *Mol Brain,* 6**,** 39.

MARX, V. 2014. A deep look at synaptic dynamics. *Nature,* 515**,** 293-7.

MATTSON, M. P. & MAGNUS, T. 2006. Ageing and neuronal vulnerability. *Nat Rev Neurosci,* 7**,** 278-94.

MCCREA, H. J. & DE CAMILLI, P. 2009. Mutations in phosphoinositide metabolizing enzymes and human disease. *Physiology (Bethesda),* 24**,** 8-16.

MCCUE, H. V., BURGOYNE, R. D. & HAYNES, L. P. 2009. Membrane targeting of the EF-hand containing calcium-sensing proteins CaBP7 and CaBP8. *Biochem Biophys Res Commun,* 380**,** 825-31.

MCCUE, H. V., BURGOYNE, R. D. & HAYNES, L. P. 2011. Determination of the membrane topology of the small EF-hand Ca2+-sensing proteins CaBP7 and CaBP8. *PLoS One,* 6**,** e17853.

MCCUE, H. V., HAYNES, L. P. & BURGOYNE, R. D. 2010a. Bioinformatic analysis of CaBP/calneuron proteins reveals a family of highly conserved vertebrate Ca2+-binding proteins. *BMC Res Notes,* 3**,** 118.

MCCUE, H. V., HAYNES, L. P. & BURGOYNE, R. D. 2010b. The diversity of calcium sensor proteins in the regulation of neuronal function. *Cold Spring Harb Perspect Biol,* 2**,** a004085.

MCCUE, H. V., PATEL, P., HERBERT, A. P., LIAN, L. Y., BURGOYNE, R. D. & HAYNES, L. P. 2012. Solution NMR structure of the Ca2+-bound N-terminal domain of CaBP7: a regulator of golgi trafficking. *J Biol Chem,* 287**,** 38231-43.

MCCUE, H. V., WARDYN, J. D., BURGOYNE, R. D. & HAYNES, L. P. 2013. Generation and characterization of a lysosomally targeted, genetically encoded Ca2+-sensor. *Biochem J,* 449**,** 449-57.

MCFERRAN, B. W., GRAHAM, M. E. & BURGOYNE, R. D. 1998. Neuronal Ca2+ sensor 1, the mammalian homologue of frequenin, is expressed in chromaffin and PC12 cells and regulates neurosecretion from dense-core granules. *J Biol Chem,* 273**,** 22768-72.

MCFERRAN, B. W., WEISS, J. L. & BURGOYNE, R. D. 1999. Neuronal Ca(2+) sensor 1. Characterization of the myristoylated protein, its cellular effects in permeabilized adrenal chromaffin cells, Ca(2+)-independent membrane association, and interaction with binding proteins, suggesting a role in rapid Ca(2+) signal transduction. *J Biol Chem,* 274**,** 30258-65.

MCGHEE, J. D. 2007. The C. elegans intestine (March 27, 2007). *WormBook, ed. The C. elegans Research Community, WormBook, doi/10.1895/wormbook.1.133.1,* http://www.wormbook.org/.

MCGINNIS, K. M., SHARIAT-MADAR, Z. & GNEGY, M. E. 1998. Cytosolic calmodulin is increased in SK-N-SH human neuroblastoma cells due to release of calcium from intracellular stores. *J Neurochem,* 70**,** 139-46.

MCKAY, S. J., JOHNSEN, R., KHATTRA, J., ASANO, J., BAILLIE, D. L., CHAN, S., DUBE, N., FANG, L., GOSZCZYNSKI, B., HA, E., HALFNIGHT, E., HOLLEBAKKEN, R., HUANG, P., HUNG, K., JENSEN, V., JONES, S. J., KAI, H., LI, D., MAH, A., MARRA, M., MCGHEE, J., NEWBURY, R., POUZYREV, A., RIDDLE, D. L., SONNHAMMER, E., TIAN, H., TU, D., TYSON, J. R., VATCHER, G., WARNER, A., WONG, K., ZHAO, Z. & MOERMAN, D. G. 2003. Gene expression profiling of cells, tissues, and developmental stages of the nematode C. elegans. *Cold Spring Harb Symp Quant Biol,* 68**,** 159-69.

MELLO, C. C., KRAMER, J. M., STINCHCOMB, D. & AMBROS, V. 1991. Efficient gene transfer in C.elegans: extrachromosomal maintenance and integration of transforming sequences. *EMBO J,* 10**,** 3959-70.

MIKHAYLOVA, M., REDDY, P. P., MUNSCH, T., LANDGRAF, P., SUMAN, S. K., SMALLA, K. H., GUNDELFINGER, E. D., SHARMA, Y. & KREUTZ, M. R. 2009. Calneurons provide a calcium threshold for trans-Golgi network to plasma membrane trafficking. *Proc Natl Acad Sci U S A,* 106**,** 9093-8.

MINKE, B. 2006. TRP channels and Ca2+ signaling. *Cell Calcium,* 40**,** 261-75.

MIURA, K., JACQUES, K. M., STAUFFER, S., KUBOSAKI, A., ZHU, K., HIRSCH, D. S., RESAU, J., ZHENG, Y. & RANDAZZO, P. A. 2002. ARAP1: a point of convergence for Arf and Rho signaling. *Mol Cell,* 9**,** 109-19.

MIYAWAKI, A., GRIESBECK, O., HEIM, R. & TSIEN, R. Y. 1999. Dynamic and quantitative Ca2+ measurements using improved cameleons. *Proc Natl Acad Sci U S A,* 96**,** 2135-40.

MIYAWAKI, A., LLOPIS, J., HEIM, R., MCCAFFERY, J. M., ADAMS, J. A., IKURA, M. & TSIEN, R. Y. 1997. Fluorescent indicators for Ca2+ based on green fluorescent proteins and calmodulin. *Nature,* 388**,** 882-7.
MOCHIDA, S., FEW, A. P., SCHEUER, T. & CATTERALL, W. A. 2008. Regulation of presynaptic Ca(V)2.1 channels by Ca2+ sensor proteins mediates short-term synaptic plasticity. *Neuron,* 57**,** 210-6.
MOLNAR, Z. & BROWN, R. E. 2010. Insights into the life and work of Sir Charles Sherrington. *Nat Rev Neurosci,* 11**,** 429-36.
MONET, M., FRANCOEUR, N. & BOULAY, G. 2012. Involvement of phosphoinositide 3-Kinase and PTEN protein in mechanism of activation of TRPC6 protein in vascular smooth muscle cells. *J Biol Chem,* 287.
MONTELL, C. 2005. The TRP superfamily of cation channels. *Sci STKE,* 2005**,** re3.
MONTELL, C. & RUBIN, G. M. 1989. Molecular characterization of the Drosophila trp locus: a putative integral membrane protein required for phototransduction. *Neuron,* 2**,** 1313-23.
MORENO, C. M., DIXON, R. E., TAJADA, S., YUAN, C., OPITZ-ARAYA, X., BINDER, M. D. & SANTANA, L. F. 2016. Ca(2+) entry into neurons is facilitated by cooperative gating of clustered CaV1.3 channels. *Elife,* 5.
MORI, I. 1999. Genetics of chemotaxis and thermotaxis in the nematode Caenorhabditis elegans. *Annu Rev Genet,* 33**,** 399-422.
MORI, I. & OHSHIMA, Y. 1995. Neural regulation of thermotaxis in Caenorhabditis elegans. 376**,** 344-348.
MORI, I., SASAKURA, H. & KUHARA, A. 2007. Worm thermotaxis: a model system for analyzing thermosensation and neural plasticity. *Curr Opin Neurobiol,* 17**,** 712-9.
MORI, M. X., IMAI, Y., ITSUKI, K. & INOUE, R. 2011. Quantitative measurement of Ca(2+)-dependent calmodulin-target binding by Fura-2 and CFP and YFP FRET imaging in living cells. *Biochemistry,* 50**,** 4685-96.
MORLEY, J. F. & MORIMOTO, R. I. 2004. Regulation of Longevity in Caenorhabditis elegans by Heat Shock Factor and Molecular Chaperones. *Mol Biol Cell.*
MOSS, J. & VAUGHAN, M. 1995. Structure and function of ARF proteins: activators of cholera toxin and critical components of intracellular vesicular transport processes. *J Biol Chem,* 270**,** 12327-30.
MOSSESSOVA, E., GULBIS, J. M. & GOLDBERG, J. 1998. Structure of the guanine nucleotide exchange factor Sec7 domain of human arno and analysis of the interaction with ARF GTPase. *Cell,* 92**,** 415-23.
MULDER, N. J., APWEILER, R., ATTWOOD, T. K., BAIROCH, A., BARRELL, D., BATEMAN, A., BINNS, D., BISWAS, M., BRADLEY, P., BORK, P., BUCHER, P., COPLEY, R. R., COURCELLE, E., DAS, U., DURBIN, R., FALQUET, L., FLEISCHMANN, W., GRIFFITHS-JONES, S., HAFT, D., HARTE, N., HULO, N., KAHN, D., KANAPIN, A., KRESTYANINOVA, M., LOPEZ, R., LETUNIC, I., LONSDALE, D., SILVENTOINEN, V., ORCHARD, S. E., PAGNI, M., PEYRUC, D., PONTING, C. P., SELENGUT, J. D., SERVANT, F., SIGRIST, C. J., VAUGHAN, R. & ZDOBNOV, E. M. 2003. The InterPro Database, 2003 brings increased coverage and new features. *Nucleic Acids Res,* 31**,** 315-8.
MURAKAMI, H., BESSINGER, K., HELLMANN, J. & MURAKAMI, S. 2005. Aging-dependent and -independent modulation of associative learning behavior by insulin/insulin-like growth factor-1 signal in Caenorhabditis elegans. *J Neurosci,* 25**,** 10894-904.
MURAKAMI, S. 2007. Caenorhabditis elegans as a model system to study aging of learning and memory. *Mol Neurobiol.* United States.

NAGAI, T., YAMADA, S., TOMINAGA, T., ICHIKAWA, M. & MIYAWAKI, A. 2004. Expanded dynamic range of fluorescent indicators for Ca(2+) by circularly permuted yellow fluorescent proteins. *Proc Natl Acad Sci U S A,* 101**,** 10554-9.
NAKANO, A. & MURAMATSU, M. 1989. A novel GTP-binding protein, Sar1p, is involved in transport from the endoplasmic reticulum to the Golgi apparatus. *J Cell Biol,* 109**,** 2677-91.
NARAYAN, A., LAURENT, G. & STERNBERG, P. W. 2011. Transfer characteristics of a thermosensory synapse in Caenorhabditis elegans. *Proc Natl Acad Sci U S A,* 108**,** 9667-72.
NG, E., VARASCHIN, R. K., SU, P., BROWNE, C. J., HERMAINSKI, J., LE FOLL, B., PONGS, O., LIU, F., TRUDEAU, L. E., RODER, J. C. & WONG, A. H. 2016. Neuronal calcium sensor-1 deletion in the mouse decreases motivation and dopamine release in the nucleus accumbens. *Behav Brain Res,* 301**,** 213-25.
NIE, Z., HIRSCH, D. S. & RANDAZZO, P. A. 2003. Arf and its many interactors. *Curr Opin Cell Biol,* 15**,** 396-404.
NIE, Z., STANLEY, K. T., STAUFFER, S., JACQUES, K. M., HIRSCH, D. S., TAKEI, J. & RANDAZZO, P. A. 2002. AGAP1, an endosome-associated, phosphoinositide-dependent ADP-ribosylation factor GTPase-activating protein that affects actin cytoskeleton. *J Biol Chem,* 277**,** 48965-75.
NILIUS, B., VOETS, T. & PETERS, J. 2005. TRP channels in disease. *Sci STKE,* 2005**,** re8.
NISHIDA, Y., SUGI, T., NONOMURA, M. & MORI, I. 2011. Identification of the AFD neuron as the site of action of the CREB protein in Caenorhabditis elegans thermotaxis. *Embo Reports,* 12.
NONET, M. L., GRUNDAHL, K., MEYER, B. J. & RAND, J. B. 1993. Synaptic function is impaired but not eliminated in C. elegans mutants lacking synaptotagmin. *Cell,* 73**,** 1291-305.
NONET, M. L., SAIFEE, O., ZHAO, H., RAND, J. B. & WEI, L. 1998. Synaptic transmission deficits in Caenorhabditis elegans synaptobrevin mutants. *J Neurosci,* 18**,** 70-80.
NUTTLEY, W. M., ATKINSON-LEADBEATER, K. P. & VAN DER KOOY, D. 2002. Serotonin mediates food-odor associative learning in the nematode Caenorhabditiselegans. *Proc Natl Acad Sci U S A,* 99**,** 12449-54.
O'CALLAGHAN, D. W., IVINGS, L., WEISS, J. L., ASHBY, M. C., TEPIKIN, A. V. & BURGOYNE, R. D. 2002. Differential use of myristoyl groups on neuronal calcium sensor proteins as a determinant of spatio-temporal aspects of Ca2+ signal transduction. *J Biol Chem,* 277**,** 14227-37.
O'CALLAGHAN, D. W., TEPIKIN, A. V. & BURGOYNE, R. D. 2003. Dynamics and calcium sensitivity of the Ca2+/myristoyl switch protein hippocalcin in living cells. *J Cell Biol,* 163**,** 715-21.
OHKUMO, T., MASUTANI, C., EKI, T. & HANAOKA, F. 2008. Use of RNAi in C. elegans. *Methods Mol Biol,* 442**,** 129-37.
OHNISHI, N., KUHARA, A., NAKAMURA, F., OKOCHI, Y. & MORI, I. 2011. Bidirectional regulation of thermotaxis by glutamate transmissions in Caenorhabditis elegans. *Embo j,* 30**,** 1376-88.
OSAWA, M., DACE, A., TONG, K. I., VALIVETI, A., IKURA, M. & AMES, J. B. 2005. Mg2+ and Ca2+ differentially regulate DNA binding and dimerization of DREAM. *J Biol Chem,* 280**,** 18008-14.
OZ, S., BENMOCHA, A., SASSON, Y., SACHYANI, D., ALMAGOR, L., LEE, A., HIRSCH, J. A. & DASCAL, N. 2013. Competitive and Non-competitive Regulation

of Calcium-dependent Inactivation in CaV1.2 L-type Ca2+ Channels by Calmodulin and Ca2+-binding Protein 1. *J Biol Chem,* 288**,** 12680-91.
PALKAR, R., LIPPOLDT, E. K. & MCKEMY, D. D. 2015. The molecular and cellular basis of thermosensation in mammals. *Curr Opin Neurobiol,* 34c**,** 14-19.
PALMER, A. E. & TSIEN, R. Y. 2006. Measuring calcium signaling using genetically targetable fluorescent indicators. *Nat Protoc,* 1**,** 1057-65.
PALMER, D. J., HELMS, J. B., BECKERS, C. J., ORCI, L. & ROTHMAN, J. E. 1993. Binding of coatomer to Golgi membranes requires ADP-ribosylation factor. *J Biol Chem,* 268**,** 12083-9.
PANDALANENI, S., KARUPPIAH, V., SALEEM, M., HAYNES, L. P., BURGOYNE, R. D., MAYANS, O., DERRICK, J. P. & LIAN, L. Y. 2015. Neuronal Calcium Sensor-1 Binds the D2 Dopamine Receptor and G-protein-coupled Receptor Kinase 1 (GRK1) Peptides Using Different Modes of Interactions. *J Biol Chem,* 290**,** 18744-56.
PASQUALATO, S., RENAULT, L. & CHERFILS, J. 2002. Arf, Arl, Arp and Sar proteins: a family of GTP-binding proteins with a structural device for 'front-back' communication. *EMBO Rep,* 3**,** 1035-41.
PATEL, S., MARCHANT, J. & BRAILOIU, E. 2010. Two-pore channels: Regulation by NAADP and customized roles in triggering calcium signals. *Cell Calcium,* 47**,** 480-90.
PEDERSEN, S. F., OWSIANIK, G. & NILIUS, B. 2005. TRP channels: an overview. *Cell Calcium,* 38**,** 233-52.
PENELA, P., MURGA, C., RIBAS, C., LAFARGA, V. & MAYOR, F. 2010. The complex G protein-coupled receptor kinase 2 (GRK2) interactome unveils new physiopathological targets. *Br J Pharmacol,* 160**,** 821-32.
PENELA, P., RIBAS, C. & MAYOR, F., JR. 2003. Mechanisms of regulation of the expression and function of G protein-coupled receptor kinases. *Cell Signal,* 15**,** 973-81.
PEREIRA, L., KRATSIOS, P., SERRANO-SAIZ, E., SHEFTEL, H., MAYO, A. E., HALL, D. H., WHITE, J. G., LEBOEUF, B., GARCIA, L. R., ALON, U. & HOBERT, O. 2015. A cellular and regulatory map of the cholinergic nervous system of C. elegans. *eLife,* 4.
PERKINS, L. A., HEDGECOCK, E. M., THOMSON, J. N. & CULOTTI, J. G. 1986. Mutant sensory cilia in the nematode Caenorhabditis elegans. *Dev Biol,* 117**,** 456-87.
PETERSEN, C. C., BERRIDGE, M. J., BORGESE, M. F. & BENNETT, D. L. 1995. Putative capacitative calcium entry channels: expression of Drosophila trp and evidence for the existence of vertebrate homologues. *Biochem J,* 311**,** 41-4.
PETERSEN, O. H., MICHALAK, M. & VERKHRATSKY, A. 2005. Calcium signalling: past, present and future. *Cell Calcium,* 38**,** 161-9.
PETERSON, B. Z., DEMARIA, C. D., ADELMAN, J. P. & YUE, D. T. 1999. Calmodulin is the Ca2+ sensor for Ca2+ -dependent inactivation of L-type calcium channels. *Neuron,* 22**,** 549-58.
PETKO, J. A., KABBANI, N., FREY, C., WOLL, M., HICKEY, K., CRAIG, M., CANFIELD, V. A. & LEVENSON, R. 2009. Proteomic and functional analysis of NCS-1 binding proteins reveals novel signaling pathways required for inner ear development in zebrafish. *BMC Neurosci,* 10**,** 27.
PEYMEN, K., WATTEYNE, J., FROONINCKX, L., SCHOOFS, L. & BEETS, I. 2014. The FMRFamide-Like Peptide Family in Nematodes. *Front Endocrinol (Lausanne),* 5**,** 90.
PIERCE-SHIMOMURA, J. T., FAUMONT, S., GASTON, M. R., PEARSON, B. J. & LOCKERY, S. R. 2001. The homeobox gene lim-6 is required for distinct chemosensory representations in C. elegans. *Nature,* 410**,** 694-8.

PITCHER, J. A., FREEDMAN, N. J. & LEFKOWITZ, R. J. 1998. G protein-coupled receptor kinases. *Annu Rev Biochem,* 67**,** 653-92.
POCOCK, R. & HOBERT, O. 2010. Hypoxia activates a latent circuit for processing gustatory information in C. elegans. *Nat Neurosci,* 13**,** 610-4.
POGORZALA, L. A., MISHRA, S. K. & HOON, M. A. 2013. The cellular code for mammalian thermosensation. *J Neurosci,* 33**,** 5533-41.
PONGS, O., LINDEMEIER, J., ZHU, X. R., THEIL, T., ENGELKAMP, D., KRAH-JENTGENS, I., LAMBRECHT, H. G., KOCH, K. W., SCHWEMER, J., RIVOSECCHI, R. & ET AL. 1993. Frequenin--a novel calcium-binding protein that modulates synaptic efficacy in the Drosophila nervous system. *Neuron,* 11**,** 15-28.
POSSIK, E. & PAUSE, A. 2015. Measuring oxidative stress resistance of Caenorhabditis elegans in 96-well microtiter plates. *J Vis Exp***,** e52746.
PRONIN, A. N., CARMAN, C. V. & BENOVIC, J. L. 1998. Structure-function analysis of G protein-coupled receptor kinase-5. Role of the carboxyl terminus in kinase regulation. *J Biol Chem,* 273**,** 31510-8.
PRONIN, A. N., SATPAEV, D. K., SLEPAK, V. Z. & BENOVIC, J. L. 1997. Regulation of G protein-coupled receptor kinases by calmodulin and localization of the calmodulin binding domain. *J Biol Chem,* 272**,** 18273-80.
RAGHURAM, V., SHARMA, Y. & KREUTZ, M. R. 2012. Ca(2+) sensor proteins in dendritic spines: a race for Ca(2+). *Front Mol Neurosci,* 5**,** 61.
RAJARAM, S., SEDENSKY, M. M. & MORGAN, P. G. 2000. The sequence and associated null phenotype of a C. elegans neurocalcin-like gene. *Genesis,* 26**,** 234-9.
RAMSEY, I. S., DELLING, M. & CLAPHAM, D. E. 2006. An introduction to TRP channels. *Annu Rev Physiol,* 68**,** 619-47.
RANDAZZO, P. A., NIE, Z., MIURA, K. & HSU, V. W. 2000. Molecular aspects of the cellular activities of ADP-ribosylation factors. *Sci STKE,* 2000**,** re1.
RECHAVI, O., HOURI-ZE'EVI, L., ANAVA, S., GOH, W. S., KERK, S. Y., HANNON, G. J. & HOBERT, O. 2014. Starvation-induced transgenerational inheritance of small RNAs in C. elegans. *Cell,* 158**,** 277-87.
RHOADS, A. R. & FRIEDBERG, F. 1997. Sequence motifs for calmodulin recognition. *Faseb j,* 11**,** 331-40.
RIBAS, C., PENELA, P., MURGA, C., SALCEDO, A., GARCIA-HOZ, C., JURADO-PUEYO, M., AYMERICH, I. & MAYOR, F., JR. 2007. The G protein-coupled receptor kinase (GRK) interactome: role of GRKs in GPCR regulation and signaling. *Biochim Biophys Acta,* 1768**,** 913-22.
RIBEIRO, F. M., FERREIRA, L. T., PAQUET, M., CREGAN, T., DING, Q., GROS, R. & FERGUSON, S. S. 2009. Phosphorylation-independent regulation of metabotropic glutamate receptor 5 desensitization and internalization by G protein-coupled receptor kinase 2 in neurons. *J Biol Chem,* 284**,** 23444-53.
RIEKE, F., LEE, A. & HAESELEER, F. 2008. Characterization of Ca2+-binding protein 5 knockout mouse retina. *Invest Ophthalmol Vis Sci,* 49**,** 5126-35.
RODERICK, H. L., HIGAZI, D. R., SMYRNIAS, I., FEARNLEY, C., HARZHEIM, D. & BOOTMAN, M. D. 2007. Calcium in the heart: when it's good, it's very very good, but when it's bad, it's horrid. *Biochem Soc Trans,* 35**,** 957-61.
ROSE, J. K. & RANKIN, C. H. 2001. Analyses of habituation in Caenorhabditis elegans. *Learn Mem,* 8**,** 63-9.
ROUSSET, M., CENS, T., GAVARINI, S., JEROMIN, A. & CHARNET, P. 2003. Down-regulation of voltage-gated Ca2+ channels by neuronal calcium sensor-1 is beta subunit-specific. *J Biol Chem,* 278**,** 7019-26.

RUAS, M., RIETDORF, K., ARREDOUANI, A., DAVIS, L. C., LLOYD-EVANS, E., KOEGEL, H., FUNNELL, T. M., MORGAN, A. J., WARD, J. A., WATANABE, K., CHENG, X., CHURCHILL, G. C., ZHU, M. X., PLATT, F. M., WESSEL, G. M., PARRINGTON, J. & GALIONE, A. 2010. Purified TPC isoforms form NAADP receptors with distinct roles for Ca(2+) signaling and endolysosomal trafficking. *Curr Biol,* 20**,** 703-9.

RUSSELL, J., VIDAL-GADEA, A. G., MAKAY, A., LANAM, C. & PIERCE-SHIMOMURA, J. T. 2014. Humidity sensation requires both mechanosensory and thermosensory pathways in Caenorhabditis elegans. *Proc Natl Acad Sci U S A,* 111**,** 8269-74.

RYU, W. S. & SAMUEL, A. D. 2002. Thermotaxis in Caenorhabditis elegans analyzed by measuring responses to defined Thermal stimuli. *J Neurosci,* 22**,** 5727-33.

SAAB, B. J., GEORGIOU, J., NATH, A., LEE, F. J., WANG, M., MICHALON, A., LIU, F., MANSUY, I. M. & RODER, J. C. 2009. NCS-1 in the dentate gyrus promotes exploration, synaptic plasticity, and rapid acquisition of spatial memory. *Neuron,* 63**,** 643-56.

SALLESE, M., MARIGGIO, S., COLLODEL, G., MORETTI, E., PIOMBONI, P., BACCETTI, B. & DE BLASI, A. 1997. G protein-coupled receptor kinase GRK4. Molecular analysis of the four isoforms and ultrastructural localization in spermatozoa and germinal cells. *J Biol Chem,* 272**,** 10188-95.

SAMMUT, M., COOK, S. J., NGUYEN, K. C., FELTON, T., HALL, D. H., EMMONS, S. W., POOLE, R. J. & BARRIOS, A. 2015. Glia-derived neurons are required for sex-specific learning in C. elegans. *Nature,* 526**,** 385-90.

SANTY, L. C. & CASANOVA, J. E. 2002. GTPase signaling: bridging the GAP between ARF and Rho. *Curr Biol,* 12**,** R360-2.

SASAKURA, H. & MORI, I. 2013. Behavioral plasticity, learning, and memory in C. elegans. *Curr Opin Neurobiol,* 23**,** 92-9.

SASAKURA, H., TSUKADA, Y., TAKAGI, S. & MORI, I. 2013. Japanese studies on neural circuits and behavior of Caenorhabditis elegans. *Front Neural Circuits,* 7**,** 187.

SATOH, Y., SATO, H., KUNITOMO, H., FEI, X., HASHIMOTO, K. & IINO, Y. 2014. Regulation of experience-dependent bidirectional chemotaxis by a neural circuit switch in Caenorhabditis elegans. *J Neurosci,* 34**,** 15631-7.

SATTERLEE, J. S., SASAKURA, H., KUHARA, A., BERKELEY, M., MORI, I. & SENGUPTA, P. 2001. Specification of thermosensory neuron fate in C. elegans requires ttx-1, a homolog of otd/Otx. *Neuron,* 31**,** 943-56.

SCHACKWITZ, W. S., INOUE, T. & THOMAS, J. H. 1996. Chemosensory neurons function in parallel to mediate a pheromone response in C. elegans. *Neuron,* 17**,** 719-28.

SCHAFER, W. R. 2012. Tackling thermosensation with multidimensional phenotyping. *BMC Biol,* 10**,** 91.

SCHRAUWEN, I., HELFMANN, S., INAGAKI, A., PREDOEHL, F., TABATABAIEFAR, M. A., PICHER, M. M., SOMMEN, M., SECO, C. Z., OOSTRIK, J., KREMER, H., DHEEDENE, A., CLAES, C., FRANSEN, E., CHALESHTORI, M. H., COUCKE, P., LEE, A., MOSER, T. & VAN CAMP, G. 2012. A mutation in CABP2, expressed in cochlear hair cells, causes autosomal-recessive hearing impairment. *Am J Hum Genet,* 91**,** 636-45.

SCHWALLER, B. 2009. The continuing disappearance of "pure" Ca2+ buffers. *Cell Mol Life Sci,* 66**,** 275-300.

SHALTIEL, L., PAPARIZOS, C., FENSKE, S., HASSAN, S., GRUNER, C., ROTZER, K., BIEL, M. & WAHL-SCHOTT, C. A. 2012. Complex regulation of voltage-dependent

activation and inactivation properties of retinal voltage-gated Cav1.4 L-type Ca2+ channels by Ca2+-binding protein 4 (CaBP4). *J Biol Chem,* 287**,** 36312-21.
SHANER, N. C., STEINBACH, P. A. & TSIEN, R. Y. 2005. A guide to choosing fluorescent proteins. *Nat Methods,* 2**,** 905-9.
SHEN, L., HU, Y., CAI, T., LIN, X. & WANG, D. 2010. Regulation of longevity by genes required for the functions of AIY interneuron in nematode Caenorhabditis elegans. *Mech Ageing Dev,* 131**,** 732-8.
SIDI, S., FRIEDRICH, R. W. & NICOLSON, T. 2003. NompC TRP channel required for vertebrate sensory hair cell mechanotransduction. *Science,* 301**,** 96-9.
SIMMER, F., MOORMAN, C., VAN DER LINDEN, A. M., KUIJK, E., VAN DEN BERGHE, P. V., KAMATH, R. S., FRASER, A. G., AHRINGER, J. & PLASTERK, R. H. 2003. Genome-wide RNAi of C. elegans using the hypersensitive rrf-3 strain reveals novel gene functions. *PLoS Biol,* 1**,** E12.
SIMMER, F., TIJSTERMAN, M., PARRISH, S., KOUSHIKA, S. P., NONET, M. L., FIRE, A., AHRINGER, J. & PLASTERK, R. H. 2002. Loss of the putative RNA-directed RNA polymerase RRF-3 makes C. elegans hypersensitive to RNAi. *Curr Biol,* 12**,** 1317-9.
SIPPY, T., CRUZ-MARTIN, A., JEROMIN, A. & SCHWEIZER, F. E. 2003. Acute changes in short-term plasticity at synapses with elevated levels of neuronal calcium sensor-1. *Nat Neurosci,* 6**,** 1031-8.
SKORA, S. & ZIMMER, M. 2013. Life(span) in balance: oxygen fuels a sophisticated neural network for lifespan homeostasis in C. elegans. *Embo j,* 32**,** 1499-501.
SMEAL, T. & GUARENTE, L. 1997. Mechanisms of cellular senescence. *Curr Opin Genet Dev,* 7**,** 281-7.
SMITH, H. K., LUO, L., O'HALLORAN, D., GUO, D., HUANG, X. Y., SAMUEL, A. D. & HOBERT, O. 2013. Defining specificity determinants of cGMP mediated gustatory sensory transduction in Caenorhabditis elegans. *Genetics,* 194**,** 885-901.
SNUTCH, T. P., HESCHL, M. F. & BAILLIE, D. L. 1988. The Caenorhabditis elegans hsp70 gene family: a molecular genetic characterization. *Gene,* 64**,** 241-55.
SOMEYA, A., SATA, M., TAKEDA, K., PACHECO-RODRIGUEZ, G., FERRANS, V. J., MOSS, J. & VAUGHAN, M. 2001. ARF-GEP(100), a guanine nucleotide-exchange protein for ADP-ribosylation factor 6. *Proc Natl Acad Sci U S A,* 98**,** 2413-8.
SONG, M. Y. & YUAN, J. X. 2010. Introduction to TRP channels: structure, function, and regulation. *Adv Exp Med Biol,* 661**,** 99-108.
STEVENS, F. C. 1983. Calmodulin: an introduction. *Can J Biochem Cell Biol,* 61**,** 906-10.
STORY, G. M., PEIER, A. M., REEVE, A. J., EID, S. R., MOSBACHER, J., HRICIK, T. R., EARLEY, T. J., HERGARDEN, A. C., ANDERSSON, D. A., HWANG, S. W., MCINTYRE, P., JEGLA, T., BEVAN, S. & PATAPOUTIAN, A. 2003. ANKTM1, a TRP-like channel expressed in nociceptive neurons, is activated by cold temperatures. *Cell,* 112**,** 819-29.
STRAHL, T., HAMA, H., DEWALD, D. B. & THORNER, J. 2005. Yeast phosphatidylinositol 4-kinase, Pik1, has essential roles at the Golgi and in the nucleus. *J Cell Biol,* 171**,** 967-79.
STRAHL, T., HUTTNER, I. G., LUSIN, J. D., OSAWA, M., KING, D., THORNER, J. & AMES, J. B. 2007. Structural insights into activation of phosphatidylinositol 4-kinase (Pik1) by yeast frequenin (Frq1). *J Biol Chem,* 282**,** 30949-59.
SULSTON, J. E. 1983. Neuronal cell lineages in the nematode Caenorhabditis elegans. *Cold Spring Harb Symp Quant Biol,* 48 Pt 2**,** 443-52.

SULSTON, J. E., ALBERTSON, D. G. & THOMSON, J. N. 1980. The Caenorhabditis elegans male: postembryonic development of nongonadal structures. *Dev Biol,* 78**,** 542-76.
SULSTON, J. E. & HORVITZ, H. R. 1977. Post-embryonic cell lineages of the nematode, Caenorhabditis elegans. *Dev Biol,* 56**,** 110-56.
SULSTON, J. E., SCHIERENBERG, E., WHITE, J. G. & THOMSON, J. N. 1983. The embryonic cell lineage of the nematode Caenorhabditis elegans. *Dev Biol,* 100**,** 64-119.
SUTTON, K. A., JUNGNICKEL, M. K., WANG, Y., CULLEN, K., LAMBERT, S. & FLORMAN, H. M. 2004. Enkurin is a novel calmodulin and TRPC channel binding protein in sperm. *Dev Biol,* 274**,** 426-35.
TADROSS, M. R., TSIEN, R. W. & YUE, D. T. 2013. Ca2+ channel nanodomains boost local Ca2+ amplitude. *Proc Natl Acad Sci U S A,* 110**,** 15794-9.
TAKAHASHI, N., HAMADA-NAKAHARA, S., ITOH, Y., TAKEMURA, K., SHIMADA, A., UEDA, Y., KITAMATA, M., MATSUOKA, R., HANAWA-SUETSUGU, K., SENJU, Y., MORI, M. X., KIYONAKA, S., KOHDA, D., KITAO, A., MORI, Y. & SUETSUGU, S. 2014. TRPV4 channel activity is modulated by direct interaction of the ankyrin domain to PI(4,5)P(2). *Nat Commun,* 5**,** 4994.
TALAVERA, K., NILIUS, B. & VOETS, T. 2008. Neuronal TRP channels: thermometers, pathfinders and life-savers. *Trends Neurosci,* 31**,** 287-95.
TAVERNA, E., FRANCOLINI, M., JEROMIN, A., HILFIKER, S., RODER, J. & ROSA, P. 2002. Neuronal calcium sensor 1 and phosphatidylinositol 4-OH kinase beta interact in neuronal cells and are translocated to membranes during nucleotide-evoked exocytosis. *J Cell Sci,* 115**,** 3909-22.
TEWSON, P., WESTENBERG, M., ZHAO, Y., CAMPBELL, R. E., QUINN, A. M. & HUGHES, T. E. 2012. Simultaneous detection of Ca2+ and diacylglycerol signaling in living cells. *PLoS One,* 7**,** e42791.
TIMMONS, L., COURT, D. L. & FIRE, A. 2001. Ingestion of bacterially expressed dsRNAs can produce specific and potent genetic interference in Caenorhabditis elegans. *Gene,* 263**,** 103-12.
TIMMONS, L. & FIRE, A. 1998. Specific interference by ingested dsRNA. *Nature,* 395**,** 854.
TIMMONS, L., TABARA, H., MELLO, C. C. & FIRE, A. Z. 2003. Inducible systemic RNA silencing in Caenorhabditis elegans. *Mol Biol Cell,* 14**,** 2972-83.
TIPPENS, A. L. & LEE, A. 2007. Caldendrin, a neuron-specific modulator of Cav/1.2 (L-type) Ca2+ channels. *J Biol Chem,* 282**,** 8464-73.
TODD, P. A., MCCUE, H. V., HAYNES, L. P., BARCLAY, J. W. & BURGOYNE, R. D. 2016. Interaction of ARF-1.1 and neuronal calcium sensor-1 in the control of the temperature-dependency of locomotion in Caenorhabditis elegans. *Sci Rep,* 6**,** 30023.
TOMIOKA, M., ADACHI, T., SUZUKI, H., KUNITOMO, H., SCHAFER, W. R. & IINO, Y. 2006. The insulin/PI 3-kinase pathway regulates salt chemotaxis learning in Caenorhabditis elegans. *Neuron,* 51**,** 613-25.
TOPALIDOU, I. & CHALFIE, M. 2011. Shared gene expression in distinct neurons expressing common selector genes. *Proc Natl Acad Sci U S A,* 108**,** 19258-63.
TRINDADE, L. S., AIGAKI, T., PEIXOTO, A. A., BALDUINO, A., MANICA DA CRUZ, I. B. & HEDDLE, J. G. 2013. A novel classification system for evolutionary aging theories. *Front Genet,* 4**,** 25.
TROEMEL, E. R., KIMMEL, B. E. & BARGMANN, C. I. 1997. Reprogramming chemotaxis responses: sensory neurons define olfactory preferences in C. elegans. *Cell,* 91**,** 161-9.

TSALIK, E. L. & HOBERT, O. 2003. Functional mapping of neurons that control locomotory behavior in Caenorhabditis elegans. *J Neurobiol,* 56**,** 178-97.
TSIEN, R. W., ELLINOR, P. T. & HORNE, W. A. 1991. Molecular diversity of voltage-dependent Ca2+ channels. *Trends Pharmacol Sci,* 12**,** 349-54.
TSIEN, R. Y. 2009. Constructing and exploiting the fluorescent protein paintbox (Nobel Lecture). *Angew Chem Int Ed Engl,* 48**,** 5612-26.
TSUJIMOTO, T., JEROMIN, A., SAITOH, N., RODER, J. C. & TAKAHASHI, T. 2002. Neuronal calcium sensor 1 and activity-dependent facilitation of P/Q-type calcium currents at presynaptic nerve terminals. *Science,* 295**,** 2276-9.
TURNER, C. E., WEST, K. A. & BROWN, M. C. 2001. Paxillin-ARF GAP signaling and the cytoskeleton. *Curr Opin Cell Biol,* 13**,** 593-9.
VAZQUEZ, G., WEDEL, B. J., KAWASAKI, B. T., BIRD, G. S. & PUTNEY, J. W., JR. 2004. Obligatory role of Src kinase in the signaling mechanism for TRPC3 cation channels. *J Biol Chem,* 279**,** 40521-8.
VENKATACHALAM, K. & MONTELL, C. 2007. TRP channels. *Annu Rev Biochem,* 76**,** 387-417.
VIVIANO, J., KRISHNAN, A., WU, H. & VENKATARAMAN, V. 2016. Data on the calcium-induced mobility shift of myristoylated and non-myristoylated forms of neurocalcin delta. *Data Brief,* 7**,** 630-3.
VOETS, T. 2014. TRP channels and thermosensation. *Handb Exp Pharmacol,* 223**,** 729-41.
VRIENS, J., NILIUS, B. & VOETS, T. 2014. Peripheral thermosensation in mammals. *Nat Rev Neurosci,* 15**,** 573-89.
WALKER, R. G., WILLINGHAM, A. T. & ZUKER, C. S. 2000. A Drosophila mechanosensory transduction channel. *Science,* 287**,** 2229-34.
WALLACE, D. J., MEYER ZUM ALTEN BORGLOH, S., ASTORI, S., YANG, Y., BAUSEN, M., KUGLER, S., PALMER, A. E., TSIEN, R. Y., SPRENGEL, R., KERR, J. N., DENK, W. & HASAN, M. T. 2008. Single-spike detection in vitro and in vivo with a genetic Ca2+ sensor. *Nat Methods,* 5**,** 797-804.
WANG, D., KENNEDY, S., CONTE, D., JR., KIM, J. K., GABEL, H. W., KAMATH, R. S., MELLO, C. C. & RUVKUN, G. 2005. Somatic misexpression of germline P granules and enhanced RNA interference in retinoblastoma pathway mutants. *Nature,* 436**,** 593-7.
WANG, D., O'HALLORAN, D. & GOODMAN, M. B. 2013. GCY-8, PDE-2, and NCS-1 are critical elements of the cGMP-dependent thermotransduction cascade in the AFD neurons responsible for C. elegans thermotaxis. *J Gen Physiol,* 142**,** 437-49.
WANG, K., YANG, Z., LIU, X., MAO, K., NAIR, U. & KLIONSKY, D. J. 2012. Phosphatidylinositol 4-kinases are required for autophagic membrane trafficking. *J Biol Chem,* 287**,** 37964-72.
WASSERMAN, S. M., BEVERLY, M., BELL, H. W. & SENGUPTA, P. 2011. Regulation of response properties and operating range of the AFD thermosensory neurons by cGMP signaling. *Curr Biol,* 21**,** 353-62.
WAUGH, M. G. 2015. PIPs in neurological diseases. *Biochim Biophys Acta,* 1851**,** 1066-82.
WEISS, J. L., ARCHER, D. A. & BURGOYNE, R. D. 2000. Neuronal Ca2+ sensor-1/frequenin functions in an autocrine pathway regulating Ca2+ channels in bovine adrenal chromaffin cells. *J Biol Chem,* 275**,** 40082-7.
WEISS, J. L. & BURGOYNE, R. D. 2001. Voltage-independent inhibition of P/Q-type Ca2+ channels in adrenal chromaffin cells via a neuronal Ca2+ sensor-1-dependent pathway involves Src family tyrosine kinase. *J Biol Chem,* 276**,** 44804-11.

WEISS, J. L., HUI, H. & BURGOYNE, R. D. 2010. Neuronal calcium sensor-1 regulation of calcium channels, secretion, and neuronal outgrowth. *Cell Mol Neurobiol,* 30**,** 1283-92.
WES, P. D., CHEVESICH, J., JEROMIN, A., ROSENBERG, C., STETTEN, G. & MONTELL, C. 1995. TRPC1, a human homolog of a Drosophila store-operated channel. *Proc Natl Acad Sci U S A,* 92**,** 9652-6.
WHITE, J. G., SOUTHGATE, E., THOMSON, J. N. & BRENNER, S. 1986. The structure of the nervous system of the nematode Caenorhabditis elegans. *Philos Trans R Soc Lond B Biol Sci,* 314**,** 1-340.
WHITE, J. Q. & JORGENSEN, E. M. 2012. Sensation in a single neuron pair represses male behavior in hermaphrodites. *Neuron,* 75**,** 593-600.
WINGARD, J. N., CHAN, J., BOSANAC, I., HAESELEER, F., PALCZEWSKI, K., IKURA, M. & AMES, J. B. 2005. Structural analysis of Mg2+ and Ca2+ binding to CaBP1, a neuron-specific regulator of calcium channels. *J Biol Chem,* 280**,** 37461-70.
WITTENBURG, N. & BAUMEISTER, R. 1999. Thermal avoidance in Caenorhabditis elegans: an approach to the study of nociception. *Proc Natl Acad Sci U S A,* 96**,** 10477-82.
WOLF, F. I. & CITTADINI, A. 1999. Magnesium in cell proliferation and differentiation. *Front Biosci,* 4**,** D607-17.
XIAO, R., LIU, J. & XU, X. Z. 2015. Thermosensation and longevity. *J Comp Physiol A Neuroethol Sens Neural Behav Physiol*.
XIAO, R., ZHANG, B., DONG, Y., GONG, J., XU, T., LIU, J. & XU, X. Z. 2013. A genetic program promotes C. elegans longevity at cold temperatures via a thermosensitive TRP channel. *Cell,* 152**,** 806-17.
YAMAUCHI, T. 2005. Neuronal Ca2+/calmodulin-dependent protein kinase II--discovery, progress in a quarter of a century, and perspective: implication for learning and memory. *Biol Pharm Bull,* 28**,** 1342-54.
YAN, J. L., K. MAGUPALLI, VG. NANOUA, E. MARTINEZA, GQ. SCHEUERA, T. CATTERALL, WA. 2014. Modulation of CaV2.1 channels by neuronal calcium sensor-1 induces short-term synaptic facilitation. *Molecular and Cellular Neuroscience,* 63**,** 124–131.
YANEZ, M., GIL-LONGO, J. & CAMPOS-TOIMIL, M. 2012. Calcium binding proteins. *Adv Exp Med Biol,* 740**,** 461-82.
YANG, P. S., ALSEIKHAN, B. A., HIEL, H., GRANT, L., MORI, M. X., YANG, W., FUCHS, P. A. & YUE, D. T. 2006. Switching of Ca2+-dependent inactivation of Ca(v)1.3 channels by calcium binding proteins of auditory hair cells. *J Neurosci,* 26**,** 10677-89.
YANG, P. S., JOHNY, M. B. & YUE, D. T. 2014. Allostery in Ca(2)(+) channel modulation by calcium-binding proteins. *Nat Chem Biol,* 10**,** 231-8.
YAO, X., KWAN, H. Y. & HUANG, Y. 2005. Regulation of TRP channels by phosphorylation. *Neurosignals,* 14**,** 273-80.
YE, H. Y., YE, B. P. & WANG, D. Y. 2008. Evaluation of the long-term memory for thermosensation regulated by neuronal calcium sensor-1 in Caenorhabditis elegans. *Neurosci Bull,* 24**,** 1-6.
YEMINI E., J. T., GRUNDY L. J., BROWN A.E.X. AND SCHAFER W.R. 2013. A database of Caenorhabditis elegans behavioral phenotypes. *Nature Methods,* 10**,** 877-879.
YU, S. C., KLOSTERMAN, S. M., MARTIN, A. A., GRACHEVA, E. O. & RICHMOND, J. E. 2013. Differential roles for snapin and synaptotagmin in the synaptic vesicle cycle. *PLoS One,* 8**,** e57842.

ZHANG, B., XIAO, R., RONAN, E. A., HE, Y., HSU, A. L., LIU, J. & XU, X. Z. 2015. Environmental Temperature Differentially Modulates C. elegans Longevity through a Thermosensitive TRP Channel. *Cell Rep,* 11**,** 1414-24.

ZHANG, M., TANAKA, T. & IKURA, M. 1995. Calcium-induced conformational transition revealed by the solution structure of apo calmodulin. *Nat Struct Biol,* 2**,** 758-67.

ZHAO, B., KHARE, P., FELDMAN, L. & DENT, J. A. 2003. Reversal frequency in Caenorhabditis elegans represents an integrated response to the state of the animal and its environment. *J Neurosci,* 23**,** 5319-28.

ZHAO, L., HELMS, J. B., BRÜGGER, B., HARTER, C., MARTOGLIO, B., GRAF, R., BRUNNER, J. & WIELAND, F. T. 1997. Direct and GTP-dependent interaction of ADP ribosylation factor 1 with coatomer subunit β. *Proc Natl Acad Sci U S A,* 94**,** 4418-23.

ZHAO, X., VARNAI, P., TUYMETOVA, G., BALLA, A., TOTH, Z. E., OKER-BLOM, C., RODER, J., JEROMIN, A. & BALLA, T. 2001. Interaction of neuronal calcium sensor-1 (NCS-1) with phosphatidylinositol 4-kinase beta stimulates lipid kinase activity and affects membrane trafficking in COS-7 cells. *J Biol Chem,* 276**,** 40183-9.

ZHENG, C. Y., PETRALIA, R. S., WANG, Y. X. & KACHAR, B. 2011. Fluorescence recovery after photobleaching (FRAP) of fluorescence tagged proteins in dendritic spines of cultured hippocampal neurons. *J Vis Exp*.

ZHENG, Y., BROCKIE, P. J., MELLEM, J. E., MADSEN, D. M. & MARICQ, A. V. 1999. Neuronal control of locomotion in C. elegans is modified by a dominant mutation in the GLR-1 ionotropic glutamate receptor. *Neuron,* 24**,** 347-61.

ZHOU, H., KIM, S. A., KIRK, E. A., TIPPENS, A. L., SUN, H., HAESELEER, F. & LEE, A. 2004. Ca2+-binding protein-1 facilitates and forms a postsynaptic complex with Cav1.2 (L-type) Ca2+ channels. *J Neurosci,* 24**,** 4698-708.

ZHOU, Q., LAI, Y., BACAJ, T., ZHAO, M., LYUBIMOV, A. Y., UERVIROJNANGKOORN, M., ZELDIN, O. B., BREWSTER, A. S., SAUTER, N. K., COHEN, A. E., SOLTIS, S. M., ALONSO-MORI, R., CHOLLET, M., LEMKE, H. T., PFUETZNER, R. A., CHOI, U. B., WEIS, W. I., DIAO, J., SUDHOF, T. C. & BRUNGER, A. T. 2015. Architecture of the synaptotagmin-SNARE machinery for neuronal exocytosis. *Nature,* 525**,** 62-7.

ZIMMER, M., GRAY, J. M., POKALA, N., CHANG, A. J., KAROW, D. S., MARLETTA, M. A., HUDSON, M. L., MORTON, D. B., CHRONIS, N. & BARGMANN, C. I. 2009. Neurons detect increases and decreases in oxygen levels using distinct guanylate cyclases. *Neuron,* 61**,** 865-79.

ZUCKER, R. S. & REGEHR, W. G. 2002. Short-term synaptic plasticity. *Annu Rev Physiol,* 64**,** 355-405.

ZUHLKE, R. D., PITT, G. S., TSIEN, R. W. & REUTER, H. 2000. Ca2+-sensitive inactivation and facilitation of L-type Ca2+ channels both depend on specific amino acid residues in a consensus calmodulin-binding motif in the(alpha)1C subunit. *J Biol Chem,* 275**,** 21121-9.